Analysis of Targeted *CYCD7;1* Expression in Seed Development

Emily Sornay

School of Biosciences

Cardiff University

A thesis submitted in partial fulfilment of the requirements for the degree of
Doctor of Philosophy
2013

Acknowledgements

I would like to express my most sincere gratitude to my supervisor, Prof. James Murray for giving me the opportunity to work on this project, and for all of the help, guidance and expert advice he has given me over the last four years. I would also like to thank Dr. Walter Dewitte for his expert scientific advice, guidance and encouragement.

I wish to thank my colleagues in Prof. Murray's lab, in particular Dr. Céline Forzani, Dr. Simon Scofield, Dr. Jeroen Nieuwland and Mr Rico Randall for their expert scientific advice and technical assistance. My further thanks go to Ms Joe Kilby and Ms Angela Marchbank for their technical assistance.

I would also like to thank Bayer CropScience for funding this project and the people involved in this project: Dr. Marc Bots at Bayer CropScience for his supervision and Mr John Teske for his bioinformatic help.

Finally, my most sincere gratitude goes to my family, parents and my sister, and Rico for the unconditional support, patience and love they have given me during all these years to make this work possible.

Analysis of Targeted *CYCD7;1* Expression in Seed Development

Emily Sornay

Summary

D-type cyclins in plants are represented by seven conserved subgroups and play a major role in controlling cell division. Relatively little is understood of their role during seed development, although their expression pattern has been characterized and ectopic expression of *CYCD3;1* has previously been shown to disrupt normal embryo development.

Here the consequences of ectopic expression of *CYCD7;1* using the early endosperm-specific promoter *FWA* in developing Arabidopsis seeds were investigated. Ectopic *CYCD7;1* expression in the maternal central cell prior to fertilization, and in the endosperm from fertilization until cellularization resulted in seeds up to 45% larger. Seed enlargement was accompanied seed lethality, shown to be due to a defect of development during early and mid stages of seed development. As expected from the maternal specific expression of the imprinted *FWA* promoter, seed size and lethality was dependent on maternal origin of the transgene. Larger seed size was correlated to mature embryo and seed coat outgrowth, and was due to cell proliferation rather than cell elongation. In particular, embryo development was accelerated during the early stages, suggesting these may be dependent on cell division rate, whereas later stages progressed at the same rate as *WT* seeds. Seed-targeted *CYCD7;1* expression phenocopies (1) the nucleus proliferation in the endosperm prior to fertilization observed in *rbr* and *fis*-class mutants and (2) the seed enlargement observed in paternal genome excess interploidy crosses. These suggest that *CYCD7;1* may act through the RBR pathway to promote cell proliferation and modify imprinting in the endosperm, thereby influencing the parental genome balance.

Mechanistically, CYCD7;1 did not interact directly with CDKA;1 but the interaction was promoted in presence of the inhibitor of CDK, ICK1/KRP1 or ICK2/KRP2 in a yeast-three-hybrid assay. However, loss of either KRP1 or KRP2 in respective mutant backgrounds did not prevent the seed enlargement phenotype.

Table of Contents

Chapter 1 : Introduction

Chapter 2 : Material and Methods

Chapter 3 : Targeting *CYCD7;1* Expression to Engineer Seed Size

Chapter 4 : Effects of Endosperm-Targeted Expression of *CYCD7;1* on Seed Development

Chapter 5 : Interaction of CYCD7;1 with CDK and KRP proteins

Chapter 6 : Final Discussion

Abbreviations

ACT	*ACTIN*
AD	Activation domain
A or **ade**	Adenine
AHK	*ARABIDOPSIS HISTIDINE KINASE*
AP2	*APETALA2*
AP-MS	Affinity purification mass spectrometry
BD	Binding domain
BiFC	Bimolecular fluorescence complementation
CAK	CDK-dependent kinase
CDK	Cyclin-dependent kinase
CKI	Cyclin-dependent kinase inhibitor
CKS	Cyclin-dependent kinase subunit
CKX	*CYTOKININ OXIDASE/DEHYDROGENASE*
Col-0	*Columbia-0*
CYCD	*Cyclin D*
DAP	Day after pollination
DNA	Deoxyribonucleic acid
dFWA	FWA protein fragment with a homedomain and a NLS
dNTP	Deoxynucleotide triphosphate
EOD3	*ENHANCER OF DA1*
FIE	*FERTILIZATION-INDEPENDENT ENDOSPERM*
FIS	*FERTILIZATION-INDEPENDENT SEED*
FWA	*FLOWERING WAGENINGEN*
G1 / G2	Gap1 / Gap2
GM	Growth medium
HAP	Hour after pollination
H or **his**	Histidine
ICK	INHIBITOR OF CYCLIN-DEPENDENT KINASE
IKU	*HAIKU*

KRP	*KIP RELATED PROTEIN*
L or **Leu**	Leucine
M	Mitosis
MEA	*MEDEA*
MET	Methionine
MET1	*DNA METHYLTRANSFERASE1*
MINI3	*MINISEED3*
MNT	*MEGAINTEGUMENTA*
MSI1	*MULTICOPY SUPRESSOR OF IRA1*
NLS	Nuclear localization sequence
PCA	Protein-fragment complementation assay
PCR	Polymerase chain reaction
PGK	*PHOSPHOGLYCERATE KINASE*
RB	Retinoblatoma protein
RBR	*RETINBLASTOMA-RELATED*
RNA	Ribonucleic acid
rpm	Revolutions per minute
RPS5A	*RIBOSOMAL PROTEIN SUBUNIT 5A*
RT-PCR	Reverse transcription PCR
S	Synthesis phase
SE	Standard error
$_{seed}$CYCD7;1	*CYCD7;1* seed-targeted expression (*pFWA:CYCD7;1*)
SHB	*SHORT HYPOCOTYL UNDERBLUE1*
SIM	*SIAMESE*
TAP	Tandem affinity purification
T-DNA	Transfer DNA
TF	Transcription factor
T	Tryptophan
TTG2	*TRANSPARENT TESTA GLABRA 2*
U	Uracil
WT	*Wild-type*

X-Gal	5-bromo-4-chloro-3-indolyl-β-D-galactoside
X-Gluc	5-bromo-4-chloro-3-indolyl glucuronide
Y2H	Yeast-two-hybrid assay
Y3H	Yeast-three-hybrid assay

Chapter 1

Introduction

Chapter 1
Introduction

Seeds are essential for dispersal and survival of Flowering plants. During seed development, the high level of mitotic cell cycle activity drives the formation of a multicellular organism from the single-celled zygote. Moreover, crop seeds constitute a major part of human nutrition. Increasing seed yield in crops is becoming more important, due to rising food demand. Understanding the plant cell cycle and its regulation during seed development might help to achieve greater seed yields. In this thesis, “plants” refers to higher land plants or ‘seed’plants.

1.1. The plant cell cycle

For any living organism, the cell division cycle is a fundamental process by which cells reproduce. The cell cycle is a highly conserved mechanism from protozoa (or prophytes) to complex metazoans (or metaphytes). For unicellular organisms, it is essential for reproduction. For multicellular organisms, it is also required for (1) the formation of a multicellular individual from a single zygotic cell and (2) the regeneration of some tissues (Nurse, 2000).

In plants, development can be continuous and occurs mostly post-embryonically due to the activity of meristems that contain pools of stem cells. The production of new organs during plant development requires active cell division. New cells, that undergo cell expansion and differentiation, are formed leading to the formation of new tissues and/or organs. Therefore, the plant mitotic cell cycle is an essential part of both embryonic and post-embryonic development. Despite the fact that the sequential phases of plant cell cycle and their regulation have been studied for decades, the regulation of some processes remains unclear (Alberts *et al.*, 2002).

1.1.1. The plant cell cycle and its regulators

Overview of the plant cell cycle

The mitotic cell cycle leads to the formation of two daughter cells carrying the same genetic information as the mother cell they were generated from. The mitotic cycle is composed of alternating DNA replication (synthesis, also named S phase) and chromosome partitioning

(Mitosis, also named M phase), interrupted by two gaps named G1 (between M and S phases) and G2 (between S and M phases) (Fig. 1.1). Cell cycle progression requires tight regulation that occurs at the two main checkpoints: G1-to-S and G2-to-M transitions (Novak *et al.*, 1998; Jakoby and Schnittger, 2004). The commitment into a cell cycle requires the integration by the cell of developmental cues such as energy availability and hormone levels respectively (Dewitte and Murray, 2003). The integration of these signals is fundamental for the cell in making the decision to initiate DNA replication and to commit itself to the mitotic process (Van't Hof, 1985).

To complete the cell cycle, the duplicated DNA has to be separated and a new cell wall synthesized. The cytoskeleton, the microtubules in particular, plays a major role in separating the daughter chromatids, which align at the site of the pre-prophase band, and in guiding membrane vesicles to the cell plate to form the new cell wall (Field *et al.*, 1999; Pickett-Heaps *et al.*, 1999).

Some plant cells undergoing differentiation can go through a modified cell cycle, called endocycle (Galbraith *et al.*, 1991). During the endocycle, the genetic material is replicated during S-phase, but mitosis does not occur. Therefore, for every endocycle, the ploidy level is doubled (Joubes and Chevalier, 2000). Endoreplication has been described for all eukaryotes (Edgar and Orr-Weaver, 2001). In Arabidopsis, the ploidy level is highly variable. It has been observed that in mature or differentiating leaves, the epidermal cells can display 2C to 16C and even reach 64C in specific leaf cells such as trichomes (Galbraith *et al.*, 1991; Melaragno *et al.*, 1993). The role of endoreduplication is not well understood, however it has been observed that endocycles are often correlated with increased cell size and it has been postulated that it might offset increased metabolism (Melaragno *et al.*, 1993; Traas *et al.*, 1998). It also has been proposed that by increasing ploidy, the plant has a greater capacity to buffer to the accumulation of mutations and/or to DNA damage (Ramirez-Parra and Gutierrez, 2007).

The mitotic cell cycle and endocycle mostly share the same regulators and similar regulatory mechanisms (Jakoby and Schnittger, 2004).

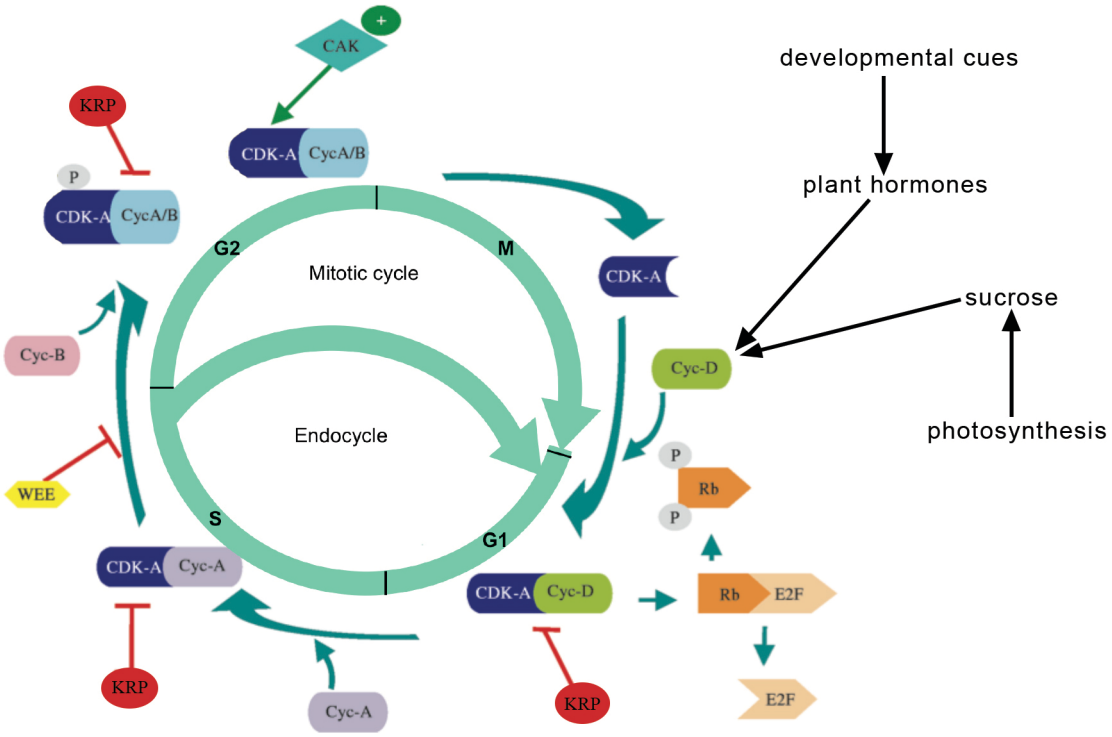

Figure 1.1. Plant cell cycle overview. The progression through the different phases G1, S, G2 and M involved the successive formation, activation and inactivation of cyclin-dependent kinases (CDKs). The control of the different phases and transition depends on the association between the different CDKs and cyclins. Activity of CDK/CYC complex can be decreased by KRPs binding and by negative phosphorylation by WEE1. CDK/CYC activity can be enhanced by positive phosphorylation by CDK-activating kinases (CAKs). Endocycle is a modified cell cycle, reduced to the alternating S and G1 phases. Modified from Andrietta *et al.* (2001) and Menges *et al.* (2005).

Cyclin-dependent Kinases (CDKs)

Eukaryotic cell cycle control involves modulation of the serine-threonine kinase activity of cyclin-dependent kinases (CDKs). The CDK usually requires the binding of a regulatory subunit called a cyclin to be functional (Fig. 1.2). In all eukaryotes analyzed to date, there is at least one CDK with the canonical amino-acid sequence PSTAIRE in the cyclin-binding domain. All eukaryotic serine-threonine and tyrosine kinases share a similar protein structure due to a closely-related sequence of 300 amino acids. This sequence gives rise to a bilobal structure forming a catalytic pocket between the N- and C-terminal tails. This pocket is the site of ATP- and substrate-binding. Access to the catalytic pocket is restricted by a so-called T-loop. Upon cyclin binding, the flexible CDK structure is shifted and the T-loop moves laterally allowing CDK substrates to access the catalytic sites. However, the catalytic activity is low and requires the phosphorylation of threonine 160 of the T-loop by

CDK activating kinases, to give full catalytic potential (Joubes *et al.*, 2000; Dissmeyer *et al.*, 2007; Jura *et al.*, 2011).

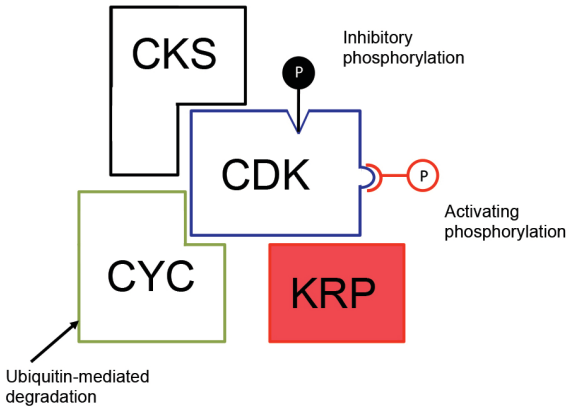

Figure 1.2. CDK/CYC complex and its regulation.

CDK can be regulated at different levels. The kinase activity is activated by CYC binding and positively enhanced by CKS binding and activation phosphorylation by CAKs. The kinase activity is inhibited upon inhibitory binding of ICKs/ Kip-related protein (KRPs) or upon inhibitory phosphorylation. Modified from Dewitte and Murray (2003).

In the Arabidopsis genome, twelve CDK-related genes have been identified based on sequence similarity. They are divided into 6 groups (CDKA-F; Fig.1.3) (Vandepoele *et al.*, 2002).

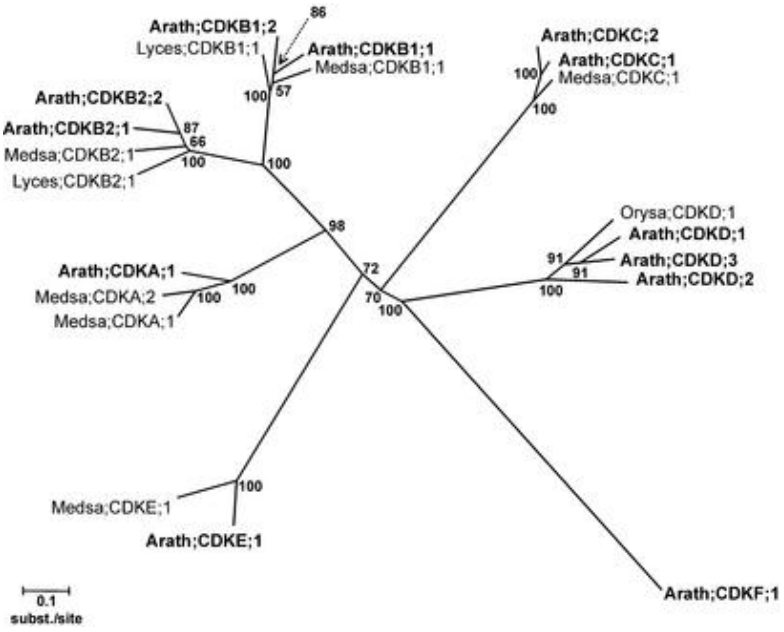

Figure 1.3. Tree of the A, B, C, D, E, and F Classes of CDKs from Arabidopsis (Arath), Lyces, tomato (*Lycopersicon esculentum*); Medsa, alfalfa (*Medicago sativa*); Orysa, rice (*Oryza sativa*) (from Vandepoele *et al.*, 2002).

In Arabidospis, a single gene coding for CDKA (CDKA;1) is present, and is the only gene that carries in its sequence the PSTAIRE amino acid hallmark. CDKB genes have the sequence PPTA/TLRE (Mironov *et al.*, 1999; Vandepoele *et al.*, 2002). The difference of the hallmarks in the CDKB group reflects the presence of two subgroups, CDKB1 and CDKB2 families, each containing 2 members in *Arabidopsis* (CDKB1;1, CDKB1;2, CDKB2;1 and CDKB2;2). CDKA;1 and CDKBs have been shown to have direct action on controlling the transition between the different phases of the cell cycle (Joubes *et al.*, 2000;

Boudolf *et al.*, 2001). CDKA;1 is involved in regulating both the transition from G1-to-S and G2-to-M, with a requirement for CDKB in the latter transition (Inze and De Veylder, 2006; Kawamura *et al.*, 2006).

CDKD displays an N(I/F)TALRE motif and, in association with a H-type cyclin, can phosphorylate CDKA/D-type cyclin complexes (De Veylder *et al.*, 2007). CDKF has also been shown to be involved in activating the CDK/CYC complexes by phosphorylating a threonine site on the T-loop (Umeda *et al.*, 1998; Shimotohno *et al.*, 2004). Therefore CDKD and CDKF are classified as CDK-activating kinases (CAKs). Recent data show that CDKF and CDKD can also phosphorylate RNA polymerase II and mutation in any of these CDKs leads to defects in transcription in plants (Hajheidari *et al.*, 2012). Since phosphorylation of both CDKs and the C-terminal tail of the RNA polymerase can be a shared function of CAKs, these results reinforce that CDKD and CDKF are CAKs. Similarly, CDKC, characterized by a PITAIRE and shown to be homologous of mammalian CDK9, is involved in phosphorylating the C-terminal domain of RNA polymerase II (Mironov *et al.*, 1999; Price, 2000; Barroco *et al.*, 2003). A more recent study also showed that CDKC shares more similarity with the mammalian CYSTEINE-RICH RLK7 (RECEPTOR-LIKE PROTEIN KINASE7, CRK7) than the mammalian CDK9, and is co-localized with splicing factors and this localization depends on its kinase activity (Kitsios *et al.*, 2008).

CDKE, carrying the hallmark SPTAIRE, has not been demonstrated to be involved regulating the cell cycle (Vandepoele *et al.*, 2002). Based on it homology with the human CDK8, it was proposed that CDKE might also be involved in regulating the RNA polymerase II (Tassan *et al.*, 1995). To date, this has not been demonstrated in plants.

Table 1.1. Arabidopsis cyclin-dependent kinases (Modified from Vandepoele *et al.*, 2002).

Gene	Accesssion Number	CDK signature motif
CDKA;1	At3g48751	PSTAIRE
CDKB1;1	At3g54180	PPTALRE
CDKB1;2	At2g38620	PPTALRE
CDKB2;1	At1g76540	PPTALRE
CDKB2;2	At1g20930	PPTALRE
CDKC;1	At5g10270	PITAIRE
CDKC;2	At5g64960	PITAIRE
CDKD;1	At1g73690	NVTALRE
CDKD;2	At1g66750	NFTALRE
CDKD;3	At1g18040	NITALRE
CDKE;1	At5g63610	SPTAIRE
CDKF;1	At4g28980	None

There are four levels of regulation to activate and/or modulate CDK activity (Fig1.3): (1) the binding with positive cofactors such as cyclins, (2) the binding of negative regulators such as CDK inhibitors, (3) positive phosphorylations and (4) negative phosphorylations, with both phosphorylations occurring on the threonine or tyrosine residues of the T-loop (Pines, 1995).

Cyclins

Monomeric CDKs do not usually possess kinase activity. The association with regulatory proteins called cyclins (CYCs) is required to activate their kinase activity (Fig. 1.3). Cyclins were first identified in sea urchin eggs in which their protein levels appear and disappear in a cyclic manner (Evans *et al.*, 1983). Interactions between CDKs and CYCs have been demonstrated using different methods and the potential interaction between the different members of these protein classes investigated (Boruc *et al.*, 2010). The interaction of human CDKs and cyclins has been visualized by crystallography (Russo *et al.*, 1996). Cyclins are characterized by a conserved region of 250 amino acids. (Nugent *et al.*, 1991; Noble *et al.*, 1997). The N-terminal region is about 100 amino acids long and corresponds to a region of highest conservation with five invariant residues. It contains a CDK-binding site also called “cyclin box” (Wang *et al.*, 2004). Over three decades, cyclins have been isolated from many organisms. The constant discovery of new plant cyclins in the 1980s-90s necessitated a unified nomenclature (Renaudin *et al.*, 1996).

Arabidopsis genome-wide analysis reveals 49 putative cyclins that could be identified based on the presence of the two N- and C-terminal regions (Fig. 1.4) (Vandepoele *et al.*, 2002; Wang *et al.*, 2004). Thirty one of these proteins have the N- and C-termini in their sequence, whereas 18 contain only the N-terminus. Phylogenetic analysis reveals homology with animal and protist cyclins, thus the plant cyclins have been classified into 10 classes homologous to those in animals and protists. They are annotated A, B, C, D, H, T, L, U. C-, T-, L-, U-type cyclins based on sequence analysis. Except for their expression pattern in different Arabidopsis tissues and the presence of homologs in rice (*Oryza sativa*), little is known about these four classes (Wang *et al.*, 2004). On the other hand, A-type, B-type, D-type and H-type cyclins have been widely described and their involvement in cell cycle control has started to be elucidated (De Veylder *et al.*, 2007). The A-type cyclin family has 10 members, B-type, 11, D-type 10 and there is a single H-type cyclin. CYCA and CYCB are divided into three subgroups (A1, A2, A3 and B1,B2, and B3) and CYCD into six (D1, D2/D4, D3, D5, D6, D7) (Vandepoele *et al.*, 2002).

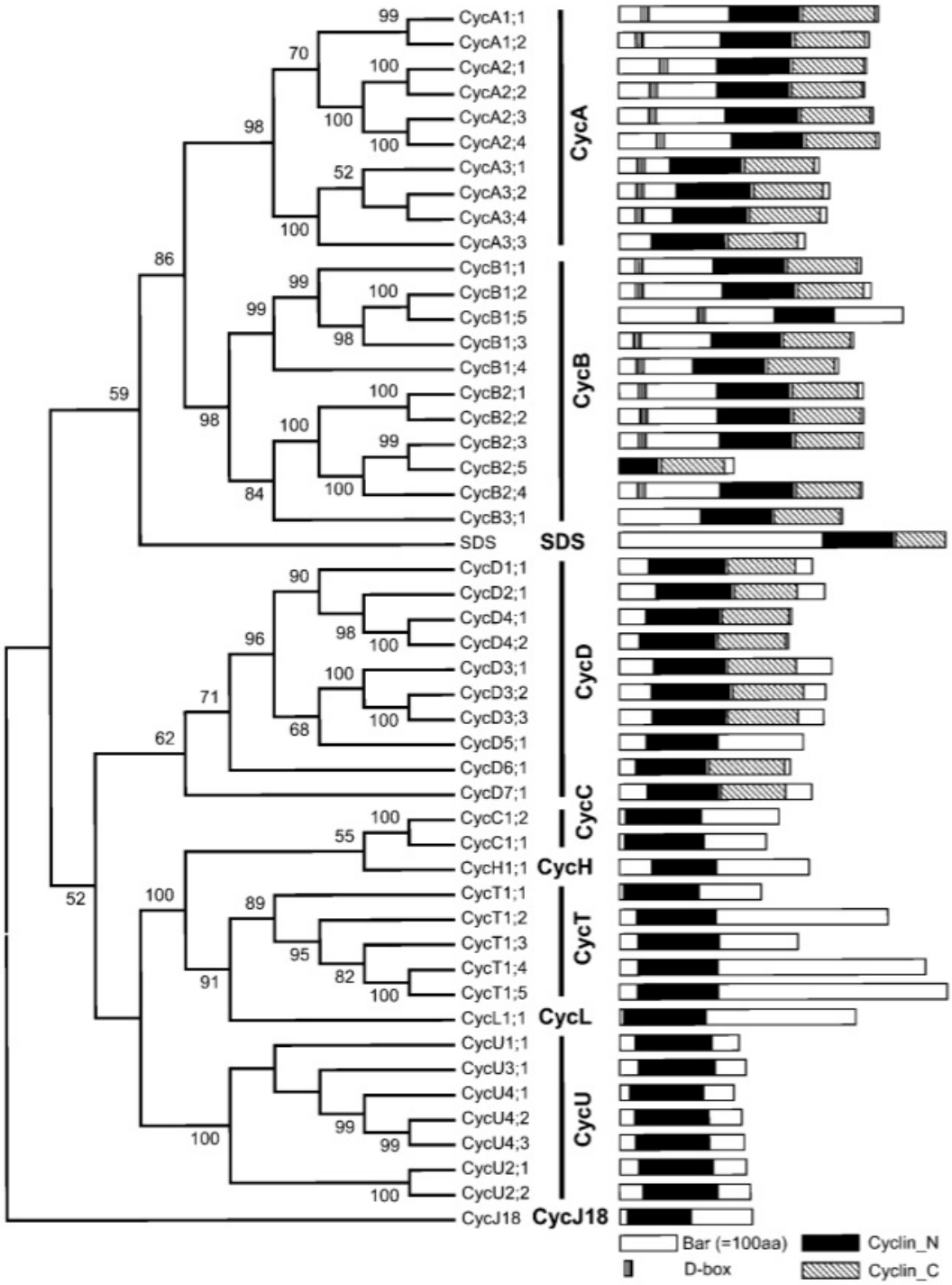

Figure 1.4. Phylogenetic tree and protein domain structure of Arabidopsis cyclin (from Wang et al., 2004).

CYCA, CYCB and CYCD form active complexs with CDKA;1 or CDKBs, whereas CYCH is associated with CDKD. Broadly speaking, the G1-S transition is controlled by CYCD/CDKA;1 and CYCA/CDKA;1 and CDKB regulate the cell cycle from the S-phase to the M-phase. The G2-M transition and the onset of M phase are regulated by CYCA, CYCB or CYCD with CDKA or CDKB (Inze and De Veylder, 2006). CYCH is associated with CDKD at the transition G2-M. The general view of the cell cycle control is corroborated by

analysis of expression of the different cyclins in synchronized cell suspension (Menges *et al.*, 2005) and the investigation of core cell cycle protein interactions (Boruc *et al.*, 2010; Van Leene *et al.*, 2010; Van Leene *et al.*, 2011). The plant D-types cyclins and their role during the cell cycle and development of plants is detailed below.

The level of each cyclin type protein is a way to regulate the activity of CDKs and control the progression of the cell cycle. This level can be regulated transcriptionally or post-translationally by targeting proteasome degradation.

CDK Subunit

CDK subunit (CKS) proteins act as docking factors that mediate the interaction between the CDKs and their substrates and regulatory proteins (Fig. 1.3) (De Veylder *et al.*, 1997; De Veylder *et al.*, 2001; Zhou *et al.*, 2002b). In Arabidopsis, two CKSs (CKS1 and CKS2) have been identified (Vandepoele *et al.*, 2002). They share 83% homology in the nucleotide sequence and 90% in the protein sequence (De Veylder *et al.*, 1997). They are located on the same chromosome, arranged in a tandem-like organization suggesting that they arise from a duplication event (Fig. 1.5) (Vandepoele *et al.*, 2002). CKS1 interacts with CDKA;1 and CDKBs and is expressed in dividing and endoreduplicating cells (De Veylder *et al.* 1997). CKS2 has been shown to interact *in vivo* with CDKA;1, CDKB1;1 and CYCD3;1 but no functional analysis has been carried out (Van Leene *et al.*, 2007).

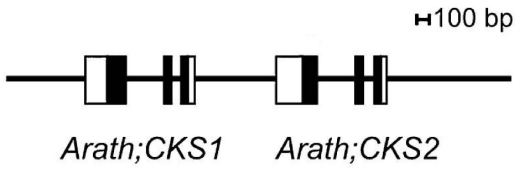

Figure 1.5. Schematic of the tandem-like structure of CKS genes in Arabidopsis. Blacks boxes represent exon and white boxes are untranslated region. (from Vandepoele *et al.*, 2002).

CDK inhibitors

CDK Inhibitors (CKIs) modulate the activity of CDKs either to direct binding of the CDK/CYC complex or by a negative by regulating phosphorylation of the CDK subunit (Fig.1.3) (Vandepoele *et al.*, 2002).

CDK/CYC binding inhibitors are divided into 2 groups: INTERACTOR/INHIBITOR OF CYCLIN-DEPENDENT KINASE (ICK) family and a more recently described class, SIAMESE (SIM) and SIM-RELATED (SMR) proteins in Arabidopsis (Walker *et al.*, 2000; Churchman *et al.*, 2006; Peres *et al.*, 2007).

Crystallography studies show that the mammalian protein related to ICKs can bind CDK on its own (Russo *et al.*, 1996) but has a greater affinity for the CDK/CYC complex. A 65

amino-acid domain of ICK, involved in the binding, interacts with a large surface of the CDK/CYC complex (Fig. 1.6) (Joubes *et al.*, 2000). The ICK binding on CDK/CYC complex prevents ATP and substrate entry in the catalytic pocket. In Arabidopsis, the first ICK isolated, ICK1, displays a homology in its C-terminus with the animal Cip/Kip family (Wang *et al.*, 1997). Therefore they were also named Kip-Related Proteins (KRPs). The Arabidopsis genome contains 7 genes encoding for KRP1-7 (Fig. 1.6) (De Veylder *et al.*, 2001). Deletion analysis indicated that the C-terminal domain of ICK1/KRP1 is required for the interaction with CDKA;1 and CYCDs (Wang *et al.*, 1998). Functional analysis of KRPs shows that the C-terminus contains three motifs conserved in the 7 Arabidopsis KRPs and the mammalian $p27^{Kip1}$ protein (De Veylder *et al.* 2001). A more recent study reveals that the homology in the C-terminus is also shared with other plant species such as *Poplar trichocarpa* and *Oryza sativa L*. (Torres Acosta *et al.*, 2011). The inhibition of kinase activity has been shown *in vitro* (Wang *et al.* 1997) and *in vivo* (Zhou *et al.*, 2003). The inhibitory effect on the cell cycle was demonstrated *in planta* by overexpressing *KRP1* and *KRP2* leading to small plants with smaller serrated leaves and *KRP1* overexpression was shown to reduce the cell number in petals.

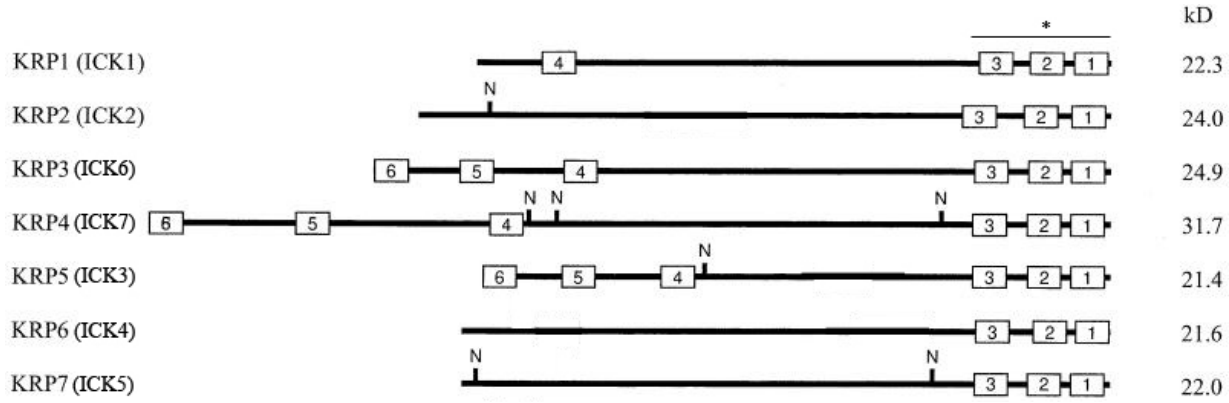

Figure 1.6. Structural organization of Arabidopsis KRPs. Conserved sequence boxes are indicated (1 to 6). N, nuclear localization signal. Asterix indicates the conserved sequences required for CDKA;1/CYCD interaction. Modified from De Veydler *et al.*, 2001).

The second class of CDK inhibitors acting by binding to the CDK/CYC complex that has been identified is the SIAMESE (SIM) proteins (Churchman *et al.*, 2006). In Arabidopsis, there are four members of the SIM family. They share a conserved EIEDFF motif with ICK/KRP and display a potential cyclin-binding motif. FRET studies show that SIM can bind both CDKA;1 and D-type cyclins. The inhibitory effect has been demonstrated in overexpressers, characterized by slow-growing plants with serrated leaves composed of enlarged epidermal cells with an increased ploidy level, very similar to *KRP* overexpressers.

Arabidopsis CDKs possess the two residues threonine-14 and tyrosine-15, that when phosphorylated, inhibit the CDK/CYC activity (Fig. 1.3). Phosphorylated tyrosine-15 brings the N-terminus into the CDK cleft by creating a hydrogen bond with glutamine-51 (Joubes *et al.*, 2000). Therefore, ATP binding and substrate docking are prevented. In Arabidopsis, one gene codes for the kinase WEE1 that is involved in phosphorylating these two residues (Sorrell *et al.*, 2002).

CDK-activating component

As mentioned above, full CDK activation can be achieved by the phosphorylation of threonine-160 or by removing the inhibitory phosphorylation on the threonine-14 and tyrosine-15 residues. T-160 phosphorylation is carried out by the CDKD/CYCH complex. Partial activation of CDK/CYC complexes can also be performed. In yeast, CDC25 phosphatase dephosphorylates these residues (Russell and Nurse, 1986). In Arabidopsis, a single gene (*Arath;CDC25*), sharing 32% homology in the catalytic domain with the yeast CDC25, has been identified (Landrieu *et al.*, 2004). Different views are found regarding its role and its possible involvement in cell cycle regulation. It has been shown that Arath;CDC25 displays a phosphatase activity *in vitro* whereas *in vivo* no effect on the cell cycle could detected since in *arath;cdc25* loss-of-function and *ArathCDC25* overexpresser mutants did not grow differently compared to *wild-type* (*WT*) plants, and DNA ploidy distribution was similar in mutant lines and *WT* plants (Landrieu *et al.*, 2004; Dissmeyer *et al.*, 2009; Spadafora *et al.*, 2011). However, *Arath;CDC25* was shown to be involved in other *in vivo* physiological processes. Since *Arath;CDC25* has some sequence homology with the arsenate reductase enzyme, its enzyme activity was tested: in an *ArathCDC25* overexpresser; its activity was increased two-fold. In *arath;cdc25* loss-of-function mutants, its activity was not detectable (Landrieu *et al.*, 2004; Dissmeyer *et al.*, 2009). These results suggest that *ArathCDC25* is not involved in cell cycle regulation but may act as an arsenate reductase.

Retinoblastoma protein

In higher eukaryotes one of the main targets of the CDK/cyclin complex is the retinoblastoma-related (RBR) protein (Goodrich and Lee, 1993; Boniotti and Gutierrez, 2001). In Arabidopsis, a single gene encodes the RBR protein (Xie *et al.*, 1996) whereas in maize, there are three RBR genes (RBR1, RBR2 and RBR3) (Xie *et al.*, 1996; Ach *et al.*, 1997; Sabelli *et al.*, 2005). During the G1 phase, the active RBR represses gene transcription by either binding the heterodimeric transcription factor E2F/Dimerisation Partner (DP) or by recruiting histone deactylases (Dyson, 1998; Ramirez-Parra *et al.*, 1999; Chen and Tian, 2007). RBR protein contains two conserved sequences that form a pocket

in which the E2F is docked (de Jager and Murray, 1999). At the G1-to-S transition RBR is phosphorylated by the CDK/CYCD complex, leading to its inactivation. Therefore RBR dissociates from its partner E2F/DP leading to the expression of E2F/DP responsive genes and histone deacetylases are not recruited. As RBR represses transcription, RBR is seen as a negative regulator of cell cycle and cell proliferation.

RBR is essential for plant development and reproduction in Arabidopsis. In an *rbr* loss-of-function mutant, meiotic defects result in impaired female and male gametogenesis .(Chen *et al.*, 2011) In addition, the *rbr* mutant fails to restrict mitosis during megagametogenesis (Ebel *et al.*, 2004; Ingouff *et al.*, 2006) and to determine the cell fate of vegetative and sperm cells during pollen formation (Chen *et al.*, 2009).

In addition to the role of RBR in the cell cycle, RBR has been shown to be involved genome silencing during seed development (discussed in section 1.2.6)(Jullien *et al.*, 2008).

E2F/Dimerisation Partner (DP)

RBR controls the activity of the E2F promoter-binding factor. In Arabidopsis, there are six genes coding for E2F proteins (E2Fa, E2Fb, E2Fc, E2Fd, E2Fe and E2Ff) and two for DP proteins (DPa and DPb) (Fig. 1.7). E2F/DP binds DNA in responsive promoters containing a canonical (TTTCCCGCC) sequence, which commonly lies upstream of genes involved in the regulation of the S-phase of the cell cycle (Albani *et al.*, 2000). The binding of E2F to DNA requires 2 motifs. E2Fa, E2Fb and E2Fc contain a single DNA-binding motif in their respective sequences whereas E2Fd (also named DP/E2F-like proteins 2 (DEL2), E2Fe/DEL1, E2Ff/DEL3 possess two binding motifs in their sequence (Dyson, 1998; Kosugi and Ohashi, 2002). Therefore, to regulate the promoter activity of a responsive gene, E2Fa, E2Fb and E2Fc require dimerization with DPa or DPb, which also contain a DNA-binding motif. E2Fa/b/c act as heterodimers and E2Fd-e-f act as monomers to regulate gene expression. RBR can interact only with E2fa/b/c. E2Fa and E2Fb are activators (De Veylder *et al.*, 2002; Rossignol *et al.*, 2002). In contrast, E2Fe/DEL1, E2Ff/DEL3 and E2Fc, the latter acting possibly with DPb, are transcriptional repressors (del Pozo *et al.*, 2002; Kosugi and Ohashi, 2002). When E2Fa/DPa are ectopically overexpressed, they induce cell divisions and endoreduplication in leaves and hypocotyls (De Veylder *et al.*, 2002; Rossignol *et al.*, 2002). Overexpression of E2Fe/DEL1 leads to reduced ploidy level in leaves or premature onset of endoreduplication suggesting that E2Fe/DEL1 is an inhibitor of endoreduplication (Vlieghe *et al.*, 2005). E2Ff/DEL3 is shown to be involved in down-regulating the expression of genes involved in cell wall biosynthesis such as *expansin*, therefore suppressing cell expansion of dividing cells (Ramirez-Parra *et al.*, 2004).

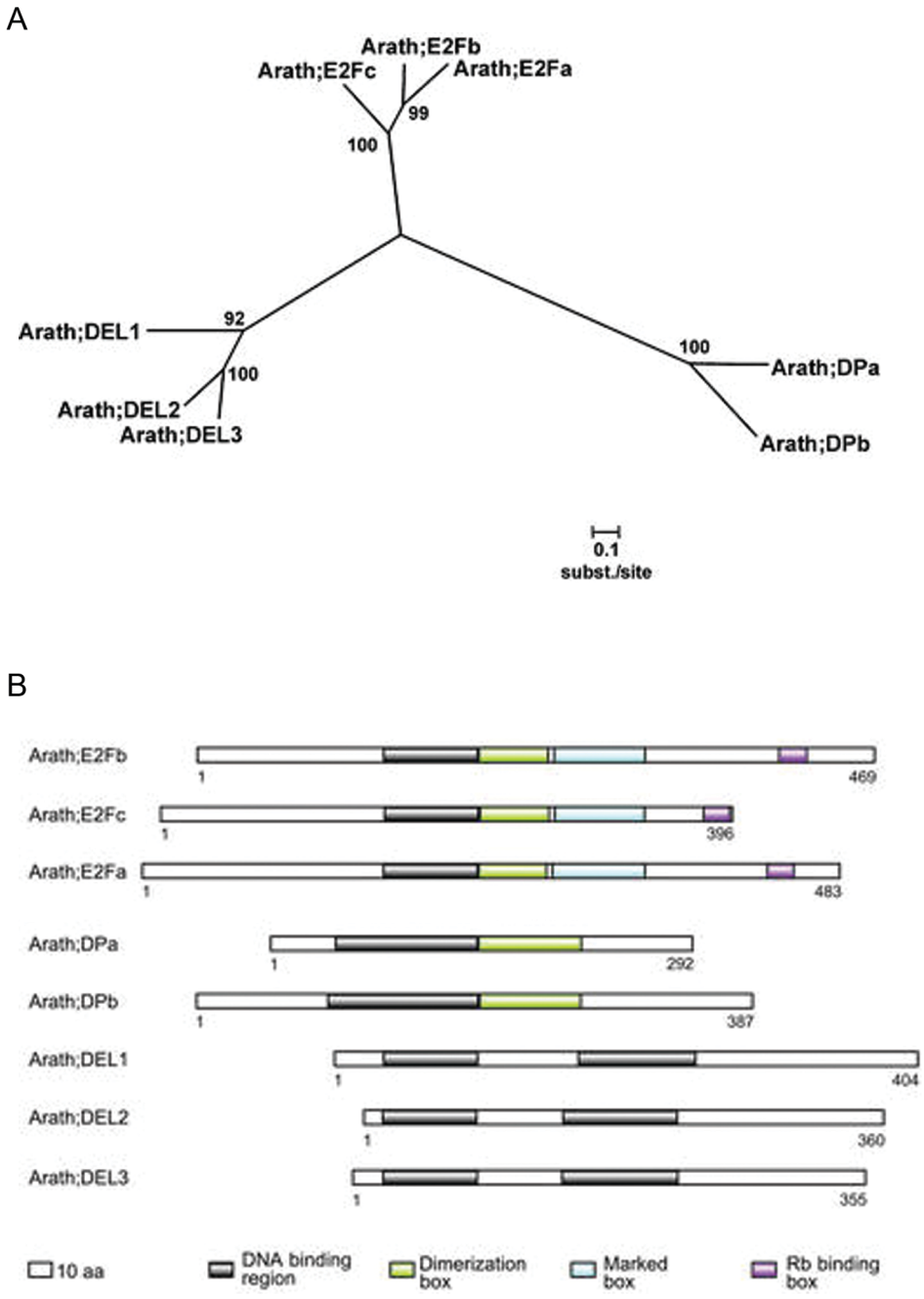

Figure 1.7. E2F and DP families in Arabidopsis: Phylogenetic Tree (A) and structural organization of E2F and DP proteins (Modified from Vandepoele *et al.,* 2002).

1.1.2. Cell cycle transitions and progression

The cell cycle progression depends on the protein level of the regulators mentioned above as well as their specific interactions.

The G1 to S-phase transition

The G1-to-S transition is a control point in the cell cycle. During G1, exogenous and endogenous cues are integrated by the cell to make the decision to commit, to exit or re-enter the cell cycle. Once the cell commits to the cell cycle, DNA replication is initiated (Gutierrez *et al.*, 2002). The regulation of the G1-S transition involves the D-type cyclins as major regulator (Oakenfull *et al.*, 2002). CYCD amino acid sequence contains the RBR binding motif LxCxE, with x any amino-acid (Menges *et al.*, 2007). Protein interaction studies show that CDKA;1 form a complex with several CYCDs such as CYCD3;1 (Wang *et al.*, 2004), CYCD2;1 (Sanz *et al.*, 2011), CYCD4;1 and CYCD4;2 (Van Leene *et al.*, 2010). CYCDs bind specifically to CDKA;1 but not CDKB1;1 (Healy *et al.*, 2001). The formation and the activity of the CDKA;1-CYCD complex depends on the factors mentioned above. As previously reviewed, the active CDKA;1/CYCD complex phosphorylates RBR (Boniotti and Gutierrez, 2001). In non-dividing cells, RBR binds to the E2F/DP complex and recruits histone deacetylases preventing the transcription of S-phase genes such as thymidine kinase and DNA polymerase (de Jager and Murray, 1999). The E2F/DP transcription factor bound to RBR is inactivated (Dyson, 1998). Deacytelation of histones maintains the positive charge conferred by lysine and arginine residues of the histone. Therefore the histones have great affinity for the negatively charged DNA, blocking the accessibility of the chromatin to transcription factors (Chen and Tian, 2007). Upon RBR phosphorylation, the inhibition of S-phase genes is removed. RBR dissociates from E2F/DP and can activate gene expression (Fig.1.8). Histones are more likely acetylated, reducing their affinity for DNA and allowing the transcription machinery to work. Therefore, transcription is active in genes whose products are needed for S-phase entry and progression. Thus the cell cycle progresses to the S phase.

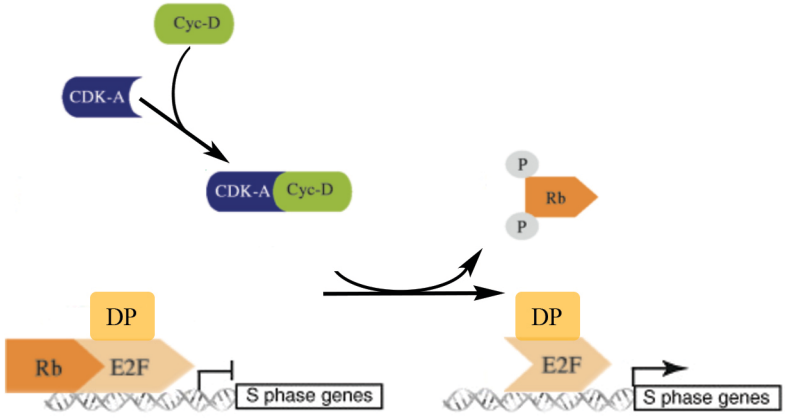

Figure 1.8. Model of G1-to-S transition control. CYCD3 in response to developmental cues, binds CDKA;1. The active CDKA;1/CYCD3 complex phosphorylates RBR releasing E2F/DP from its inhibitory binding. S phase genes are therefore expressed (Modified from Tromas *et al.,* 2010 and Andrietta *et al.,* 2001).

The G2 to M-phase transition

The control of the G2/M transition is responsible for entry into mitosis. At this checkpoint the cell commits to either divide or endoreduplicate. The control depends on CDK-CYC kinase activity. The typical mitotic CDK is CDKB as its expression level peaks at G2; however, CDKA;1 is also thought to be involved in the transition (Menges *et al.*, 2002). It has been shown that CDKA;1 is required for cell entry into mitosis (Nowack *et al.*, 2006). CYCB transcript level increases from S phase to G2 and interact with CDKA and CDKB. Moreover, CYCA can also interact with CDKA and CDKB to control the progression from G2-to-M as it has been shown that CDKB1;1 and CYCA2;3 form a complex at the G2-to-M transition and their activity inhibits the switch between mitosis and endocycle (Boudolf *et al.*, 2009). The negative regulation of CYC/CDK by WEE1 occurs during the G2-M transition (Sorrell *et al.*, 2002).

CDK/CYC complexes phosphorylate specific transcription factors that activate the expression of genes required for mitosis (Ito *et al.*, 1998; Ito *et al.*, 2001). In addition, CYC/CDK were shown to be associated with microtubules during mitosis (Criqui and Genschik, 2002). It was demonstrated that a CYC/CDK complex phosphorylates microtubule-associated proteins that are involved in the regulation and stabilization of microtubular structure assembly. CYC/CDK complexs may have an essential role for the formation of the preprophase band, mitotic spindle and phragmoplast (Criqui and Genschik, 2002).

Endoreduplication

Certain cells that have completed DNA replication do not go through mitosis in response to developmental cues. The cell cycle is shortened to alternating S-phase and G1 phase without DNA partitioning and cytokinesis (Edgar and Orr-Weaver, 2001). The switch to the endoreplication cycle lies in the down-regulation of M-phase-specific CDKs and CYCs such as CDKBs, CYCAs and CYCBs (Jacqmard *et al.*, 1999; Imai *et al.*, 2006). CDKB transcripts cannot be detected whereas CDKA;1 is still present but in much lower abundance. Interestingly, it has been shown that the down-regulation of CYCD3;1 promotes endocycles in leaves (Dewitte *et al.*, 2007). Down-regulation of the components of a CYC/CDK complex can be achieved by negative phosphorylation by WEE1 and/or by targeting the CDK/CYC for degradation via CCS52A-mediated proteolysis (Kondorosi and Kondorosi, 2004). ICK can act as a repressor or an activator of endocycles: high overexpression of ICK1 or ICK2 leads to endocycle and mitotic cycle repression (Verkest *et al.*, 2005b), whereas a weak overexpression results in premature onset of endocycles (Verkest *et al.*, 2005a; Weinl *et al.*, 2005).

Overexpression of E2Fa/DPa promotes endocycles correlated with RBR deficiency (De Veylder *et al.*, 2002; Wildwater *et al.*, 2005). On the other hand, overexpression of DEL1 (E2Fe) represses the endocycle (Vlieghe *et al.*, 2005). In maize endosperm, inactivation of RBR by hyperphosphorylation correlates with an increase of ploidy due to enhanced endoreduplication (Grafi *et al.*, 1996). Hence E2Fa and RBR appear to be involved in both mitotic and endocycle control.

1.1.3. D-type cyclins in plants

D-type cyclin gene in plants

There is a high degree of homology of cell cycle core components between plants and animals. D-type cyclins are conserved among higher eukaryotes. Despite the low sequence similarity of D-type cyclins between animals and plants (Wang *et al.*, 2004), they share key features required for their function during the cell cycle, especially during the G1-S transition. In the plant kingdom, 14 CYCDs are found in rice (*Oryza sativa*), 22 in poplar (*Populus trichocarpa*), 1 in moss, 10 in *Arabidopsis thaliana* (Fig. 1.9) (Menges *et al.*, 2005) and at least 17 were isolated from maize (Buendía-Monreal *et al.*, 2011). Their sequence organization has been widely reported for plants and the gene organization regarding exon length and distribution of exons and introns is conserved (Renaudin *et al.*, 1996; Vandepoele *et al.*, 2002; Menges *et al.*, 2007). The 10 Arabidopsis CYCDs are divided into 6 subgroups. The CYCD3 family has 3 members (CYCD3;1, CYCD3;2, and CYCD3;3), CYCD2-4 contains 3 members (CYCD2;1, CYCD4;1 and CYCD4;2), whereas the CYCD1,

CYCD5, CYCD6 and CYCD7 subgroups, each have a single member. CYCDs have an N-domain containing 120 amino acids highly conserved among plants. The C-terminal domain is more variable and can even be absent. Only the Arabidopsis CYCD5;1 does not have the C-domain, whereas 2 of the rice cyclins and 3 of the poplar cyclins do not possess the C-domain (Menges *et al.*, 2007). The absence of the C-domain suggests that it is not critical for its function but might give some specificity (Wang *et al.*, 2004). The N-domain spans fours regions essential for cyclin function: the CDK-binding region, the RBR binding region, the cyclin signature and five non-contiguous highly conserved residues (R, W, D, L and K, Table 1.2). The CDK-binding region, also named the "cyclin box" contains a highly conserved 8 amino-acid W(I/M)LKV motif. The cyclin box spans the first and second exons except for CYCD3 where it is localized in the first exon (Menges *et al.*, 2007). The RBR binding motif is characterized by the LxCxE sequence. CYCD5;1 has a modified LxCxE motif to FxCxE and CYCD4;2 and CYCD6;1 do not contain the motif in their sequence. The RBR interaction motif has been shown to be conserved in poplar and rice (Menges *et al.*, 2007). In human CYCD, the PEST sequence (proline, glutamine, serine and threonine rich) is involved in targeting the CYCD for ubiquitin-mediated proteolysis by phosphorylation of T-286. To date, potential PEST sequences were only identified in plants and they were found in Arabidopsis CYCDs with exceptions of the CYCD2/4 group, CYCD3;3; CYCD6;1 and CYCD7;1.

Table 1.2. Arabidopsis D-type cyclins and the conserved domains. nd not determined

Gene name	Accession number	CDK-binding motif	RBR-binding motif
CYCD1;1	At1g70210	ILK--VQAYY	LFCGE
CYCD2;1	At2g22490	ILKVCAHY	LACGE
CYCD3;1	At4g34160	ILRVNAHY	LYCEE
CYCD3;2	At5g67260	VLRVKSHY	LYCEE
CYCD3;3	At5g50070	IFKVKSHY	LFCEE
CYCD4;1	At5g65420	WIWKACEVH	LLCTE
CYCD4;2	At5g10440	WIWKACEEL	nd
CYCD5;1	At4g37360	ILTTRTRF	LYCEE
CYCD6;1	At4g03270	ITQYSRKF	nd
CYCD7;1	At5g02110	LIQTSRL	LLCDEE

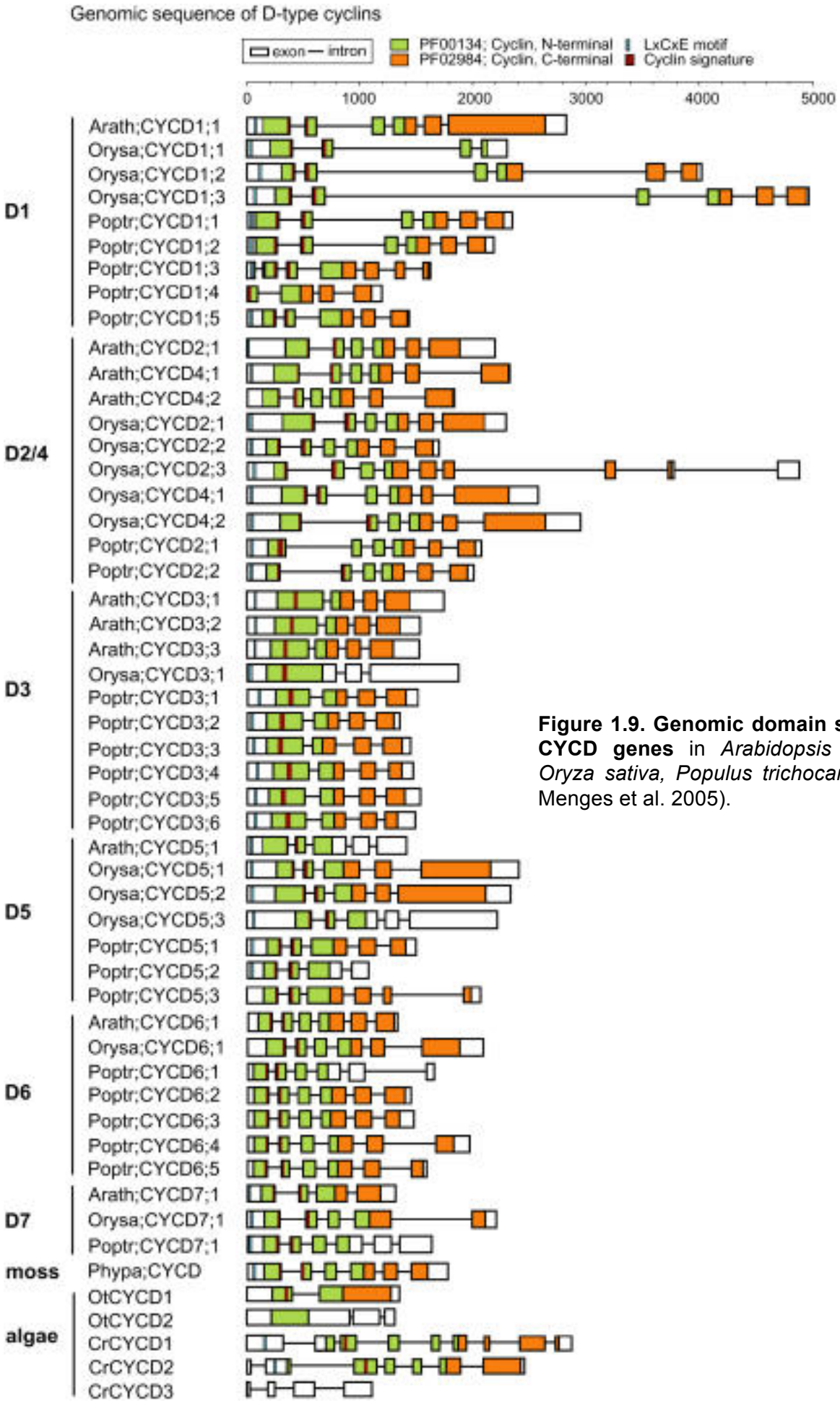

Figure 1.9. Genomic domain structure CYCD genes in *Arabidopsis thaliana*, *Oryza sativa, Populus trichocarpa* (from Menges et al. 2005).

D-type cyclin role in plant development

In Arabidopsis, ten genes encode for D-type cyclins. However, their differential roles in controlling the cell cycle are not well characterized. The study of *CYCD* gene activity during plant development demonstrated discrete and overlapping spatio-temporal expression patterns that may be associated with their different roles in controlling cell cycle progression (Dewitte and Murray, 2003).

The study of *CYCD* expression during the plant cell cycle provides insight into the differential roles in controlling the cell cycle. Cell suspensions were used in combination with Affymetrix GeneChip arrays. Conveniently, the cell cultures could be synchronized in cell cycle progression with sucrose induction and aphidicolin supplementation (Menges and Murray, 2002). This allows molecular analysis of the cell cycle and the control of its progression. It has been shown that the ten CYCDs are expressed during the cell cycle with some differences in their patterns (Menges *et al.*, 2002; Menges *et al.*, 2003; Menges *et al.*, 2005). *CYCD3;3* and *CYCD5;1* are expressed early in G1, whereas *CYCD3;1* and both of the *CYCD4* genes accumulate at the end of G1 prior to the G1-S transition. Whereas *CYCD3;1* transcript level is high throughout the cell cycle, *CYCD4*, *CYCD5.1* and *CYCD3;3* transcript levels decrease. *CYCD6;1* and *CYCD7;1* are also expressed during late G1. These data are consistent with the CYCDs being regulators of the G1/S transition during the cell cycle.

In the context of plant development the balance between cell mitotic cycle, endocycle and differentiation requires fine-tuning. The great diversity of plant D-type cyclins may suggest that the individual genes have exclusive or partially overlapping roles. However, such roles are yet to be fully elucidated. The expression of most of the CYCDs has been investigated during plant development using promoter reporters, fluorescent protein fusions and mRNA transcript detection techniques. *CYCD1;1* expression is detectable only in the embryonic root and especially in the lens-shaped cell that will be incorporated into the root meristem during embryo development (C. Forzani, unpublished data). *CYCD2;1* has been shown to be expressed in the shoot and the root (Cockcroft *et al.*, 2000). CYCD2;1 protein localized in the root apical meristem (RAM) apart from the quiescent center and the adjacent initials and their progeny of primary and lateral roots. In the elongation zone of the root closest to the RAM, *CYCD2;1* is still distinguishable in the endodermis (Sanz *et al.*, 2011). *CYCD3* genes are expressed in the SAM, in the inflorescence stem and the meristem throughout floral development. They are restricted to the gynoecium at later stages of floral development (Riou-Khamlichi *et al.*, 1999; Swaminathan *et al.*, 2000; Dewitte *et al.*, 2007).

CYCD3 expression is also detected in the RAM. *CYCD3;2* is expressed in stomata. *CYCD4;1* is expressed in the root meristem, the SAM, hypocotyl, as well as the vascular tissues (Kono *et al.*, 2003; Barroco *et al.*, 2005; Kono *et al.*, 2007). *CYCD6;1* is specifically expressed in the cortex-endodermis initials and their daughter cell from heart stage of embryo development to 5-day-old seedlings as well as in young developing leaves (Sozzani *et al.*, 2010). *CYCD7;1* is expressed in late meristemoids and guard mother cells during stomatal development and in sperm cells of pollen grain (Patell *et al.,* manuscript under revision). These expression patterns support the idea that *CYCD* gene activity is associated with tissues being able to divide.

To understand the roles of CYCDs in plant development, gain-of-function and loss-of-function mutants have been analyzed.

cycd1;1 and *cycd4;1* mutants delay the onset of cell division in the RAM during seed germination, leading to a delay of radicle emergence, suggesting that they are rate-limiting (Masubelele *et al.*, 2005). In addition, the generation of the *cycd4;1-cycd4;2* double mutant reveals that non-protruding cells of the hypocotyl that give rise to the stomata lineage were reduced. This indicates an essential role of CYCD4 is to control cell division in the initial step of stomata formation (Kono *et al.*, 2007). Constitutive overexpression of *CYCD1;1*, *CYCD2;1* and *CYCD3;1* causes an increase of the number of dividing cells. However, *CYCD1;1*, and *CYCD2;1* affect the cells in the radicle, leading to more rapid germination, whereas *CYCD3;1* overexpression induced ectopic cell division in the hypocotyl and does not induce a faster germination rate (Masubelele *et al.*, 2005). In *CYCD3;1* overexpresser seedlings, leaf development is impaired, likely due to hyperproliferation of leaf cells, a failure to differentiate leaf tissues and an inhibition of endocycles (Dewitte *et al.*, 2003). The loss of the three *CYCD3* class genes leads to the onset of endoreduplication in the petals and young leaves. In addition, in young *cycd3* leaves, the number of cells is reduced but not the average leaf area. In the SAM, cell number is also reduced. Impaired SAM development leads to defects in aerial organ formation. *cycd3* cannot generate callus without exogenous cytokinin and even with exogenous cytokinin no shoot could be formed. These results suggest that *CYCD3* genes may be involved in restraining endocycles in favor of mitotic cycle and are rate-limiting for cytokinin responses (Dewitte *et al.*, 2007). It appears that the loss of several *CYCD* genes gives stronger phenotypes than in single mutants.

In summary, during plant development, D-type cyclins regulate the cell cycle in order to coordinate cell proliferation and tissue differentiation.

1.2. Seed development in *Arabidopsis thaliana*

1.2.1. Fertilization and formation of seeds

In Spermatophytes, seeds are composed of three compartments: the embryo, the endosperm and the seed integuments or seed coat (Dumas, 2001). They arise from fertilized ovules. The ovule is composed of the embryo sac surrounded by the maternal sporophytic integuments (Fig. 1.10) (Shi and Yang, 2011). The embryo sac or female gametophyte contains seven cells: two synergids, one egg cell, one central cell and three antipodiales. These cells are haploid with the exception of the central cell, which contains two haploid nuclei. In flowering plants, reproduction is characterized by a double fertilization event: both the egg cell and the central cell are fertilized by one haploid sperm cell each (Faure *et al.*, 2002). This implies that the male gametophyte or pollen grain contains two haploid sperm cells (Hamamura *et al.*, 2012). A vegetative cell surrounds the two sperm cells. After its hydration, the pollen grain germinates developing a pollen tube. The vegetative cell supports the growth of the pollen tube along the septum in the ovary. It brings the two sessile sperm cells to the embryo sac (Higashiyama *et al.*, 1998). A key feature of fertilization is that the female and male gametes can only fuse in the same phase of the cell cycle (Berger *et al.*, 2006). Prior to fertilization, the sperm cell is in G2 (Nowack *et al.*, 2006) and it is assumed that the female gametes are also in G2 (Berger *et al.*, 2006). Upon fertilization, the ovule becomes a seed containing two zygotic tissues, the diploid embryo derived from the fertilization of the egg cell and the triploid endosperm arising from the fertilization of the central cell, and a sporophytic tissue, the seed integuments (Fig. 1.2B). Seed development requires a co-ordination of growth between the different seed comparments and it has been postulated that signals between endosperm and seed integuments may be essential for determination of seed size in Arabidopsis (Berger *et al.*, 2006).

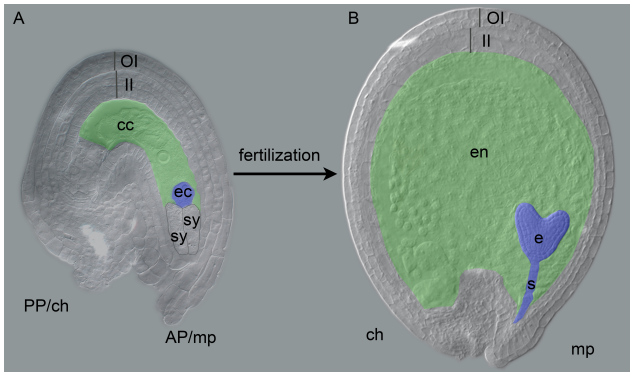

Figure 1.10. Ovule (A) becomes a seed (B) upon a double fertilization event of the female gametophyte. The two female gametes: the central cell (cc, in green) and the egg cell (eg, in blue) are both fertilized by one sperm cell giving rise to two genetically different zygotic tissues, the triploid endosperm (en; 2m/p) and a diploid zygote (m/p) that develops into an embryo (e) and a suspensor (s), respectively. The two synergids (sy) release peptides that serve as chemical guidance for pollen tube growth. A 2-cell layered outer integument (OI) and 3-cell layered inner integument (II) protect the female gametophyte and the zygotic tissues. The antero pole (AP) is at the micropyle (mp) and the postero pole (PP) at the chazalal pole (ch). Abbreviations: m, maternal genome; p, paternal genome.

1.2.2. Embryo development

Morphological development of the embryo

In Arabidopsis, embryogenesis is initiated by the fusion of the haploid sperm cell and the haploid egg cell. It gives rise to a diploid zygote. The development of the embryo is characterized by a well-defined order of cell division planes and cell fate specification, although this organization is not apparent in all species (Fig. 1.11, top panel) (West and Harada, 1993; Kaplan and Cooke, 1997; Capron *et al.*, 2009; Peris *et al.*, 2010)

Just after fertilization, the zygotic cell elongates and forms the “proembryo”. Then the proembryo divides asymmetrically and anticlinally to give rise to a small apical cell toward the endosperm and a larger basal cell at the micropylar region. The apical cell is referred to as the embryo proper. The basal cell undergoes several rounds of anticlinal divisions forming a file of cells. The top cell of the file is the hypophysis and the file itself is the suspensor. The suspensor anchors the embryo to the mother plant. It regulates nutrient exchange between the mother and the embryo. Most of the embryo body derives from the apical cell except for the embryonic root apex that comes from the hypophysis. The apical cell undergoes two longitudinal divisions, producing four cells, followed by transverse divisions giving rise to an octant stage embryo. An apico-basal axis can be distinguished with an upper and a lower tier, each consisting of four cells. The next division is periclinal and differentiates the outer layer, the protoderm precursor of the epidermis, and the inner cells, precursors of the ground and vascular tissues. At this stage the embryo contains 16 cells. The following globular stage is defined by anticlinal divisions in the protoderm, leading to the expansion of the protoderm around the ground and vascular tissue precursors, and longitudinal and transverse divisions of the inner cells. At this stage, the hypophysis divides asymmetrically and transversally, forming the lens-shaped cell and a lower cell. These two cells are incorporated into the embryonic root apex, establishing the quiescent center and the columella root cap respectively. The embryo progresses to the transition stage when the two lobes of the cotyledon start bulging and a bilateral symmetry appears. At the transition stage, ground tissues, epidermis, vascular tissues and root meristem are distinguishable and the shoot apical meristem is determined. The heart stage is characterized by the emergence of the cotelydons. Cotyledon expansion carries on until the torpedo stage then the bent-cotyledon stage (also called walking stick) until they reach their full length in mature embryos. From late heart stage onwards, the shoot meristem is discernible as well as the fundamental three layers of the shoot apex (L1-L2-L3). In Arabidopsis, embryo maturation is characterized by the accumulation of nutrient storage mainly in cotyledons. Finally the embryo metabolism slows down for the embryo to become dormant and sustain desiccation.

Figure 1.11. Seed development in Arabidopsis.

Arabidopsis seed begins development following a double fertilization event, giving rise to two zygotic tissues: the diploid embryo and the triploid endosperm. The top part represents the different stages of embryo development. The lower part represents the endosperm development. The pictures that are my own and the diagrams (modified from Berger (2003)) are not to scale.

Embryo development starts upon the fertilization of the haploid egg cell by a haploid sperm cell. It gives rise to a diploid cell called zygote. The first division of the zygote is transversal and leads to the formation of an apical cell towards the endosperm, giving rise to the embryo itself and, a basal cell toward the micropyle giving rise to the suspensor. Early developmental stages are named according to the number of cells constituting the embryo. At 16-Cell stage, also called dermatogen stage, the protoderm is specified and the hypophysis is visible. At the triangular stage, the hypophysis divides transversally and the upper cell forms the lens cell that will be incorporated in the embryonic root to form part of the root apical meristem (RAM) at the heart stage. The heart stage is characterized by the emerging cotyledons and the shoot apical meristem (SAM) is specified in the connecting region between the cotyledons. From fertilization to the torpedo stage, cell division is the prevailing process by which the embryo develops. From bent-cotyledon (BC, walking stick WS) stage onwards, embryo growth is supported by cell expansion rather than cell division.

Endosperm development starts with several rounds of synchronous syncytial mitosis from stage I to stage VI. From stage VII, division starts being asynchronous between the chalazal and micropylar pole resulting in morphologically distinct zones. From stage VIII, the endosperm starts its cellularization from the micropylar pole. Cellularization at the chalazal pole is delayed and is visible from stage X. After full cellularization, the endosperm is a source of nutrients to support the development of the embryo as it reaches the torpedo stage. In an Arabidopsis mature seed, the endosperm is limited to a single cell layer called aleurone.
The endosperm arises from the fertilization of the diploid central cell and a haploid sperm cell, therefore it is a triploid with a 2m/p genome balance. The change in maternal/paternal genome balance leads to a disruption of endosperm development, affecting the length of the syncytial and asyncytial phases. The bottom diagrams illustrate these changes.

Abbreviations: A, anterior pole; ap, apical cell; BC, bent-cotyledon stage; bp, basal cell; c, cotyleon; cp, chalazal pole; gt, ground tissue; h, hypohysis; hy, hypocotyl; lc, lens cell; mp; micropylar pole; P, posterior pole; pd; protoderm; pv, provasculature; QC, quiescent centre; ra; radicle; RAM root apical meristem; SAM, shoot apical meristem; su, suspensor; WC, walking-stick stage; z, zygote.

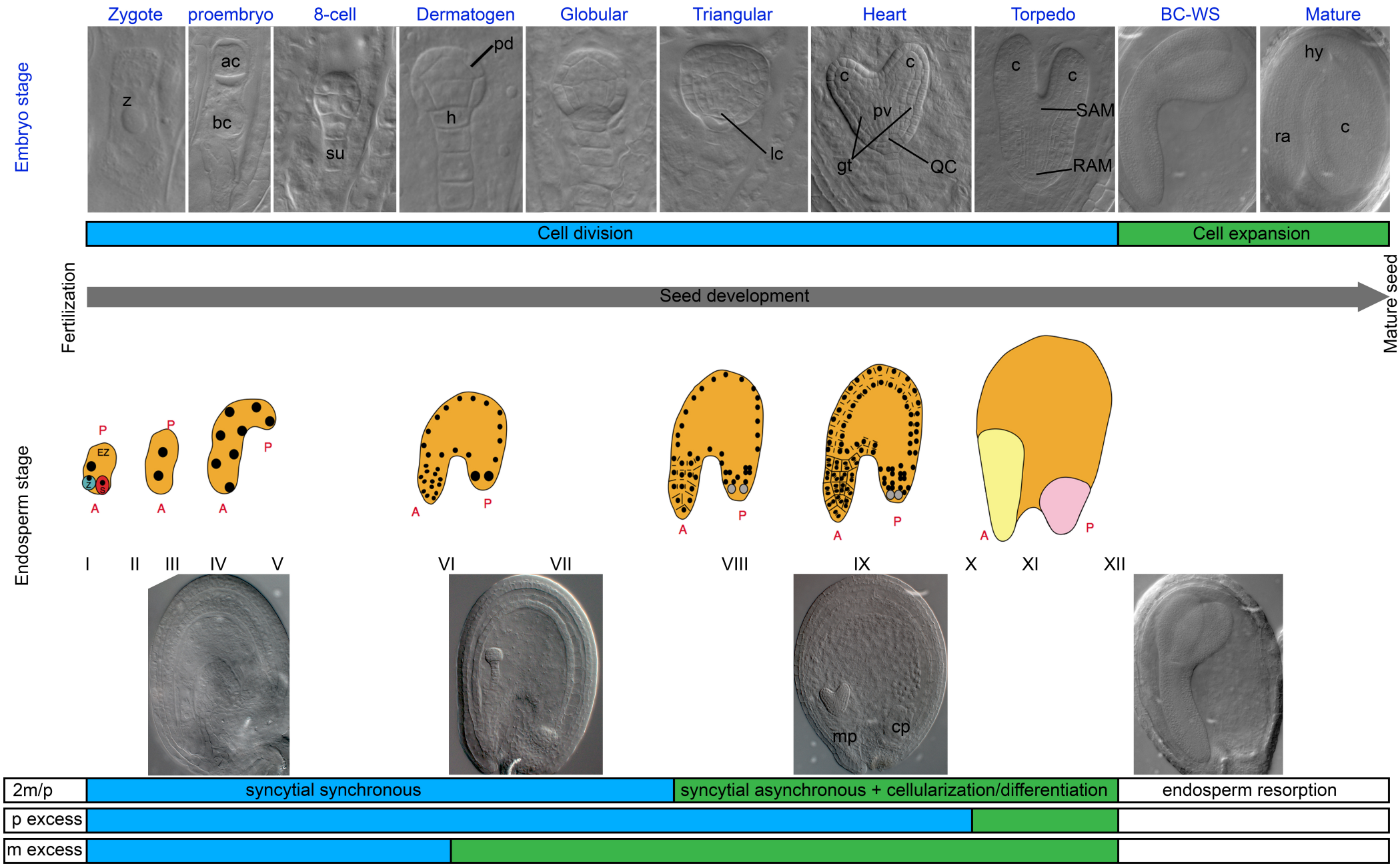
Embryo stage
Zygote
proembryo
8-cell
Dermatogen
Globular
Triangular
Heart
Torpedo
BC-WS
Mature
z
ac
bc
su
pd
h
lc
c
pv
gt
QC
SAM
RAM
hy
ra
Cell division
Cell expansion
Fertilization
Seed development
Mature seed
Endosperm stage
P
EZ
Z
S
A
I
II
III
IV
V
VI
VII
VIII
IX
X
XI
XII
mp
cp
2m/p
syncytial synchronous
syncytial asynchronous + cellularization/differentiation
endosperm resorption
p excess
m excess

Molecular genetics of embryo development

In Arabidopsis, embryo development is characterized by a strict control of cell proliferation and cell fate acquisition. This is essential to correctly pattern the plant body with the specific tissues in the appropriate domains. During embryo development, the determination of cell and tissue types is controlled by many different transcription factors. The coordinated development is the product of specific gene expression from the early embryonic events following fertilization (Table 1.3).

Prior to the first asymmetric division, the zygote elongates. This elongation depends on the expression of *GNOM* (*GN*). A defect in *GN* expression leads to a symmetric division and the development of a ball-shaped embryo. (Mayer *et al.*, 1993; Steinmann *et al.*, 1999; Wolters *et al.*, 2011). This elongation is coupled with the acquisition of a polarity of the zygote. The zygote polarity appears to be established by the differential expression of the *WUSCHEL-RELATED HOMEOBOX* (*WOX)* transcription factor. In the mature egg cell and in the central cell region nearest to the egg apparatus, *WOX2* and *WOX8* are expressed. This expression persists in the zygote. After the first division, the expression becomes differential along the apical-basal axis with *WOX8* and *WOX9* in the basal cell and *WOX2* in the apical cell (Haecker *et al.*, 2004; Breuninger *et al.*, 2008). A recent study shows that differential *WOX8* expression is directly activated by the transcription factor WRKY2 leading to a polar organelle localization that appears to be required for asymmetric division of the zygote (Ueda *et al.*, 2011). The embryo polarity and patterning depend on the directional transport of the plant hormone auxin and its signaling (Friml *et al.*, 2003). After the first zygotic division occurring in an auxin-independent manner (Ueda *et al.*, 2011), auxin is transported from the basal to the apical cell via the auxin efflux carrier *PIN-FORMED 7* (*PIN7*) (Friml *et al.*, 2003). Removing the directional auxin transport leads to longitudinal division correlated with a defect in specifying the apical cell. The transverse division is also observed in auxin deficient mutants such as *monopteros/auxin response factor5* (*mp/arf5*) from the two-cell stage onwards and *bodenlos/indole-3-acetic acid inducible12* (*bdl/iaa12*). *GN* has also been shown to the involved in maintaining the auxin gradient. *GN* encodes for a protein regulating the intracellular trafficking and is involved in the positioning of multiple auxin transport membrane proteins (Steinmann *et al.*, 1999). These results suggest that auxin is essential for early formation of the apical-basal axis of the embryo.

As the embryo progresses through the 16-cell/dermatogen stage, asymmetric periclinal divisions generate an outer cell layer with protoderm specification and inner cells giving rise to provasculature and ground tissue. At this stage, the radial axis begins to be established.

The asymmetric divisions are linked to the expression of *MP*, *BDL* and *WOX* genes that are expressed differentially after the transverse division. *MP* is excluded from the protoderm layer, and *WOX2* and *WOX9* are specifically expressed in the protoderm layer (Mansfield and Briarty, 1991; Haecker *et al.*, 2004; Breuninger *et al.*, 2008). In addition, the expression of the transcription factors *ARABIDOPSIS THALIANA MERISTEM LAYER 1* (*ATML1*) and *PROTODERMAL FACTOR2* (*PDF2*) is confined in the protodermal layer (Lu *et al.*, 1996; Abe *et al.*, 2003). The *atml1/pdf*2 mutant does not form a distinct epidermis layer (Abe *et al.*, 2003). The inner cells express *ARGONAUTE 10* (*AGO10*) shown to be involved in SAM maintenance (Lynn *et al.*, 1999). During progression of embryo development at the transition stage, the inner cells divide separating the inner vascular tissues from the outer ground tissues. The transcription factor *SHORT-ROOT* (*SHR*) is expressed in the provasculature (Helariutta *et al.*, 2000). *SHR* acts non-autonomously in the adjacent ground tissue to activate the expression of *SCARECROW* (*SCR*). *SCR* promotes ground tissue periclinal division and specification of the endodermal identity during and post-embryogenesis (Nakajima *et al.*, 2001; Sozzani *et al.*, 2010). Therefore SHR and SCR are involved in establishing the radial pattern of the embryonic and mature root. SHR also directly activates expression of a number of cell cycle genes, including CYCD6, to promote division of the cortical/endodermal initial cell post-embryonically (Sozzani *et al.*, 2010).

Establishment of the root system and its positioning occurs at the 8/16-cell stage. Specification of the root pole is seen as a consequence of developmental events taking place at the apical pole of the embryo (Weijers *et al.*, 2006). Auxin synthesized by the apical cells is accumulated in the hypophysis by a directional transport involving the efflux carrier PIN1 located at the basal membrane of each cell (Friml *et al.*, 2003; Friml *et al.*, 2004). *PIN1* expression is controlled by *MP* and *BDL* (Weijers *et al.*, 2006). Several genes, such as *TARGET OF MONOPTEROS 7* (*TMO7*), *SHR* and *PLETHORA* (*PLT*), have been shown to confer hypophysis specification (Nakajima *et al.*, 2001; Aida *et al.*, 2004; Schlereth *et al.*, 2010). Once the hypophysis is specified, a transverse asymmetric division produces an upper lens-shaped cell. At the heart stage, several divisions of the lens-shaped cell and its progeny give rise to three cell types : the quiescent center (QC), the columella cell and columella stem cell constituting the root cap.

During embryogenesis, shoot apical meristem (SAM) specification and cotyledon initiation occur in the apical domain of the embryo. SAM specification is marked by the expression of stem cell identity genes such as *WUSCHEL* (*WUS*), *SHOOT MERISTEMLESS* (*STM*) and *HOMEODOMAIN LEUCINE SIPPER III* (*HD-ZIPIII*) (Mayer *et al.*, 1998; Aida *et al.*, 1999; Emery *et al.*, 2003). The expression of these genes is activated early during

embryogenesis at the 16-cell stage. *WUS* expression is restricted to a few cells of the SAM during embryo development due to negative regulation by the *CLAVATA* genes (*CLV*) (Schoof *et al.*, 2000). The expression of *STM* in the central domain is promoted by the *CUP-SHAPED COTYLEDON* (*CUC*) genes. In a negative feedback loop, *STM* restricts the expression of *CUC*, creating a boundary between the SAM and the cotyledon primordia (Aida *et al.*, 1999). In the SAM, *STM* counteracts *ASYMETRIC LEAVES* genes (*AS*), preventing the formation of lateral organ primordia in the *STM* expression domain. In the adjacent regions of the SAM where *AS* genes are expressed, cotyledon primordia are initiated (Byrne *et al.*, 2000). Evidence shows that at the globular stage, the incipient cotyledon primordia represent a maximum of auxin response correlated with PIN1 localization mediating the flow toward these maxima (Benkova *et al.*, 2003). The study of *CUC* expression in *mp* and *pin1* mutant shows that these genes are required for proper *CUC* expression (Aida *et al.*, 2002). The link between auxin and *AS* for cotyledon primordia initiation has not been resolved.

Table 1.3. Genes mentioned involved in embryo development.

Abbreviation	Full Gene name
AGO	*ARGONAUTE*
ARF	*AUXIN RESPONSE FACTOR*
AS	*ASYMETRIC LEAVES*
ATLM	*ARABIDOPSIS THALIANA MERISTEM LAYER*
BD	*BODENLOS*
CLV	*CLAVATA*
CUC	*CUP-SHAPED COTYLEDON*
GN	*GNOM*
HD-ZIPIII	*HOMEODOMAIN LEUCINE SIPPER III*
IAA	*INDOLE-3-ACETIC ACID INDUCIBLE*
MP	*MONOPTEROS*
PDF	*PROTODERMAL FACTOR*
PIN	*PIN-FORMED*
PLT	*PLETHORA*
SCR	*SCARECROW*
SHR	*SHORT ROOT*
STM	*STEM MERISTEMLESS*
TMO	*TARGET OF MONOPTEROS*
WOX	*WUSCHEL-RELATED HOMEOBOX*
WUS	*WUSCHEL*

1.2.3. Endosperm development

Morphological development of the endosperm

In higher plant endosperm development is characterized by four biological processes: syncytial divisions, cellularization, differentiation and degeneration (Lopes and Larkins, 1993; Berger, 1999). These phases can occur in a discrete manner or can overlap with one another. However the length of these phases and the degree of division, cellularization, differentiation and degeneration vary in different plant species (Lopes and Larkins, 1993).

During syncytial divisions in Arabidopsis, mitoses take place without cytokinesis leading to the formation of the coenocytic endosperm. Cellularization is defined cell walls formation around the syncytial nuclei at the end of mitotic cycles. And so during this process, individual cells can be visualized (Boisnard-Lorig *et al.*, 2001). The cellularization of the endosperm overlaps with syncytial mitosis at the end of the syncytial phase and happens gradually throughout the endosperm. The differentiation of the endosperm into tissues carrying out different functions is concomitant with the cellularization of the endosperm. It has been postulated that the differentiation may originate from heterogeneous distribution of mRNA within the cœnocytic endosperm (Doan *et al.*, 1996). During these two processes, three endosperm compartments are morphologically and cytologically distinguishable. These compartments are patterned along the antero-posterior axis, consisting of the micropylar endosperm (MCE) with a dense cytoplasm surrounding the globular embryo, the chalazal endosperm (CZE) with few large nuclei, and the peripheral endosperm (PEN) in the region linking the CZE and the PEN (Scott *et al.*, 1998; Boisnard-Lorig *et al.*, 2001; Sorensen *et al.*, 2002). The polarity along the antero-posterior axis is present in the central cell even before fertilization. The anterior pole (AP) of the ovule is where the micropyle, the site of sperm cell entry, is located. The posterior pole (PP), at the side opposite the micropyle, is the chalaza where the vascular tissues supply the ovule with nutrients (Berger, 2003).

Finally, in Dicot plant, the endosperm is degraded by the embryo and persists a single layer called the aleurone layer (Berger, 1999). In Arabidopsis endosperm degeneration occurs after full cellularization of the endosperm whereas in peas, the endosperm is degraded after syncytial division and before cellularization. In Monocot plants, the endosperm is persistent in the mature seed (Lopes and Larkins, 1993). Degeneration of the endosperm is linked to seed germination. During germination, embryo revival and growth is supported by the use of nutrients stored in the endosperm, allowing the resumption of embryo metabolism (Berger, 1999). Despite a possible involvement of ethylene signaling in maize (Young *et al.*, 1997), little is known about the factors triggering degeneration or from where the signals originate.

Endosperm development of Arabidopsis has been described in detail by Boisnard-Lorig *et al.* (2001). It has been divided into 12 developmental stages (annotated I to XII) where the four phases mentioned previously overlap (Fig 1.11, bottom panel). Stage I is defined by fertilization of the endosperm by a haploid sperm cell. During stage I to IV, three rounds of synchronous syncytial divisions take place, giving rise to 8 free nuclei in the tube-like endosperm. At stage IV, one or two nuclei migrate to the chalazal pole and the endosperm appears like an enlarged tube. From stage V onwards, nuclear divisions start being asynchronous with nuclei dividing faster at the anterior pole. During the fourth nuclear mitosis at stage V, the nuclei appear to have a different size with larger nuclei containing larger nucleoli at the posterior pole than at the anterior pole. At stage VIII, the three domains MCE, PEN and CZE are recognizable. At stage IX, the eighth mitotic cycle is followed by cytokinesis around the nuclei of the MCE. The event characterizes the end of the syncytial phase and the beginning of the cellularization phase. From stage IX onwards, the formation of the cell wall progresses from the MCE to the PEN and CZE.

Molecular genetics of endosperm development

Endosperm development is triggered by fertilization and it has been shown to be dependent on the activity of *FERTILIZATION-INDEPENDENT SEED* (*FIS*) genes prior to fertilization (Table 1.4). FIS proteins are homologous to the animal Polycomb group (PcG) proteins that are chromatin-remodeling proteins (Grossniklaus *et al.*, 1998; Kohler *et al.*, 2003; Leroy *et al.*, 2007). Three FIS genes have been identified in Arabidopsis: *FIS1/MEDEA* (*MEA*) (Grossniklaus *et al.*, 1998), *FIS2* (Luo *et al.*, 1999), *FIS3/ FERTILIZATION-INDEPENDENT ENDOSPERM* (*FIE*)(Ohad *et al.*, 1996) and MULTICOPY SUPPRESSOR OF IRA 1 (MSI1) (Kohler *et al.*, 2003; Guitton *et al.*, 2004). The *FIS* genes are expressed in the embryo sac during the late stages of its maturation and in the embryo and endosperm post-fertilization (Luo *et al.*, 2000). MEA encodes for a protein containing a SET domain, which is known in histone lysine methyltransferases and required for their enzymatic activity (Grossniklaus *et al.*, 1998) (Thorstensen *et al.*, 2011). FIE and MSI1 proteins contain a WD40 domain known to function as a protein-protein or protein-DNA (Guitton *et al.*, 2004; Xu and Min, 2011). The FIS protein has a VEFS domain characterized by an acidic tryptophane/methionine-rich sequence (Chanvivattana *et al.*, 2004). The FIS proteins interact to form the Polycomb repressive complex 2 (PCR2) (Kohler *et al.*, 2003). *fis* mutants show automonous development of the embryo sac. In the absence of fertilization, *mea*, *fis2* and *fie/fis3* mutants display nuclear proliferation in the central cell (Ohad *et al.*, 1996; Grossniklaus *et al.*, 1998; Luo *et al.*, 1999). In addition to endosperm-autonomous development, *msi* mutants show additional divisions in the egg

cell (Guitton and Berger, 2005). These results suggest that, firstly, the FIS complex is required in the female gametophyte to control the arrest of the cell cycle prior to fertilization, and secondly that the control of the egg cell arrest may rely on a discrete mechanism from the one for the central cell (Berger *et al.*, 2006). *FIS2* and *MEA/FIS1* are imprinted and only the maternal allele is expressed during seed development, but *MSI1* and *FIE/FIS3* are not (Kinoshita *et al.*, 1999; Luo *et al.*, 2000; Jullien *et al.*, 2006). *FIS2* silencing in the sperm cell relies on the methylation of a CpG rich region of its promoter by the methyltransferase MET1 (Jullien *et al.*, 2006; Schmidt *et al.*, 2013) and the imprinting removal depends on DNA glycolsylase DEMETER (DME) activity (Gehring *et al.*, 2006). Similarly the *FLOWERING WAGENINGEN* (*FWA*) gene, whose function in seed development is still unknown, is expressed in the maternal gametophyte and is subject to the same silencing mechanism as *FIS2*, involving MET1 and DME (Kinoshita *et al.*, 2004). By contrast, *MEA* silencing relies on the presence of a methyl group on the lysine residue 27 of the HISTONE H3 (H3K27) (Jullien *et al.*, 2006). Similarly to FIS2, DME is responsible for relieving silencing of the maternal allele at the end of ovule development (Choi *et al.*, 2004).

PHERES1 (PHE1) and the SKP1-like protein MEIDOS have been showed to be direct targets of the FIS complex (Kohler *et al.*, 2003). The function of these two genes is still unknown but their expression is repressed upon FIS binding. In addition, *PHE1* has been shown to be imprinted and so only the paternal allele is expressed in the endosperm.

As previously stated, *FIS* genes appear to be involved in the control of cell cycle arrest in the female gametophyte prior to fertilization. Several data show that cell cycle regulators are involved in endosperm development. It has been shown that RBR is a direct target of MSI1 (Jullien *et al.*, 2008). The *rbr1-1* mutant also shows nuclear divisions in the central cell in the absence of fertilization, a phenotype similar to that seen in the *msi1* mutant as well as in the male gamete (Ingouff *et al.*, 2006; Chen *et al.*, 2009).

FIS genes and their targets are involved in endosperm development in late stages of gametophyte maturation onwards. *FIS2* is also involved in endosperm cellularization as *fis2* fails to cellularize and the embryo development arrests (Hehenberger *et al.*, 2012). Other genes are involved in controlling the endosperm development at later stages during the cellularization process. Mutants with impaired endosperm cellularization are *knolle* (*kn*), *keule* (*keu*), *hinkel* (*hin*), *open house* (*opn*), *runkel* (*ruk*), *späztle* (*spa*), *pleiade* (*ple*) and *endosperm defective 1* (*ede1*) (Sorensen *et al.*, 2002; Hehenberger *et al.*, 2012). These mutants display absence of cellularization in the syncytial endosperm visualized by multinucleate enlarged cells in the endosperm. In addition, they often display defects of

cytokinesis in the embryo. *PILZ* group genes include *TITAN1* (*TTN1*) and *TTN5*. *pilz* mutants do not cellularize due to a lack of organized microtubules (Mayer *et al.*, 1999). Other *ttn* mutants, *ttn7* and *ttn8* show giant nuclei and non-cellularized endosperm (Liu *et al.*, 2002).

All these genes encode for components involved in the basic machinery of cytokinesis and chromosome partitioning at the anaphase of mitosis. KNOLLE is a protein involved in vesicle docking and fusion at the cell plate (Lukowitz *et al.*, 1996). KEULE interacts with a protein involved in regulating vesicle trafficking (Sorensen *et al.*, 2002). HINKEL is a kinesin-like protein that functions in reorganizing the phragmoplast microtubules (Strompen *et al.*, 2002). PLEIADE is a microtubule-associated protein (Müller *et al.*, 2002). RUNKEL is a protein with a microtubule-binding domain (Krupnova *et al.*, 2009). *PILZ* encodes for proteins of the tubulin-folding complex (Steinborn *et al.*, 2002).

On the contrary, genes like *AGAMOUS-LIKE 62* (*AG62*), *HAIKU2* (*IKU2*) and *MINISEED3* (*MINI3*) are shown to repress cellularization. *ag62*, *iku2* and *mini3* endosperms show precocious cellularization (Garcia *et al.*, 2003; Luo *et al.*, 2005; Kang *et al.*, 2008). It has been demonstrated that in *WT,* the *AG62* level drops prior to cellularization suggesting that *AG62* may act as a suppressor of cellularization during the syncytial development (Kang *et al.*, 2008).

Control of the cell cycle plays important roles in the endosperm. Endosperm development depends on control of cell cycle arrest in the central cell before fertilization. Proliferation of nuclei during the syncytial stage involves multiple rounds of nuclear divisions. Then the cellularization stage of the endosperm relies on cytokinesis machinery components required for chromosome segregation and formation of the new cell wall.

Table 1.4. Genes mentioned involved in endosperm development.

Abbreviation	Full Gene name
AG62	*AGAMOUS-LIKE 62*
DME	*DEMETER*
EDE1	*ENDOSPERM DEFECTIVE1*
FIE	*FERTILIZATION INDEPENDENT ENDOSPERM*
FIS	*FERTILIZATION-INDEPENDENT SEED*
FWA	*FLOWERING WAGENINGEN*
HIN	*HINKEL*
IKU2	*HAIKU2*
KEU	*KEULE*
KN	*KNOLLE*
MEA	*MEDEA*
MINI3	*MINISEED3*
MSI1	*MULTICOPY SUPPRESSOR OF IRA1*
PHE1	*PHERES1*
PLE	*PLEIADE*
OPN	*OPEN HOUSE*
RUK	*RUNKEL*
SPA	*SPAZTLE*
TTN	*TITAN*

1.2.4. Seed coat

The seed coat or testa is a protective layer for zygotic tissues. It is typically a sporophytic tissue and derives from the diploid integuments surrounding the female gametophyte. In the mature ovule, there are two integuments, the outer integument composed of two cell layers and the inner integument that consists of one cell layer at the micropylar and gradually becomes a three cell layer at the chalazal end (Schneitz *et al.*, 1995; Enugutti *et al.*, 2013). In response to fertilization, the integument cells divide, elongate and finally differentiate into a seed coat (Windsor *et al.*, 2000). Seed coat differentiation is associated with the secretion of mucilage by the outer layer and accumulation of flavonoids such as proanthocyanidin throughout the seed coat. The mucilage is secreted between the cell wall and the plasma membrane of the outermost layer. The final stage of differentiation occurs when the inner layer of the outer integument is completely compressed. During imbibition of seed prior to germination, the mucilage layer is hydrated by passive entry of water into the cells. The pressure increases within the cell, causing the outer cell wall to break from the transverse walls, thus weakening the seed coat (Windsor *et al.*, 2000). Flavonoid accumulation gives the brown color to the seed coat. Fertilization is required for the proanthocyanidin deposit. Single fertilization of the egg cell is sufficient to induce flavonoid

production (Ungru *et al.*, 2008), since in an autonomous endosperm seed, flavonoid production is induced. However, the lack of pigment accumulation does not appear to impair the development of the embryo and the endosperm (Debeaujon *et al.*, 2003).

1.2.5. Cross-talk between seed compartments

Seed development requires control of the individual seed components but also coordination of growth between these components. Communication between the embryo, the endosperm and the integuments has been unraveled (Fig. 1.12). Signal and communication pathways have been partially identified.

The first piece of evidence showing signals from the embryo was illustrated by the work on *cdka;1*$^{+/-}$ mutants. Half of the *cdka;1*$^{+/-}$ pollen grain population carries a single sperm cell that can fertilize the egg cell leaving the diploid central cell unfertilized. Then, the embryo initiates its development. Concomitantly, nuclear proliferation in the central cell is visible and the acquisition of endosperm fate is demonstrated by the use of an endosperm-specific marker (Nowack *et al.*, 2006; Ungru *et al.*, 2008; Zhao *et al.*, 2012). Ultimately embryo development ceases at the transition stage, likely due to an under-developed endosperm carrying 32 nuclei. Identical results have been reported for *fbl17* mutants (Gusti *et al.*, 2009). These results suggest that a positive signal from the fertilized egg cell activates endosperm development during early seed development. However, when *cdka;1*$^{+/-}$ fertilizes a *fis*-class mutant (*mea*, *fie* and *fis2*), in which seed abortion is linked to the arrest of autonomous endosperm development, seeds complete embryogenesis with a maternal genome-derived endosperm. Cellularization and differentiation of the endosperm is restored and embryo development carries on (Nowack *et al.*, 2007). This result suggests the existence of a signal between the endosperm and the embryo at later stages of seed development, in addition to signals emitted just after fertilization.

Existence of signal emitted from zygotic tissues to the maternal integument is illustrated by the production of flavonoid by the maternal integument trigged by fertilization of the female gametophyte. Flavonoid production is the key event marking the transformation of the maternal integument into a seed coat. In the *cdka;1* mutant, Similarly, seed containing autonomous endosperm also produces flavonoids in the seed coat (Ingouff *et al.*, 2006). These results raise the question whether the signal triggering seed coat formation comes from the embryo or the endosperm, once its proliferation has been elicited.

Signals to the embryo, which originate from the endosperm, have been demonstrated by the specific ablation of the endosperm after its initiation (after two or three rounds of

nucleus divisions) using diphtheria toxin A. Following the removal of the endosperm, the embryo arrests and seeds abort (Weijers *et al.*, 2003). The *glauce* mutant also illustrates the existence of signals from the endosperm to the embryo. In *glauce*, two sperm cells are produced. The egg cell is fertilized and the embryo develops whereas the endosperm does not develop due to either a defect in fertilization of the central cell or a defect in division of the primary endosperm nucleus (Ngo *et al.*, 2007). *glauce* embryos stop their development at the late globular stage. Similarly the *capulet 2* mutant stops endosperm development after one to five divisions and the embryo arrests in the late globular stage (Grini *et al.*, 2002). This collection of mutants with a seed abortion phenotype reveals the existence of the signal(s) from the endosperm to the embryo that allow(s) coordination of seed component development. Interestingly, although such mutant phenotypes point to the existence of signals, their nature is unknown. It is also unclear to what extent they act to co-ordinate relative growth.

As mentioned above, it appears that the endosperm emits signals to the maternal integuments, which in response enter the seed coat differentiation process. The production of flavonoids in the integuments of an endosperm-autonomous seed is one piece of evidence (Ingouff *et al.*, 2006). *iku2* and *mini3* mutants produce decreased endosperm, embryo and integument size leading to smaller seeds. However, *IKU* and *MINI3* are specifically expressed in the endosperm shortly after fertilization (Garcia *et al.*, 2003; Luo *et al.*, 2005). Data show that *IKU2* and *MINI3* are in a common pathway. This result suggests that the loss-of-function in the endosperm impacts on cell elongation in the seed integument and embryo.

A

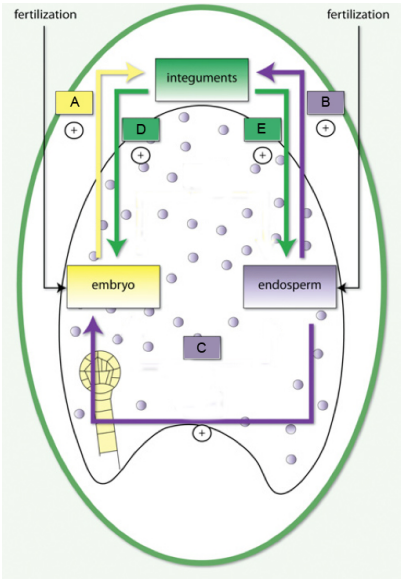

B

Signal	Known gene involved
A	n.d.
B	*IKU2, MINI3*
C	*FIS1/2/3, GLAUCE, CAPULET2*
D/E	*SIN1, AP2, GL2, TTG2*

Figure 1.12. Cross-talk between seed compartments. (A) Diagram of a seed and the communication existing between the different tissues. (B) List of genes reviewed in this section known to be involved in the cross-talk between seed compartment.

Reciprocally, maternal integuments engender signals to influence embryo and endosperm development. The existence of signals to the embryo can be illustrated by the studies of *short integument 1* (*sin1*), *glabra2, apetala 2* (*ap2*) and *megaintegumenta (mnt)/auxin-response factor 2 (arf2)* mutants. In *sin1*, the integument growth is disrupted. In *sin1*$^{+/-}$, embryos fail to specify/produce a SAM and only one cotyledon emerges (Robinson-Beers *et al.*, 1992; Ray *et al.*, 1996b). *AP2*, initially identified as a floral homeotic gene, has been shown to be involved in the production of seed coat epidermal structures. In *ap2*, integuments are longer with more elongated cells. Consequently, the endosperm and the embryo undergo an outgrowth (Jofuku *et al.*, 1994). *mnt/arf2* mutants exhibit cell overproliferation in the integuments. A larger endosperm is developed and the final seed size enhanced (Schruff *et al.*, 2006). With *ap2* and *mtn*/*arf2* examples, a question is raised regarding whether the embryo and endosperm phenotype is due to a signal produced by the integuments to trigger zygotic tissue growth or whether the outgrowth is a consequence of a mechanical constraint exerted by the seed integument that is released.

TRANSPARENT TESTA GLABRA2 (*TTG2*) is involved in integument differentiation and especially in flavonoid production (Johnson *et al.*, 2002). In *ttg2*, not only flavonoid deposits are affected but also the integument cell size and the endosperm is reduced and thus the overall seed size is reduced (Garcia *et al.*, 2005).

1.2.6. Seed Development, cell cycle and D-type cyclins

Interface between seed development and cell cycle

Seed development is characterized by cell proliferation and cell fate specification leading to the ultimate cell differentiation, often with an intermediate step of cell elongation (Mansfield *et al.*, 1991). As it has been demonstrated, *CDKA;1* is essential for seed development as the homozygous loss-of-function mutant is embryo lethal (Nowack *et al.*, 2006). The study of a dominant-negative *cdka;1* mutant reveals defects in embryo patterning such as distortion in the apical-basal pattern. Impaired embryo patterning leads to seed germination failure, leaf growth defects and incorrect phyllotaxy (Hemerly *et al.*, 2000). The study of tobacco *CYCA3;2* shows that in antisense expression lines, mature embryos do not display properly formed roots, cotyledons or hypocotyls due to a defect of cell proliferation (Yu *et al.*, 2003). Other cyclins have been shown to be expressed during seed development. *CYCA2;1* is expressed in developing embryos and endosperm, from zygote formation to the torpedo stage and from the syncytial to cellularized stages respectively (Burssens *et al.*, 2000). Studies show that *CYCB1;1* is expressed in the three mitotic domains of the syncytial endosperm (Boisnard-Lorig *et al.*, 2001) as well as throughout the embryo from the globular to the heart stage, in the cotyledons and the vascular tissues at the torpedo

and finally in only a few dividing cells of the cotyledons in a mature embryo (Collins *et al.*, 2012).

RBR, another cell cycle regulator, has been shown to have an essential role during female gametogenesis and seed development. *rbr1* shows overproliferation of nuclei in the central cell (Ebel *et al.*, 2004); however, the central cell does not acquire endosperm fate (Ingouff *et al.*, 2006). RBR has been shown to interact with MSI1 leading to a transcriptional repression of MET1. In turn, MET1 repression leads to a reduced of methylation level of DNA allowing gene expression which was previously repressed by MET1. As mentioned in section 1.2.3., the MET1 known targets in seed development are *FWA* gene and *PcG* genes such as *FIS2* and *MEA/FIS1* (Jullien *et al.*, 2008). Therefore these results suggest that RBR has a role in the FIS pathway to control proliferation in the female gametophyte.

Pieces of information now start coming together to understand how cell cycle regulation is involved in seed development and the developmental coordination of the seed components.

Seed development and D-type cyclins

Data describing D-type cyclin expression were not collected until recently: it has been shown that *CYCD4;1* is expressed in fertilized ovules and in embryos at heart and torpedo stages (De Veylder *et al.*, 1999) and *CYCD3;2* is expressed in developing ovules and early developing seeds (Swaminathan *et al.*, 2000). A recent study describes in detail the expression pattern of the 10 D-type cyclins during seed development and starts to unravel the role of CYCD during seed development (Collins *et al.*, 2012). The use of reporter genes shows that CYCDs have both discrete and overlapping expression profiles during seed development. For example *CYCD3;1* is expressed in early endosperm at the chalazal pole. It expression is detected in the embryo from globular to heart stage and is restricted to the cotyledons from the torpedo stage onwards. On the other hand, *CYCD7;1* does not appear to be expressed in the mature ovule or in the developing seed. *CYCD3* class genes are required for proper seed development as loss-of-function mutants display aborted seeds and a delay in embryo development. CYCD3 over-expressers show cell overproliferation leading to a delay in embryo development with abnormal and additional divisions. However, the *CYCD3* overexpressers do not show a defect in endosperm development although this might be linked to the RIBOSOMAL PROTEIN SUBUNIT 5A (RPS5A) promoter used, which is highly active in the embryo. This study is the first to give some insights into the role of D-type cyclins during seed development. However, information remains limited.

1.3. Seed size

1.3.1. Economical impact of seed size

The population of the Earth is expected to reach 9.6 billion by 2050 (UN News, 2013). The population increase implies an increase in demand for food production and the UN predicts that a 70% increase in global food production is required by 2030 (FAO, 2009). However, arable land has become less available and is likely to continue to do so. To cope with the requirement of food production increase, new varieties and/or genetically modified crops are potential solutions. These strategies cannot only increase crop yields but may also improve the nutritional quality. The majority of food consumed by humans is and/or derived from seeds, primarily maize, barley, wheat, soybean and rice. Other seeds are used to extract compounds (i.e. oil from *Brassica napus,* commonly named oilseed rape, and from sunflower, *Helianthus annus*). The drive to improve crop yield through creative engineering is reflected in the recent increase of reports concerning the biology and the genetic control of seed development. The sequencing of the genome of many crop species (wheat, oilseed rape, rice, soybean) will help in engineering crops (International Rice Genome Sequencing, 2005; Schmutz *et al.*, 2010; Brenchley *et al.*, 2012; Huang *et al.*, 2013).

1.3.2. Determination and regulation of seed size

The regulation of final seed size depends on gene expression in each seed compartment, the parent-of-origin effect as well as a trade-off between seed size and number.

The final seed size is affected by the maternal and zygotic tissues. As previously mentioned, *TTG2*, *AP2*, *MTN/ARF2* and the *cytochrome P450/KLUH (KLU*) are expressed in the maternal integuments (Jofuku *et al.*, 1994; Garcia *et al.*, 2005; Schruff *et al.*, 2006; Adamski *et al.*, 2009). *TTG2* and *KLU* promote cell expansion of the seed integuments whereas *AP2* and *ARF2* limit integument expansion (Garcia *et al.*, 2005; Jofuku *et al.*, 2005; Schruff *et al.*, 2006; Ohto *et al.*, 2009). *TTG2* and *AP2* control cell expansion and *KLU* and *ARF2* regulate cell proliferation. In addition, *AP2* has been shown to be involved in controlling the accumulation of proteins and oils during seed development (Jofuku *et al.*, 2005). *AP2* controls some the main features that plant breeders are interested in, however *ap2* mutants are not a good candidate as its mutation has pleiotropic effects (Jofuku *et al.*, 1994). In Arabidopsis, several factors expressed in the zygotic tissues influence seed size. *IKU*, *MINI3* and *SHORT HYPOCOTYLE* are expressed in the endosperm and promote endosperm growth (Garcia *et al.*, 2003; Luo *et al.*, 2005; Zhou *et al.*, 2009). The loss-of-function of each of these genes leads to the production of seeds with a reduced size suggesting that these genes are involved in controlling seed size. Other genes controlling the seed size are *DA1* and *ENHANCER OF DA1* (*EOD3*) genes encoding for a predicted

ubiquinin receptor and the cytochrome P450/CYP78A6, respectively (Li *et al.*, 2008; Fang *et al.*, 2012). *DA1* is expressed throughout the developing ovule and the torpedo embryo and loss-of-function of *da1-1* leads to enlarged seeds. Despite that *EOD3* could not be detected in any ovule or seed tissues, overexpression of *EOD3* produces enlarged seeds both due to cell expansion and cell proliferation in the maternal integuments. Despite the fact that *DA1* and *EOD3* do not act in the same regulatory pathway and are also independently of TTG2, their functions in a regulatory pathway have not been found.

Seed size also appears to be regulated by the plant hormone cytokinin. Plants overexpressing the *CYTOKININ OXIDASE/DEHYDROGENASE* (*CKX*) gene have a reduced level of cytokinin (Werner *et al.*, 2001). In *CKX* overexpresser plants, seeds produces were larger and contained an enlarged embryo constituted of more cells that were larger (Werner *et al.*, 2003). Similarly, mutants lacking cytokinin receptor (Arabidopsis thaliana sensor histidine kinase (*ahk*)) were shown to produce larger seeds and embryos (Riefler *et al.*, 2006). However in this study, it has not been resolved by which mechanism the enlargement occurs, whether cell elongation or cell number is affected and whether it is a maternal or zygotic effect (Riefler *et al.*, 2006). It is interesting to note that cytokinin can regulate cell cycle components. For example, it has been shown that *CYCD3;1* expression is induced by cytokinin treatment in cell suspension culture and that *cycd3* triple mutants are impaired in cytokinin responses suggesting that *CYCD3* genes link plant hormone levels and cell proliferation (Riou-Khamlichi *et al.*, 1999; Dewitte *et al.*, 2003).

The parental genome dosage is also involved in regulating the seed size and studies have shown that the maternal versus paternal expression of genes can influence seed size. In the study performed on several Arabidopsis ecotypes, interploidy crosses show that doubling the maternal genome (2n) with respect to paternal genome (1n) inhibits endosperm development and leads to smaller seeds, whereas the reciprocal crosses, with a doubled amount of paternal genome produce enlarged seed. If the parental genome number is triple the maternal genome number, the seeds abort (Scott *et al.*, 1998). Inter-ecotype crosses in Arabidopsis show that seed viability depends only on the male genotype independently of the fertilization success whereas the seed size is influenced by both the maternal and paternal genotypes (House *et al.*, 2010).

To increase crop yield, breeders have already considered increasing the relative parental genome abundance by creating amphidiploid, tetraploid or even hexaploid species. Therefore, to increase seed size, new solutions must be looked at. The recent study on D-type cyclin function in seed development may point to a new direction (Collins *et al.*, 2012). Overexpression of *CYCD3;1* and *CYCD7;1* using a promoter active in dividing tissues

(*RIBOSOMAL PROTEIN SUBUNIT 5A*, *RPS5A*) induces overproliferation of the suspensor, the embryo and the endosperm. However, there is a large proportion of aborted seeds correlated mainly with embryo defects. These data raise the idea that final seed size enlargement can be achieved by increasing the number of cells. The increase of cell number might be accomplished by modifying cell cycle regulation. This can be done by changing the spatio-temporal expression of its regulators. In addition, Collins carried out a preliminary experiment in which *CYCD3;1* and *CYCD7;1* were expressed using a two component system (GAL4/UAS) under the *FWA* promoter (Collins, 2008). The aim was to investigation the role of seed-targeted expression of a cyclin natively expressed in the seed (CYCD3;1) and one that is not natively expressed (CYCD7;1). These initial results suggest that *CYCD7;1* expression under the *FWA* promoter increased final seed size whereas no effect on final seed size could be observed when expressing the CYCD3;1 gene under the *FWA* promoter. Furthermore, considering that the project was in collaboration with Bayer CropScience, and the patent situation, it was interesting to pursue the investigation of endosperm-targeted *CYCD7;1* expression.

1.4. Project aims

With the worldwide increasing pressure to supply more food, the need to increase crop yield is urgent. In this work, I aimed to explore the potential for ectopic *CYCD* expression to engineer seed size. This idea was to attempt to increase the number of cells within the seed by expression of the limiting cell regulator *CYCD*. The chosen *CYCD* is *CYCD7;1,* as it is not natively expressed in the seed and hence might be less prone to other overriding regulation. Given the initial results of Collins, seed-targeted expression was chosen to be driven by the endosperm-specific promoter, *FWA*. The effects of ectopic *CYCD7;1* expression on final seed size and on seed development, as well as molecular mechanisms were to be investigated.

The system of choice is *Arabidopsis thaliana*, a model plant that has its genome sequenced and is very convenient to work with considering its short life cycle. Moreover, Arabidopsis belongs to the same family as commercially relevant species such as *Brassica napus* (oilrape seed), *Brassica oleracea* (wild cabbage) or *Brassica rapa* (wild turnip), which have a longer life cycle. Arabidopsis can be used for a low cost proof a concept. Then any useful technology can potentially be transferred to the other Brassicas.

Objectives:

1- Establish the phenotype of final seed size in lines expressing *CYCD7;1* in the endosperm during early stages of seed development using available lines with

the GAL4/UAS system, and to confirm the effect of ectopic expression with newly generated lines in which *CYCD7;1* is directly expressed under the *FWA* promoter.

2- Confirm the spatio-temporal window of *FWA* expression and follow the expression of CYCD7;1 protein using a fluorescent tag.

3- Carry out a detailed analysis of seed development with seed-targeted *CYCD7;1* expression, looking at mature female gametophyte, embryo and endosperm development, effects on the seed coat and the overall seed production by plants.

4- Understand the molecular mechanism by which CYCD7;1 may act for the seed size phenotype, by looking for cell cycle interactors of CYCD7;1 and investigating the seed phenotype in any relevant mutant backgrounds of these interactors.

Chapter 2

Materials and Methods

Chapter 2
Material and Methods

All chemicals and enzymes were purchased from Sigma-Aldrich Company Ltd., Promega-UK Ltd., New England Biolabs, Melford Laboratories Ltd, Roche Diagnostics Ltd., Life Technologies Corporation or Bioline Reagent Ltd., unless otherwise stated. All media and solutions were prepared using demineralized ultra-purity (UHP) distilled water and were sterilized by autoclaving at 115°C at 15 psi for 20 minutes or filter sterilized using a 0.2 µm filter. When concentrated buffers are listed the final concentration in the reaction was always 1X, unless otherwise stated. Unless otherwise stated, all procedures were performed at room temperature (RT).

2.1. General DNA techniques

2.1.1. Isolation of Arabidopsis genomic DNA

For cloning procedure

Genomic DNA used for cloning was extracted from plant tissue (leaf) with Nucleon Phytopure Genomic DNA Extraction Kits (GE Healthcare, UK) according to the manufacturer's instructions. Plant tissue was frozen using liquid nitrogen and ground finely. First 600 µl of Reagent I was added to the plant powder, mixed and then 200 µl of Reagent II was added. After mixing, the samples were incubated at 65°C with constant shaking for 10 minutes followed by a 20 minute incubation on ice. The DNA extraction was performed by adding 500 µl of ice-cold chloroform, then 100 µl of Nucleon PhytoPure DNA extraction resin suspension, shaking for 10 minutes at room temperature, centrifugation at 13,000 g for 10 minutes and finally by transferring the upper phase containing the DNA into a fresh tube. DNA was precipitated with an equal volume of ice-cold isopropanol and centrifuged for 5 minutes at 4,000 g. The DNA was washed with 70% ethanol and air-dried. The DNA was finally resuspended in 50 µl of TE (10 mM Tris-HCl and 1 mM EDTA, pH 8.0).

For genotyping

Genomic DNA extraction was performed with REDExtract-N-Amp^{TM} Plant PCR Kits (Sigma, USA) for genotyping. Fresh plant tissue was collected in a tube and 50 µl of Extraction Solution was added. After 10 minutes incubation at 95°C, 50 µl of Dilution Solution was added. After mixing, the extracted DNA was stored at 4°C.

2.1.2. Isolation of plasmid DNA

Plasmid extraction was performed with commercial kits, QIAprep Spin Miniprep Kit (QIAGEN GmbH, Germany) or with Wizard Plus SV Minipreps, DNA Purification system (Promega, USA). These two kits are based on the same principles. Plasmid isolation was carried out on 5 to 10 ml of overnight culture according to manufacturer's instructions. Cells were first pelleted and resuspended in the appropriate buffer. Cell lysis was performed by adding an alkaline buffer and, after 5 minutes incubation the lysis was stopped with a neutralization solution. The lysate was centrifuged for 10 minutes at maximum speed and the cleared supernatant containing the plasmid DNA was bound to a column. After several washes, the DNA was eluted with elution solution and stored at -20°C.

2.1.3. Determination of DNA concentration

DNA concentration was first estimated by comparing the intensity of the band of interest to the intensity of the different bands of the DNA fragment size-marker SmartLadder (Eurogentec, Belgium), that represents a precise amount if used according to the manufacturer's instructions.

DNA concentration was determined more precisely using a NanoDrop-1000 spectrophotometer (ThermoFisher Scientific, USA). This measures on one hand the concentration of DNA and on the other hand the purity of DNA samples by measuring the ratio of absorbance at 260 nm and at 280 nm. Ratios of 1.8 ± 0.1 are typical of pure DNA samples.

The results from these two methods can be compared.

2.1.4. Concentration of DNA

DNA was precipitated by adding 1/10 volume 3M sodium acetate (CH_3COONa), pH 5.2 and 2 volumes of ice-cold 100% ethanol. After mixing thoroughly, samples were incubated at -20°C for at least 1h30 and centrifuged at 14,000 rpm at 4°C for 20 minutes. The DNA pellet was washed twice with ice-cold 70% ethanol and centrifuged for 5 minutes, 14,000 g at 4°C. The pellet was resuspended in an appropriate volume of water and stored at -20°C.

2.1.5. Restriction endonuclease digestion of DNA

DNA samples were digested with restriction endonucleases purchased from New England Biolabs (UK) or Promega (UK). Typically 0.5 to 1 µg of DNA was incubated with 5-10 units of restriction enzymes, 10X of appropriate buffer and 100X BSA (bovine serum albumine, for NEB enzymes requiring BSA) in a 20 µl volume reaction. Depending on enzyme characteristics, reactions were incubated at 25°C or 37°C for at least 1 hour 30 minutes.

When necessary, enzymes were inactivated at 65°C for 15 minutes. The digestion was analyzed by agarose gel electrophoresis.

2.1.6. Agarose gel electrophoresis

1% agarose gels were prepared by dissolving agarose (for routine use, Sigma, life Science) in 1X TAE buffer (40 mM TrisAcetate, pH 8.0 and 2 mM Na_2EDTA, AlphaLaboratories, Hampshire, UK).

SafeView Nucleic Acid Stain (NBS Biologicals, UK) was added to the molten agarose in the amount advised by the manufacturer in order to stain the DNA.

Gel loading buffer (6X bromophenol blue: 0.25% in 30% sterile glycerol) was added to DNA samples to visualize the sample prior to sample-loading into the wells, and during electrophoresis.

DNA fragment size-marker SmartLadder was run alongside the DNA samples to estimate DNA fragment size and concentration in the sample.

DNA was electrophoresed at a constant voltage of 80V using BioRad Power Pack 300.

Bands were visualized using an UV transilluminator U:genius (Syngene) connected to an integrated camera to acquire gel images.

2.1.7. Recovery of DNA from agarose gel and PCR clean-up

DNA was recovered using the NucleoSpin® Extract II PCR clean-up gel extraction protocol (Macherey and Nagel, Germany). For gel recovery, the DNA fragment of interest was cut out of the gel. For each 100 mg of gel or 100 µl of digestion solution, 200 µl of binding buffer was added and heated together at 50°C until the gel was completely dissolved (10 minutes maximum). The DNA-gel solution was run through a column. DNA was retained and washed with the appropriate buffer. Finally, DNA was eluted with the elution buffer.

2.1.8. Subcloning of DNA

5’ ends dephosphorylation

To prevent recircularisation and religation of digested plasmid DNA after blunt end restriction digestion reactions, 5’-ends were dephosphorylated using a shrimp alkaline phosphatase (SAP, Promega). 10 units SAP/µg of vector were used. Typically 2 µl of SAP were directly added to a 40 µl restriction-digestion reaction and incubated at 37°C for the time of the digestion reaction. SAP was inactivated by heating to 60°C for 15 minutes.

Blunting reaction

Blunting reactions were performed by removing 3' overhang or by filling-in 5' overhang, using T4 DNA polymerase (New England Biolabs, UK). Restriction digested DNA fragments were blunted by adding dNTPs to a final concentration of 100 µM, 1 unit T4 DNA polymerase per microgram DNA and any 10X NEBuffer. The reaction was incubated for 15 minutes at 12°C and stopped by adding EDTA to a final concentration of 10 mM and heating to 75°C for 20 minutes. The chelating agent EDTA was removed from the solution using a PCR clean-up protocol as mentioned above.

Ligation reaction

Purified restriction digested DNA fragments were ligated using T4 DNA ligase (New England Biolabs, UK). Ligations were performed in a final volume of 10-15 µl. Typically a ratio 3:1, DNA fragment:vector was used with 10X DNA ligase buffer and 1 µl of T4 DNA ligase (1-2 Units). Reactions were incubated at room temperature, approximately 20-24°C for at least 1 hour for cohesive ends and 2 hours for blunt ends. The plasmid mixture was used immediately to transform *E. coli*.

TOPO® cloning (Invitrogen™)

Invitrogen™ developed a cloning method using topoisomerase I. The enzyme cleaves a phosphodiester bond of a double stranded DNA vector releasing the energy that is, in turn, used to synthesize a new phosphodiester bond between the opened vector and the PCR product. There are several vectors available: pCR®-Blunt-II-TOPO® used with blunt pCR product, pCR®2.1-TOPO™ and pCR®II-TOPO® used with 3'A-overhang PCR product and, pENTR™/D-TOPO® that requires a forward primer designed with an 5' CACC overhang prior to the sequence of interest. TOPO™ reactions were performed according to manufacturer's instructions: 0.5-1 µl of TOPO™ vector containing the topoisomerase, 1 µl of salt solution and 0.5 to 4 µl of fresh PCR product were mixed in a 6-µl volume reaction. PCR clean-up was always performed prior to the reaction. The reactions were incubated for 1 hour at RT and 1 to 6 µl were used to transform chemically competent *E. coli* bacteria (see section 2.4).

LR reaction for GATEWAY® cloning

Gateway® cloning, developed by Invitrogen™, allows the assembly of multiple DNA segments by recombination between specific sites (*att* borders) using a mixture of recombinase enzymes, called LR clonase.

LR reactions were performed according to manufacturer's instructions. LR reactions were performed with 10 fmoles each of *att*L/*att*R entry clones (formula to calculate femtomoles

from ng of DNA is provided in the instruction), 20 fmoles the plant binary vector (called pDEST™)(0.4 µl) and dH_2O up to an 8 µl final volume. To enhance the success of LR reaction, entry clones with *att*L or *att*R sites were linearized by digestion with a restriction enzyme cutting the vector outside the *att* sites once. The digestion was subsequently desalted from the enzyme buffer using the PCR clean-up method (section 2.1.7.).

2.2. Polymerase Chain Reaction (PCR)

Amplification of DNA from Arabidopsis plants, bacterial cells or purified DNA was performed using the Polymerase Chain Reaction, PCR. Depending on the aim of the PCR, three different enzymes were used.

Primers used were synthesized by Eurofins, MWG operon (Ebersberg, Germany) or Sigma-Aldrich. Generally primers were designed using PCR Primer Design Tool (Eurofins) or AmplifX software (Jullien, 2004). Parameters used were 15-30 base pairs (bp), a melting temperature of 55-65°C, a G+C content between 40-55% and a low sequence complementarity at their termini to avoid primer-dimers and hair-pin loop formation. The primer sequences are reported in Table 2.1.

The samples were placed into a thermal cycler (Mastercycler pro, Eppendorf AG, Hamburg) and parameters were adjusted to enzyme features.

All resultant PCR products were analyzed by gel electrophoresis.

2.2.1. Phusion High-Fidelity DNA polymerase, Finnzymes: cloning purposes

Cloning requires a high accuracy in synthesis, therefore amplification of promoter and full-length coding sequences was carried out with Phusion High-Fidelity DNA polymerase (New England Biolabs). Typical PCR reactions were performed in a 50 µl volume consisting of 5X Phusion HF buffer, 200 µM of each dNTP (Invitrogen), 0.5 µm of each forward and reverse primer, 1 unit DNA polymerase and 1 µl DNA template, made up to 50 µl with milliQ ultrapure water.

A typical PCR cycle was an initial template denaturation at 98°C for 30 seconds, followed by 30 cycles of denaturation at 98°C for 10 seconds, annealing at or below the primer melting point for 30 seconds and extension at 72°C for 30 seconds/1kb template length and a final extension at 72°C for 5-10 minutes followed by cooling to 4°C.

2.2.2. Taq polymerase: bacterial recombinant plasmid DNA screen

PCR reactions were performed to detect *Agrobacterium tumefaciens* and *E. coli* transformed with recombinant plasmids. They were carried out with GoTaq® (Promega, UK) or with Taq PCR Master Mix (Qiagen) in a 10 µl volume.

GoTaq® PCR reactions were performed with 5X green GoTaq® flexi buffer, 25 mM $MgCl_2$ to a final concentration of 2.0 mM, 0.2 mM dNTPs, 0.5 µM of each primer, 5 units/µl GoTaq® DNA polymerase and one colony as DNA template was directly transfer to the PCR mix.

2X Taq PCR Master Mix from Qiagen (1.5 mM $MgCl_2$, 200 µM each dNTP, 5 units/µl Taq DNA polymerase) was mixed with 0.5 µl of each primer, and the same amount of DNA template.

A typical PCR cycle was an initial template denaturation at 94°C for 10 minutes, followed by 30 cycles of 94°C denaturation for 30 seconds, annealing temperature at the primer melting point for 30 seconds and 72°C extension for 1 minute / 1 kb template length and a final extension at 72°C for 5 minutes and gradual cooling to 4°C.

2.2.3. RedExtract-N-Amp Plant PCR (Sigma-Aldrich): genotyping

RedExtract-N-Amp Plant PCR (Kit, Sigma-Aldrich) was performed for genotyping. A typical reaction was performed in 10 µl volume using 2X REDExtract-N-Amp PCR ReadyMix complemented with 2 µl of the prepared DNA extract (stored at 4°C, see section 2.1.1) and 0.4 µM of each primer.

A typical PCR cycle was an initial template denaturation at 94°C for 3 minutes, followed by 30 cycles of 94°C denaturation for 30 seconds, annealing at the primer melting point for 30 seconds and 72°C extension for 1 minute / 1 kb template length and a final extension at 72°C for 5 minutes followed by a gradual cooling to 4°C

Table 2.1. Primers used in PCR and RT-PCR, and their associated sequences.

Primer name	DNA sequence (5'→3')	Number
CYCD7-F-BamHI	ggatccATGGATAATCTACTCTG	1
CYCD7-R-SacI	acgagctcCTAAATGTAATTTGACATTTCAATTG	2
pFWA-F-HindIII	caagcttGGTAGGCTAATAATCAGAAGCCCT	3
pFWA-R-BamHI	acggatccTTTCCCTCAATGCAATAACCTGGACA	4
pFWA-F-SacII	gacccgcggTAGGCTAATAATCAGAAGCCCT	5
FWA-R-Ex2-AscI	agcggcgcgccCTTCTCGAGATTTCTTTTATTCTGGAACCA	6

Table 2.1. Primers used in PCR and RT-PCR, and their associated sequences (continued).

Primer name	DNA sequence (5'→3')	Number
M13-F (Uni -21)	TGTAAAACGACGGCCAGT	7
M13-R (-29)	CAGGAAACAGCTATGACC	8
ACT2-F	GAAGAACTATGAATTACCCGATGGGC	9
ACT2-R	CCCGGGTTAGAAACATTTTCTGTGAACG	10
rt-FWA-5UTR-F2	GGTCGAAGTGCTATTTGGTTGTTTAAGG	11
rt-CYCD7-Rv5'-2	CGGTTAACTTCTTTGAGACGA	12
KRP1-F	ATGGTGAGAAAATATAGAAAAGCTAAAGG	13
KRP1-R	TCACTCTAACTTTACCCATTGG	14
KRP1-rt-Fw_{340}	GAATTTGAATCGGCGGTTAA	15
KRP2-rt-F_{10}	CGGTTAGGAGAAGAGAACGAG	16
KRP2-rt-R_{600}	CGTATCTTCCTCCACCAAGTG	17
BAR-F	CGGTCTGCACCATCGTC	18
BAR-R	TGCCAGAAACCCACGTC	19
LB1a	TGGTTCACGTAGTGGGCCATCG	20
FWA-F	ACAGAGGTACGAGCTTGGAC	21
UAS-F	GCTGCAGCAAGACCCTTCCT	22
GAL4-R2	GCGTCTTTGTTCACGTTGTC	23
EGFP1	AGTCGTGCTGCTTCATGTGGTCG	24

2.3. Sequence analysis

PCR products were sequenced using an external service on an ABI3730XL sequencing analyzer (Eurofins, MWG, London, UK) or Illumina Genome Analyzer (GeneService, Cambridge, UK). Sample preparation was performed according to the manufacturer's instruction. Computer based sequence analysis was performed using Sequencher 4.0 software (Gene Codes corporation, USA) MACVECTOR 12.7.1 (MacVector, Inc, USA) or BLAST online tool (NCBI).

2.4. General *Escherichia coli* techniques

2.4.1. *E. coli* strains and growth conditions

All routine recombinant DNA procedures were performed using *E. coli* OneShot TOP10 (Invitrogen) or DG1 (Eurogentec, Delphi genetics) chemically competent cells. These strains are sensitive to ampicillin, kanamycin, spectinomycin. These antibiotics can be used for selecting transformed colonies and the *LacZ* test for white/blue screen of recombinant clones can be performed.

E. coli strains were cultivated at 37°C in Luria-Bertani (LB) medium (bacto-tryptone 100g/L, yeast extract 5g/L, NaCl 10g/L, pH7). Liquid cultures were incubated with gentle shaking at 200 rpm. Solid medium was obtained by adding Bacto-agar (15 g/L) and incubated in a static incubator.

2.4.2. Transformations of *E. coli* strains

Chemically competent cells were transformed using the heat-stock method (Sambrook and Russell, 2001). A 50 µl aliquot of chemically competent cells was allowed to thaw on ice before adding 1-5 µl of circular plasmid DNA and incubating on ice for 30 minutes. Cells underwent a 42°C heat-shock for 30 seconds and were then incubated on ice for 2 minutes. To recover, 250 µl of LB was added and cells were incubated for 1 hour at 37°C with gentle shaking. 100-250 µl of cells were spread on LB-agar plates with appropriate antibiotics and were incubated overnight at 37°C.

2.4.3. Selection of transformants

Transformed cells were selected by incorporating appropriate antibiotics into the medium (Table 2.2.). Only cells containing the plasmid DNA of interest carrying an antibiotic resistance gene are able to grow on such medium. The *LacZ* test was employed to screen for white recombinant colonies by spreading 0.8 mg/ml of X-Gal (dissolved in dimethylformamide, DMF) on top of the agar prior to the 37°C, 24-hour incubation with cells.

Clones identified as recombinant were analyzed by PCR to confirm that they were carrying the plasmid DNA of interest. Restriction digestion was carried out to ensure the presence of the DNA of interest and discriminate PCR false positives. Ultimately the plasmid DNA was checked by sequencing (see 2.3).

Table 2.2. List of plasmids used and the resistance associated for selection in bacteria and plants. NA: Not Applicable (when the vector does not carry T-DNA borders required for insertion into the plant genome)

Plasmid Name	Resistance (Bacteria; Plant) µg/ml
pCR®-Blunt-II-TOPO®	25 µg/ml Zeocin or 50 µg/ml Kanamycin; NA
pCR®2.1-TOPO™	50 µg/ml Ampicillin or 50 µg/ml Kanamycin; NA
pCR®II-TOPO®	50 µg/ml Ampicillin or 50 µg/ml Kanamycin; NA
pENTR™/D-TOPO®	50 µg/ml Kanamycin; NA
pGPTV-Bar	50 µg/ml Kanamycin; 15 µg/ml phosphinothricin PPT
pBluescript SK$^-$ II	50 µg/ml Ampicillin; NA
pH7m34GW	100µg/ml Spectinomycin; 25 µg/ml Hygromycin
pDONR R2/L3 (venus)	50 µg/ml Kanamycin; NA
pDONR L4/R1	50 µg/ml Kanamycin; NA
pENTR/D L1 L2	50 µg/ml Kanamycin; NA
pGreenI 0029	50 µg/ml Kanamycin; 50 µg/ml Kanamycin

2.5. Construction of binary vector for endosperm-targeted *CYCD7;1* expression

To achieve specific seed-targeted expression, *CYCD7;1* expression was placed under the control of the *FLORAL WAGENINGEN* (*FWA*) promoter. The different cloning steps are summarized in figure 2.1 and 2.2. First the 1026 bp coding sequence of *CYCD7;1* was amplified by PCR using high-fidelity DNA polymerase. *BamH*I and *Sac*I restriction sites were added at the 5' and 3' ends respectively. The primers used were CYCD7-F-BamHI and CYCD7-R-SacI. *CYCD7;1* amplicons were inserted in pCR®-Blunt-II-TOPO® according to procedure described in section 2.1.8 to give pCR®-Blunt-II-TOPO®_CYCD7;1 (Fig. 2.1A). *CYCD7;1* was transferred into pBluescript SK$^-$ II using *BamH*I and *Sac*I, allowing, in the next step, the insertion of the promoter fragment at the 5' end (pBSC_CYCD7;1, Fig. 2.1B). The *FWA* promoter was amplified by PCR using high-fidelity DNA polymerase and the primers pFWA-F-HindIII and pFWA-R-BamHI (3272 bp), thereby adding *Hind*III and *BamH*I sites at the 5' and 3' ends respectively. The *FWA* promoter was inserted into pCR®2.1-TOPO™ by a TOPO reaction (pCR®2.1-TOPO™_pFWA, Fig. 2.1C). The *FWA* promoter was introduced 5' of the *CYCD7;1* in pBluescript SK$^-$ II using *Hind*III *and BamH*I (pBSC_ pFWA:CYCD7;1, Fig. 2.1D). The cassette p*FWA:CYCD7;1* was

cut out of pBluescript SK- II with *Hind*III and *Sac*I and inserted in the plant binary vector pGPTV-bar to yield pGPTV-bar_ pFWA:CYCD7;1 (Fig. 2.1E) (Becker *et al.*, 1992).

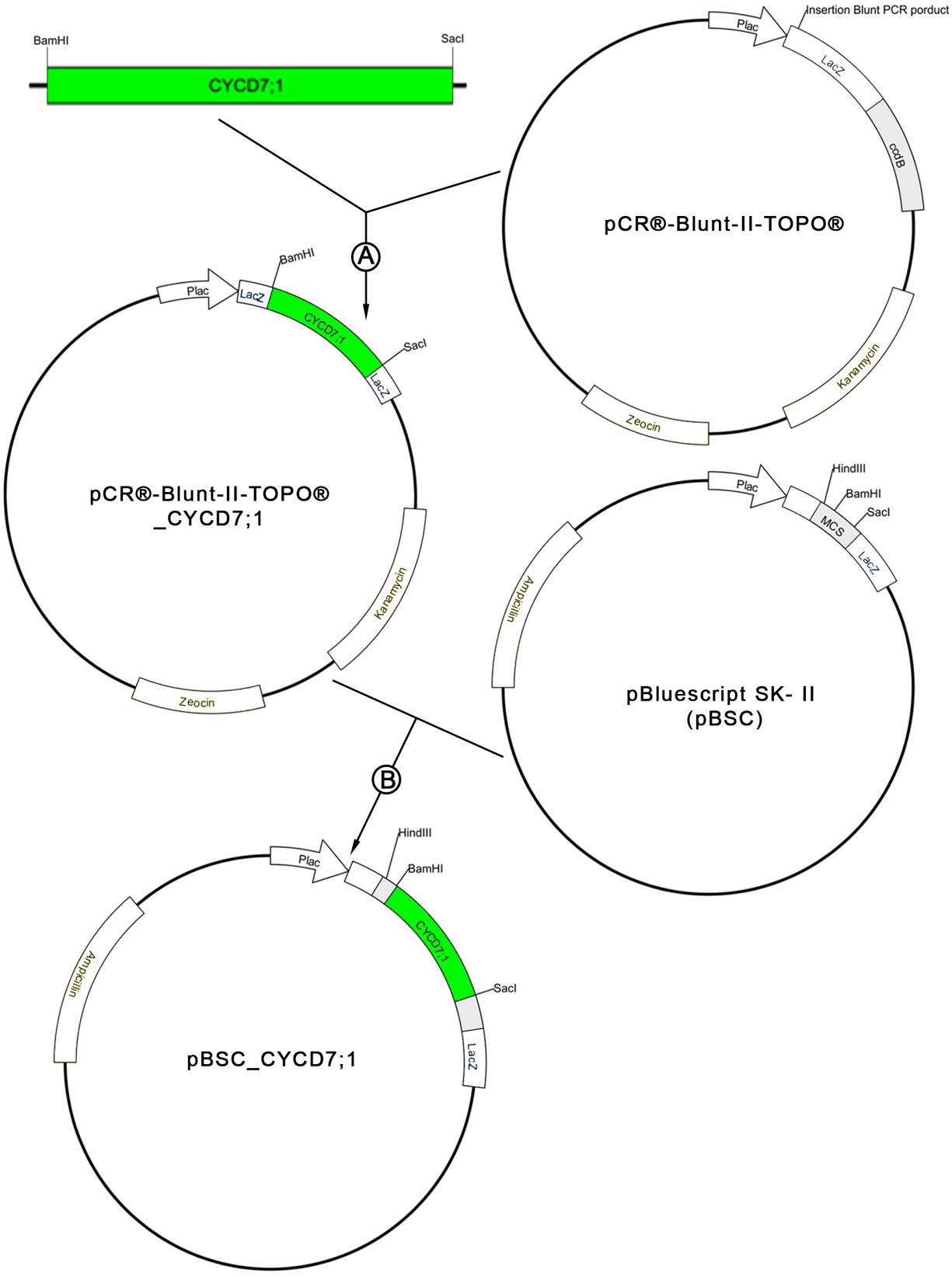

Figure 2.1. Cloning strategy to construct binary expression vector pGPTV-bar with *pFWA:CYCD7;1* cassette containing the *CYCD7;1* coding sequence under the control of the *FWA* promoter for endosperm-targeted *CYCD7;1* expression.

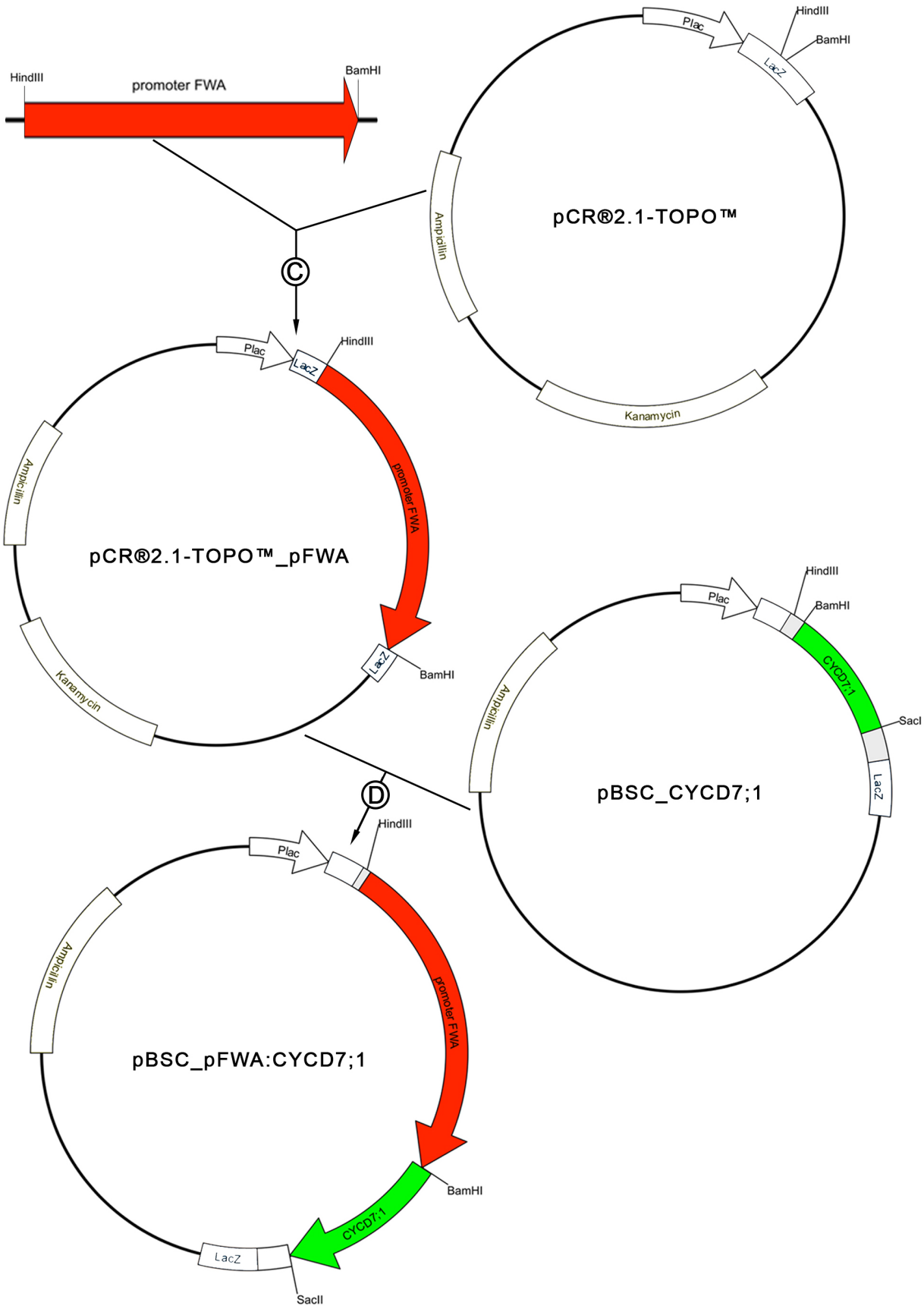

Figure 2.1. Cloning strategy to construct binary expression vector pGPTV-bar with *pFWA:CYCD7;1* cassette containing the *CYCD7;1* coding sequence under the control of the *FWA* promoter for endosperm-targeted *CYCD7;1* expression (continued).

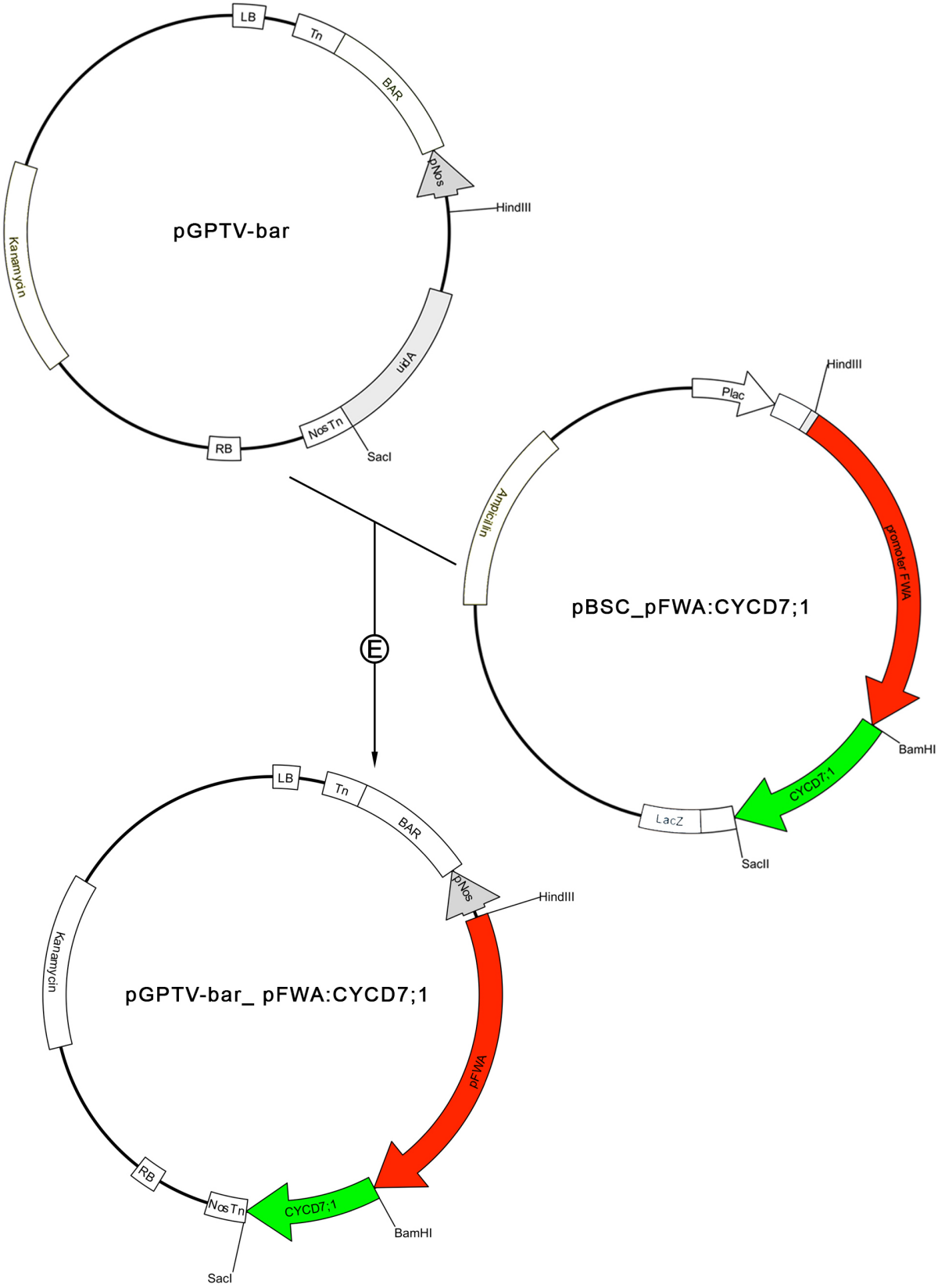

Figure 2.1. Cloning strategy to construct binary expression vector pGPTV-bar with *pFWA:CYCD7;1* cassette containing the *CYCD7;1* coding sequence under the control of the *FWA* promoter for endosperm-targeted *CYCD7;1* expression (continued).

A second construct containing the *FWA* promoter together with 409 bp of the *FWA* gene annotated *dFWA* consists of the first two exons and the first intron of *FWA* encoding for a 96 amino acid fragment. *dFWA* contains a homedomain and a nuclear localization sequence and might be involved in gene regulation (Soppe *et al.*, 2000; Kinoshita *et al.*, 2004). *dFWA* was cloned in frame with the *CYCD7;1* coding sequence. The *FWA:dFWA* fragment was excised from pBCH2-pFWA:dFWA:GFP plasmid (Kinoshita *et al.*, 2004) using *Hind*III and *BamH*I and inserted upstream of *CYCD7;1* in pBluescript SK- II (pBSC_pFWA:dFWA-CYCD7;1, Fig. 2.2A). The cassette *FWA:dFWA-CYCD7;1* was cut out of pBluescript SK- II with *Hind*III and *Sac*I and inserted in the plant binary vector pGPTV-bar to pGPTV-bar_ pFWA:dFWA-CYCD7;1 (Fig. 2.2B). Sequencing of the recombinant vectors was performed to ensure the correct sequence and frame between *dFWA* and *CYCD7;1* had been obtained.

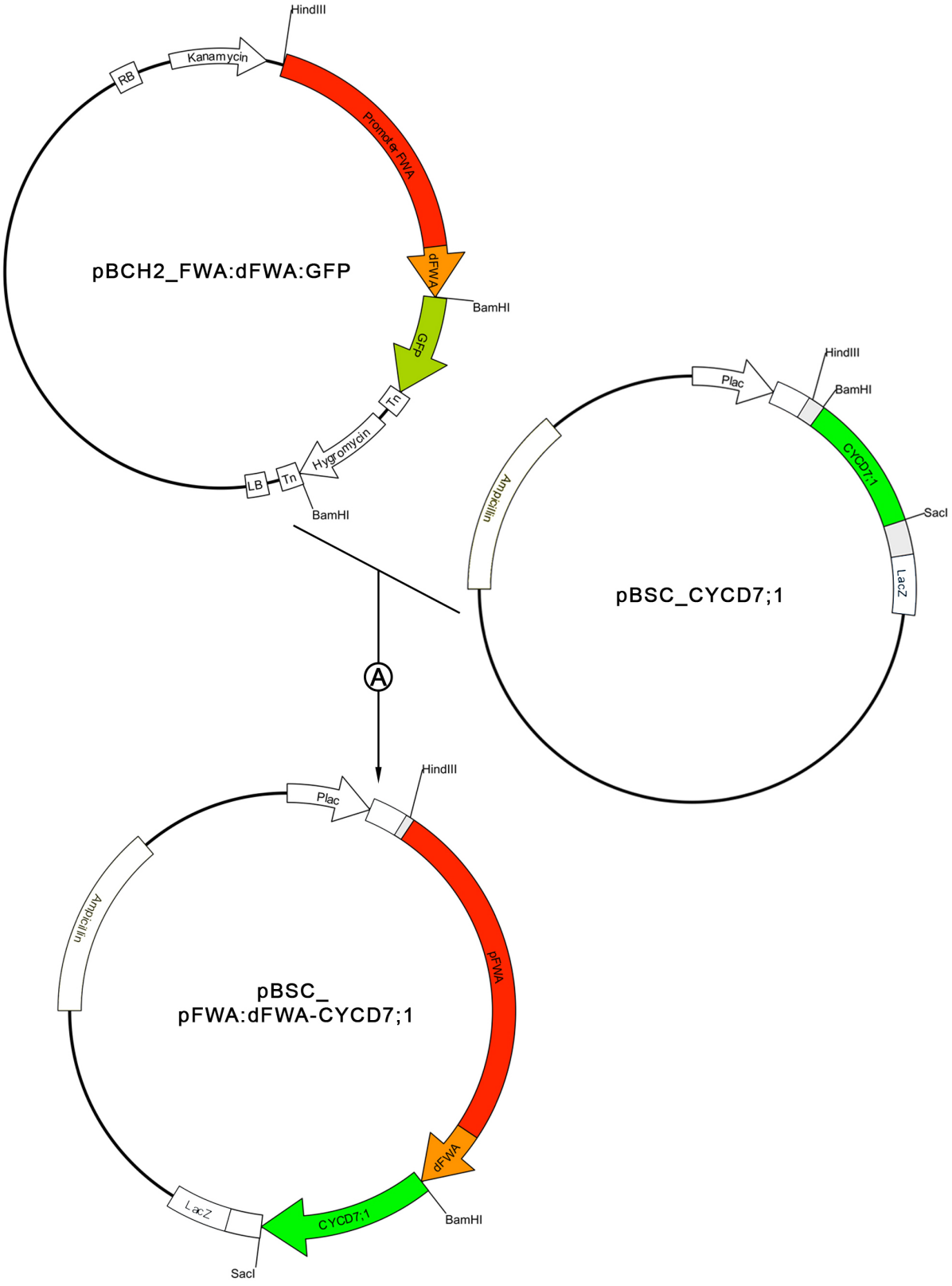

Figure 2.2. Cloning strategy to construct binary expression vector pGPTV-bar with *pFWA:dFWA-CYCD7;1* cassette containing the sequence coding for *dFWA* in frame with the *CYCD7;1* coding sequence under the control of the *FWA* promoter for endosperm-targeted *CYCD7;1* expression.

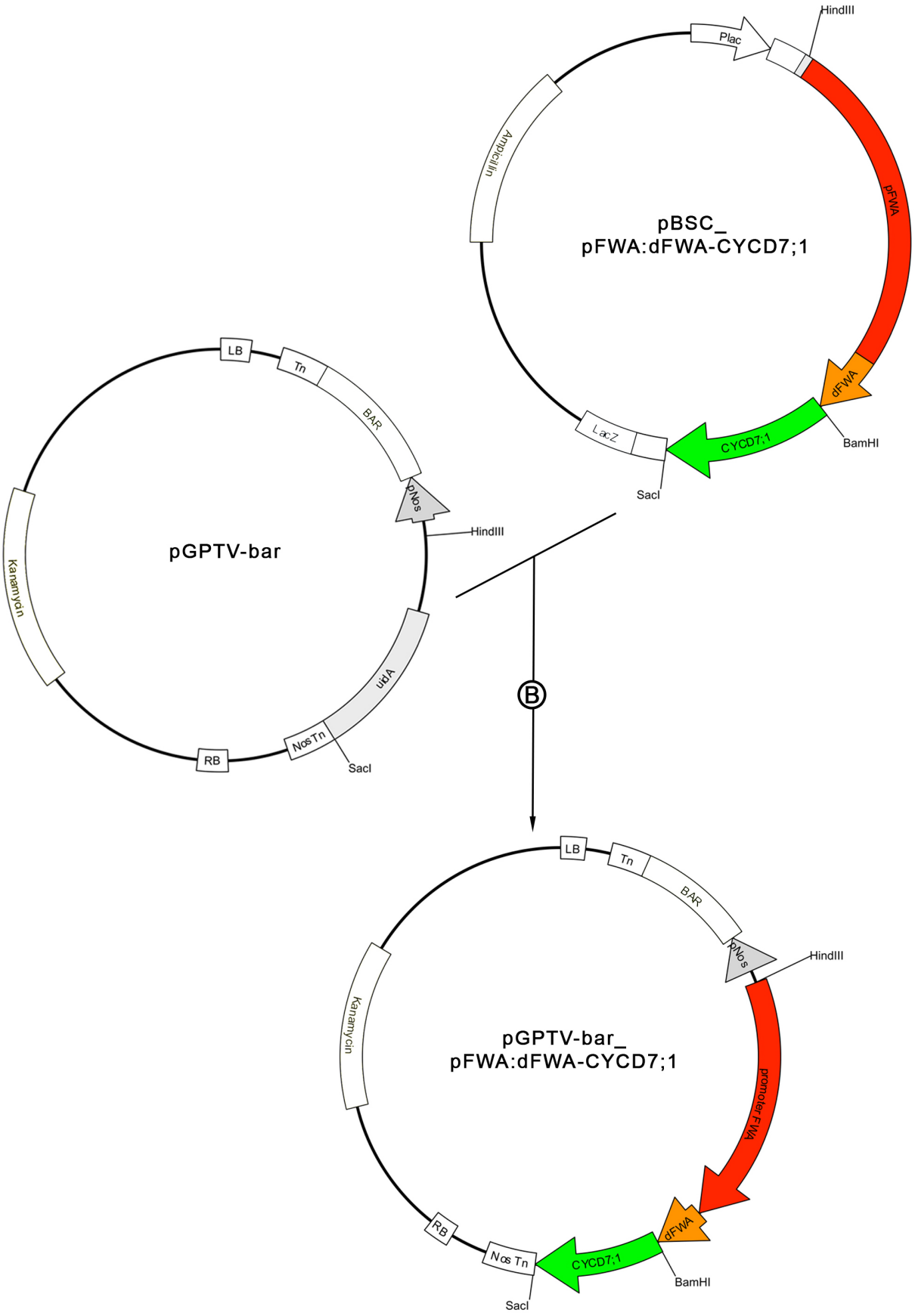

Figure 2.2. Cloning strategy to construct binary expression vector pGPTV-bar with *pFWA:dFWA-CYCD7;1* cassette containing the sequence coding for *dFWA* in frame with the *CYCD7;1* coding sequence under the control of the *FWA* promoter for endosperm-targeted *CYCD7;1* expression (continued).

2.6. Construction of reporters to follow endosperm-targeted *CYCD7;1* expression

The pBCH2_FWA:dFWA:GFP plasmid was available (Kinoshita *et al.*, 2004). In addition two constructs to examine the expression of *CYCD7;1* under the control of *FWA* were built: a transcriptional reporter *pFWA:3xVENUS* and a translational reporter *pFWA:dFWA-CYCD7;1-VENUS*. The "VENUS" marker is the fast folding yellow fluorescent protein (YFP) variant (Nagai *et al.*, 2002).

pFWA:3xVENUS was inserted into pGreenI 0029 by one step cloning (Fig. 2.3). The *FWA* promoter was cut from pBSC_pFWA:CYCD7;1 using *Hind*III and *BamH*I. The *3xVENUS* consists of three repeats of the VENUS protein. The 3xVENUS fragment was cut out of pCUC2:3xVENUS (Heisler *et al.*, 2005) using *BamH*I and *Not*I. The *3xVenus* fragment also contains the *N7* nuclear localization sequence. The two fragments *pFWA* and *3xVENUS* were inserted, in one step ligation, into pGreenI 0029 previously cut with *Hind*III and *Not*I (pGreenI 0029_pFWA:3xVENUS-N7; Fig. 2.3).

The *pFWA:dFWA-CYCD7;1-VENUS* translational reporter was made using 3-way Gateway® (Fig 2.4). The expression vector pH7m34GW carries *att*R4 and *att*R3 sites. R4 and R3 sites recombine with L4 and L3 respectively. The entry vector pDONR containing the fluorescence tag, VENUS, carries R2 and L3 (pDONR_R2-VENUS-L3). The entry vector pENTR/D with L1 and L2 contains coding sequence of *CYCD7;1* without the STOP codon (pENTR/D L1 L2_CYCD7;1). The entry vector pDONR L4/R1 has the *FWA* promoter between the recombination sites (pDONR_L4-pFWA:dFWA-R1). pDONR_R2-VENUS-L3, pENTR/D_L1-CYCD7;1-L2 and pDONR_L4-GAL4-R1 were already available (Forzani C., unpublished data). The latter vector contains *Sac*I and *Asc*I *sites* 5' and 3' of GAL4 respectively and between the L4 and R1 borders. *pFWA:dFWA* was amplified by PCR using high-fidelity DNA polymerase, with the pFWA-F-AscI and FWA-R-Ex2-AscI primers and using pBSC_pFWA:dFWA-CYCD7;1 as template. PCR product pDONR_L4-GAL4-R1 was digested with *Asc*I and *Sac*II and the *pFWA:dFWA* fragment inserted into pDONR L4/R1 in place of GAL4 (Fig. 2.4A). The three entry vectors, pDONR_R2-VENUS-L3, pENTR/D_L1-CYCD7;1-L2 and pDONR_L4-pFWA:dFWA-R1 and the expression vector pH7m34GW were used together to perform the LR reaction (see 2.1.8) (Fig. 2.4B). The plant expression vector pH7m34GW_pFWA:dFWA-CYCD7;1-venus was checked by sequencing and used to transform Arabidopsis plants.

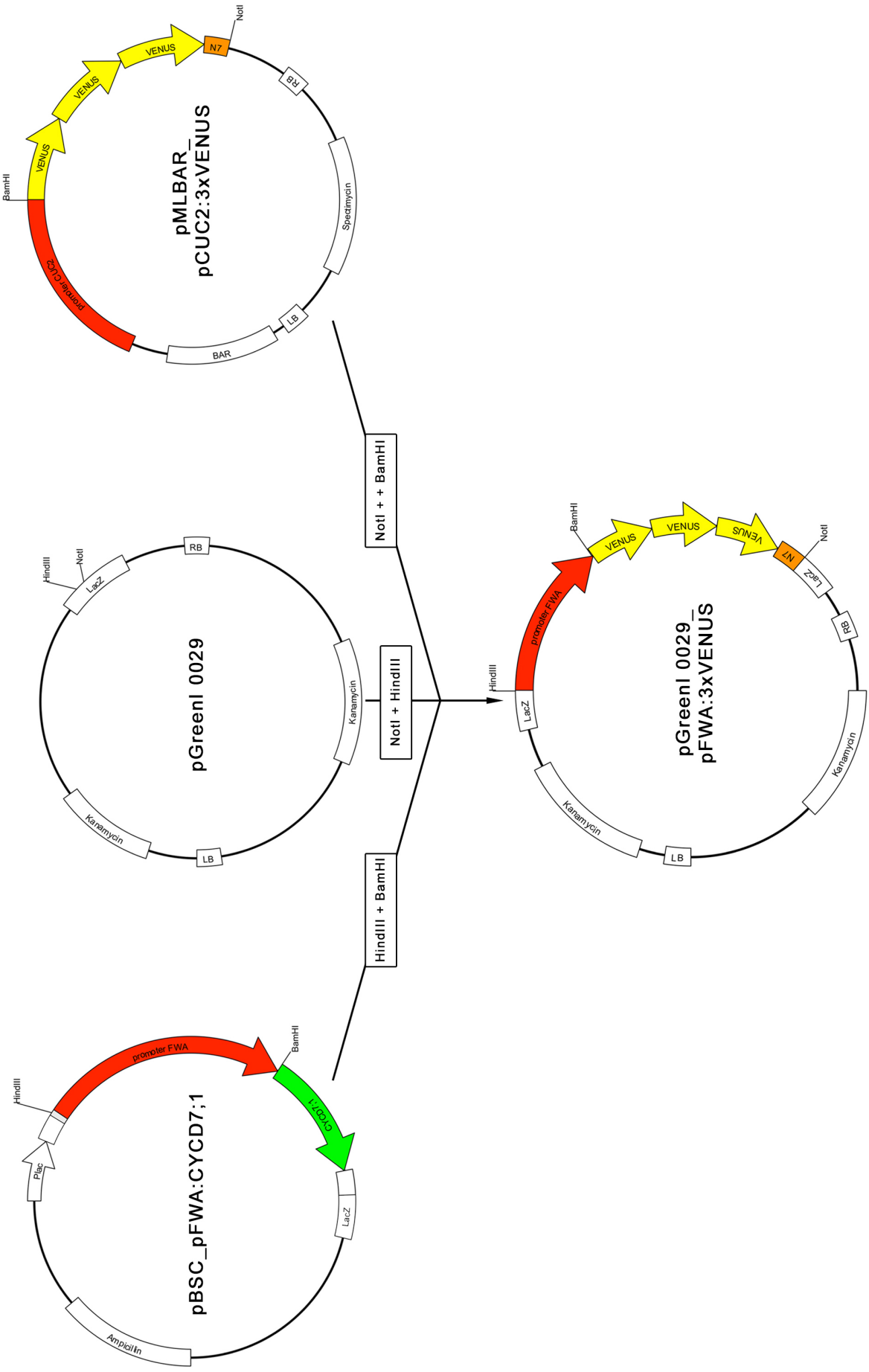

Figure 2.3. Cloning strategy to construct an expression vector with *FWA* promoter driving the expression of the 3xVENUS.

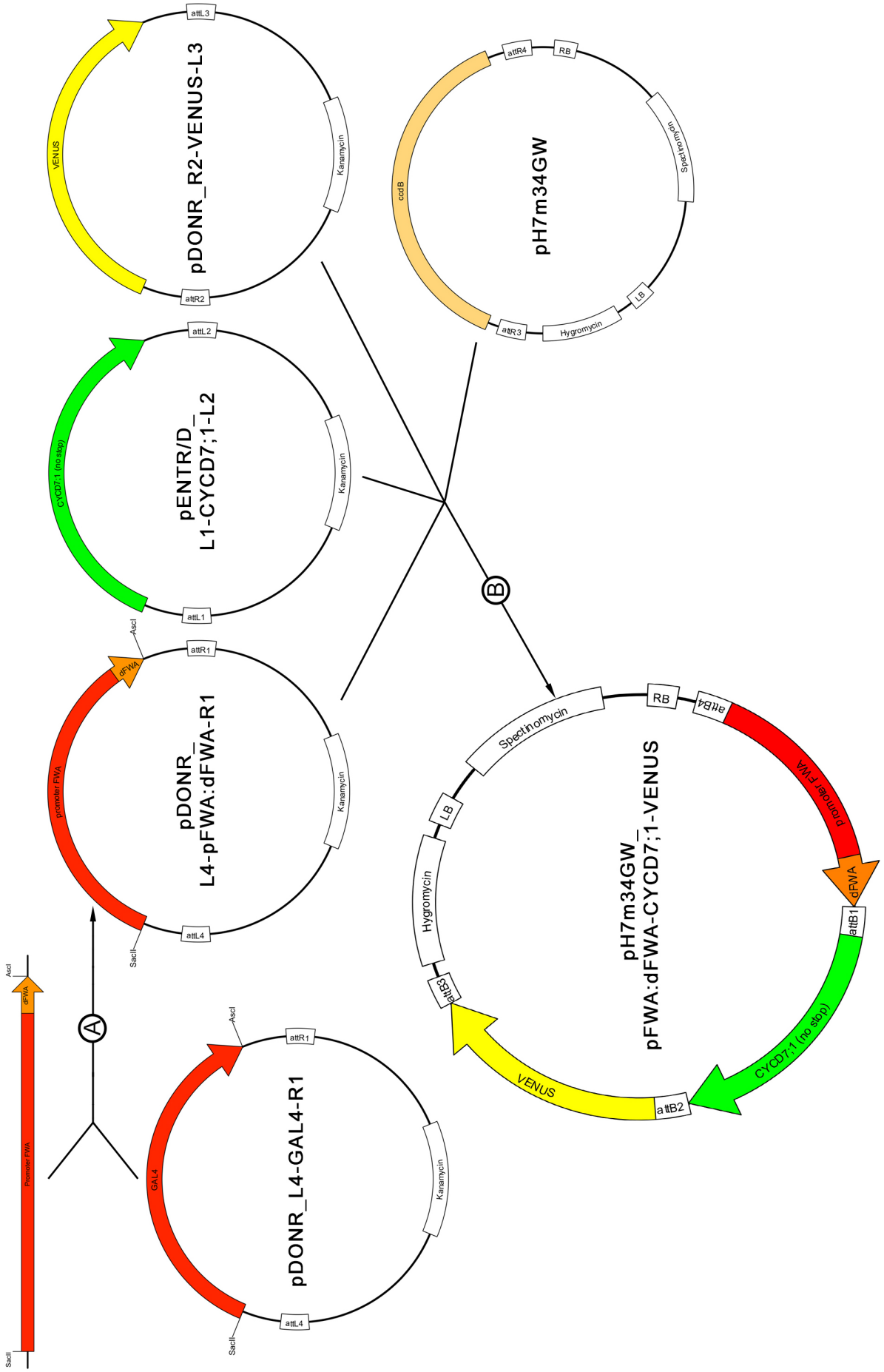

Figure 2.4. Construction of FWA:dFWA-CYCD7;1-VENUS reporter using 3-way GATEWAY® cloning system.

2.7. RNA techniques and reverse transcription PCR (RT-PCR)

RNA is sensitive to degradation therefore care was taken to use ribonuclease-free solutions and tubes. All consumables (plasticware, glassware) were autoclaved prior to use.

2.7.1. RNA isolation

RNA was isolated from inflorescence tissue using TriPure Isolation Reagent (Roche) and from developing seeds using RNeasy Plant mini kit (Quiagen). Two apices of inflorescence stems (cut below the third silique coming out of the flower) or seeds from 10 siliques (at different developmental stages) were ground in liquid nitrogen using a 1.5 ml tube and pellet pestle.

TriPure Method

To disrupt cells and denature proteins (such as nucleases), 1 ml of TriPure was added to the powder, which was then homogenized and incubated for 5 minutes at room temperature. Then 0.3 ml chloroform was added to the mixture, inverted several times and left incubating for 15 minutes. The solution was centrifuged at 10,500 rpm for 15 minutes at 4°C. The colourless upper aqueous phase was transferred to a fresh tube. The RNA was precipitated by adding an equal volume of isopropanol followed by inversion and a 10-minute incubation at RT. The RNA was pelleted by a 10-minute centrifugation at 4°C and the supernatant was discarded. The RNA pellet was washed twice with 70% ethanol, then air-dried and finally dissolved in 100 µl pre-heated (50°C) RNase-free water.

RNeasy Plant Mini Kit (Qiagen)

The Qiagen RNeasy Plant Mini kit was used according to manufacturer's instructions. Cell disruption and protein denaturation were performed by adding 450 µl Buffer RLC supplemented with β-mercaptoethanol and vigorous vortexing. The lysate was transferred to a QIAshredder spin column to homogenize it. After 2-minutes full speed centrifugation, the flow-through was transferred to a fresh tube. 0.5 volumes of ethanol was added and mixed. The sample was transferred to a RNeasy spin column to bind the RNA and centrifuged for 30 seconds at 10,000 rpm. The RNA was washed once with 750 µl buffer RW1 and twice with 500 µl Buffer RPE. 15-second centrifugation at 10,000 rpm was applied between each wash. Finally the RNA was recovered from the column using 50 µl of RNase-free water and a 30-second centrifugation at 10,000 rpm.

Removal of DNA contamination

The TURBO DNA-free™ kit was used according to manufacturer's instructions (Ambion). Half of the RNA sample was incubated with DNaseI and 10X TURBO DNase buffer at 37°C for 30 minutes. DNase inactivation was performed by adding 0.1 volume DNase inactivation buffer. After a gentle mix and 5-minute incubation at room temperature, the solution was centrifuged for 1.5 minutes at 10,000 rpm. The upper clear phase containing the RNA was transferred to a fresh tube.

2.7.2. Determination of RNA yield and purity

The total amount and purity of RNA was quantified by UV spectrophotometry using a NanoDrop-1000 spectrophotometer (ThermoFisher Scientific, USA). The absorbance of samples at 260 nm (A_{260}), 280 nm (A_{280}) and 230 nm (A_{230}) was measured. The amount was determined at A_{260} whereas a high purity was defined by A_{260}/A_{280} ratio and A_{260}/A_{230} ratio, that should be greater than 2.0.

The integrity of RNA samples was determined by gel electrophoresis. Prior to use, electrophoresis apparatus was cleaned with 20% SDS (Sodium dodecyl sulfate) solution to remove any trace of RNases. A 1% agarose gel was used to visualize two discrete bright bands (28S and 18S ribosomal RNA) as well as few fainter bands of lower molecular weight. RNA samples with sufficient yield and of good quality were used for analysis.

2.7.3. Single stranded cDNA synthesis

The first strand cDNA synthesis was performed using RETROscript RT-PCR kit (Ambion) or RevertAid M-MuLV Reverse Transcriptase (RT, Fermentas) and oligo(dT) primer (T11VN, Eurogentec) according to the manufacturer's instructions. Both methods follow the same principle. Firstly, 0.5-1 µg of total RNA was added to 2 µl 50 µM oligo(dT) and nuclease-free water was added to a final volume of 12 µl. The mixture was incubated at 65°-70°C for 3-5 minutes and chilled on ice to facilitate the hybridization of oligo(dT) with the poly(A) tails of mRNAs. Then the following components were added to a total volume of 20 µl: RT buffer (10X Ambion buffer or 5X Fermentas buffer), 2-4 µl dNTP mix (1 mM final concentration), RNase inhibitor (20 units), RT (100 units Ambion or 200 units Fermentas). Reactions were incubated at 42°C for 1 hour followed by a 10-minute incubation at 94°C (Ambion) or 70°C (Fermentas). Single stranded cDNA samples were stored at -20°C and analyzed by PCR.

2.7.4. Semi-quantitive RT-PCR amplification using cDNA or RNA template

The expression level of a gene of interest was estimated using semi-quantitative RT-PCR. RT-PCR was performed using one of two methods based on the nucleic acid template

used: (1) cDNA template or (2) RNA samples using OneStep RT-PCR kit (Qiagen). For each gene, primer sets, annealing temperature (Tm) and number of cycles were optimized to stop the reaction before the point of product saturation. After gel electrophoresis and DNA staining, the amplicons produced in different samples could be compared by correlating the amplicon band intensities on a gel.

RT-PCR on cDNA was performed using Taq PCR master Mix (Qiagen) using the conditions described in section 2.2.2, but the initial denaturation step was performed at 94°C for 3 minutes instead of 10 minutes.

The OneStep RT-PCR kit allows cDNA synthesis and PCR in a single step. RT-PCR mix was made in a final volume of 50 µl (in 200-µl PCR tube) using 100 ng of total RNA, 5X Qiagen OneStep RT-PCR buffer, 2 µl dNTP mix (with a final concentration of 400 µM of each dNTP), each primer at 0.6 µM final concentration and 2 µl OneStep RT-PCR enzyme Mix. The thermal cycler was set for 4 distinct steps: first a 30-minute incubation at 50°C to produce singled stranded cDNA by reverse transcription, then an initial PCR activation step at 95°C for 15 minutes inactivating the reverse transcriptase, denaturating the cDNA as well as activating the HotStartTaq DNA polymerase, thirdly a 3-step-cycling repeated 25 to 35 times with a 30-second denaturation at 94°C, 30-second annealing at 5°C below the Tm required by the primer set and 1-minute extension at 72°C, and a final extension performed at 72°C for 10 minutes.

2.8. *Agrobacterium* mediated transformation of Arabidopsis

Electrocompetent *Agrobacterium tumefaciens* (GV3101 strain containing pMP90 plasmid) were used to transform *Columbia-0* ecotype of *Arabidopsis thaliana*.

2.8.1. Electrocompetent *Agrobacterium*

GV3101 *A. tumefaciens* were grown for two days at 28°C on LB agar plates with 50 µg/ml rifampicin to select for the *Agrobacterium* genomic DNA containing the integrated rifampicin resistance gene and 20 µg/ml gentamycin to select for pMP90. One colony was used to inoculate 5-10 ml LB with the same antibiotics mentioned above and grown overnight at 28°C. 400 ml of LB complemented with antibiotics was inoculated with the overnight culture and incubated at 28°C until OD_{600} reached 0.6. Cells were centrifuged at 4500 rpm for 15 minutes at 4°C. Several washes were performed by resuspending the pellet sequentially in 1, 0.5. and 0.02 volumes of ice-cold 10% glycerol, with an intervening centrifugation step. Finally cells were resuspended in 0.005 volumes of 10% ice-cold glycerol, aliquoted in 50 µl volume and quickly frozen in liquid nitrogen. Cells were stored at - 80°C until required.

2.8.2. Agrobacterium transformation

1 µl of plasmid DNA was added to a 50 µl aliquot of GV3101 cells and transferred into a pre-chilled electroporation cuvette. A pulse was then applied (Ec2 program, 2.4 kV, 25 µF) with a BioRad electroporator. After adding 1 ml of LB, the bacterial suspension was incubated for 2 hours at 28°C with gentle shaking. The bacterial culture was spread on LB agar plates containing 50 µg/ml rifampicin, 20 µg/ml gentamycin and the appropriate antibiotic to select for the plasmid of interest. The growth occurred during 2 days at 28°C. One colony containing the plasmid of interest – checked by PCR – was used to inoculate 5 ml LB with the antibiotics mentioned above.

2.8.3. Arabidopsis transformation using the floral dipping method

A. thaliana was transformed using the floral dipping method (Weigel and Glazebrook, 2006). One single *A. tumefaciens* colony containing the desired plasmid was picked and used to inoculate 5 ml LB supplemented with 50 µg/ml rifampicin, 20 µg/ml gentamycin and the appropriate antibiotic for the antibiotic resistance carried by the plasmid of interest. Cultures were incubated for 24 hours at 28°C, 200 rpm shaking. 1 ml of 24-hour culture was used to inoculate 200-400 ml LB culture with antibiotics as above. After a 24-hour incubation, OD_{600} was recorded. The cells were harvested by centrifugation at 4500 rpm for 15-20 minutes and the supernatant was discarded. Cells were resuspended at a concentration of OD_{600} = 0.8 in infiltration medium containing 5% sucrose and 0.05% Silwet L-77. Plants with multiple floral stems were transformed by inverting them in the infiltration medium and allowing them to soak for 1 minute. Plants were then placed in sealed plastic bags and left under low light for about 16 hours. The plants then were removed from the bags and grown under normal conditions.

2.8.4. Recovery of transgenic plants

Agrobacterium-mediated transformation of Arabidopsis shows a 0.1-1% efficiency (Weigel and Glazebrook, 2006). Seeds harvested from the plants dipped are named T1 seeds. To identify transgenic T1 plants, all seeds were surface sterilized (see below) and sown on GM medium containing the selective agents for which resistance was carried by the T-DNA inserted and 200 µg/ml cefotaxime to kill any agrobacteria present on T1 seeds. After 7-15 days of growth, transformed T1 seedlings produced true leaves and the lawn of sensitive plants turned either yellow for kanamycin and phosphinothricin (PPT) selection or stayed small and green for hygromycin selection. Resistant T1 seedlings were transferred onto soil.

2.9. Plant growth conditions

2.9.1. Seed sterilization

Sterilization solution (5 g/L sodium dichloroisocyanurate dihydrate (Chlorifix, Bayrol), 70% ethanol) was prepared by first dissolving an appropriate mass of sodium dichloroisocyanurate dehydrate in water and then adding 100% ethanol to a final concentration of 70%. Seeds were sterilized in the sterilizing solution for 10 minutes. Seeds were washed with 95% ethanol 3 times before drying.

2.9.2. Growth condition *in vitro*

After seed sterilization, plants were grown *in vitro* on germination medium (GM) plates containing 4.4 g/L Murashige and Skoog medium (MS), 1.5% sucrose, 1% agar, 0.5 g/L MES buffer (2-(N-morpholino) ethansulfonic acid), pH 5.8. For transgenic plants carrying resistance genes, GM plates were supplemented with the appropriate selective agent (50 µg/ml kanamycin, 15 µg/ml PPT, 25 µm/ml hygromycin). To screen for transformant T1 plants, 200 µg/ml cefotaxime was also added to GM plates to kill agrobacteria that could still be on seeds. Seeds on plates were left at 4°C for 2-3 days and then transferred to a growth chamber with 16h-light/8h-dark, 21°C and 70% humidity. After about 15 days, resistant seedlings were scored and transplanted to soil.

2.9.3. Growth conditions on soil

Seedlings grown *in vitro* were transferred to a mixture of 1 part horticultural sharp sand and 2 parts Sinclair professional All Purpose Growing Medium compost. Plants were watered once every 2-3 days. Plants were grown in controlled environment rooms at 21°C, with a 16-hour photoperiod.

2.10. Arabidopsis genetics and crossing

2.10.1. Determination of apparent transgene copy number

Following Arabidopsis transformation, the number of unlinked copies of the transgenic cassette containing a resistance gene (see table 2.2) that had integrated into the genome of transformants (T1 plants) was estimated. T2 seeds harvested following self-fertilization of T1 plants were surface sterilized and plated on GM supplemented with the appropriate selective agent. The ratio of resistant:sensitive seedlings was recorded. Based on Mendelian genetics, a typical ratio of 3 resistant: 1 sensitive suggests a single T-DNA insertion in the Arabidopsis genome. These resistant T2 plants were transferred onto soil.

2.10.2. Isolation of homozygous lines

The selected T2 plants were allowed to self-fertilize. T3 seeds generated were harvested and sown on GM with the appropriate antibiotics. T3 seeds showing 100% resistance were kept as homozygous for the insert based on the resistance marker. For each construct, several independent lines containing a single homozygous T-DNA were used for further analysis.

2.10.3. PCR confirmation of transgene integration

To confirm that the T-DNA did not integrate only the selectable marker but also the DNA cassette of interest, PCR was performed using RedExtract-N-Amp Plant PCR (Sigma-Aldrich) and primers to specifically amplify fragments of the transgene of interest (primers are detailed for each result chapter). In parallel, RT-PCR was performed to compare the level of expression of the transgene between the different lines and a *wild-type Columbia-0* (*WT Col-0*) (see 2.7).

2.10.4. Procedure for crossing

All parent lines used for crossing were homozygous. Flowers from the primary inflorescence stem were used for crossing. 2-3 unopened flowers in which petal elongation had started were emasculated by removing sepals, petals and finally stamens with fine forceps. The unwanted flowers on the stem were removed. After leaving the gynoecium to develop for 2 days, pollination was performed by transferring the pollen from ripe stamens onto the stigmatic papillae of the gynoecium until the latter was saturated with the donor plant pollen. To avoid contamination with unwanted pollen, forceps were regularly rinsed between crosses with 70% ethanol followed by a wash with dH_2O. Successful pollination of gynoecia was observed 2 days later by the gradual elongation of developing siliques.

This procedure was also used to follow seed development at specific time points.

The emasculation procedure and pistil development was also performed to study the mature female gametophyte in chapter 4.

2.11. Assay for β-glucuronidase activity (GUS)

GUS staining was performed on seedlings, flowers and seeds (Jefferson *et al.*, 1987; Stangeland and Salehian, 2002). For seeds, siliques were sampled and cut open at each end and along the septum using single-edge blades. Plant samples were fixed in 90% ice-cold acetone for 15-30 minutes before being washed twice with 50 mM sodium phosphate buffer pH 7.2. Specimens were immersed in GUS buffer (50 mM sodium phosphate buffer pH 7.2, 0.5 to 2 mM $K_3Fe(CN)_6$, 0.5 to 2 mM $K_4Fe(CN)6$, 1 mg/ml X-Gluc and 0.2% Tween

20). Samples were vacuum infiltrated for 5 minutes and then incubated at 37°C in the dark for 6-24 hours. The staining buffer was removed. Seedlings and flowers were cleared in 100% ethanol for 1-2 days and then rehydrated with an ethanol series of 70%, 50% and 30% prior to microscopic examination. Siliques were washed several times with ethanol: acetic acid (1:1). A clearing solution of chloral hydrate:dH_2O:glycerol (4:3:1) was used to mount sampled seeds from the siliques or seedlings and floral organs, 24 hours or 1 hour respectively prior to exanimation.

2.12. Histological techniques

2.12.1. Sample fixation

For microscopic analysis, samples were fixed. Prior to DAPI staining, pistils containing unfertilized ovules were cut at both ends and opened along the septum. Samples were placed in FAA fixative solution (2 volumes 35% formaldehyde, 17 volumes 95% ethanol, 1 volume acetic acid) and a vacuum was applied for 10 minutes. Samples were incubated at 4°C overnight. After washing twice with dH_2O, ovules were extracted with a surgical needle (0.3x13 mm, BD Microbalance) and placed in 50 µl of DAPI stain (see below). Samples were stored at 4°C in the dark for 7 days prior to analysis.

When ovules or seeds were observed using Differential Interference Contrast (DIC), a fixative solution of ethanol:acetic acid (Et:Ac; 3:1) was used. Siliques or pistils were cut open and incubated in Et:Ac for 1- 24 hours at 4°C. Ovules or seeds were then cleared and mounted in chloral hydrate:dH_2O:glycerol (4:3:1) and observed under DIC.

2.12.2. Cell wall staining

Embryo cell walls were stained with Schiff and propidium iodide (PI) allowing optical sectioning of plant tissue using confocal laser scanning microscopy (Truernit *et al.*, 2008). Arabidopsis seeds were imbibed in water at 4°C for 2 days. Seed coats were removed using surgical needles. Embryos were transferred to 1 ml fixative (50% methanol and 10 % acetic acid) and stored at 4°C until observation. Prior to confocal imaging, fixative was removed and embryos were washed with dH_2O. Embryos were incubated for 20-40 minutes at RT in 1% periodic acid. Embryos were washed with dH_2O and incubated in Schiff reagent with PI (100 mM sodium metabisulphite and 0.15N HCl ; PI to final concentration of 0.1 mg/ml was freshly added for 1-2 hours or until the embryos were visibly stained). The embryos were rinsed with dH_2O and cleared in chloral hydrate solution for a few days before being mounted in chloral hydrate:dH_2O:glycerol (4:3:1) for confocal observation.

2.13. Microscopy, image processing and phenotype analysis

2.13.1. Microscopy and photography

Wholemount preparations were examined using a Nikon SMZ-U dissecting microscope and photographed with the attached digital zoom camera Kodak DC290/MDS90. All pictures were captured with Adobe Photoshop 6.0.

Seed pictures for seed size measurement were acquired using a LeicaFire Cam digital camera attached to a Leica MZ16F dissecting microscope.

Cleared samples such as ovules and seeds were observed under a Zeiss Axio Imager M1 microscope equipped with DIC optics. Pictures were acquired using an attached Axiocam MRC5 camera and pictures were processed using AxioVision 4.7 image analysis software.

Live imaging of fluorescent proteins was carried out with a Zeiss LSM 710 Meta confocal microscope, using a DIC filter. Laser, filter and range of fluorescent protein emission wavelengths used are detailed in table 2.3. DAPI staining of nuclei used VECTASHIELD® mounting medium for fluorescence with DAPI (Vector Laboratories, Inc). Prior to DAPI staining, samples were fixed in FAA as mentioned above. Green fluorescent protein (GFP) and modified yellow fluorescent protein (VENUS) were added to the protein of interest during cloning procedures. PI was diluted 250X from 4 mg/ml to stain cell walls.

Table 2.3. Confocal microscope settings and fluorescence

Stain	Laser for excitation (nm)	Filter	Range of fluorescence emission (nm)
DAPI	405	MBS 405	410-585
GFP	488	MBS 488	493-592
VENUS	514	MBS 458/514	519-621
PI	543	MBS 488/543	493-572

2.13.2. Image analysis

Images were processed using ImageJ. Cell length, cell area, cell counting and embryo length were acquired using the tools provided by the package.

Seed parameters were generated using Seed Measurer, a purpose-written ImageJ plug-in (Forero-Vargas M., unpublished data). The program gives seed area, length and width as features.

Embryo volume was measured from Z-stacks covering the whole volume. An ImageJ plug-in, Embryo 3D, reconstitutes the 3-D structure of the embryo and calculates the volume (Forero-Vargas M., unpublished data).

2.13.3. Statistical analysis

Statistical analysis was performed with the statistics package PASW 16.0 (SPSS Inc. 2007. Chicago). Statistical analyses were performed using one-, two-way ANOVA and χ^2 tests depending on the experiment and the data comparison.

Prior to performing ANOVA test, four main assumptions were verified: the samples were (1) randomly selected and (2) independent by experimental design, (3) the population was normally distributed and (4) the homoscedasticity (or equality of variance of the different populations) was verified. The normality assumption was tested using Kolmogorov-Smirnov or Shapiro-Wilk tests. The homoscedasticity was verified using Levene's test. Normality and homoscedasticity were verified when p-value of these latter tests was greater than the significance level (α) of 0.05 (p-value> α =0.05). Therefore ANOVA tests were performed. When the normality and homoscedasticity were not verified (p-value<0.05 for Kolmogorov-Smirnov, Shapiro-Wilk and Leneve's tests), non-parametric test (Kruskal-Wallis test) was performed. When performing ANOVA or Kruskal-Wallis tests, a significant difference of the mean between the different populations was concluded when the p-value was smaller than 0.05. When performing ANOVA test, Bonferroni multiple comparison tests were run simultaneously to compare each mean of the different sample to another, in order to discriminate the one(s) that was/were significantly different.

χ^2 or Goodness-of-fit test was used to conclude whether the observed frequencies in the different populations fit a particular (hypothezised) distribution (Table 4.2 and Fig. 4.5A). A significant difference between the observed and hypothesized frequencies was concluded when the p-value was smaller than 0.05.

2.14. Yeast-Hybrid assay

2.14.1. Yeast strain and media

Yeast-hybrid assays were performed in the yeast strain *S. cerevisiea* PJ69-4A (*MATa leu2-3,112 ura3-52 trp1-901 his3-200 gal4Δ gal80Δ GAL-ADE2 lys2::GAL1-HIS3 met2::GAL7-LacZ*) (James *et al.*, 1996). PJ69-4A was grown at 30°C in YDP broth (1% yeast extract, 2% peptone and 2% dextrose) or on YDP agar (YDP supplemented with 2% bacto-agar).

Selection for transformants or for interaction was performed on SD medium (1.67g/l yeast nitrogen base without amino acids and containing ammonium sulfate, 2% glucose and

specific amino acids required for strain growth; SD agar was obtained by adding 2% bacto-agar).

Yeast strain PJ69-4A is auxotrophic for methionine (M), uracil (U), tryptophan (T), leucine (L), histidine (H) and adenine (A). Once transformed with the following plasmid DNA (see below), it became prototrophic for tryptophan, leucine and uracil respectively. Hence to select transformed cells, SD medium was supplemented with 20 µg/ml L-methionine, 20 µg/ml L-histine and 40 µg/ml adenine.

2.14.2. Vectors for Yeast-Three-Hybrid (Y3H) assay

Y3H assays were performed to test the interaction between three proteins at the same time: CYCD7;1, CDKs and KRPs. Vectors containing the GAL4 DNA binding domain (BD) were pDEST32 (Invitrogen) and pBI880, a derivative of pPC62 (Chevray and Nathans, 1992). Vectors containing activation domain (AD) were pDEST22 (Invitrogen) and pPC86 (Chevray and Nathans, 1992). The third protein was cloned in pFL61, a vector carrying a 2µ plasmid origin, and expressed under the constitutive *PHOSPHOGLYCERATE KINASE* (*PGK*) promoter (Minet *et al.*, 1992). The 7 *KRPs* and *CYCD2;1* cDNA fused to the GAL4 AD in pPC86_KRP and pBI880_CYCD2;1 respectively were available in the laboratory (Sanz *et al.*, 2011). All the *CDKs* (*CDKA;1 CDKB1;1 CDKB1;2 CDKB2;1* and *CDKB2;2*) and *CYCD7;1* cDNA fused either to the GAL4 AD in pDEST22 or to the BD in pDEST32 (de Jager S. unpublished data) were also available. All the KRPs were inserted in pFL61. pFL61_KRP2 was already available (Sanz *et al.*, 2011). KRP3/4/5/6/7 cDNAs were excised from pPC86 with *Sal*I and *Not*I and introduced into the *Not*I site of pFL61 after blunting. The KRP1 cDNA was amplified by PCR with KRP1-F and KRP1-R (see table 2.1) at Tm 58°C. After PCR clean-up (Macherey and Nagel, see section 2.1.7), KRP1 was cloned in pCR®-Blunt II TOPO vector (Zero Blunt® TOPO® PCR technology, Invitrogen^{TM}) according to the manufacturer's instructions (see section 2.1.8). The KRP1 cDNA was excised from the pCR®-Blunt II TOPO vector with *EcoR*I-HF and introduced into the *Not*I site of pFL61 after blunting. To ensure the right orientation of the KRP cDNA sequence in pFL61, pFL61_KRP vectors were sequenced.

2.14.3 Yeast transformation

Yeasts were co-transformed with 3 different plasmids (1 with AD, 1 with BD and 1 pFL61, as mentioned above) using high efficiency yeast transformation protocols (Amberg *et al.*, 2006). A starter culture was initiated by inoculating 5-10 ml YDP with one colony from a YPD plate and incubating overnight at 30°C, 200 rpm. A new culture was inoculated to 0.2 OD_{600} with the overnight culture and incubated at 30°C, 200 rpm. Typically the culture volume used was equivalent to 10 ml for each transformation to be performed. When the

OD_{600} reached 0.5-0.8 (3-5 hours), cells were centrifuged for 3 minutes at 3000g and washed with 5 ml sterile water or half of the initial culture volume. Cells were centrifuged again, washed in 1 ml LiAc/TE (1X TE, 0.1M LiAc, 1/10 initial volume) and transferred to a 1.5 ml tube. Cells were centrifuged for 30 seconds at top speed. Finally cells were resupended in transformation mix by gentle vortexing in 50 µl LiAc/TE, 25 µl 2 mg/ml salmon sperm single-stranded carrier DNA (previously boiled at 95°C for 5 minutes and chilled on ice), 300 µl 40% PEG (freshly made from 50% PEG, polyethylene glycol MW 3350, Sigma P3640) and 0.5 µg/µl of each plasmid DNA. Cells were incubated in the transformation mix for 30 minutes at 30°C and then underwent a heat-shock at 42°C for 20 minutes. Cells were pelleted for 1 minute at 3000 rpm and the transformation mix was removed. Cells were resuspended in 100 µl of sterile water by gently pipetting. Cells were spread out on plates to select the transformants carrying all the plasmid DNAs of interest (SD-TLU) and incubated at 30C for 2-4 days.

2.13.4. Selection for interactions

Histidine and adenine auxotrophy as well as *lacZ* expression were used to select interactions between the proteins of interest. Growth on plates lacking histidine and adenine and the expression of the *lacZ* reporter indicate an interaction between proteins expressed from the plasmid DNA.

Histidine and Adenine auxotrophy

2-4 days after transformation and for each plasmid combination, 4 -5 transformants growing on SD-TLU were used to inoculate 2 ml SD-TLU culture. After overnight growth at 30°C, 200 rpm, each culture was diluted to 0.5 OD_{600} and 10 µl was spotted onto plates non-selective for the interaction (SD-TLU), but selective for transformants carrying the three plasmids of interest, and onto plates selective for the interaction, lacking either adenine or histidine. Histidine selection has low stringency creating false positive results, thus 30 mM of the inhibitor of the enzyme activity encoded by the *HIS3* gene, 3-amino-1,2-4-triazole (3-AT, 1M filtered sterilized stock added to molten medium) was added. Spotted plates were incubated at 30°C for 3-7 days. At 3 days, the SD-TLU plates were checked for the growth of viable transformants and subsequently used to perform the β-galactosidase assay. At 7 days, the plates selecting for the interaction were checked and colony growth was examined to confirm interactions.

Identification of lacZ expression

Expression of the *lacZ* reporter gene in transformants was detected using the X-Gal agarose overlay assay (Duttweiler, 1996). After 3-day growth on SD-TLU, yeast plates

were overlaid with 10 ml 5 mg/ml agarose in 0.45 M potassium phosphate buffer (KPO_4, pH 7.0), 6% DMF, 0.1% SDS, 5 µl β-mercapto-ethanol and 0.5 mg/ml X-gal. The agarose was allowed to set and plates were incubated at 30°C for 24 hours until a blue color developed.

2.15. Accession numbers and T-DNA insertion mutants

Sequence data can be found in the Arabidopsis Information Resource database (www. Arabidospsi.org) under the following accession numbers : At4g25530 (FWA), At5g02110 (CYCD7.1), At2g23430 (ICK1/KRP1), At2g23430 (ICK2/KRP2), At5g48820 (ICK6/KRP3), At2g32710 (ICK7/KRP4), At3g24810 (ICK3/KRP5), At3g19150 (ICK4/KRP6) At1g49620 (ICK5/KRP7), At3g48750 (CDKA;1), At3g54180 (CDKB1;1), At2g38620 (CDKB1;2), At1g76540 (CDKB2;1), At1g20930 (CDKB2;2).

Mutants used were: *krp1-1* (SALK 100189) and *krp2-3* SALK (110338) (Sanz *et al.*, 2011).

Chapter 3

Targeting *CYCD7;1* Expression to Engineer Seed Size

Chapter 3
Targeting *CYCD7;1* Expression to Engineer Seed Size

Introduction

Ectopic expression is a common technique to assess the potential function of a gene. This method can lead either to a misplaced and/or enhanced expression (gain-of-function) or to a direct silencing effect by expressing an interfering RNA (RNAi) that hybridizes with the targeted mRNA triggering the destruction of the double stranded hybrid and thereby preventing translation of the target mRNA (loss-of-function) (Waterhouse *et al.*, 1998; Chuang and Meyerowitz, 2000; Muranaka, 2011). In both cases, the method gives insights into gene function through the analysis of the phenotypic consequences. In plants, gain-of-function has commonly been generated by placing a gene of interest under the transcriptional control of the *Cauliflower Mosaic Virus 35S* (*CaMV 35S*) promoter (Benfey *et al.*, 1989). Originally the *CaMV 35S* promoter was responsible for driving the expression of a gene of the *CaMV* genome. The *35S* promoter is a strong promoter leading to constitutive expression of the gene under its control. However, it has been shown that constitutive expression under the control of the *35S* promoter of some genes can be responsible for abnormal plant development, and may induce sterility or, in extreme cases, lethality. Hence, the use of the *35S* promoter can lead, in some cases to misinterpretation of results (Yoo *et al.*, 2005; Zheng *et al.*, 2007). To overcome deleterious effects of constitutive overexpression, studies using more directed expression have been performed. They rely on the choice of a promoter that defines the timing and pattern of expression.

The genetic modification of crops was initially based on the transgenic expression method in which the target gene is often from another organism. For example, genetically modified (GM) crops have been engineered to be herbicide or pest-resistant by expressing a herbicide tolerance gene coming from a bacterial genome or a bacterial toxin that once ingested becomes toxic to the insects. Furthermore, GM crops have also been developed to improve nutritional quality as illustrated by the “golden rice” example. This GM rice variety produces elevated levels of provitamin A in the rice grain (http://www.goldenrice.org). With the growing demand and strain on the food supply and arable land becoming limited, increasing crop yield appears to be unavoidable and since

most crops are harvested as seed, increasing the seed yield is considered a primary target. As reviewed in chapter 1, seed arises from the fertilization of the ovule by sperm cells. Its development involves a well-characterized sequence of cell division, expansion and differentiation. Therefore, one approach considered for increasing yield is to increase the final seed size by stimulating cell proliferation during the appropriate stages (see below).

A mitotic cell cycle is a tightly regulated process. As previously reviewed, cell cycle progression is governed by the activity of the complex cyclin-dependent kinase/cyclin complexes. The transition G1-S is under the control of CDKA;1 kinase complexes. CDKA can form active kinase complexes with cyclins expressed in the G1 phase, such as the D-type cyclins (Dewitte and Murray, 2003; Inze and De Veylder, 2006; Van Leene *et al.*, 2010). The study of the 10 *CYCD* gene reporter constructs during seed development indicates that they have discrete and overlapping expression patterns in the different seed tissues, which change throughout development (Collins *et al.*, 2012). Of the 10 *CYCLIN* genes, *CYCD7;1* uniquely does not appear to be expressed during seed development. It has been shown that *CYCD7;1* native expression is in late meristemoids and guard mother cell during stomatal development, as well as in sperm cells of pollen grains (Patell *et al.*, manuscript under revision).

Hence, the ectopic expression of *CYCD7;1* was performed using two methods: (1) the GAL4/UAS system and, (2) a direct construct where a specific promoter was cloned upstream (5') of the *CYCD7;1* coding sequence. The *GAL4/UAS* system has been used successfully for decades in *Drosophila melanogaster* (Fischer *et al.*, 1988; Brand and Perrimon, 1993), mammalian cells (Kakidani and Ptashne, 1988) and in plants upon adaption of the codon usage (Ma *et al.*, 1988; Haseloff and Hodge, 2001). Specific promoters drive the expression of the yeast transcription factor (TF) GAL4 that binds to the *Upstream Activator Sequence* (*UAS*) leading to the transcription of the gene placed under the control of the *UAS*. The GAL4 protein used has been modified: the activation domain of GAL4 has been interchanged with the activation domain of the TF VP16 from *Herpes simplex virus* conferring a greater potency of the TF GAL4:VP16 (Moore *et al.*, 2006). The GAL4:VP16/UAS combination has been further optimized for Arabidopsis (Haseloff and Hodge, 2001). The GAL4 DNA-binding nucleotide sequence has been modified to enhance its expression in plants (mGAL4), although the amino-acid sequence remains identical.

After fertilization and during seed development, cell division activity persists until the bent cotyledon stage. After this stage, cell expansion becomes the predominant growth-driving process (Garcia *et al.*, 2005; Le *et al.*, 2010). The divisions occur in all three components of the seed, the embryo, the endosperm and the integuments. Thus, to increase cell division,

it seems beneficial to express *CYCD7;1* during the early to mid stages of seed development. To date, a promoter has not been reported that would be active in all three seed compartments from fertilization to torpedo stage, therefore it was essential to decide in which seed compartment *CYCD7;1* would be expressed during the time of expression previously chosen. As discussed in chapter 1, studies show that the endosperm controls seed size and therefore embryo development and the proliferation and differentiation of the integuments (Garcia *et al.*, 2003; Luo *et al.*, 2005; Zhou *et al.*, 2009). Reciprocally, it has been shown that integument proliferation promotes seed and endosperm growth (Garcia *et al.*, 2005). From these studies, no specific seed compartment was obvious in which *CYCD7;1* should be expressed. However it has been shown that endosperm development and thus its nucleus proliferation was active shortly after fertilization and the endosperm goes through several rounds of syncytial mitotic division even before the zygote enters its first mitotic cycle (Boisnard-Lorig *et al.*, 2001). Moreover, the endosperm is fully developed when the embryos reach heart/torpedo stage, after which the endosperm is used to support embryo development. Therefore it seems judicious to use an endosperm-specific promoter. The promoter chosen that most closely meets the requirements of timing and pattern of expression was the *FLOWERING WAGENINGEN* (*FWA*) promoter (Kinoshita *et al.*, 2004). The *FWA* gene was primarily identified by a late-flowering phenotype in a gain-of-function mutant (Soppe *et al.*, 2000). The ectopic expression of *FWA* was due to loss of DNA methylation in the promoter region and in the first two exons and introns. The *FWA* promoter was first shown to be expressed in the flower and more specifically in the endosperm, but was not active in any of the other plant and floral tissues (Kinoshita *et al.*, 2004). The *FWA* promoter region is imprinted (Soppe *et al.*, 2000), thus *FWA* is only silenced in the mature pollen due to methylation of the promoter and is expressed in the mature female gametophyte and in the endosperm upon fertilization, until endosperm cellularization (Kinoshita *et al.*, 2004). *FWA* silencing depends on MET1, and *FWA* expression relies on the demethylation of the promoter region by DME (Kinoshita *et al.*, 2004). Moreover preliminary experiments by Collins (Collins, 2008) suggested that *FWA*-driven expression of *CYCD7;1* might increase seed size.

When studying ectopic expression of a target gene, it is desirable to verify that the target gene is expressed in the target domain and developmental window and, for this, the use of reporter genes is extremely convenient. Such reporters can be informative regarding the tissue and and developmental window of gene activity, at organ, tissue or cellular level during plant development. There is a wide variety of reporter genes that can be used, such as β-glucurodinase (GUS) or fluorescent proteins. The GUS gene (*uidA*) encodes an

enzyme β-glucurodinase that cleaves the substrate X-Gluc (5-bromo, 4-chloro, 3-indolyl β-glucuronide) producing a blue dye (Jefferson *et al.*, 1987).The presence of the cyan color indicates the tissues and time of gene activity. The first fluorescent protein isolated from the jellyfish, *Aequoria victoria* is the green fluorescent protein (GFP). Other fluorescent proteins are now available such as YFP (Yellow), CFP (Cyan) both modified GFP and DsRed (Red) naturally present in the coral *Discosoma*.

The GUS assay requires destructive sampling whereas fluorescent protein imaging is a non-destructive and sensitive method that allows subcellular localization via microscopy (Prasher *et al.*, 1992; Haseloff, 1999). The reporter can be a transcriptional or translational fusion. The first reports on the promoter activity of a gene of interest by placing the reporter gene under the control of the promoter of the native gene. The second gives information about the protein itself, by fusing in frame the reporter gene to the target gene under a desired promoter.

Here, I explore the endosperm-targeted expression of *CYCD7;1* using the *FWA* promoter. The pattern and timing of expression was analyzed using four different reporter constructs. The phenotypic consequences of the ectopic expression were analyzed based on the final seed size.

Results

3.1. Expression of *FWA* during seed development

3.1.1. Activity of the *FWA* promoter during seed development

The expression pattern of the *FWA* promoter was investigated in order to evaluate whether it was appropriate to drive the expression of *CYCD7;1* during seed development. To report *FWA* activity, two reporter lines were used: *pFWA:dFWA-GFP* (Kinoshita *et al.*, 2004) and *pFWA:3xVENUS*, constructed as part of my work. Using RT-PCR, previous results showed that *FWA* was not expressed in vegetative tissues and *FWA* transcripts were detected only in the seed during its development (Kinoshita *et al.*, 2004; Collins *et al.*, 2012). Therefore, the analysis of *FWA* reporter activity was verified in mature ovules, extracted from flowers two days following emasculation, and during seed development using developmental stages defined by Boisnard-Lorig *et al.* (2001).

My analysis of the published *pFWA:dFWA-GFP* transgenic line revealed that dFWA-GFP protein was found to be localized in the nucleus of the central cell prior to fertilization and the triploid nucleus of the endosperm 6 hours after pollination (HAP) when driven by the *pFWA* cis regulatory sequence (Fig 3.1B-C). Following fertilization, fluorescent protein was

visible in the nuclei of syncytial endosperm from stage III to V (Fig 3.1D-E). At stage VI, the dFWA-GFP was detectable in the nuclei of the endosperm, which could be characterized into domains defined by the different nucleus sizes (Fig 3.1F). The GFP signal started decreasing in early cellularized endosperm at stage VIII and disappeared completely in cellular endosperm surrounding a heart stage embryo (Fig 3.1G-H). dFWA-GFP signal was absent in a mature male gametophyte (Fig. 3.1A). These results corroborate the expression pattern published by Kinoshita *et al.* (2004).

The p*FWA:dFWA-GFP* construct contains the first two exons and the intervening intron of the *FWA* gene (*dFWA*, as described in chapter 2), corresponding to the homeodomain and a nuclear localization signal of FWA protein. To assess whether the presence of *dFWA* affects reporting the activity of the promoter, by for example stabilizing the GFP, a p*FWA:3xVENUS* line was constructed. This was also intended to provide information on whether the targeted expression of CYCD7;1 could be achieved by a direct *FWA* promoter-*CYCD7;1* fusion (*FWA:CYCD7;1*). To facilitate the monitoring of *FWA* expression, the fluorescent protein was targeted to the nucleus of expressing cells by a nuclear localization signal. In mature ovules prior to fertilization, *FWA* activity was detectable through VENUS fluorescence in the nucleus of the central cell (Fig 3.1K). From stage II of endosperm development, concomitant with zygote formation arising from the fertilization of the egg cell up to stage IV-V, VENUS protein was visible in the nuclei of the syncytial endosperm (Fig 3.1L-M). At the dermatogen stage of embryo development, the fluorescent signal was observed in the nuclei throughout the endosperm that was reaching stage VI (Fig. 3.1N). At endosperm stage VII, *FWA* activity was detected in the nuclei localized at the micropylar and chalazal poles (Fig. 3.1O). *FWA* activity was not visible in any seed compartment or the cellularized endosperm concomitant with heart stage of embryo development (Fig. 3.1P). Occasionally the VENUS signal could be observed in mature pollen grains (Fig 3.1I-J).

The analysis of the *pFWA:dFWA-GFP* and *pFWA:3xVENUS* reporters showed similar activity of FWA in the central cell of the female gametophyte prior to fertilization and after fertilization, in the endosperm until its cellularization. However, stochastic expression of *pFWA:3xVENUS* was found in mature pollen grains, whereas *pFWA:dFWA-GFP* was not.

Figure 3.1. Activity of the *FWA* promoter during seed development.

Activity of the *FWA* promoter during seed development was observed using a *pFWA:dFWA-GFP* line (Kinoshita *et al.*, 2004) and a *pFWA:3xVENUS* line. Activity of the *FWA* promoter was followed by the fluorescent proteins, dFWA-GFP or 3xVENUS respectively. Seed developmental stages are those described in Boisnard-Lorig *et al.* (2001).

(A-H) Localization of dFWA-GFP in the mature pollen grain and during seed development

(A) dFWA-GFP is absent in mature pollen grains.
(B) Expression in the nucleus of the central cell, two-day maturation after emasculation.
(C) Expression in the triploid nucleus of the endosperm 6 hours after pollination (HAP).
(D) Detectable dFWA-GFP in the syncytial endosperm at stage III.
(E) Detectable dFWA-GFP in the syncytial endosperm at stage V.
(F) Presence of fluorescence protein in nuclei of stage VI endosperm.
(G) Expression of dFWA-GFP in nuclei of stage VIII endosperm.
(H) No visible dFWA-GFP in a cellular endosperm surrounding a heart stage embryo.

(I-O) Localization of 3xVENUS nucleus-targeted in the mature pollen grain and during seed development, reflecting the activity of the *FWA* promoter region in the absence of the homeodomain dFWA.

(I-J) Occasional expression of the *FWA* promoter is detectable in the mature pollen grain.
(K) 3xVENUS signal is visible in the nucleus of the central cell, two-day maturation after emasculation.
(L) After the first syncytial mitosis in the endosperm the signal is detectable in the 2 daughter nuclei.
(M) VENUS protein was visible in the syncytial endosperm at stage IV-V.
(N) Fluorescent protein was observed in the nuclei throughout the endosperm at stage VI.
(O) Fluorescent signal is localized mainly at the micropylar and chalazal poles of the endosperm.
(P) 3xVENUS is not visible in the cellularized endosperm at stage VIII-IX.

Scale bars: A, I and J, 25 µm; B-H and K-P, 50 µm. B-H and K-P: scale bars are only shown in B and K.

Abbreviations: cc, central cell; ec, egg cell; sy, synergids; I, integuments; en, endosperm; e, embryo; su, suspensor; ch, chalzal pole; mp, micropylar pole.

pFWA:dFWA-GFP
A
B
i
cc
ec
+
sy
ch
mp
C
en
z
D
E
F
G
H
e
pFWA:NLS-3xVENUS
I
J
K
L
M
N
O
P

3.1.2. Expression of *CYCD7;1* under the *FWA* promoter

To achieve seed-targeted expression of *CYCD7;1*, two strategies were used. The first was to use transgenic lines with the two component *GAL4/UAS* system (Collins *et al.*, 2012), and the second was to generate new constructs which used the *FWA* promoter upstream of the *CYCD7;1* coding sequence (see below). To verify that *CYCD7;1* is indeed expressed in the endosperm at the early stages of seed development, two reporters were available: *FWA>>CYCD7;1/*eGFP (Collins *et al.*, 2012) and *FWA:dFWA-CYCD7;1-VENUS*, the latter being constructed as part of this work.

FWA>>CYCD7;1 lines also carried a *UAS:eGFP-GUS* cassette on the same T-DNA. As *eGFP* and *CYCD7;1* are expressed under the same promoter, *GFP* expression should inform on *CYCD7;1* expression. A recent study using the same lines showed that expression of *UAS:eGFP* did not display any visible GFP in the absence of GAL4, ruling out background activation, and *FWA>>CYCD7;1/eGFP* was never detectable in vegetative tissues (Collins *et al.*, 2012). Staged analysis of this latter line, *FWA>>CYCD7;1/eGFP*, during seed development showed that GFP signal was detectable in endosperm tissue from stage I, matching the early event of fertilization, to stage VIII, at which point the endosperm starts to become cellularized and the embryo reaches early heart stage (Fig 3.2B-F). GFP signal was localized in the cytoplasm and not in the nucleus, due to the native GFP protein not carrying a nucleus-targeting signal domain. From stage IX of endosperm development, the GFP was not visible in the endosperm or in any other seed tissues (Fig. 3.2G). In mature pollen grains no signal was observed (Fig. 3.2A). The GFP localization from the *FWA>>CYCD7;1/eGFP* line appeared to match the *FWA* promoter activity determined from the analyses of the *pFWA:dFWA-GFP* and *pFWA:3xVENUS* reporters.

To monitor the expression of *CYCD7;1* under the control of the *FWA* promoter region and the accumulation of CYCD7;1 protein, two translational reporters were generated: *FWA:CYCD7;1-VENUS* and *FWA:dFWA-CYCD7;1-VENUS*.

The analysis of more than 50 lines of *FWA:CYCD7;1-VENUS* revealed no detectable GFP fluorescence during any stages of seed development. This could be caused by a technical issue in generating transgenic lines such as low expression of the *CYCD7;1* from the construct or a rapid turn-over of the protein preventing the detection of any GFP signal, GFP requiring post-protein folding maturation of the chromophore. The second hypothesis is that the absence of signal in *FWA:CYCD7;1-VENUS* lines reflects that the protein is not

expressed in this tissue possibly due to premature termination of transcription before GFP is transcribed.

However, the monitoring of *CYCD7;1* seed-targeted expression was possible using the *FWA:dFWA-CYCD7;1-VENUS* construct during seed development. As the VENUS is at the C-terminus of CYCD7;1 and no cleavage site had been added between the CYCD7;1 and the VENUS, the presence of the signal is likely to report accurately the presence of the protein. The protein is localized in the diploid nucleus of the central cell or in the triploid nucleus of the endosperm at stage I, as the fertilization event was in this case difficult to assess (Fig. 3.2I). The signal persisted in nuclei of endosperm at stage II and stage V (Fig. 3.2J-K). From stage VIII-IX, when the endosperm cellularized, the VENUS signal disappeared (Fig. 3.2L). As *FWA:dFWA-CYCD7;1*-VENUS carries the two methylated DNA regions restricting the expression in the female parts, it is not surprising that I did not find any signal in mature pollen grains (Fig. 3.2H).

Transcriptional and translational reporters of the *FWA* promoter and CYCD7;1 protein appeared to have matching localization and timing of detectable GFP meaning that the expression patterns are similar. Under the control of the *FWA* promoter region, CYCD7;1 protein appeared to be localized to the mature central cell of the female gametophyte prior to fertilization and in the endosperm of developing seeds until stage IX of endosperm development, matching the heart stage of embryo development. These results also show that the *FWA* promoter used is sufficient to give a normal expression pattern and the dFWA containing a portion of FWA is not required.

Figure 3.2. *CYCD7;1* expression under the *FWA* promoter region.

The localization of CYCD7;1 was followed during seed development using *FWA>>CYCD7;1/*eGFP and *FWA:dFWA-CYCD7;1-VENUS.* Seed developmental stages are those described in Boisnard-Lorig *et al.* (2001).

(A-G) In the *FWA>>CYCD7;1* line, the localization of *CYCD7;1* protein can be inferred by the use of green fluorescent protein GFP that is under the control of the same promoter, *UAS*. When the *UAS* promoter is activated by the TF GAL4, itself expressed under the control of the *FWA* promoter, CYCD7;1 and GFP are expressed. Hence, *GFP* expression should reflect *CYCD7;1* expression. In this construct the GFP is not nuclear targeted.

(A) No GFP detectable in the mature pollen grains.
(B) GFP is localized in the mature cell or stage I endosperm (Fertilization event was not recorded, hence the two stages are complex to distinguish).
(C) Expression of GFP is noticeable in stage II endosperm.
(D) GFP signal is observed in stage IV endosperm.
(E) Detectable GFP in the syncytial endosperm at stage V.
(F) Detectable GFP in the syncytial endosperm at stage VI-VII.
(G) Presence of fluorescence protein was not detectable in the endosperm at stage VIII-IX.

(H-L) In the transgenic *FWA:dFWA-CYCD7;1-VENUS* line, CYCD7;1 is tagged with modified yellow fluorescent protein (VENUS) at its N-terminal. Therefore the visualization of VENUS reflects the localization of CYCD7;1. Homeodomain dFWA has a nuclear localization sequence; thus the signal appears in the nuclei of the expressing tissues.

(H) No detectable expression in the mature pollen grain.
(I) VENUS signal is visible in the diploid nucleus of the central cell or in the triploid nucleus of the endosperm at stage I as the fertilization was in this case difficult to assess.
(J) After the first syncytial mitosis in the endosperm, the signal is detectable in the 2 daughter nuclei.
(K) VENUS protein was visible in the syncytial endosperm at stage V.
(L) Fluorescent protein was observed in the nuclei throughout the endosperm at stage VI.

Scale bars: A and J, 25 µm; B-G and I-L, 50 µm. B-G and I-L. Scale bars are only shown in B and I.

Abbreviations: cc, central cell; ec, egg cell; sy, synergids; I, integuments; en, endosperm; ch, chalzal pole; mp, micropylar pole.

FWA>>CYCD7;1/eGFP
A
B
I
cc
ec + sy
ch
mp
C
en
D
E
F
G
pFWA:dFWA-CYCD7;1-VENUS
H
I
J
K
L

3.2. Endosperm-targeted *CYCD7;1* expression using a GAL4/UAS enhancer trap system

3.2.1. GAL4/UAS system for endosperm-targeted *CYCD7;1* expression

The above analysis shows that the mGAL4:VP16/UAS system is suitable for specific expression of *CYCD7;1* in the endosperm of seeds during early development. As shown above, the *FWA* promoter has a domain-specific expression pattern restricted to the central cell and endosperm, and a time-specific expression pattern from mature central cell to cellularization of endosperm concomitant with the heart/torpedo stage of embryo development. *FWA:GAL4* and *UAS:CYCD7/UAS:eGFP-GUS* lines and lines with both constructs (referred to as *FWA>>CYCD7;1*) were available in the laboratory (Fig. 3.3A) (Collins *et al.*, 2012). The first step was to confirm that the lines were carrying the T-DNA of interest and were homozygous for the insert. The presence of the T-DNA was verified using diagnostic primers which discriminate between the integrated and native *CYCD7;1* and *FWA* promoter. The homozygosity of the antibiotic or herbicide resistance marker present on the T-DNA was confirmed: homozygous plants will produce seeds that are 100 % resistant on GM plates supplemented with the antibiotic or herbicide for which they carry the resistance marker.

A diagnostic primer pair binding the *FWA* promoter and *GAL4* was used to screen resistant seedlings for transgenes and *FWA:GAL4* and *FWA>>CYCD7;1* lines showed a DNA band of 320 bp following PCR analysis, suggesting that the insert was present in both of these lines (Fig. 3.3B). The *UAS:CYCD7;1* insert was detected using primers amplifying a 200 bp fragment between *UAS* and *CYCD7;1*. Both *FWA>>CYCD7;1* and *UAS:CYCD7;1* lines were confirmed to carry the insert. To confirm that lines with the *UAS:CYCD7;1-UAS:eGFP-GUS* insertion carried the whole cassette the presence of *UAS:eGFP-GUS* was also examined by PCR, revealing a 400 bp fragment. Hence both the control line *FWA:GAL4* and *UAS:CYCD7;1* and the line of interest *FWA>>CYCD7;1* carried the integrated transgene. Moreover, *Columbia-0 WT* (*Col-0*) controls did not reveal the presence of these transgenes. *Col-0* was sensitive to both PPT and kanamycin. *FWA:GAL4* was 100% resistant on kanamycin but 100% sensitive on PPT, indicating that the line is homozygous for *FWA:GAL4* transgene. *UAS:CYCD7;1* seeds were 100% resistance on PPT and 100% sensitive on kanamycin, consistent with the line being homozygous for the *UAS:CYCD7;1* construct. *FWA>>CYCD7;1* was 100% resistant on both PPT and kanamycin suggesting that the line is homozygous for both constructs.

For each confirmed line, fresh seeds were harvested and used to grow plants from which seeds collected were analyzed for their final seed size.

3.2.2. Endosperm-targeted *CYCD7;1* expression using *GAL4* driven by the *FWA* promoter produced seeds with an enhanced final size.

The line of interest, *FWA>>CYCD7;1*, was compared to three experimental controls: *WT* (*Col-0)*, a line without activator (*UAS:CYCD7;1-UAS:eGFP-GUS)* and a line without effector (*FWA:GAL4)*. Mature dry seeds were collected at the same time and stored under the same conditions. Pictures of seeds were taken at low magnification with a dissection microscope and analyzed using a plug-in for ImageJ custom designed by Dr Manuel Forero-Vargas to determine projected seed area, length and width (see Chapter 2).

WT seeds measured on average 95,952 ± 9,039 μm^2 (n=1086), with a length of 439 ± 19 µm and a width of 258 ± 17 µm (Fig. 3.3C-F). *FWA:GAL4* (n=998) and *UAS:CYCD7;1-UAS:eGFP-GUS* (n=909) seeds had an area of 95,034 ± 7,852 μm^2 and 94,861 ± 7,742 μm^2, respectively, with a length of 456 ± 15 and 463 ± 17 µm respectively and a width of 263 ± 15 µm and 261 ± 14 µm respectively. *WT*, *UAS:CYCD7;1-UAS:eGFP-GUS* and *FWA:GAL4* seeds were not significantly different (two-way ANOVA, p=0.46 and 0.12) (Fig. 3.3C-F). *FWA>>CYCD7;1* seeds (n=743) measured 491 ± 21 µm long and 282 ± 14 µm wide, significantly longer (12% increase) and 9% wider than *WT*, *UAS:CYCD7;1-UAS:eGFP-GUS* and *FWA:GAL4* seeds (one-way ANOVA, $p=3.6x10^{-6}$ for the length compared to *WT* and $p=4.1x10^{-5}$ for the width compared to *WT*). The projected surface was of 108,870 ± 7,564 μm^2. On average *FWA>>CYCD7;1* seeds were larger than the *WT* ($p=1.20x10^{-8}$), with an increase of 13% in the seed area.

Figure 3.3. Seed-targeted expression of *CYCD7;1* using the *GAL4/UAS* system.

(A) Schematic representation of *mGAL4:VP16/UAS* system implemented for Arabidopsis. The activator line contains a promoter sequence - in this study, *FWA* promoter – driving the expression of the modified yeast transcription factor (TF) mGAL4:VP16. Expression of the GAL4 TF is restricted to cells expressing the *FWA* promoter. Effector line contains *Upstream Activation Sequence* (*UAS*), the target sequence of the GAL4 TF which drives the expression of the genes of interest: in this study, the *CYCD7;1* and *eGFP/GUS* reporters. When the activator and effector cassettes are in the plant (often generated by crossing), *GAL4* expressed specifically in the domain and time of *FWA* activity is able to activate the *UAS* promoter leading to the expression of *CYCD7;1* and *eGFP/GUS*.
Arrows indicated with number show the position of primers used for genotyping. (Modified from Weijers *et al.*, 2003).

(B) DNA gel showing the genotype of lines used to evaluate a seed size variation. Primer set 21 + 23 amplifies a 320 bp fragment from the *FWA:GAL4* insert. Primer set 22 + 25 amplifies a 200 bp fragment from *UAS:CYCD7;1* insert and primer set 22 + 24 amplifies a 400 bp fragment from the *UAS:eGFP/GUS* transgene (when using an elongation time of 20 second). Table below the gel shows the percentage of resistant seedlings growing on GM with PPT (% PPT^R) or with kanamycin (%Kan^R). RPS5A was used as a loading control.

(C-E) Comparison of seed area (C), seed length (D) and seed width (E). Error bars show ± SE. (*) indicates a statistical difference in variation of seed size parameters.

(F) Mature dried seeds from self-fertilization of *WT*, *FWA:GAL4*, *UAS:CYCD7;1* and *FWA>>CYCD7;1* plants. Scale bars: 500 µm.

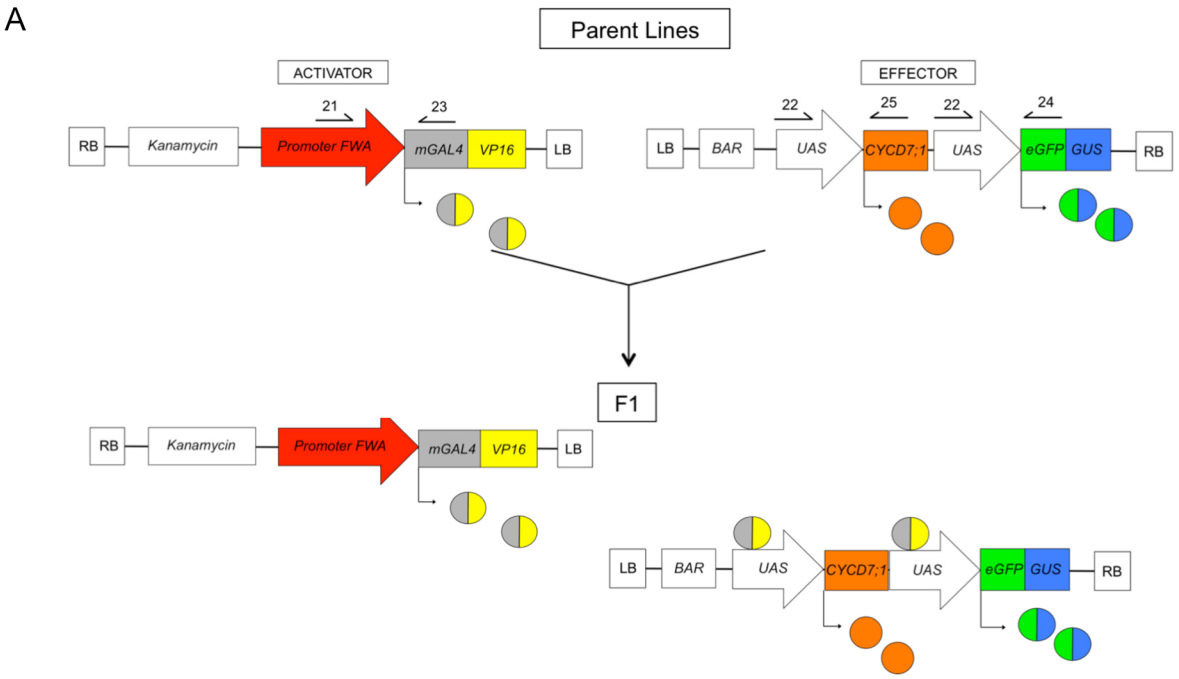

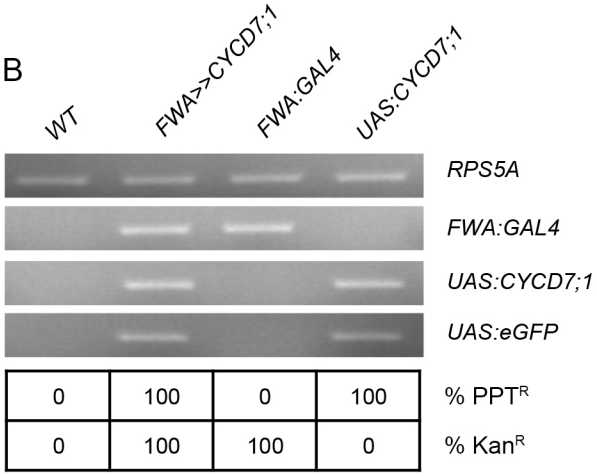

0	100	0	100	% PPT^R
0	100	100	0	% Kan^R

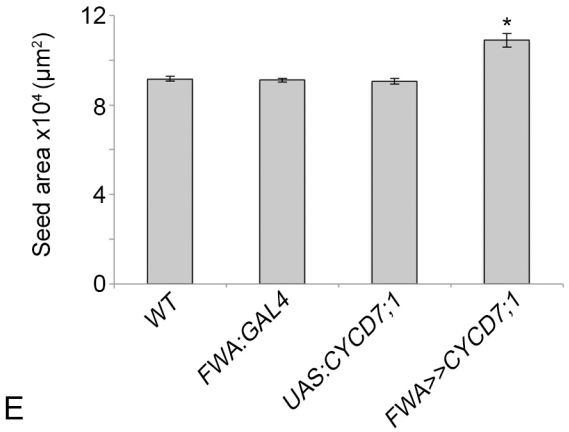

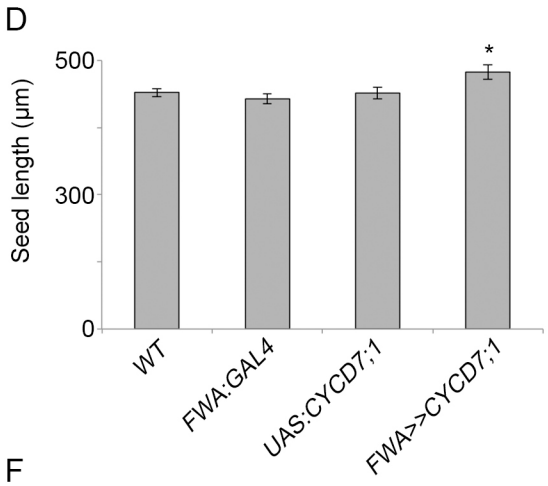

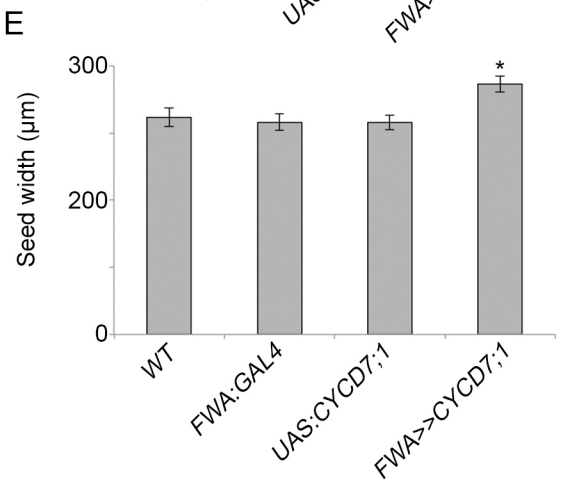

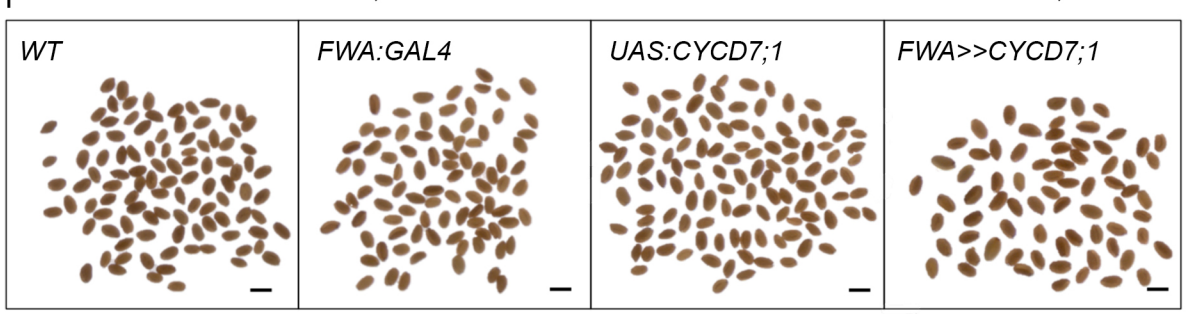

3.2.3. *CYCD7;1* has a greater effect on size seed when the number of seeds produced is reduced.

Some studies suggest that the number of seeds produced by the sporophyte has an effect on individual seed size (Paul-Victor and Turnbull, 2009; Herridge *et al.*, 2011). I sought to address whether the effect of $_{seed}$*CYCD7;1* expression depended on the resources available. Each plant was grown in identical conditions using single pots but the plant architecture was modified forming three different groups. Plants of the first group had only a primary stem growing and producing seeds; all axillary and secondary branches were removed. In this case, referred to as "SUPRA" conditions, the resources were allocated to a presumably smaller number of siliques/ seeds (Fig. 3.4A). In the second group, plant architecture was untouched and plants were grown in "NORMAL" conditions. In the last group, the primary stem was cut soon after the floral transition. This leads to the production of many stems producing a larger number of side branches and presumably a higher number of seeds. This was referred as "SUB" conditions. For each group, SUPRA, NORMAL and SUB, nine plants were grown.

An effect of plant architecture on seed size was found (two-way ANOVA, $p=1.18x10^{-47}$; Fig 3.4B). However, a Bonferroni test showed that the seed size of *WT* plants was not significantly different between NORMAL and SUPRA conditions (98,063 ± 7,053 μm^2 and 99,684 ± 8,819 μm^2 respectively; p=0.94) but in SUB conditions the seed size was about 4% smaller (94,573 ± 8,994 μm^2). The same was observed for *FWA>>CYCD7;1* seeds: grown on normal and supra conditions, plants produced seeds with a similar area (106,364 ± 9,377 μm^2 and 108,550 ± 10,241 μm^2 respectively, p=0.76), and smaller seeds when grown in SUB conditions (90,621 ± 8,793 μm^2). These results suggest that maximum seed size is not strongly resource limited, since removal of side branches had little effect.

There is also an effect of genotype on final seed size (two-way ANOVA, $p=3.95x10^{-45}$). In NORMAL plants, *FWA>>CYCD7;1* seeds were significantly 8% larger than the *WT*, confirming previous results. In SUPRA conditions *FWA>>CYCD7;1* seeds also showed a 9% increase on the overall area. However, in SUB growth conditions *FWA>>CYCD7;1* seeds were 4% smaller than the *WT*. The study of length and width showed results similar to those observed for the overall size (Fig 3.4C-D). This suggest that the manifestation of the CYCD7;1 conferred enlarged seed phenotype is dependent on the availability of sufficient resources.

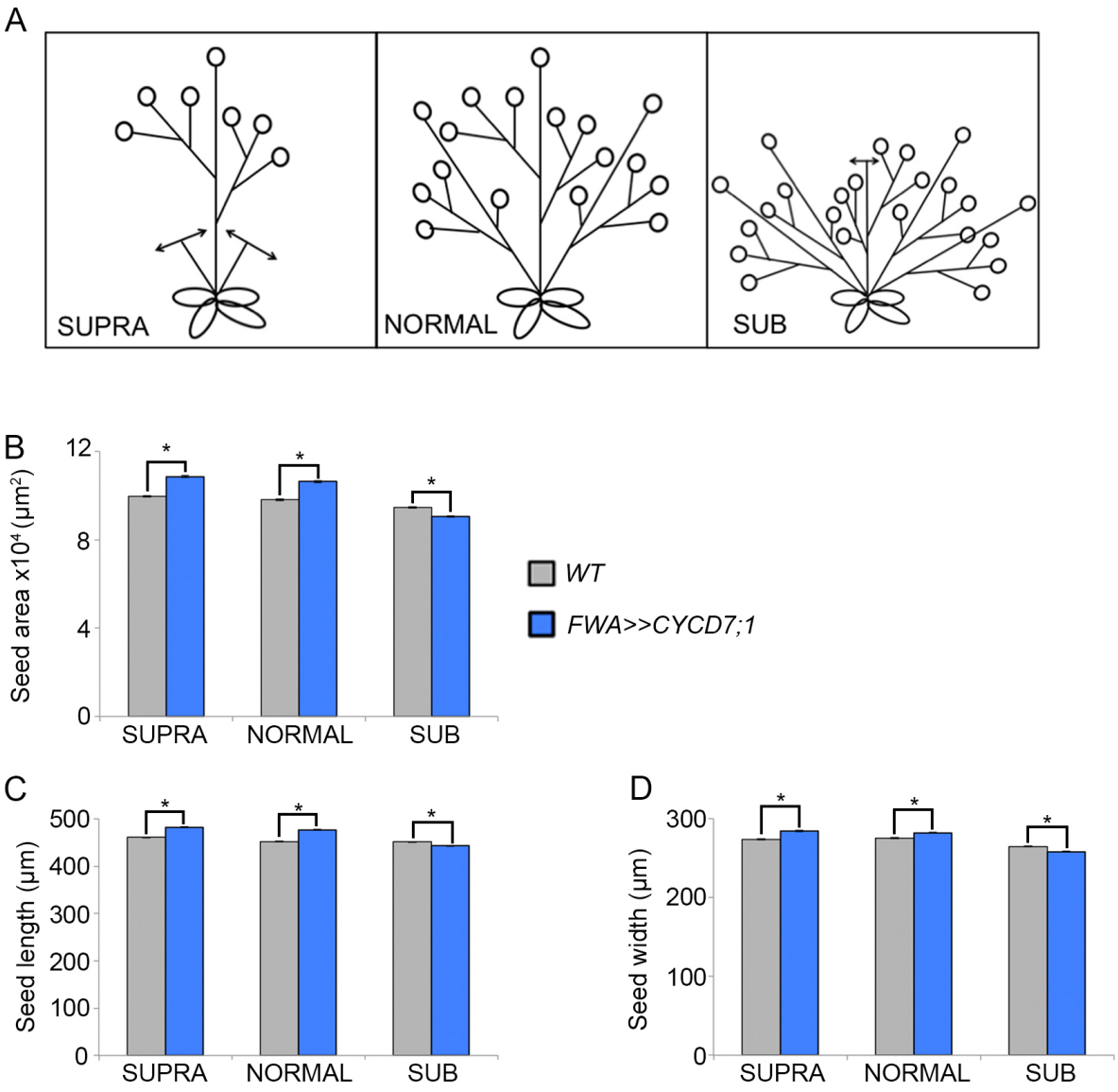

Figure 3.4. Influence of plant architecture and resource availability on seed size.

(A) Experimental design. In SUPRA conditions, all axillary and secondary branches were removed leading a reduced number of seeds produced. In NORMAL conditions plant architecture was untouched. In SUB conditions, the primary stem was cut soon after the floral transition thus allowing of the branching stem producing a higher number of seeds.

(B-C) Comparison of seed features between the different growth conditions. Mean seed area (B), mean seed length (C) and mean seed width (D). Error bars show ± SE. (*) indicates a statistical difference in variation of seed size parameters.

3.3. Endosperm-targeted *CYCD7;1* expression using a single direct promoter-gene construct

Ultimately the enlarged seed phenotype could be introduced into crops, especially in *Brassica* crops such as oilseed rape. Crops are often hybrid and carry multiple copies of their genome. For example, *Brassica napus* is an amphidiploid carrying the *Brassica rapa* and *Brassica oleracea* ancestral genome. The GAL4/UAS system has two main drawbacks in this respect. Firstly, it has never been used in *B. napus* before and it is therefore not known whether the system could work. Secondly, the GAL4/UAS as it has been used in this study requires homozygosity for both of the two T-DNAs, one carrying the *GAL4* activator under control of the desired promoter and the second carrying the effector protein of interest under the control of *UAS.* Given the time-consuming procedure for transforming *B. napus,* and the generation time, it would take a long time to generate this system in *B. napus* (4n chromosomes). Finally regulatory issues would be expected in a crop using an additional transgene. A transformation where the promoter *FWA* driving the expression of *CYCD7;1* directly seems more appropriate for crop transformation.

3.3.1. Generation of *FWA* promoter constructs directly driving *CYCD7;1* expression

Before potentially transferring the technology to crops, it was necessary to check in *Arabidopsis* that a single construct for endosperm-specific expression of *CYCD7;1* by the *FWA* promoter confers the same phenotype as the one obtained with the GAL4/UAS two component system. Two constructs were designed and created (Fig 3.5A). The same *FWA* promoter used in GAL4/UAS was used, corresponding to ~3300 bp upstream of the start codon. This promoter fragment also contains the 5'UTR of *FWA* gene. Moreover, in the *FWA:GAL4* cassette, the *FWA* promoter was followed by *dFWA* (section 2.6 and 3. 1.1) cloned in frame with *GAL4*. Therefore, in the first construct, the *FWA* promoter fragment plus *dFWA* was cloned in frame with the *CYCD7;1* coding sequence previously used in the GAL4/UAS system (section 2.6 and 3.1.1; Fig. 3.5A). Although previously *CYCD7;1* expression in endosperm could not be visualized without the homeodomain, the possible effect of *CYCD7;1* activity was unknown, so an untagged version containing 3300bp of the *FWA* promoter upstream the *CYCD7;1* coding sequence was also constructed to assess the consequence of the homeodomain on the enlarged seed phenotype.

Based on the herbicide resistance markers carried by the T-DNA, independently transformed lines carrying a single T-DNA insertion were isolated (T2 seeds showing a 3:1 resistant:sensitive ratio on selection medium): four with *FWA:CYCD7;1* transgenes and three with *FWA:dFWA-CYCD7;1.* They were annotated 6499, 6484, 12489 and 14054 for

FWA:CYCD7;1 and, 8543, 8555 and 8591 for *FWA:dFWA-CYCD7;1.* RT-PCR was performed to compare the level of *CYCD7;1* expression. RNA extraction was performed on 3 siliques starting their elongation after pollination and having the stigma and style emerging from the flower. Primers used were amplifying the 3' region of *CYCD7;1* but the comparison with the *WT* sample did not show overexpression. This was presumably due to the fact that the native *CYCD7;1* is expressed in the stomatal lineage of the epidermis of floral organs (Patell *et al.,* manuscript under revision). As spatial and temporal windows of *FWA:(dFWA)-CYCD7;1* expression in seed development are narrow, the overexpression was likely not detected in the background of native CYCD7;1 expression. Ultimately, RT primers were designed to amplify a fragment specific to the inserted region and the level of expression was compared relatively between the different transgenic lines (Fig 3.5B*). FWA:CYCD7;1* lines 6499 and 6484 showed the strongest levels of expression of the transgene, *FWA:CYCD7;1* lines 12489 and 14054 had lower levels, with line 14054 the lowest. The three *FWA:dFWA-CYCD7;1* lines showed an ectopic expression level lower than the lowest *FWA:CYCD7;1* line 14054. Among the three *FWA:dFWA-CYCD7;1* lines, 8543 showed the strongest level of ectopic *CYCD7;1* expression.

3.3.2. *FWA:CYCD7;1* produces enlarged seeds and the increase is greater than that using the GAL/UAS system

The four *FWA:CYCD7;1* lines and the three *FWA:dFWA-CYCD7;1* lines were grown and the size of the seed produced was further characterized. In order to compare the final size of dry, homozygous T3 $_{seed}$*CYCD7;1* seeds, lines were grown next to *WT* controls. Lines were sown at the same time, grown side-by-side under the same conditions of light and humidity. After harvesting, T4 seeds simultaneously with *WT* seeds were left at 42°C for 7 days. Pictures of seeds were taken and seed area, length and width measurements were generated using the SeedAnalyzer plug-in in ImageJ (see chapter 2). For each experiment, 6 to 9 plants were grown for each genotype and line, and at least 500 seeds were scored. After verifying normality of the population and homoscedasticity, ANOVA tests were performed using a significance level (α) of 0.05.

Col-0 WT seeds measured on average 101,841 ± 9,266, being on average 459 ± 22 µm long and 279 ± 14 µm wide (n=783) (Fig 3.5C-E,G). *FWA:CYCD7;1* line 6499 produced seeds with a mean area of 145,835 ± 21,2103 µm^2 . On average, the length was of 592 ± 38 µm and the width 309 ± 20 µm (n=862). The *FWA:CYCD7;1*$_{6499}$ seeds were significantly larger with an average increase of 43% for the area, 29% for the length and 11% for the width ($p=4.81\times10^{-58}$ for the area, $p=1.86\times10^{-79}$ for the length and $p=4.03\times10^{-35}$ for the width). Seeds from *FWA:CYCD7;1* line 6484 had a mean area of 13,3192 ± 19,925 µm^2, corresponding to an increase of 28% (n=807 , $p=5.32\times10^{-23}$). Seed length and width were

551 ± 35 µm and 307 ± 19 µm respectively, equivalent to an increase of 19% and 10% respectively ($p=1.37x10^{-38}$, $p=1.85x10^{-47}$, respectively). *FWA:CYCD7;1* line 12489 produced seeds 19% larger than the *WT* with a mean area of 121,742 ± 15,501 μm^2 ($n=625$, $p=3.68x10^{-30}$), a length of 522 ± 32 µm (13% increase, $p=2.83x10^{-43}$) and a width of 298 ± 18 µm (6% enlargement, $p=1.96x10^{-39}$). *FWA:CYCD7;1* line 14054 seeds underwent an area increase of 15% with a mean value of 117,198 ± 17,658 μm^2 ($n=904$, $p=6.9x10^{-67}$). The seeds were on average 501 ± 35 µm long and 298 ± 18 µm wide ($p=1.75x10^{-75}$; $p=2.37x10^{-56}$).

In order to determine if the *FWA* imprinted promoter region is sufficient or if the homeodomain *dFWA* is also required for the enlarged seed phenotype, or alternatively whether *dFWA* sequence affects the *CYCD7;1* fusion, the seed size of the transgenic line carrying *FWA:dFWA-CYCD7;1* was investigated (Fig 3.5C-E,G). Line 8543 had seeds with a mean area of 112,642 ± 9,997 μm^2 (11% increase with $p=7.43x10^{-26}$, $n=530$), average length of 490 ± 20 µm (7% increase, $p=3.14x10^{-12}$) and an average width of 292 ± 15 µm (4% increase, $p = 3.76x10^{-10}$). Line 8555 seeds were 10% larger than WT (111,879 ± 8,243 μm^2, $p=2.03x10^{-15}$, $n=831$), 5% longer (483 ± 21 µm, $p=4.57x10^{-13}$) and 5% wider (293 ±14 µm, $p=6.25x10^{-7}$). Seeds from line 8591 were 5% larger (106,594 ± 8,309 μm^2, $p=5.90x10^{-7}$, $n=755$) with a 4.5% increase length (480 ± 22 µm, $p=1.43x10^{-9}$) but a width that was not significantly different from that of *WT* (281 ± 16 µm, $p=0.402$).

The seed size range from *FWA:CYD7;1* lines 6499 and 6484 was wider than that of *WT* even though the population distribution followed a normal distribution (Fig 3.5F). *FWA:CYD7;1* line 12489, 14054 as well as *FWA:dFWA-CYD7;1* line 8543 showed a distribution similar to the *WT*, whereas *FWA:dFWA-CYD7;1* line 8555 and 8591 had a population with a narrower distribution than that of *WT.*

Figure 3.5. Seed-targeted expression of *CYCD7;1* using direct expression driven by the *FWA* promoter.

(A) Schematic representation of *FWA:CYCD7;1* (top) and *FWA:dFWA-CYCD7;1* (bottom) transgenes. The first construct was constructed by cloning ~3300 bp *FWA* promoter including the 5'UTR of *FWA* in upstream of the *CYCD7,1* coding sequence. The second cassette was constructed by cloning ~3300 bp *FWA* promoter and the 2 first exons with the intron in between, in frame with the *CYCD7,1* coding sequence. The *FWA* promoter region and the 5' genic region, and CYCD7;1 coding sequence were identical to the one used with the GAL4/UAS system.
Arrows indicated with numbers show the positions of primers used for RT-PCR.

(B) Expression of *FWA:CYCD7;1* and *FWA:dFWA-CYCD7;1*. cDNA was prepared from 3 siliques starting their elongation based on the stigma and style protruding from the flower. RT-PCR was performed using *ACTIN2* (*ACT2*, primer pair 9 and 10 in chapter 2) for normalization and transgene-specific primers (primer pair 11 and 12 in chapter 2). A ~950 bp fragment was amplified for *FWA:CYCD7;1* and ~1400 bp for *FWA:dFWA-CYCD7;1*.
Col-0 WT was used to ensure that the primer set 11+12 was specific to the transgene.

(C-E) Comparison of seed area (C), seed length (D) and seed width (E).

(F) Histogram showing the population distribution for the seed area. Curve represents an expected normal distribution. Similar histograms could be observed for length and width (not shown).

(G) Mature dried seeds from self-fertilization of *FWA:CYCD7;1* and *FWA:dFWA-CYCD7;1* plants. Scale bars: 500 µm

On graphs: Error bars show ± SE. (*) indicates a statistical difference in variation of seed size parameters compared to the *WT*.

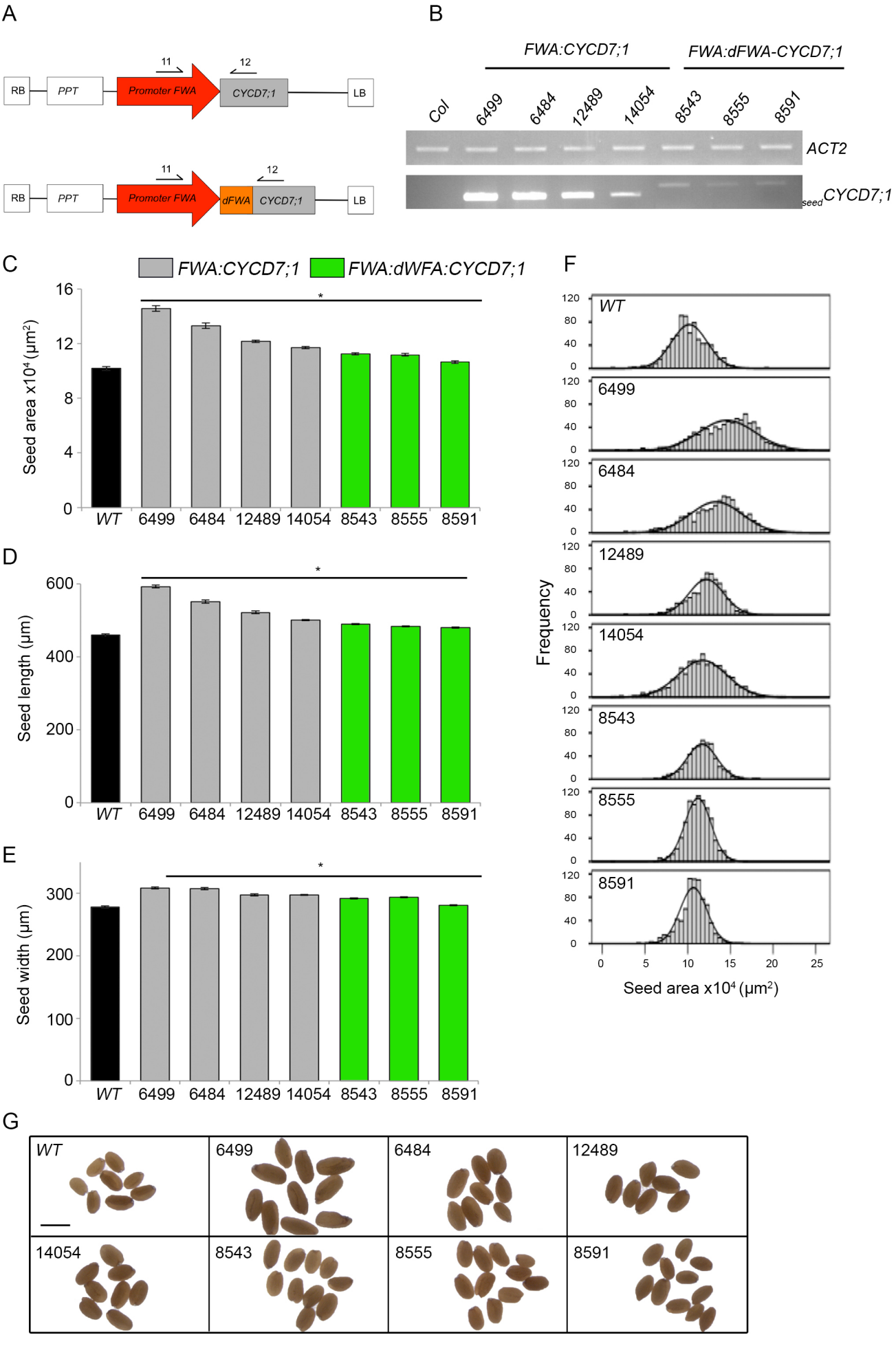
A
RB
PPT
Promoter FWA
CYCD7;1
LB
11
12
dFWA
B
FWA:CYCD7;1
FWA:dFWA-CYCD7;1
Col
6499
6484
12489
14054
8543
8555
8591
ACT2
seed CYCD7;1
C
FWA:CYCD7;1
FWA:dWFA:CYCD7;1
Seed area x10⁴ (µm²)
WT
D
Seed length (µm)
E
Seed width (µm)
F
Frequency
Seed area x10⁴ (µm²)
G

Comparing segregated siblings to establish the effects of CYCD7;1

To ensure that the enlarged seed size phenotype is due to the additional copy of *CYCD7;1* with seed targeted expression, and not due to indirect effects conferred by the transformation procedure, the seed size of $_{seed}$*CYCD7;1* was compared to seeds from *WT* plants isolated from a segregating population. Heterozygous T3 seeds were grown on soil and T4 seeds were collected from individual plants. According to Mendelian genetics, 25% of T4 seeds should be homozygous *WT*, 25% homozygous for the insert, and 50% hemizygous for the transgene. Based on the antibiotic resistance marker, homozygous *WT* and $_{seed}$*CYCD7;*1 were isolated. These seeds were measured and analyzed as above (Fig. 3.6).

WT seeds had a mean area ranging from 110,977 μm^2 (line 12489) to 128,764 μm^2 (line 6499). *Col-0 WT* control not coming from a segregating population had a mean area of 118,477 μm^2. In the same experiment, *WT* seeds from line 6499 were slightly bigger than *Col-0* seeds (p=0.015) whereas *WT* seeds from line 12489 were smaller than untransformed *WT* seeds (p=0.026). *WT* seeds from 6484 and 14054 were not significantly different than the untransformed *WT* seeds (120,433 μm^2, p=0.89 and 115201 μm^2, p=0.34, respectively). Homozygous $_{seed}$*CYCD7;1* seeds had an area of 158,603 μm^2 (line 6499), 154,275 μm^2 (line 6484), 149,006 μm^2 (line 12489) and 135,532 μm^2 (line 14054). For each line, the homozygous mutant seeds were all significantly larger than the segregating *WT* and untransformed *WT* (two-way ANOVA, p=7.17x10^{-19}).

WT seeds coming from a segregating population have a distribution similar to the untransformed *WT*. As previously observed, homozygous gain of function *CYCD7;1* mutant seeds have a broader distribution of population and consistently produce larger seeds (Fig. 3.5H-I).

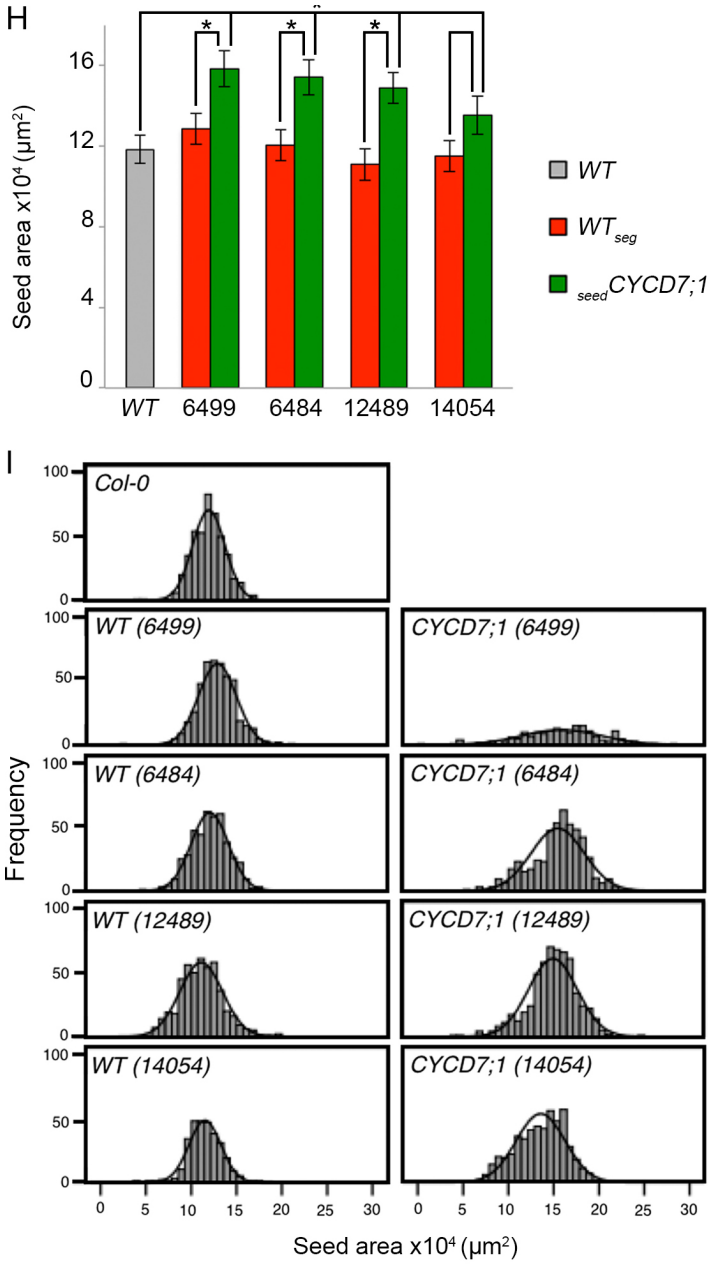

Figure 3.6. Seed-targeted expression of *CYCD7;1* using direct expression driven by the *FWA* promoter (continued).

(H) Comparison of seed area. *WT* (grey bar) is an untransformed *WT*. WT_{seg} (red bars) is a homozygote *WT* plant isolated from a segregating population. $_{seed}CYCD7;1$ (green bars) is from a homozygous plant for the *FWA:CYCD7;1* transgene. (*) indicates a statistical difference.

(I) Histogram showing the population distribution for the seed area. Curve represents an expected normal distribution. Similar histograms could be observed for length and width (not shown).

On graphs: Error bars show ± SE. (*) indicates a statistical difference in variation of seed size parameters compared to the *WT*.

3.3.3. The enlarged seed size phenotype is conferred by the expression of *CYCD7;1* in the female gametophyte

The $_{seed}$*CYCD7;1* transgenic line produced seeds with an enlarged overall size, and in these lines CYCD7;1 expression was under the control of the *FWA* promoter. The imprinting of the *FWA* promoter region confers female gametophyte specific expression due to a lack of methylation of the maternal genome (Kinoshita *et al.*, 2004). However it has also been shown that part of the imprinting lies in the 5' genic region of *FWA* (Soppe *et al.*, 2000) and I previously showed that occasional expression of *FWA* could be picked up in the mature pollen grain. To determine whether the cause of the enlarged seed phenotype lies in the expression of *CYCD7;1* in the female gametophyte and developing endosperm, reciprocal crosses between *Col-0 WT* and *FWA:CYCD7;1* lines were performed. If the imprinting is not disrupted, *FWA:CYCD7;1* should be expressed only in the female gametophyte and only maternal copies of *FWA:CYCD7;1* should be sufficient to confer the phenotype. Therefore, analyzing F1 seeds coming from directional crosses can be used to address this question.

WT x *WT* seeds had an area of 102,289 ± 10,456 μm^2 (Fig. 3.7). When pistils were pollinated with pollen coming from the plant *FWA:CYCD7;1,* seeds were significantly larger with areas 148,347 ± 24,947 μm^2 (line 6494, 45% increase), 143991 ± 21,835 μm^2 (line 6484, 40% increase), 125761 ± 21,355 μm^2 (line 12489, 23% increase), 116749 ± 18,356 μm^2 (line 14054, 14% increase), (one-way ANOVA, $p=3.4x10^{-47}$). When *FWA:CYCD7;1* pistils were pollinated with *WT* pollen, seed sizes were similar to the seeds produced by self fertilization (one-way ANOVA, p=0.32). For the four $_{seed}$*CYCD7;1* lines, seeds were larger than *WT* x *WT* (one-way ANOVA, $p=1.44x10^{-20}$). *WT* pistils were pollinated with *FWA:CYCD7;1* pollen. Seeds produced had an average area that was not significantly different from the size of seeds from *WT* x *WT* (p=0.35), but were significantly smaller than the size of seeds from *FWA:CYCD7;1* self-fertilized plants ($p=3.9x10^{-4}$).

These results show that the production of enlarged seed is defined by the genotype of the female gametophyte.

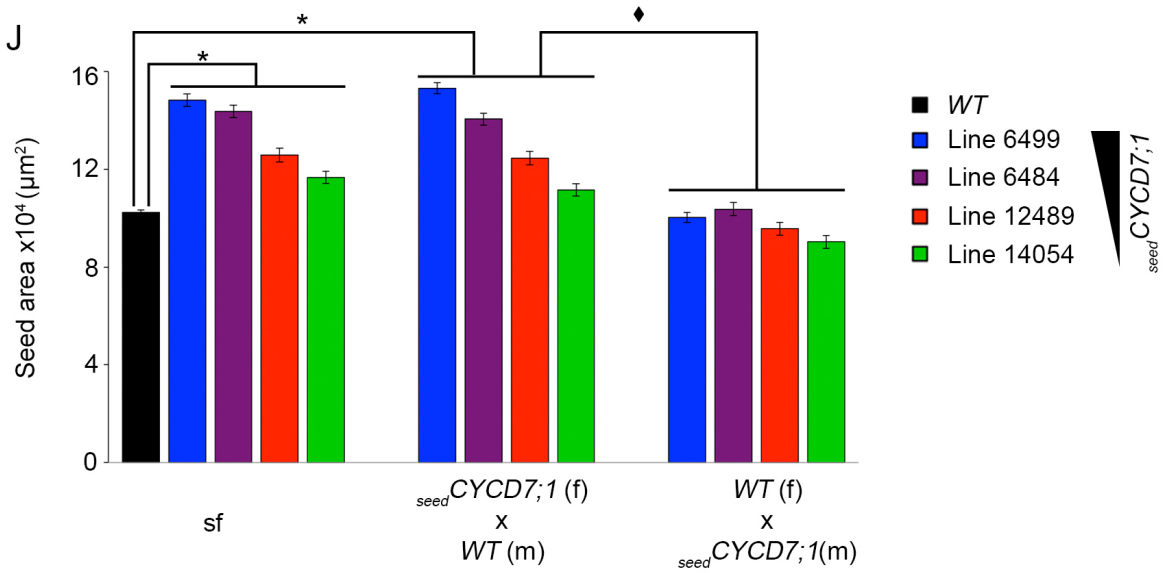

Figure 3.7. Enlarged seed produce by the seed-targeted *CYCD7;1* expression lines is maternally conferred.

Comparison of F1 seed generated by crossing *WT* and $_{seed}$*CYCD7;1*. (sf) F1 seeds are from a cross where the pistil and the pollen are from the same plant. Genotype of the female gametophyte (f) and genotype of the male gametophyte (m). (♦) indicates that seed size between $_{seed}$*CYCD7;1* (f) x *Col-0* (m) and (*) *Col-0* (f) x $_{seed}$*CYCD7;1* (m) is statistically different, comparing line by line.

Error bars show ± SE. (*) indicates a statistical difference in variation of seed size parameters compared to the *WT*.

Discussion

Endosperm-targeted ectopic expression of *CYCD7;1* was performed in the attempt to engineer seeds with an enhanced size. *FWA* activity has been shown to be maternal gametophyte-specific (Kinoshita *et al.*, 2004). This specificity is due to a hypomethylation in the promoter and 5' genic regions of *FWA* (Soppe *et al.*, 2000). Another study showed that the methylation required for the imprinting lies in two tandem repeat sequences located in the promoter region of the *FWA* gene (Fujimoto *et al.*, 2008). Initially, I confirmed that the *FWA* promoter was suitable for endosperm-specific expression and determined whether the 5' genic region (dFWA) was required for the endosperm-specific expression. Therefore, *FWA* activity was followed using one reporter line containing the *FWA* promoter and the 5' genic region encoding the dFWA protein fragment fused to GFP (*FWA:dFWA-GFP)* (Kinoshita *et al.*, 2004) and one reporter line containing the *FWA* promoter only, driving VENUS, a fast folding YFP variant (*FWA:3xVENUS)*. My results showed that, with both reporters (*pFWA:dFWA:GFP* and *pFWA:3xVENUS*), prior to fertilization, the *FWA* activity was detectable in the mature central cell of the female gametophyte. After fertilization, I showed that the *FWA* activity occurred in the endosperm during its development until stage IX when it cellularizes, concomitant with the embryo reaching the heart stage. Corroborating results have been published by Kinoshita *et al.* revealing a similar expression pattern of *FWA* in the female gametophyte and the seed during its development (2004). Moreover, in this same study, RT-PCR results showed that the *FWA* activity is detectable only in the female gametophyte and developing seed and no *FWA* mRNA could be found in vegetative tissues, buds, placenta and embryos. However, I also showed that without the 5' genic region of *FWA* (*dFWA*), a stochastic expression could be observed in a fraction of the mature pollen grains. This novel result may suggest that the degree of methylation is lower due to the absence of the 5' genic region, and thus the *FWA* expression is not restricted to the female side.

In this study, using *FWA>>CYCD7;1/eGFP* and *FWA:dFWA-CYCD7;1-VENUS* reporters, *CYCD7;1* expression under *FWA* promoter activity showed that CYCD7;1 protein was expressed and localized in the mature ovule and in the developing endosperm until its cellularization (Stage IX). The absence of detectable expression in the mature male gametophyte from these two lines could be explained by the presence of the *dFWA* fused to either GAL4 or to CYCD7;1 directly. No clear results regarding the requirement of *dFWA* for CYCD7;1 to display an endosperm-specific expression were found, as none of the *FWA:CYCD7;1-VENUS* reporter lines showed a detectable signal allowing me to follow the expression.

To engineer seed size by expressing *CYCD7;1* in seeds, two approaches were taken. The first one used the *GAL4/UAS* system where the *FWA* promoter drives the expression of the GAL4 transcription factor that activated the activity of the *UAS* promoter controlling the expression of *CYCD7;1*. The second method was to generate transgenic lines with *FWA:CYCD7;1* and *FWA:dFWA-CYCD7;1* transgenes. This method has two main advantages: (1) it can be transferable to crop plants such as Brassica and (2) it allows to assess whether or not the *dFWA* homeodomain-containing fragment fused to the *CYCD7;1* is required to engineer seed size.

$_{seed}$*CYCD7;1* expression led to the production of enlarged seeds. Using the GAL4/UAS system, the *FWA>>CYCD7;1* line produced seeds that were 13% larger than *WT*. Both length and width were increased but the length underwent a greater change (12%) than the width (9%). Here the investigation of the effect of plant architecture and theoretically the number of siliques and thus seeds produced per each parent sporophyte on final seed size was performed. The plant architecture was modified by either removing side branches reducing the number of seed produced, or removing the main stem thus allowing branching and a greater number of seeds to be produced. There were genotype effects, growth condition effects and an interactive effect between the genotype and the growth condition on the final seed size. When comparing growth conditions, both *WT* and $_{seed}$*CYCD7;1* produced larger seed in normal and supra conditions compared to the sub conditions. In normal and supra conditions, $_{seed}$*CYCD7;1* expression lead to the production of enlarged seeds whereas in sub conditions, $_{seed}$*CYCD7;1* expression produced smaller seeds than the *WT* plants. When the number of side branches and presumably the number of seeds produced was reduced, $_{seed}$*CYCD7;1* expression conferred a beneficial trait in terms of seed size increase but when the number of side branches is increased by removal of the primary shoot $_{seed}$*CYCD7;1* expression has a deleterious effect on size by reducing the size below the *WT* average.

Using *FWA:CYCD7;1* and *FWA:dFWA-CYCD7;1*, seeds displayed an enhanced size ranging from a 15% to a 43% increase for the first transgene and from 5 to 10% for the second transgene. There was a correlation between the level of expression and the enlargement: the line with a higher level of *CYCD7;1* expressed during seed development produced a greater increase in seed size than the line with a lower level of expression. The line with the higher level of $_{seed}$*CYCD7,1* expression had a population distribution with wider spread. The averages of seed features were increased but the characteristics of half of the population overlap with the *WT*. Another feature of seed size increase was that the length appeared to be more affected than the width, producing slender seeds that were less round

than the *WT*. The presence of the *dFWA* protein fragment fused to *CYCD7;1* during early seed development did not seem to give an additional effect on seed size. However, isolated lines expressing the chimeric *dFWA-CYCD7;1* showed a lower level of *dFWA-CYCD7;1* than the line expressing *CYCD7;1*. To show a biological effect of the *dFWA* protein fragment, lines with a similar level of expression would be necessary. While doing the screening of transgenic lines with one T-DNA insert and normal development, only a low level expressing line could be isolated.

The enhanced seed size phenotype was confirmed to be due to *CYCD7;1* expression in seed by comparing the size of seed from plants homozygous for the transgene to *WT* plants coming from the same segregating population. Both *WT* plants, *Col-0 WT* untransformed and *WT* plants coming from a segregating population, produced seeds with a size similar to the *Col-0 WT* and to the homozygous. Therefore, the enlarged seed size phenotype arose from the expression of *CYCD7;1* in the endosperm during early seed development and not from a secondary effect of the transformation process.

Here I showed that *CYCD7;1* can be expressed in the ovule and endosperm of developing seeds. Moreover, *CYCD7;1* endosperm-specific expression led to an enlarged seed size that depends on the maternal origin of the *pFWA:CYCD7;1* transgene, as revealed by directional crosses with *WT*. These results supports that imprinting of the *FWA* promoter is sufficient to target *CYCD7;1* expression only in the female gametophyte and confers a increased final seed size phenotype.

Chapter 4

Effects of Endosperm-Targeted Expression of *CYCD7;1* on Seed Development

Chapter 4
Effects of Endosperm-Targeted Expression of *CYCD7;1* on Seed Development

Introduction

In flowering plants, the seed develops from a double fertilization event. The male pollen grain delivers two sperm cells via a pollen tube to the female ovule. Both the haploid egg cell and the diploid central cell are fertilized by one of the sperm cells, giving rise to a diploid embryo and a triploid endosperm respectively. Seed development is characterized by the coordinated growth of the zygotic tissues, consisting of the embryo and the endosperm, and maternal tissues that give rise to the seed coat. In Arabidopsis, a series of well-defined cell divisions patterns the embryo from the zygote to the bent cotyledon stage. From the bent cotyledon stage onwards, embryo growth occurs primarily through cell expansion (Goldberg *et al.*, 1994). Endosperm development goes through a series of synchronous syncytial divisions, then syncytial divisions become asynchronous accompanied by differentiation processes. The endosperm reaches maturity when it has become fully cellularized (Boisnard-Lorig *et al.*, 2001).This stage onwards, the endosperm tissue is used being the embryo to sustain its development. The maternal sporophytic tissues become a seed coat upon fertilization that triggers cell divisions, cell elongation and differentiation, characterized by deposition of flavonoids (Debeaujon *et al.*, 2003).

The production of viable seeds involves two fundamental steps: pollination and fertilization. Pollination requires the proper development of male and female reproductive structures, the androœcium and the gynœcium respectively (Smyth *et al.*, 1990; Bowman, 1994). In Arabidopsis, the androœcium is composed of a set of six stamens, each composed of an anther and a filament. The gynœcium is the set of carpels, each consisting of the stigma, which is composed of papilla cells onto which the pollen adheres, the style, and the ovary, in which the ovules attached along placenta by the funiculus. In self-pollinated plants such as Arabidopsis, coordinated development of these structures allows the deposition of pollen grains from the opened anther onto the stigma. This was suggested by the study of the *mtn* mutant where the defect in seed production was correlated with failure in the opening of flowers and manual pollination could rescue female fertility (Schruff *et al.*, 2006). However, even though pollination is an essential step, it does not by itself lead to seed

development. The fusion of male and female gametes is the key element to transform an ovule into a seed, and fertilization can happen only if the male and female gametophytes develop properly.

The male gametophyte or pollen grain is composed of one vegetative cell and two sperm cells. All arise from the two rounds of mitotic division of a haploid microspore: the first division produces one vegetative cell and one generative cell. The vegetative cell supports the development of a pollen tube that brings the two sessile sperm cells from the stigma to the female gametophyte. The generative cell divides to produce two sessile sperm cells (Twell, 2011). The female gametophyte or embryo sac arises from four mitotic divisions of one haploid megaspore. The embryo sac is therefore composed of 7 cells of which 6 are haploid (two synergids, one egg cell, three antipodiales), plus the central cell which is a diploid fusion of two haploid nuclei (Drews and Koltunow, 2011). The proper development of the gametophytes is required for physiological processes such as the pollen tube growth of the pollen grain and the production of small protein signals from the synergids leading to the attraction of the pollen tube to the embryo sac.

Micro and megagametogenesis involve a series of divisions and the control of cell cycle progression is essential for the formation of gametophytes. For example, in the *fis* mutant, the divisions of the central cell fail to arrest, producing an autonomous-endosperm in the absence of fertilization, leading to seed development failure likely linked to the absence of a developing embryo (Grossniklaus *et al.*, 1998; Kohler *et al.*, 2003; Leroy *et al.*, 2007). *MSI1* is a *FIS*-class gene, which has been shown to be directly bound by RBR (Jullien *et al.*, 2008). Indeed, the *rbr1* mutant displays supernumerary nuclei in the sperm cells of the pollen as well as in the central cell in the absence of fertilization, but unlike *fis*, the central cell does not acquire endosperm identity (Ingouff *et al.*, 2006; Johnston *et al.*, 2008; Chen *et al.*, 2009). As reviewed in chapter 1, *CDKA;1* is a regulator of the transition between the cell cycle phases (De Veylder *et al.*, 2003). In *cdka;1-1/+*, bicellular pollen is produced that fertilizes only the egg cell leading to developing seeds that eventually abort (Nowack *et al.*, 2006). The bicellular pollen of the *cdka;1-1* mutant results from a failure to complete mitosis producing the two sperm cells from the generative cell, therefore the single generative cell remains in G2. It has been postulated that the fusion of gametes occurs only if the gametes are in the same cell cycle phase (Berger *et al.*, 2006). In tricellular pollen such as Arabidopsis, male gametes are arrested in S-phase (Friedman, 1999). The control of the cell cycle is essential to achieve normal gametophyte development.

Upon fertilization, a seed is generated and the coordination of various cellular processes in the three compartments determines its size (Chaudhury and Berger, 2001). As reviewed in chapter 1, defects in embryo development in *fis2-5* and *ede1-1* mutants as well as defects of endosperm development in *iku2* and *mini3* lead to smaller seeds correlated with a reduction of cell elongation in the seed integuments (Garcia *et al.*, 2003; Hehenberger *et al.*, 2012). Changes in the cell proliferation, elongation and differentiation of the seed integuments impair seed size and embryo and/or endosperm development. In *sin1-2* mutants, ovule integuments do not develop properly; however, 30% of the ovules generated can be fertilized and produce seed with a decreased size suggesting that integuments influence seed size and proper embryo development (Robinson-Beers *et al.*, 1992; Ray *et al.*, 1996a). Defects in integument differentiation during seed development in *ttg2* also lead to integument cell size reduction with an associated reduction of endosperm size, leading to the production a smaller seeds (Johnson *et al.*, 2002). Reciprocally, overproliferation of ovule integuments in the *mtn* mutant leads to enlarged seeds with larger embryos (Schruff *et al.*, 2006). These studies show that growth of seed components is coordinated and that cross-talk between the components determines final seed size. Seed size can also be influenced by other factors such as the dosage of parent-of-origin genomes (Scott *et al.*, 1998) and the cytokinin hormone (Werner *et al.*, 2003; Riefler *et al.*, 2006). Interploidy crosses show that plants with doubled ratio of maternal genomes to paternal genomes produce smaller seeds, whereas plants with doubled paternal genome contribution produce enlarged seeds (Scott *et al.*, 1998). As previously reviewed in Chapter 1, mutants impaired in cytokinin sensing (*ahk*) or cytokinin-deficient mutants (*ckx*) produce larger seeds (Werner *et al.*, 2003; Riefler *et al.*, 2006).

In chapter 3, I showed that seed size can also be modulated by expression the *CYCD7;1* in endosperm during early phases of seed development. In this chapter, I investigated the developmental origin of the enlarged seed. Examination of the seed components was performed at tissue and/or cellular levels during seed development and seed maturation. As seeds arise from fertilization of the cells of the female gametophyte, female and male gametophytes were also inspected. The studies were performed using the *FWA:CYCD7;1* lines described in chapter 1 and these lines were referred as $_{seed}$*CYCD7;1*.

Results

4.1. Effect of endosperm-targeted expression of *CYCD7;1* on mature female gametophytes

The formation of ovules occurs within the pistil and is one of the key steps to produce viable seed. In order to investigate the effect of endosperm-targeted *CYCD7;1* expression on the mature female gametophyte, unfertilized mature gynœcia were examined. Therefore flowers were emasculated and after two days of maturation pistils and ovules were sampled.

4.1.1. Effect of endosperm-targeted *CYCD7;1* expression on ovule initiation within the pistil

Two-day elongated pistils were prepared in order to record the ovary length (from the bottom to the top of the ovary at the junction with the style) and the number of ovules prior to fertilization using a microscope with bright field illumination. *WT* pistils measured 2.08 ± 0.15 mm long and carried on average 55 ± 8 ovules (Fig. 4.1A,B,D). $_{seed}$*CYCD7;1* pistils were significantly longer with a length of 2.28 ± 0.17 mm for line 6499, 2.27 ± 0.14 mm for line 6484, 2.32 ± 0.12 mm for line 12489 and 2.34 ± 0.22 mm for line 14054 (Fig. 4.1AC; one-way ANOVA, n=30, p=0.03). The number of ovules initiated per pistil was significantly lower with 41 ovules for line 6499, 43 for line 6484, 49 for line 12489 and 47 for line 14054 compared to 55 in the *WT* (Fig. 4.1D; one-way ANOVA, n=30 pistils, $p=3.2x10^{-8}$). These results suggest that prior to fertilization the number of ovules produced is lower in $_{seed}$*CYCD7;1* and the ovule density within the cavity of the ovary was lower in $_{seed}$*CYCD7;1*. Potentially the seeds therefore have more space to grow and have less mechanical constraint and therefore more space to grow, particularly as the pistil length is increased.

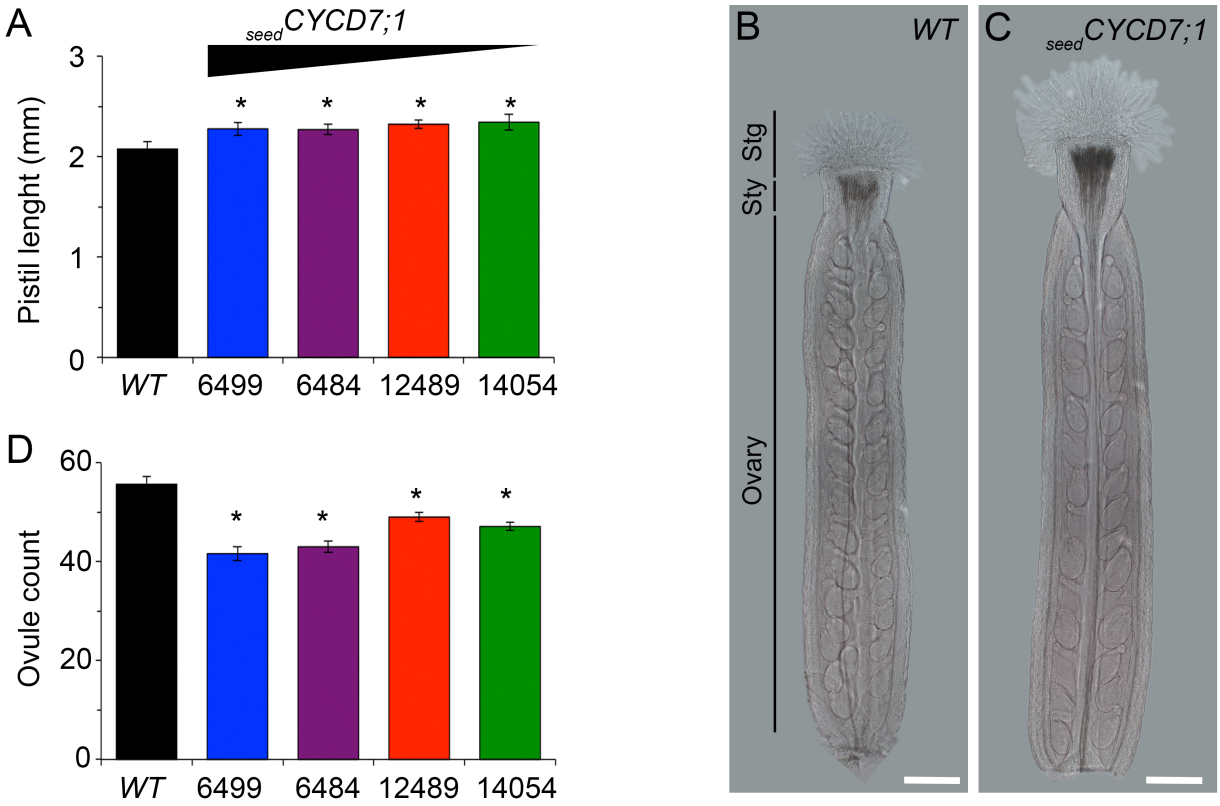

Figure 4.1. Effect of endosperm-targeted *CYCD7;1* expression on ovule initiation and associated pistil elongation.

Two-day elongated pistils from emasculated flowers were cleared and examined under a microscope. Comparison of ovary length of mature pistils (A) and number of ovules produced within the ovary (D). (B,C) DIC images of mature pistils of *WT* (B) and *seedCYCD7;1* (line 6499) (C).

Error bars show ± SE. (*) indicates a statistical difference between *WT* and *seedCYCD7;1* (n=30; p=0.03 for pistil length and p=3.2x10-8 for ovule count).

Scale bars: 200 µm.

Abbreviations: sty, style; stg, stigma.

4.1.2. Effect of endosperm-targeted *CYCD7;1* expression on cell cycle arrest in the female gametophyte prior to fertilization

As demonstrated in chapter 3, $_{seed}$*CYCD7;1* is expressed in the central cell prior to fertilization. Moreover, $_{seed}$*CYCD7;1* produced larger mature seeds and the reciprocal crosses showed that *CYCD7;1* acts maternally to influence seed size. To determine the origin of the size difference, mature ovule size was investigated. To do so, pistils were emasculated and after 2 days of maturation, ovules were cleared and observed using differential interference contrast (DIC) microscopy. *WT* ovules had an average cross sectional area of 15,097 ± 1,112 μm^2 and $_{seed}$*CYCD7;1* ovules were similar in size with 14,495 ± 1,320 μm^2 (line 6499), 15,415 ± 1,234 μm^2 (line 6484), 15,104 ± 1,070 μm^2 (line 12489), and 15,612 ± 1,359 μm^2 (line 14054) (one-way ANOVA, n=30, p=0.51; Fig. 4.2A-E).

However, the analysis of unfertilized ovules showed that in $_{seed}$*CYCD7;1* mature ovules several nuclei in the central cell were visible prior to fertilization (Fig. 4.2B-E). To confirm the presence of several nuclei in the central cell, three independent experiments in which flowers were emasculated and pistils left to mature for 2 days were performed. In two experiments, ovules were harvested, cleared and analyzed using DIC microscopy. In the third experiment, pistils were fixed (according to the procedure described in chapter 2, section 2.12.1) and ovules were stained with DAPI, then examined using confocal imaging. The overall result is shown in Fig. 4.2F. The *WT* central cell contained a single nucleus located toward the egg apparatus (Fig. 4.2B,D,F). In $_{seed}$*CYCD7;1,* depending on the line, between 20% to 50 % of the analyzed ovule, had a single nucleus (Fig. 4.2F). On average, 23% of $_{seed}$*CYCD7;1* ovules had 2 nuclei, 15% had 3 nuclei and 9% with 4 nuclei. For line 6484 and 12489 had 33% and 30 % ovules with more than 5 nuclei, respectively.

These results suggest that $_{seed}$*CYCD7;1* expression can affect the size of structures other than the seed.

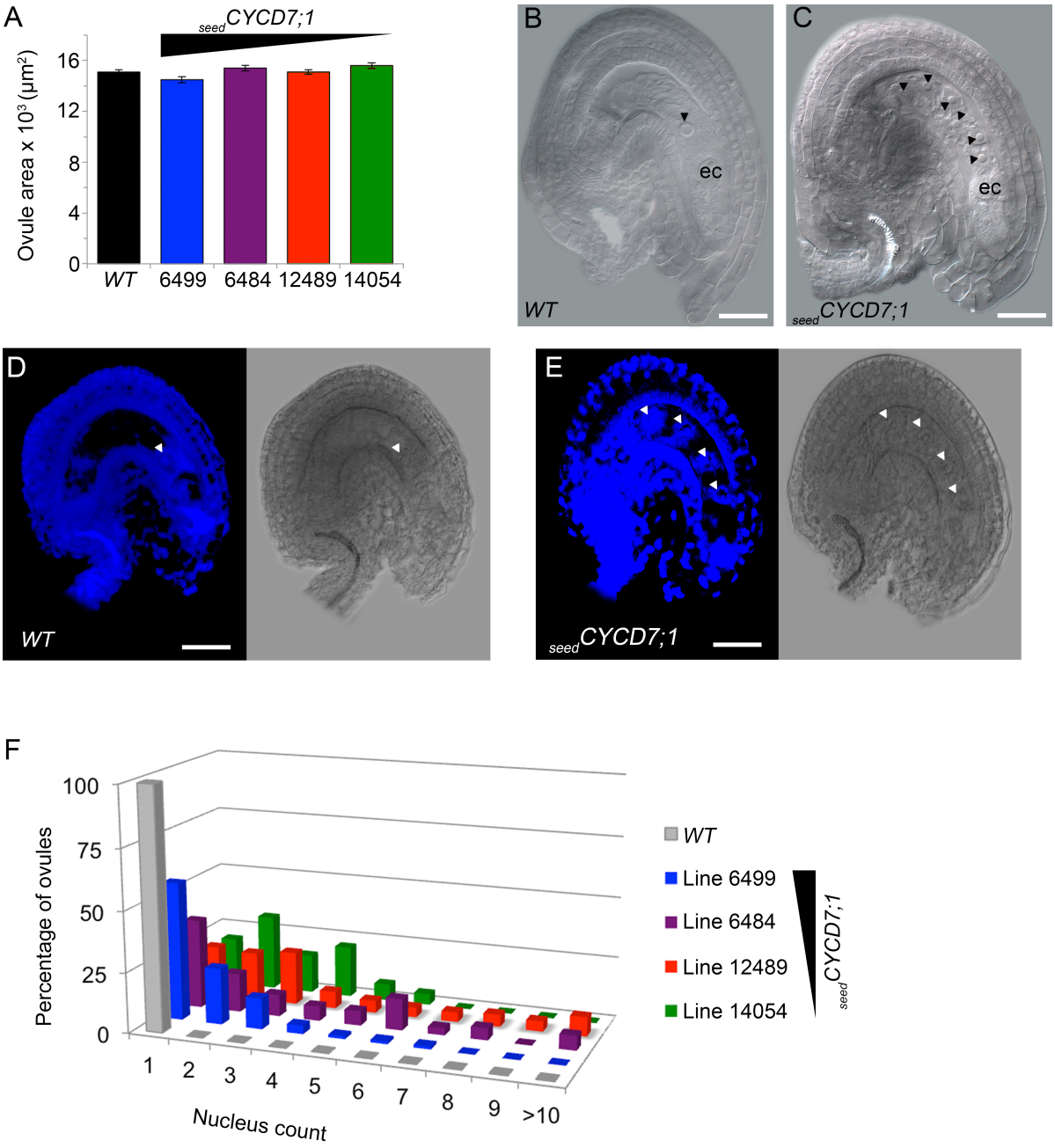

Figure 4.2. Effect of endosperm-targeted *CYCD7;1* expression on mature female gametophyte prior to fertilization.

(A-G) Comparison of mature ovule area with error bars showing ± SE (A). DIC images of *WT* ovule (B) and *seed*CYCD7;1 (line 6499) (C). Confocal images of mature ovule from *WT* (D) and *seed*CYCD7;1 (line 6499) (E) with the left-hand side picture of each panel showing DAPI-stained images and the right-hand side picture showing images using transmitted light. Arrow heads in (B-E) show a single nucleus in the mature central cell of *WT* (B,D) and supernumerary nuclei in *seed*CYCD7;1 (line 6484).

(F) Comparison of nucleus number in a non-fertilized central cell.

Scale bars: 20 µm.

Abbreviation: ec, egg cell.

4.2. Effect of endosperm-targeted expression of *CYCD7;1* on developing seeds

4.2.1. Effect of endosperm-targeted *CYCD7;1* expression on seed size during seed development

$_{seed}$CYCD7;1 produced seeds with an increased final size. To determine from which stage of development the seed size phenotype manifested itself, I recorded the size of developing seeds following controlled self-pollination. Developing seeds were dissected out and cleared with chloral hydrate for examination under DIC optics at 3, 4, 5, 6, 7, 9, days after pollination (DAP). As previously suggested in section 4.1, the ovules were no different in size and the enlargement was not visible prior to fertilization. 3 DAP, *WT* seed area measured 69,689 ± 9,368 μm^2 and *$_{seed}$CYCD7;1* seeds were not larger with an area of 64,546 ± 11,366 μm^2 (6499), 66,265 ± 13,398 μm^2 (6484), 60,230 ± 11,403 μm^2 (12489) and 61903 ± 10,338 μm^2 (14054) (one-way ANOVA, n>50, p=0.6; Fig. 4.3 and Fig. 4.3). From 4 DAP, *$_{seed}$CYCD7;1* seeds displayed a seed size larger than that of *WT*. *$_{seed}$CYCD7;1* seed area were 187,890 ± 16,643 μm^2 (6499) and 150174 ± 14,875 μm^2 (14054) and 92,836 ± 9,536 μm^2 for the *WT* seeds (two-way ANOVA, effect of the genotype on seed size, n>50, $p=5.47x10^{-7}$). At 9 DAP, the last time point recorded, *$_{seed}$CYCD7;1* areas were 237,067 ± 15,986 μm^2 (6499), 224,919 ± 19,567 μm^2 (6484), 214,672 ± 17,982 μm^2 (12489) and 186,847 ± 15,935 μm^2 (14054), and *WT* seed area was 140,552 ± 12,987 μm^2. The seed area was compared between *WT* and *$_{seed}$CYCD7;1* lines at each time point but also between the different time points (3, 4, 5, 6, 7, 9 DAP) by performing a two-way ANOVA with a Bonferroni test. Statistical analysis suggested that for each line, the seed size increased during development From 3 DAP to 6 DAP. From 6 DAP onwards, the seed size increase was not significant except for the *$_{seed}$CYCD7;1* 6499 line, which showed a significant seed size increase until 9 DAP. These results suggest that the enlarged seed size phenotype conferred by *$_{seed}$CYCD7;1* arises in the early stages of seed development (from 3 to 4 DAP) correlated with the largest relative increase in growth compared to the *WT* (191% for 6499 and 143% for 14054 relative to 33% for *WT*).

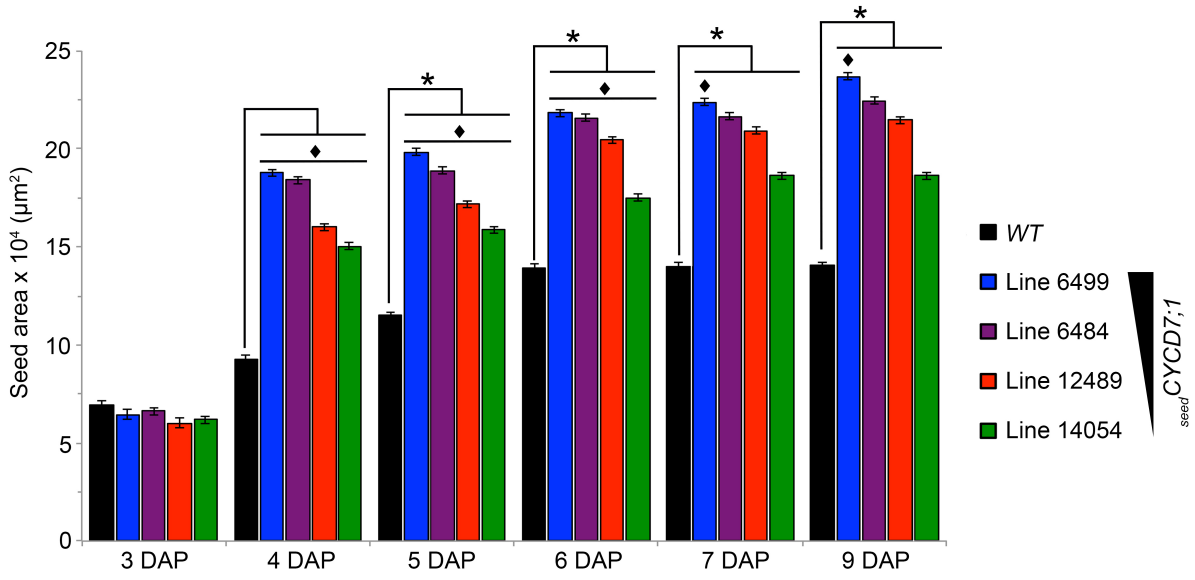

Figure 4.3. Area of developing seeds in *WT* and *seedCYCD7;1* plants.

At each time point, (*) indicates a significant difference between *WT* seeds and *seedCYCD7;1* seeds. (◆) indicates a significant different for each line with the previous time point. Error bars show ± SE.

4.2.2. Effect of endosperm-targeted *CYCD7;1* expression on seed viability in the silique

Silique length and frequency of developing seeds

Strikingly, mature siliques from $_{seed}$*CYCD7;1* plants were shorter than the *WT*. Therefore, The silique length difference was quantified by measuring the length of 5 mature siliques (stage 17 described by Alvarez-Buylla *et al.*, 2010) at position 10 to 14 from the rosette on the primary stem of 15 different plants: A *WT* mature silique measured on average 1.61 ± 0.17 cm, whereas $_{seed}$*CYCD7;1* siliques were significantly shorter with an average length of 0.86 ± 0.17 cm (line 6499), 1.20±0.22 cm (line 6484), 1.36 ± 0.17 cm (line 12489) and 1.28 ± 0.2 cm (line 14054) (one-way ANOVA, n=75, $p=3x10^{-6}$; Fig. 4.4A-B). Since the siliques were shorter, the total number of developing and aborting seed produced in each pod was recorded. In *WT* plants, the average seed count in a mature silique was 54 ± 6 (Fig. 4.4C). $_{seed}$*CYCD7;1* siliques contained on average 43 ± 7 seeds (line 6499), 46 ± 7 seeds (line 6484), 48±8 seeds (line 12489) and 48 ± 9 seeds (line 14054). The total number of seed produced in $_{seed}$*CYCD7;1* plants is significantly smaller than in *WT* plants (one-way ANOVA, n=75 $p=2x10^{-6}$). The reduced number of total seeds per silique arose during ovule initiation in the placenta, as the number of ovules produced by each transgenic line and the *WT* was similar to the final number of total seeds in a mature silique (one-sample t-test for each line: *WT*, p=0.85; 6499, p=0.71; 6484, p=0.56; 12489, p=0.91; 14054, p=0.86; Fig. 4.1). In addition, the number of aborted and developing seeds was also recorded (Fig. 4.4D), and the relative proportion of aborted/developing is shown in Fig. 4.4E. In *WT* plants, 5% of the total amount of seeds produced were aborted, whereas in $_{seed}$*CYCD7;1* plants, 80% of seeds were aborted in line 6499, 65% in line 6484, and 50% in lines 12489 and 14054. In $_{seed}$*CYCD7;1*, plants the relative proportion of lethality is substantially greater than in the *WT* (one-way ANOVA, n=75, $p=1.33x10^{-13}$).

Therefore, these results suggest that the silique length reduction is due to fewer female gametophytes being produced prior to fertilization, although the pistil is actually longer, and a larger number of aborted seeds.

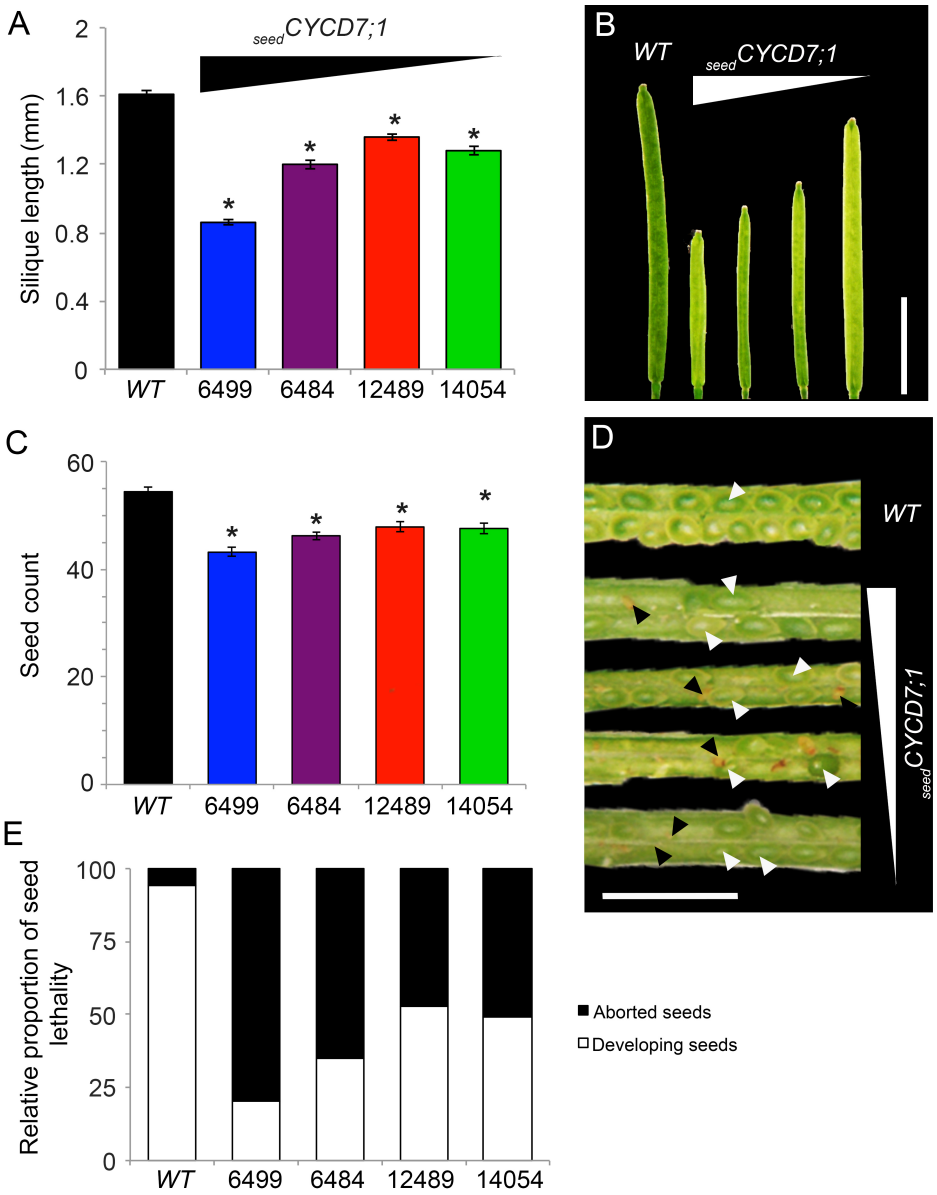

Figure 4.4. Seed lethality in developing siliques and developmental characterization of seed abortion.
Mature siliques were analyzed. The siliques developing on the primary stem from position 10 to 14 were harvested. The length, the total count of seeds and the proportion of developing/aborting seeds were recorded.

(A) Length comparison of siliques from *WT* and *seedCYCD7;1* plants.
(B) Picture of siliques at position 10 on the main stem from *WT* (first on the left) and *seedCYCD7;1* plants (from the second of the left line 6499, 6484, 12489 and 14054).
(C) Total seed count including developing and aborted seeds of the siliques from *WT* and *seedCYCD7;1* plants.
(D) Opened siliques revealing aborted seeds (black arrowhead) and developing seeds (white arrowhead) of *WT* (first on the left) and *seedCYCD7;1* plants (from the second of the left line 6499, 6484, 12489 and 14054).
(E) Relative proportion of developing/aborted seeds in siliques from *WT* and *seedCYCD7;1* plants.

Scale bars: B, 5 mm; D; 2 mm.(*) indicates a statistical difference between *WT* and *seedCYCD7;1*.

Developmental characterization of seed abortion

In $_{seed}$*CYCD7;*1 mature siliques, a large proportion of seeds aborted. It has been previously shown that the reduced fertility can be caused by mechanical failure of pollination (Schruff *et al.*, 2006). Indeed, stamens of $_{seed}$*CYCD7;1* flowers appeared to be shorter than in the *WT*. In addition, the degree of pollen deposition on the stigma seemed lower in $_{seed}$*CYCD7;1* with the reduction in the strongest $_{seed}$*CYCD7;1* expresser (6499) being higher than in the lowest $_{seed}$*CYCD7;1* expressers (12489 and 14054). Manual crosses in which stigmas were saturated with pollen from the same plant revealed that *WT* siliques produced 49 seeds with 7±8 aborting, whereas $_{seed}$*CYCD7;1* produced 38 total seeds with 26 aborting seeds (6499), and 48 seeds including 21 aborting seeds (12489, Table 4.1). When performing a manual pollination, the lethality was increased by 10% in *WT* and by 16 % and 3% in the $_{seed}$*CYCD7;1* 6484 and 14054 lines respectively (Fig. 4.4.E; table 4.2). In contrast, for $_{seed}$*CYCD7;1* 6499 the lethality was reduced by 16% and 6% in 12489 when plants were pollinated manually instead of being allowed to self-pollinate. However, the increase or decrease of lethality is not statistically significant (Table 4.2, χ^2 test, using the lethality proportion in naturally occurring pollination as expected values, p-value≤0.05).

This result suggests that mechanical pollination is unlikely to be the main factor explaining the level of seed abortion seen in $_{seed}$*CYCD7;1.*

Table 4.1. Count of aborting and developing seeds in siliques at stage 17 (mature green silique analyzed 8 DAP;(Alvarez-Buylla *et al.*, 2010)) from manually self-fertilized crosses.

		n	developing seeds	aborted seeds	total number seed
WT	*WT* x *WT*	54	42±13	7±8	49±8
$_{seed}$*CYCD7;1*	6499 x 6499	32	11±11	26±11	38±9
	6484 x 6484	52	8±5	35±8	43±7
	12489 x 12489	52	27±11	21±9	48±7
	14054 x 14054	56	22±9	25±9	47±8

Table 4.2. Comparison of seed lethality in siliques at stage 17 between naturally occuring pollination and manual crosses.

		Naturally occurring pollination		Manual pollination		
		n	% of abortion	n	% of abortion	χ^2 (p-value)
WT	*WT* x *WT*	54	14%	75	5%	0.2
seedCYCD7;1	6499 x 6499	32	80%	75	68%	0.2
	6484 x 6484	52	65%	75	81%	0.05
	12489 x 12489	52	50%	75	44%	0.4
	14054 x 14054	56	50%	75	53%	0.7

As pollination failure did not explain the observed seed abortion, early events of seed development were analyzed. Therefore, manual crosses were performed and 29 hours after pollination (HAP) seeds were cleared and examined using DIC microscopy. In *WT* plants, 100 % of the harvested seeds contained a developing embryo (Fig. 4.5A,C,D). In *seedCYCD7;1*, a developing zygote could be observed in 46% of harvested seeds of 6499, in 75% of 6484 seeds, 61% of 12489 seeds and 81% of 14054 sampled seeds. This result suggested that there is a delay or an arrest early in development. However the proportion of abortion is increased during maturation of the silique (Fig. 4.5A). This suggests that a proportion of developing embryos arrest their development. To investigate this assumption, aborted seeds from manually pollinated siliques (5 DAP) were cleared and observed under DIC optics. All arrested seeds failed to get through the globular stage, and the arrest seem to occur between the 8-cell to globular stage. However, arrested embryos seemed to be patterned correctly (Fig. 4.5E,F). These data suggest that seed development arrest happens early during development and is due to a delay early in development and a reduced potential to make the transition from a globular to heart stage embryo.

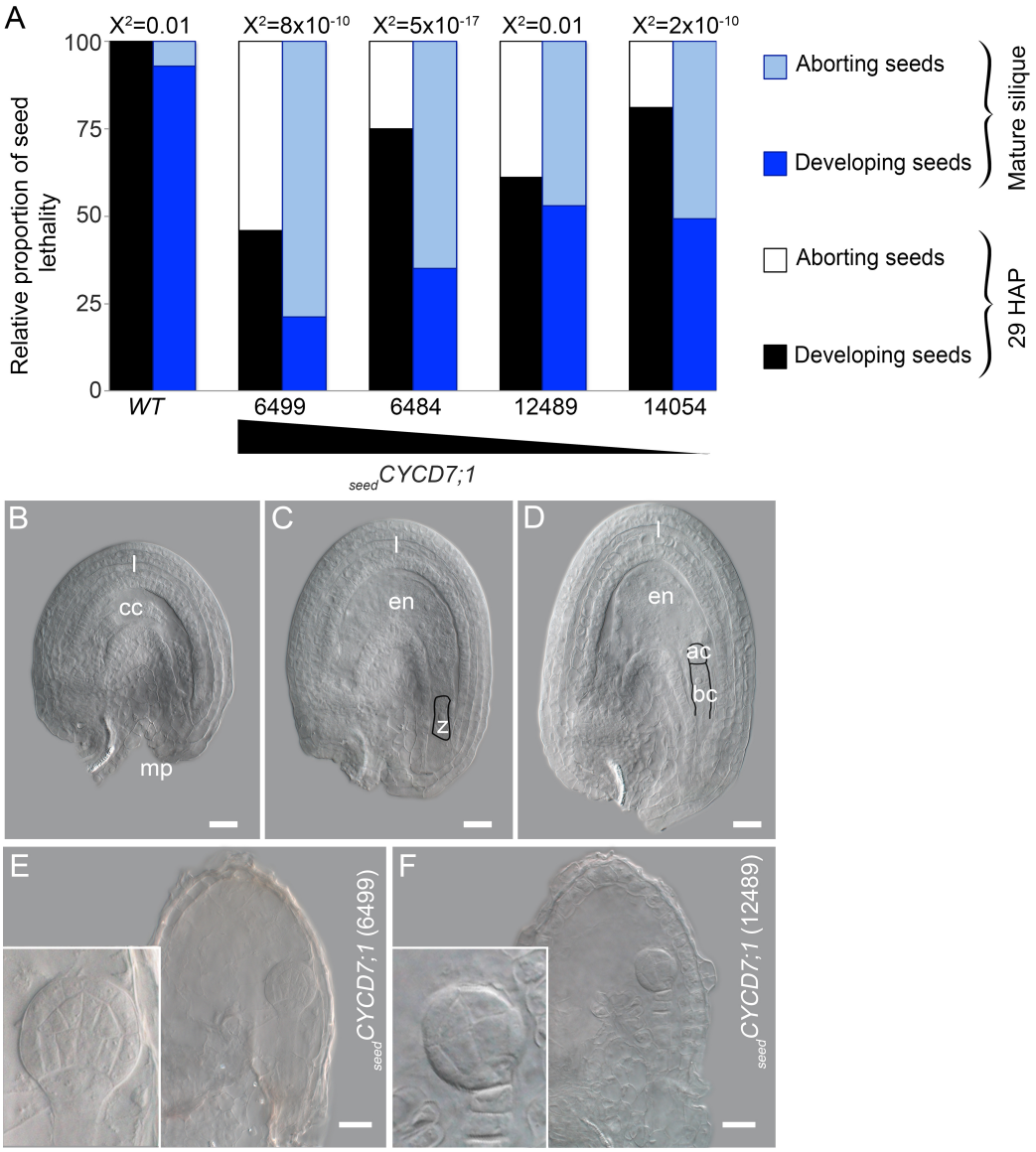

Figure 4.5. Developmental characterization of *seedCYCD7;1* seed abortion.

(A) Graph showing the proportion of developing and aborted seeds when performing manual crosses.

(B) Typical unfertilized ovule. This absence of individualized zygote and synergids, on the micropylar pole, marks the onset of degeneration.

(C,D) Progression of seed development: fertilization is indicated by the formation of the zygote on the micropylar pole and expansion of the syncytial endosperm (D). The first division of the zygote produces the two-celled embryo proper with the apical cell towards the endosperm and the basal cell towards the micropyle (E).

(E,F) 5 DAP, *seedCYCD7;1* aborting seeds were sampled. Seed integuments are degenerating, confirming that the seeds are dying. Embryos arrest at globular stage (E) and at the 16-cell stage at which point the protoderm is noticeable (F).

Scale bars: B-F, 20 µm.
Abbreviations: ac, apical cell of the embryo proper; bc, basal cell of the embryo proper cc, central cell; en, endosperm; I, integuments; mp, micropylar pole; z, zygote.

Parental-origin of seed lethality

CYCD7;1 is expressed in these experiments under the control of the *FWA* promoter. The *FWA* promoter is imprinted and active only in female reproductive structures (Soppe *et al.*, 2000; Kinoshita *et al.*, 2004). Moreover, I showed that the seed size phenotype has a maternal origin. Therefore I investigated whether the seed lethality was also due to a maternal effect. Reciprocal crosses were performed between *WT* and $_{seed}$*CYCD7;*1 plants, and the abortion proportion was recorded in both mature siliques and during early stages.

A self-fertilized manual cross on *WT* plants produced 49±8 seeds per silique with 7±8 aborting, corresponding to 14% of abortion (Table 4.3). Self-fertilized $_{seed}$*CYCD7;*1 plants produced 38 seeds per silique (line 6499), 43 for line 6484, 48 (line 12489) and 47 (line 14054). When $_{seed}$*CYCD7;*1 pistils were pollinated with *WT* pollen, the total number of seeds produced per silique and the proportion of lethality is comparable to $_{seed}$*CYCD7;*1 pistils pollinated with $_{seed}$*CYCD7;*1 pollen. For example, the pistil of the line 6499 pollinated with 6499 pollen produced 11 developing seeds and 26 aborted seeds and when pollinated with *WT* pollen, 15 seeds developed and 21 aborted (df=1, p=0.12). On the other hand a *WT* pistil pollinated with $_{seed}$*CYCD7;*1 pollen produced 50 developing seeds and 3 aborting (for the line 6499), similar to the number of seeds developing and aborting in the *WT* pistil pollinated by a *WT* pollen (df=1, p=0.54). Similar results were found for the three other $_{seed}$*CYCD7;*1 lines. This result suggests that the seed lethality is due to a maternal-origin effect.

Table 4.3. Count of aborting and developing seeds in manually self-fertilized crosses. Genotype of (f) female and (m) male.

					χ^2 test (p-value) Expected values are from the cross with	
	n	developing seeds	aborted seeds	total number seed	OE pistil	*Col-0* pistil
Col f x Col m	54	42±13	7±8	49±8		
Col f x 6499 m	30	50±5	3±3	53±4		0.544826851
Col f x 6484 m	27	44±11	5±8	50±6		0.345231072
Col f x 12489 m	33	35±10	7±7	43±5		0.236723571
Col f x 14054 m	30	40±6	3±3	43±4		0.473200418
6499 f x 6499 m	32	11±11	26±11	38±9		
6499 f x col m	36	15±2	21±5	36±4	0.12	
6484 f x 6484 m	52	8±5	35±8	43±7		
6484 f x Col m	31	8±10	34±7	42±6	0.865772375	
12489 f x 12489 m	52	27±11	21±9	48±7		
12489 f x Col m	30	21±7	20±8	41±8	0.239938989	
14054 f x 14054 m	56	22±9	25±9	47±8		
14054 f x col m	30	24±8	22±9	47±4	0.461680188	

4.2.3. Effect of endosperm-targeted *CYCD7;1* expression on embryo development

Time course of seed development

The developmental progression of $_{seed}$*CYCD7;1* lines and *WT* seeds was compared. A time course of seed development was generated in order to establish when the enlarged seed size phenotype is visible. Time points chosen were 2, 3, 4, 5, 6, 7, 9 DAP. Seeds were harvested and cleared with chloral hydrate for examination under DIC optics. 99 to 234 individual embryos were recorded for each line at each time point. The stages of embryo development recorded were those described in Fig. 1.5. In *WT* plants, 2 DAP, 56% of seeds reached the 2/4-cell stage, 36% were at the embryo proper stage and 8% were at the zygote stage (Fig. 4.6). In the strongest $_{seed}$*CYCD7;1* expresser (line 6499), only 3% of embryos reached the 2/4-cell stage, 33% the embryo proper stage and 64% were still at the zygote stage. In the lower $_{seed}$*CYCD7;1* expresser (line 14054), 23% of seeds were at the 2/4-cell stage, 54% at the embryo proper stage and 23% at the zygote stage. At 3 DAP, in *WT* plants, 20% of embryos reached the 16-cell stage, 41% the 8-cell stage, 24% the 2/4-cell and 15% were in the embryo proper stage. In $_{seed}$*CYCD7;1* plants, up to 60% of embryos were at the globular stage (line 12489), only 10% were at the 2/4-cell stage and no embryos were still at the embryo proper stage. 4 DAP, 54 % of *WT* embryos reached the globular stage, 22% the triangular stage and 5 % the heart stage, 19% were still in the 16-cell stage. $_{seed}$*CYCD7;1* embryos were mainly at the triangular and globular stages with less than 10% in the 16-cell stage and none at stages earlier than 16-cell : line 6499 had 72% embryos at the heart stage and 17% at triangular stage; line 14054 had 28% at the heart stage and 41% at the triangular stage. 5 DAP, in *WT* plants, the majority of seeds (50%) reached the globular stage but 25% were still at the transition stage and 25% at the heart stage whereas in $_{seed}$*CYCD7;1* seeds were at heart stage (74% for line 14054) or at the torpedo stage (52% for line 12089) and under 10% were at the triangular and globular stages. At 6 DAP, 32% of *WT* embryos reached the bent cotyledon stage, 52% the torpedo stage, and 16% were still at the heart and transition stages. At this specific time, the $_{seed}$*CYCD7;1* line 6499 (with the strongest expression level) showed a retarded development compared to the *WT*, with 15% of seeds at the bent cotyledon stage, 42% at the torpedo stage, 36% at heart stage and 7% at the triangular and globular stages. The $_{seed}$*CYCD7;1* line 12489 (with the one of the lowest expression level) still showed an accelerated development with 46% at the bent cotyledon stage, 49% at the torpedo stage and 5% at the heart and triangular stages. 7 DAP, 40% of *WT* seeds were at the mature embryo stage, 48% at the bent cotyledon stage and 11% between the torpedo and triangular stages. The stronger $_{seed}$*CYCD7;1* expresser 6499 still displayed a retarded

development compared to the *WT*, with 11% at the mature embryo stage, 19% of seeds at the bent cotyledon stage, 45% at torpedo stage, 22% at heart stage and 6% at triangular and globular stage. In contrast, the *$_{seed}$CYCD7;1* line 14054 (one of the lines with the lowest expression level) showed a similar development to the *WT* with 10% deviation (with 98% of seeds at the two last stages of embryo development compared to 88% in *WT*). However, in *$_{seed}$CYCD7;1* line 14054, 69% were at the mature embryo stage, 29% at the bent cotyledon stage and 2% at the torpedo stage. 100% of the *WT* and *$_{seed}$CYCD7;1* seeds reached the mature embryo stage at 9 DAP.

At very early stages of seed development (2 DAP), *WT* seeds appeared to progress faster through embryogenesis with a larger proportion of the population at the 2/4-cell stage compared to the *$_{seed}$CYCD7;1* seeds. Moreover, the stronger the level of the *$_{seed}$CYCD7;1*, the more retarded this early development was. This result is consistent with the fact that in *$_{seed}$CYCD7;1* overexpresser there is seed lethality due to a defect either at early stages of seed development or during the fertilization event. Slightly later in seed development, from 3 DAP to 5 DAP, *$_{seed}$CYCD7;1* seeds reached later stages of embryo development quicker than the *WT* seeds. This apparent early delay in *$_{seed}$CYCD7;1* might be explained if the fertilization happens at a different time in *WT* and in *$_{seed}$CYCD7;1*, or it could be a retardation of the earliest divisions. Once the fertilization occurs, the presence of CYCD7;1 in the early endosperm then supports a faster development as long as it is expressed. Finally, from 6 DAP onwards, *$_{seed}$CYCD7;1* seed development progression is similar to *WT* seed development. This could be consistent with a reduction of CYCD7;1 expression within the endosperm at this time. However, detailed analysis of the different *$_{seed}$CYCD7;1* lines showed that from 7 DAP onwards, the line with the strongest level of expression tends to be slower than the *WT* whereas seeds from the line with the lowest expression level are still further ahead in seed development progression than *WT* seeds. Interestingly, the accelerated embryo progression through the globular-heart stage occurred between 3 to 4 DAP. This time window also corresponds to the greatest relative increase of seed area (Fig.4.4).

Figure 4.6. Seed development in *WT* and $_{seed}$*CYCD7;1*.

Manual crosses were performed and seeds were cleared and examined 2, 3, 4, 5, 6, 7, 9 days after pollination. Progression of seed development was observed in $_{seed}$*CYCD7;1* lines and compared to *WT* seed development.

(A) Radar diagrams show the proportion of seed at different stages for each time point.

(B) Characteristic pictures of the typical stage present in higher proportion for each time point and in each line.
First row: seed development from *WT* plants; second row: seed development from one of the strongest $_{seed}$*CYCD7;1* (6499) and third row: seed development from one of the weakest $_{seed}$*CYCD7;1* (12489)
In all images, the chalazal pole is at the left end the micropylar pole, where the embryo is located at early stages and from which the embryo expands at later stages, is on the right. Scale bar: 50 µm (shown only in the first of B).

A

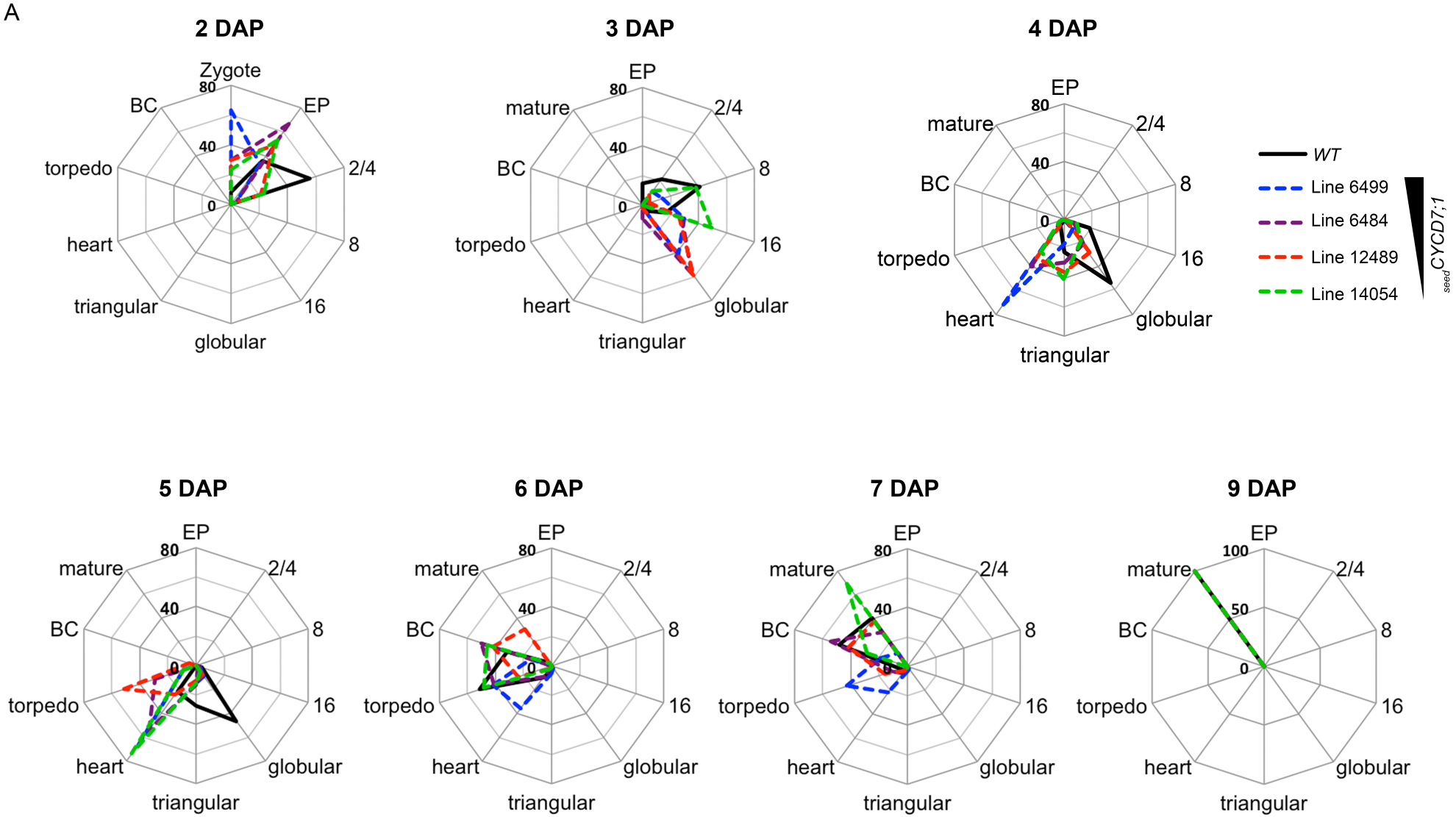
2 DAP
Zygote
EP
2/4
8
16
globular
triangular
heart
torpedo
BC
80
40
0
3 DAP
EP
2/4
8
16
globular
triangular
heart
torpedo
BC
mature
4 DAP
EP
2/4
8
16
globular
triangular
heart
torpedo
BC
mature
WT
Line 6499
Line 6484
Line 12489
Line 14054
seed CYCD7;1
5 DAP
6 DAP
7 DAP
9 DAP
100
50

B
2 DAP
3 DAP
4 DAP
5 DAP
6 DAP
7 DAP
9 DAP
WT
Seed CYCD7;1(6499 (+++))
Seed CYCD7;1 (12489 (+))

Heart stage embryo size

The study of the progression of embryo development revealed that *WT* embryos started reaching the heart stage at 5 DAP, one day later than $_{seed}$*CYCD7;1*. However, the time window in which each embryo transited the heart stage was shorter in the *WT* (2 days from 5 to 6 DAP) whereas $_{seed}$*CYCD7;1* had a slower average progression through the heart stage from 4 DAP to 7 DAP. Despite the slower rate of embryo development and the wider time window through heart stage, the patterning of *WT* and $_{seed}$*CYCD7;1* embryos was morphologically similar at early and late heart stage (Fig. 4.7A-F). This could suggest that the coordination between embryo progression and tissue formation was not disturbed by faster embryo development progression in $_{seed}$*CYCD7;1*. In addition the embryo area of every heart stage embryos was recorded (Fig. 4.7G). *WT* embryos measured on average 4378 μm^2 and $_{seed}$*CYCD7;1* embryos measured 4489 μm^2 (6499), 4583 μm^2 (6484), 4312 μm^2 and 4410 μm^2 (14054). $_{seed}$*CYCD7;1* embryos were not significantly different from *WT* (one-way ANOVA, $n>35$, $p=0.26$). Despite the fact that $_{seed}$*CYCD7;1* seeds started undergoing a significant enlargement compared to the *WT*, the embryos were not significantly larger. Taken together with the fact that $_{seed}$*CYCD7;1* embryo patterning was not disturbed and that the $_{seed}$*CYCD7;1* reached heart stage quicker, it is likely that the transition from triangular to heart stage in $_{seed}$*CYCD7;1* was accelerated. As embryo patterning is correlated with cell division rate, it is also plausible that the accelerated rate of embryo development at this triangular/heart stage transition was due to a faster rate of cell divisions.

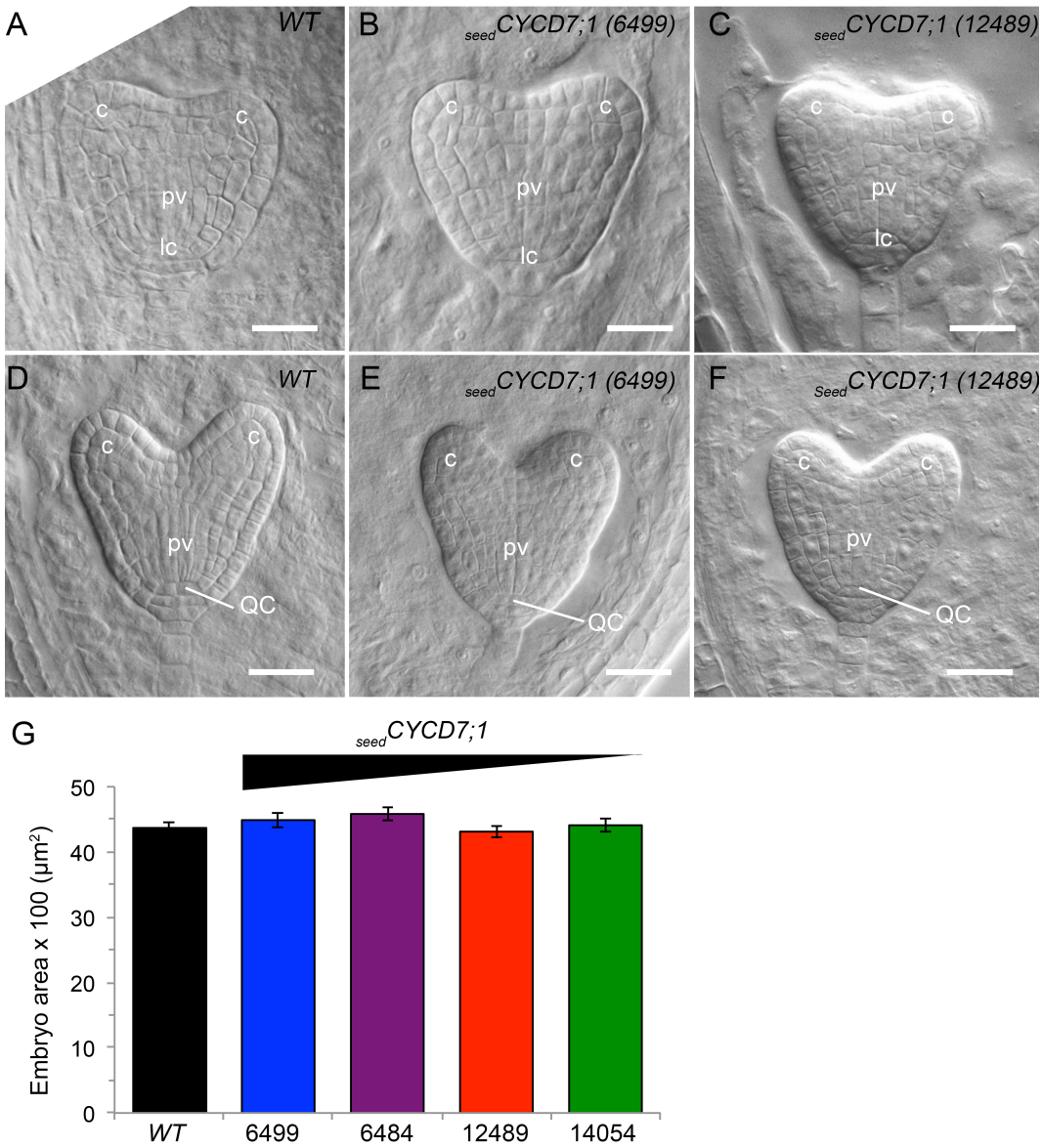

Figure 4.7. Characterization of heart-stage embryos in *WT* and *seedCYCD7;1*.

(A-C) Early heart stage embryo where the cotyledon-to-be starts forming a bump. Toward the future root tip, the division of the upper cell of the hypophysis formed the lens-shaped cell. From the lens-shaped cell, the provascular tissues are distinguishable at the centre and the ground tissues at the outside surrounded by the epidermis.

(D-F) Mid-heart stage embryo where the cotyledons have started their outgrowth. The lens-shaped cell underwent divisions giving rise to the quiescent centre and one cell-layer of collumela stem cells. The vascular tissues are still distinguishable at the centre and the ground tissues at the outside surrounded by the epidermis

(A,D) *WT* embryo. (B,E) *seedCYCD7;1* line 6499 and (C,F) *seedCYCD7;1* line 12489.

(G) Embryo area at heart-stage. Error bars show ± SE. No statistical difference between *WT* and *seedCYCD7;1* is observed.

Scale bars: A-F, 15 µm.
Abbreviations: c, cotyledon; lc, lens-shaped cell; QC, quiescent centre; pv, provasculature.

4.3. Effect of endosperm-targeted expression of *CYCD7;1* on the compartments of mature seeds

In chapter 3, I showed that $_{seed}$*CYCD7;1* produced seeds with a final seed area enlarged by 15% to 43%. To investigate the overall consequences on the seed components, I looked at the mature embryo released from of mature seeds, as well as the seed coat, especially the outer layer of the outer integument.

4.3.1. Effect of endosperm-targeted *CYCD7;1* expression on final embryo size

A *Col-0 WT* mature embryo measured on average 894 µm long, whereas $_{seed}$*CYCD7;1* mature embryos had a length of 1226 µm for line 6499, 1122 µm for line 6484, 1035 µm for line 12489 and 996 µm for line 14054 (Fig. 4.8A,B). Hence $_{seed}$*CYCD7;1* mature embryos were significantly longer by 12% to 37% depending on the transgenic line (one-way ANOVA, n>37, $p=8.47x10^{-7}$). The volume of a mature embryo was determined by imaging the whole embryo with confocal Z-stacks and by picture integration with an ImageJ plug-in developed by M. Ferero-Vargas (personal communication). A *WT* embryo had a volume of $25x10^6$ µm^3. $_{seed}$*CYCD7;1* embryos were $61x10^6$ µm^3 (line 6499), $40x10^6$ µm^3 (line 6484), $41x10^6$ µm^3 (line 12489) and $38x10^6$ µm^3 (line 14054). These results show a significant increase in volume ranging from 50% to 139% (one-way ANOVA, n>37, $p=2.8x10^{17}$; Fig. 4.8A,C).

To determinate whether the increase in mature embryo size was due to a cell overproliferation effect or to an effect on cell elongation, the cotyledon areas and the epidermal pavement cell areas were measured in the mature embryo. The ratio of cotyledon surface:epidermal pavement cell surface gives a calculated number of pavement cells on the cotyledon surface. The *WT* cotyledon surface measured on average $75x10^3$ µm^2. $_{seed}$*CYCD7;1* measured $120x10^3$ µm^2 (line 6499), $116x10^3$ µm^2 (line 6484), $106x10^3$ µm^2 (line 12489) and $97x10^3$ µm^3 (line 14054). As the embryo volume increased, $_{seed}$*CYCD7;1* cotyledon area was significantly larger with a 29% to 60% increase (one-way ANOVA, n>74, $p=1.29x10^{-5}$; Fig. 4.8A,H). The average surface areas of epidermal pavement cells were 194 µm^2 for the *WT* and 210 µm^2, 196 µm^2, 200 µm^2 and 199 µm^2 for $_{seed}$*CYCD7;1* line 6499, 6484, 12489 and 14054 respectively. A Bonferroni multi-comparison test revealed that only from $_{seed}$*CYCD7;1* 6499 were the pavement cells significantly larger (n>555, $p=0.3x10^{-4}$; Fig. 4.8F,G). The calculated ratio of cotyledon surface:epidermal pavement cell surface showed that the *WT* area were consisted of 388 cells and the $_{seed}$*CYCD7;1* of 572, 589, 529 and 448 cells for line 6499, 6484, 12489 and 14054 respectively. *WT* cotyledons had fewer pavement cells than the $_{seed}$*CYCD7;1* (one-

way ANOVA, n>74, $p=7.5x10^{-20}$; Fig. 4.8I). By measuring cell area in the shoot, I inferred that cell proliferation was stimulated in cotyledons.

As the whole embryos were larger, I next determined whether the embryo radicle anatomy and the cell length were different. *WT* radicle consists of concentric single-cell layers of epidermis, cortex and endodermis from the outside to the inside. The inner layers consist of the stele, where the single-layer pericycle surrounds the vascular tissues (Marchant *et al.*, 1999). The analysis of Z-stacks showed that *$_{seed}$CYCD7;1* radicles did not appear to have extra layers and the root pattern in the radial dimension was similar to that of *WT* (Fig.4.8D). The lengths of sixteen cortical cells, starting from the first cortical cell after the cortical-endodermis initials (CEI), were measured. The first cortical cell length in a *WT* root was 6.5 µm. In the *$_{seed}$CYCD7;1* cortical cell lengths ranged from 5.5 to 6 µm depending on the line observed. The sixteenth cortical cell length measured was 9.2 µm in *WT* and were between 8.8 µm and 10.6 µm for *$_{Seed}$CYCD7;1*. Overall the cell length was increasing up the root except for the second cortical cell with slightly greater cell length than *$_{seed}$CYCD7;1*. A two-way ANOVA test showed that the cortical cell length is not significantly different between *WT* and *$_{seed}$CYCD7;1* (n>74 cortical files, α=0.05, p=0.23). However, for both genotypes the cortical cell length is statistically different depending on the position from the CEI (n>74 cortical files, α=0.05, $p=4.6x10^{-6}$; Fig. 4.8E). As the cells from the cortex were not larger, the contribution of the root to produce a larger embryo is presumably due to cell overproliferation.

4.3.2. Effect of endosperm-targeted *CYCD7;1* expression on the seed coat of mature seeds

As the *$_{seed}$CYCD7;1* lines produced larger seeds with larger embryos containing more cells, I investigated the effect on the seed coat. The cells of the outer layer of the outer integument were measured on mature dry seeds. Cells of the outer integuments had on average an area of 778 μm^2 for *WT* (Fig. 4.8J). The average cell area for *$_{seed}$CYCD7;1* was 854 μm^2 (6499), 857 μm^2 (6484), 821μm^2 (12489) and 807 μm^2 (14054) and is not significantly different from the *WT* cell area (one-way ANOVA, n=450, p=0.18). The projected seed area was measured and the ratio projected seed area:average cell area gives a calculated number of cells contributing to the size of the seed coat. The *WT* seed area was $12.3x10^4$ μm^2 whereas *$_{seed}$CYCD7;1* seed areas were significantly larger with an average of $17.4x10^4$ μm^2 (6499), $17.3x10^4$ μm^2 (6484), $16.2x10^4$ μm^2 (12489) and $14.3x10^4$ μm^2 (14054) (Fig. 4.8K; one-way ANOVA, n=30, $p=5.9x10^{-4}$). Therefore, the calculated counts of cells in the outer integument inferred by the ratio projected seed area:average cell area were 159 for the *WT*. The *$_{seed}$CYCD7;1* lines contained significantly more cells with averages of 204, 203, 197 and 181 for lines 6499, 6484, 12489 and 14054

respectively (Fig. 4.8L; one-way ANOVA, n=450, $p=6x10^{-4}$). Therefore, The $_{seed}$*CYCD7;1* seed coat is larger and the enlargement is due to cell proliferation rather than cell expansion.

Figure 4.8. Characterization of enlarged mature seeds from $_{seed}$*CYCD7;1* plants.

(A-I) Embryo features

(A) Confocal stacks showing embryos removed from mature dried seeds.
Length (B) and volume (C) of mature embryos from *WT* and $_{seed}$*CYCD7;1* plants.
(D) Embryo radicle revealing a concentric single-celled layer radial pattern (from the outside to the inside: the epidermis, the cortex, the endodermis and the pericycle) the inner part of radicle is the stele constituted of vascular tissues.
(E) Length of cortical cells from the cortex-endodermis initials (CEI)

(A) Trace of mature embryo cotyledon epidermis showing pavement cells, stomata and lineage cells of stomata.
(B) Comparison of cell area of pavement cells of mature embryo cotyledons.
(C) Comparison of cotyledon area of mature embryos.
(D) Inferred numbers of pavement cells of cotyledons by calculating the ratio cotyledon surface:epidermal pavement cell surface.

(J-L) Seed coat features looking at the outermost layer of the integuments.
(E) Comparison of cell area of the outermost layer of the mature seed integuments.
(F) Comparison of seed surface.
(G) Inferred numbers of cells in the outer integument by calculating the ratio seed surface:integument cell surface.

Scale bars: A,D, 100 µm; F, 50 µm
Error bars show ± SE. (*) shows a statistical difference between *WT* and $_{seed}$*CYCD7;1.*

Abbreviations: co, cortex; ed, endosermis; ep, epidermis; p, pericycle; st, stele.

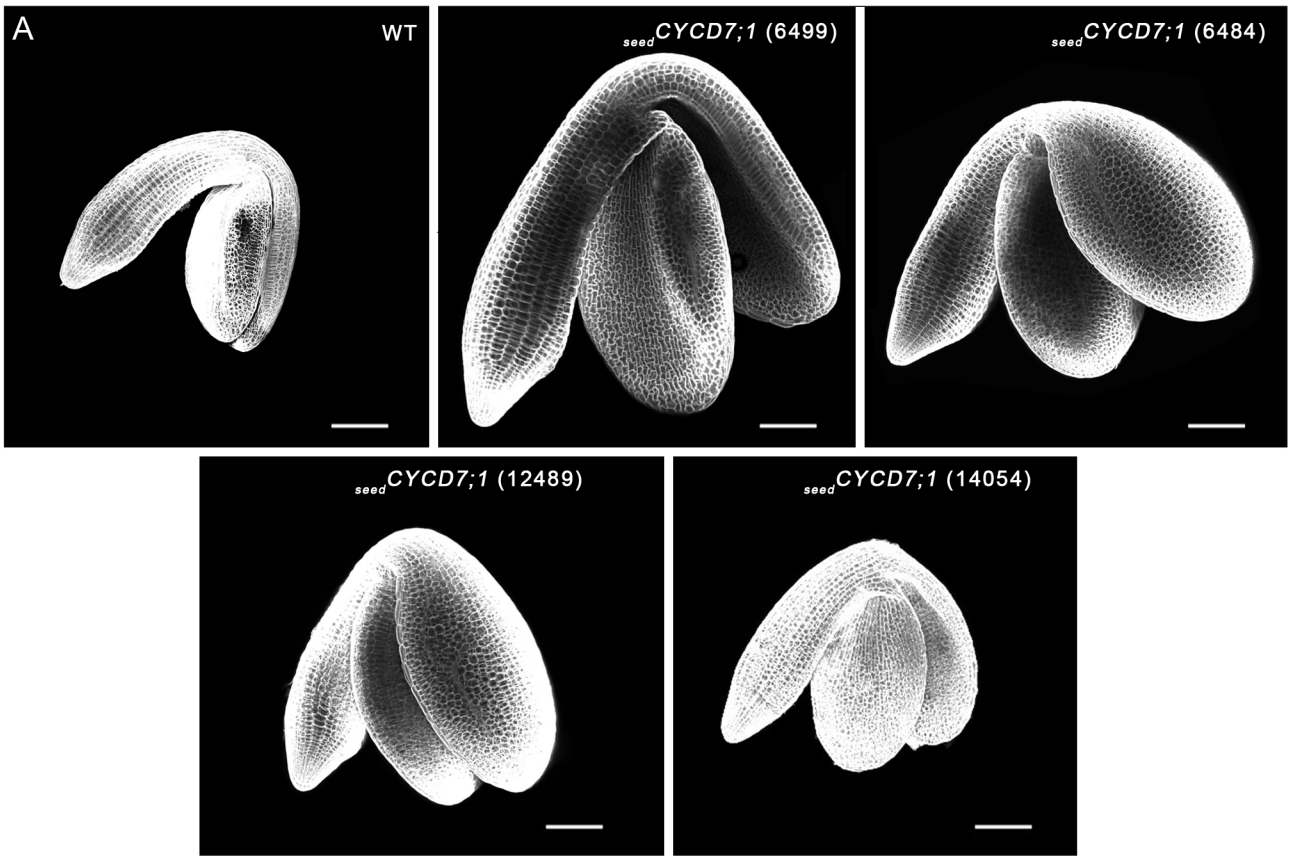
A
WT
seedCYCD7;1 (6499)
seedCYCD7;1 (6484)
seedCYCD7;1 (12489)
seedCYCD7;1 (14054)

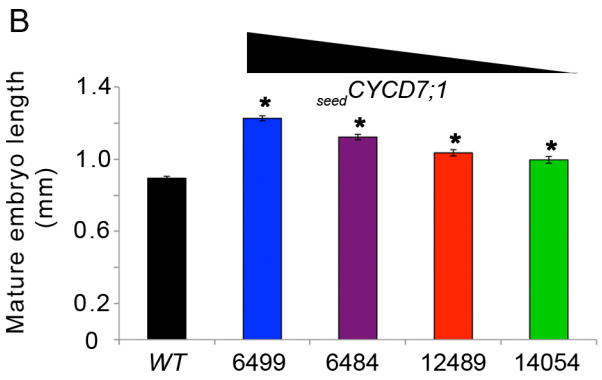
B
Mature embryo length (mm)
1.4
1.0
0.6
0.2
0
seedCYCD7;1
WT
6499
6484
12489
14054

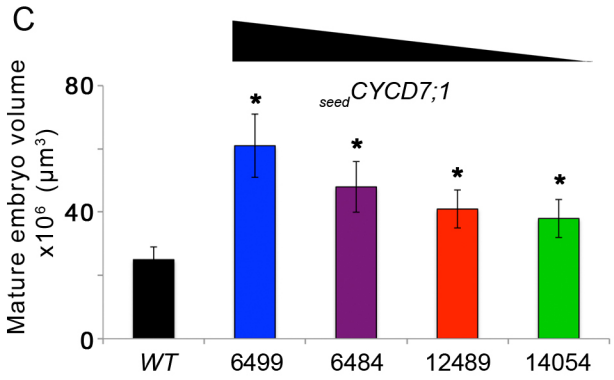
C
Mature embryo volume x10⁶ (µm³)
80
40
0
seedCYCD7;1
WT
6499
6484
12489
14054

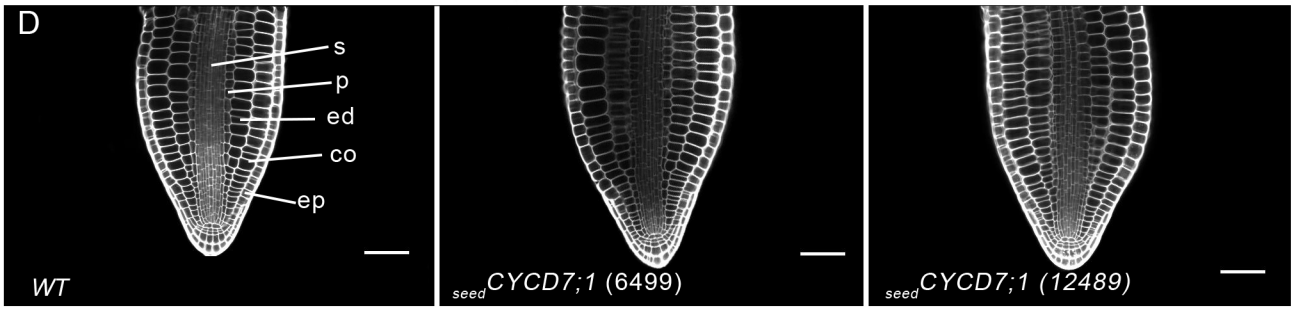
D
s
p
ed
co
ep
WT
seedCYCD7;1 (6499)
seedCYCD7;1 (12489)

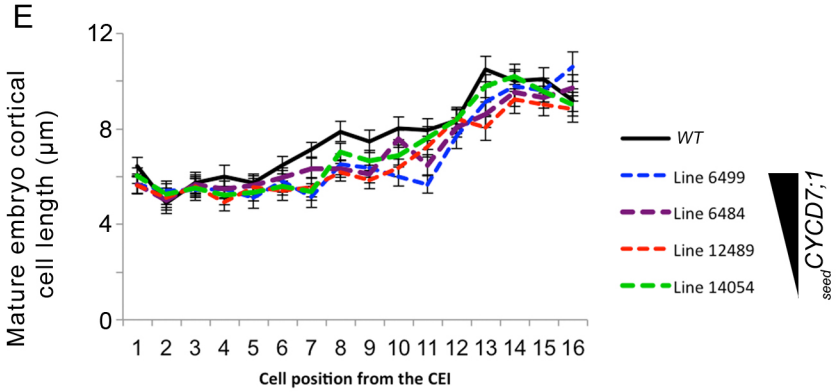
E
Mature embryo cortical cell length (µm)
12
8
4
0
1 2 3 4 5 6 7 8 9 10 11 12 13 14 15 16
Cell position from the CEI
WT
Line 6499
Line 6484
Line 12489
Line 14054
seedCYCD7;1

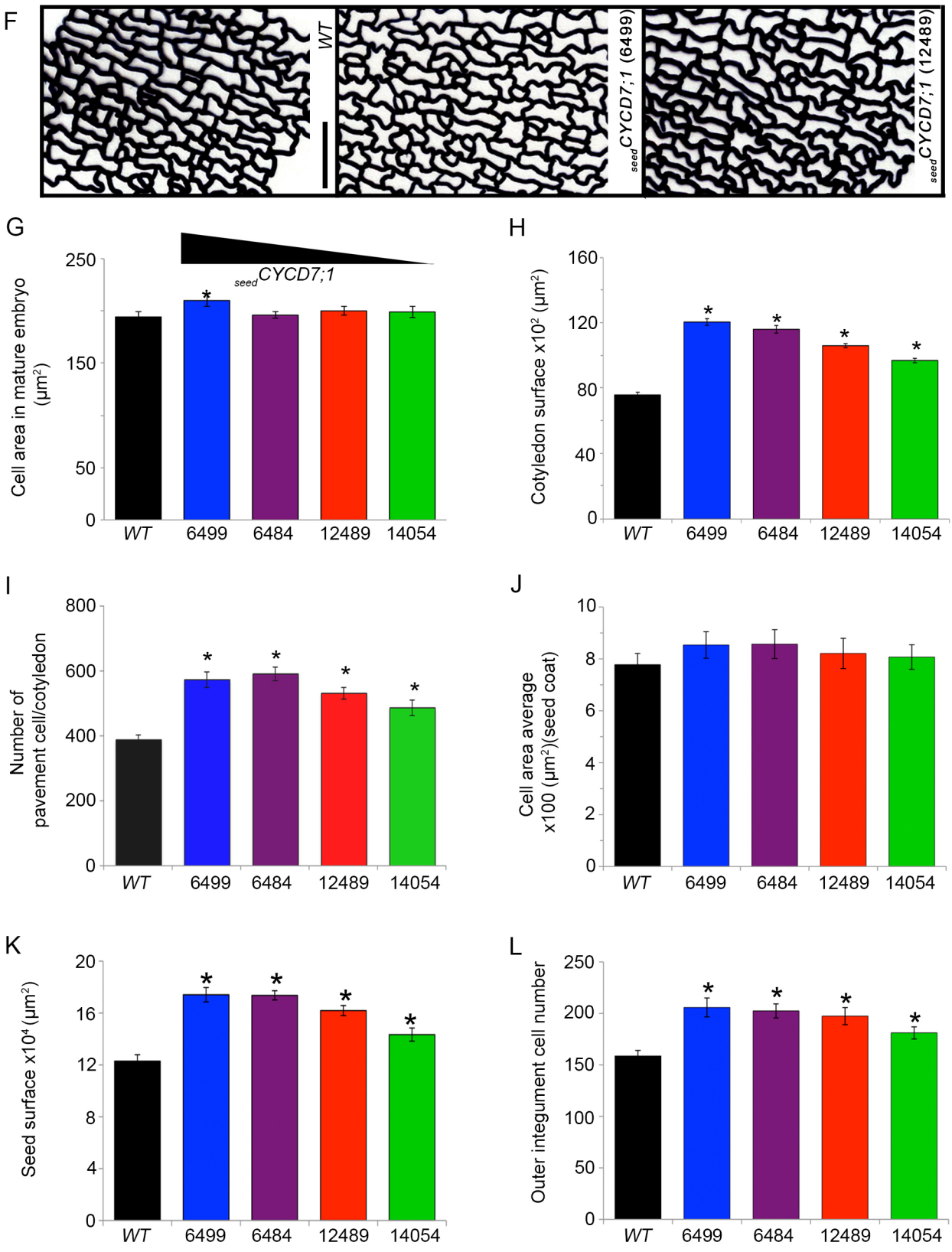

Figure 4.8. Characterization of enlarged mature seed from $_{seed}$*CYCD7;1* plants (continued).

4.4. Effect of endosperm-targeted expression of *CYCD7;1* on seedlings post-germination

As the final embryo size of $_{seed}$*CYCD7;1* was increased, an investigation was carried out to determine whether the $_{seed}$*CYCD7;1* has a prolonged effect beyond its window of expression during post-embryonic development. In 7 day-old seedlings, root length and cotyledon area were measured. In *WT*, the root length of 7 day-old seedling was 21.9 mm (Fig. 4.9C). In $_{seed}$*CYCD7;1*, roots were 31.3 mm long for line 6499, 31.1 mm for line 6484, 29.7 mm for 12489 and 28.6 mm for 14054. $_{seed}$*CYCD7;1* roots were significantly longer than *WT* roots (one-way ANOVA, $30<n<45$, $p=6.09\text{x}10^{-9}$). The average cotyledon surface per seedling was 5.1 mm^2 in *WT* and the cotyledon area was larger in $_{seed}$*CYCD7;1* seedlings with an average of 9.5 mm^2 for the line 6499, 8.5 mm^2 for 6484, 7.9 mm^2 for 12489 and 7.7 mm^2 for 14054 (one-way ANOVA, $p=2.5\text{x}10^{-10}$; Fig. 4.9A,B). In addition, in $_{seed}$*CYCD7;1* the first true leaves were more advanced in their development that the ones in *WT* (Fig. 4.9B). Whether the emergence of the first true leaves is faster in $_{seed}$*CYCD7;1* or whether the leaves grow faster, still needs to be investigated.

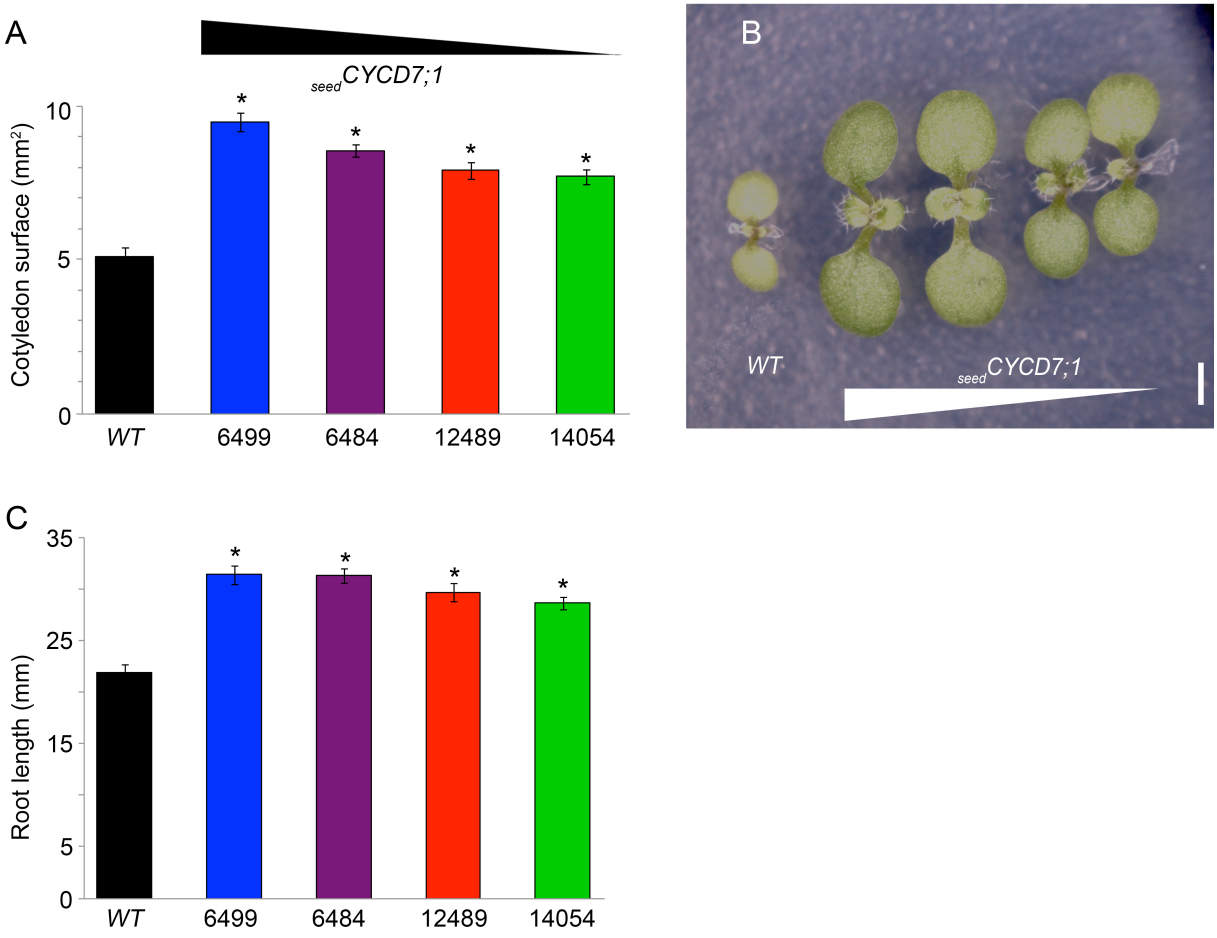

Figure 4.9. *seedCYCD7;1* has an effect on seedling growth 7 days after germination.

(A) Comparison of cotyledon surface between 7 day-old seedling WT and seedCYCD7;1.

(B) 7 day-old seedling. Cotyledon surface is wider in seedCYCD7;1 than in the WT and the development of the true leaves is more advanced.

(C) Comparison of root length between 7 day-old WT and seedCYCD7;1 seedlings.

Scale bar: 1 mm.

Discussion

Changes in seed size have been reported in a number of genes including *AP2*, *EOD3* and *MTN* that encode for an AP2 class transcription factor, a cytochrome P450 and AUXIN RESPONSE FACTOR 2, respectively. Seed-targeted expression of *CYCD7;1* promotes seed growth by promoting cell proliferation in the embryo and the seed coat rather than cell expansion (Fig. 4.8), unlike *ap2* and *eod3-1D* in which both cell proliferation and cell expansion are affected (Ohto *et al.*, 2005; Fang *et al.*, 2012). Despite the expression of $_{seed}$*CYCD7;1* in the central cell of the mature female gametophyte (Chapter 3), the size of mature ovules was similar in the *WT* and $_{seed}$*CYCD7;1*, suggesting that the effect of *CYCD7;1* expression in the central cell has no visible effect prior to fertilization, although the number of ovules was reduced. Therefore I can assume that the seed size difference happens post-fertilization and time-course experiments revealed that the enlarged seed size was distinguishable 4 DAP. Similarly, the mature ovule of *eod3-1D* mutants have a size similar to the *WT* and the enlarged seed phenotype from the *eod3-1D* mutants arises post-fertilization at 2 DAP, whereas in *mtn* the enlargement is observable in mature ovules pre-fertilization (Schruff *et al.*, 2006; Fang *et al.*, 2012). At 4 DAP, the seed size enlargement was noticeable in $_{seed}$*CYCD7;1* and is correlated with a faster rate of embryo development until the embryos reach the heart stage. Despite the quicker embryo development progression, heart stage embryos did not display an enhanced size or abnormalities in embryo patterning, unlike *RPS5A:CYCD7;1* (Collins *et al.*, 2012). It has been shown that under the control of the *RPS5A* promoter, *CYCD7;1* is expressed in all proliferating tissues (Weijers *et al.*, 2001; Collins *et al.*, 2012). This expression leads to abnormal embryo development characterized by cell overproliferation in the suspensor and in the embryo. Morphologically the embryo patterning is impaired. However embryos still progress through the different stages of development and reach maturity (Collins *et al.*, 2012). Interestingly, the defects of embryo patterning have also been observed with *RPS5A:CYCD3;1*, reinforcing the hypothesis that control of the cell cycle progression is essential for normal seed development. The normal embryo patterning and heart stage embryo size suggests that the accelerated rate of cell division and embryo patterning were still coordinated to form normal tissues rather than a disturbed coordination leading to aberrant patterning.

In addition to seed enlargement, $_{seed}$*CYCD7;1* line exhibit a high proportion of non-developing seeds. The level of lethality appeared to be positively correlated with the level of $_{seed}$*CYCD7;1*. The seed abortion in $_{seed}$*CYCD7;1* appeared to be only partially due to a defect of reproductive structure architecture limiting the efficiency of pollination. In the *mtn*

mutant the reduced fertility is rescued by performing manual crosses (Schruff *et al.*, 2006). In contrast, in $_{seed}$*CYCD7;1*, manual crosses (Fig. 4.5) only partially rescued the number of seeds produced in the strongest expresser, suggesting the pollination event is not the key step in the reduction of developing seeds. As the *CYCD7;1* was expressed exclusively on the female side and I previously showed that *CYCD7;1* acts maternally to promote seed growth leading to an enlarged seed size, reciprocal crosses were performed to reveal that similarly the reduction of developing seed is due a maternal effect. The present results do not allow a conclusion as to whether the increase of seed size is due to reduced fertility as observed in *ap2* and *mtn/arf2* or is independent of fertility impairment, as in *eod3-1D* (Schruff *et al.*, 2006; Fang *et al.*, 2012). Therefore these data raise the question of $_{seed}$*CYCD7;1* effects on seed development: does $_{seed}$*CYCD7;1* induce a reduction of the number of developing seeds leading to a lower steric bulk within the closed silique and also indirectly increasing the nutrient flow to the remaining seeds and therefore allowing the seeds to enlarge? Or, does the endosperm-targeted *CYCD7;1* expression induces seed enlargement and lethality is induced by an independent mechanism? The hypothesis that $_{seed}$*CYCD7;1* induces lethality, and as a consequence the seeds enlarge, is backed up by the fact that arrested seeds are at the globular stage (3 DAP). The proportion of seed progressing beyond the heart stage had therefore more room and this could be correlated with the fact that the enlarged seed phenotype arises at 4 DAP. This hypothesis is also supported by the study of *eod3* that showed that mutant plants producing seeds that were 80% larger that *WT* seeds also displayed an increased lethality compared to that of *WT* (Fang *et al.*, 2012).

I demonstrated that seed development arrest was due on one hand to a defect during early phases of seed development but also to embryo arrest prior to or at globular stages. In $_{seed}$*CYCD7;1* lines, embryos reached the globular stage 3 DAP, at which time the embryo development progression and rate of cell divisions were faster in $_{seed}$*CYCD7;1* than in *WT.* This suggests that the globular stage may be particularly sensitive to changes in the developmental program. This is supported by studies showing that embryo patterning, shoot apical meristem specification and emergence of future cotyledons depend on the proper establishment of auxin flow from the zygote to the transition stage (Mayer *et al.*, 1993; Aida *et al.*, 2002; Friml *et al.*, 2003; Friml *et al.*, 2004). Moreover, the examination of aborted seeds did not reveal aberrations in the morphological patterning of the globular embryo as has been recently published with overexpression of *CYCD3;1* in the seed (Collins *et al.*, 2012). The use of cell fate markers might help to ascertain whether the cell fate is established properly during early onset of divisions. For example, *WOX2,8,9* or *WUS*

would highlight the cell fate acquisition until globular stage and *PIN1, PIN7, MP* and *DR5* reporters would indicate the proper establishment of auxin flow and auxin response, essential for patterning the embryo (Moller and Weijers, 2009). At early stages, it was unclear whether the arrest was due to a non-fertilization event or an arrest at the zygote stage. Initial observations indicated an absence of fertilization, as no zygotes were distinguishable in the degenerating ovules. A way to determine whether the fertilization happened or not, would be to use a sperm cell nucleus marker such as the *Histone Three Related 12* (HTR12, *pHTR12:HTR12-RFP*) (Ingouff *et al.*, 2007). HTR12 marks initially the nucleus of the microspore and during male gametogenesis is restricted to the generative cell and finally to the two sperm cell nuclei. After fertilization, HTR12 is visible in the nuclei of the developing endosperm and the zygote. Twelve hours after fertilization, when the endosperm contains 8 nuclei and the zygote undergoes the first mitotic division, the expression becomes weaker.

Interestingly, $_{seed}$*CYCD7;1* displayed nucleus overproliferation in the central cell without pollination and fertilization (Fig 4.2). *CYCD7;1* under the *FWA* promoter is expressed during seed development but also in the mature central cell. Therefore the multinuclear phenotype in central cell suggests that CYCD7;1 may have an effect in the central cell prior to fertilization. The first hypothesis to explain this phenotype could be pollen contamination. It seems unlikely since the styles of pistils were examined prior to ovule sampling to ensure the absence of pollen contamination. However, to rule out this hypothesis, the use of the HTR12 marker in the $_{seed}$*CYCD7;1* background would determine whether the ovules were fertilized by some pollen grains. However, the nucleus proliferation phenotype in the central cell or in the endosperm in the absence of fertilization has previously been reported in the *rbr1-1* mutant and *fis* class mutants respectively. In *rbr1-1* mutants, the multiple nuclei phenotype in the central cell was due to a failure in arresting the cell cycle prior to fertilization and thus the central cell does not acquire endosperm fate, whereas in *fis* class mutants, the multiple nuclei phenotype in the endosperm is due to autonomous seed development in the absence of fertilization (Ohad *et al.*, 1996; Grossniklaus *et al.*, 1998; Kiyosue *et al.*, 1999; Luo *et al.*, 1999; Kohler *et al.*, 2003; Guitton and Berger, 2005; Ingouff *et al.*, 2006). To investigate whether the central cell acquires the endosperm fate, examination of the presence flavonoid (pro-anthocyanidins) deposits in the endothelium with vanillin staining could be done. In addition, a marker of the female gametophyte central cell such as *pMEDEA:GUS* could indicate whether or not the central cell acquires endosperm fate (Luo *et al.*, 2000). These two methods would suggest an autonomous endosperm development mimicking fertilization of the central cell (Ingouff *et al.*, 2006).

Little is known about the molecular mechanism by which CYCD7;1 acts in plant development. As a member of the D-type cyclins, it is plausible that CYCD7;1 acts with CDKA;1 to inactivate RBR function by phosphorylation (Boniotti and Gutierrez, 2001). Therefore, overexpressing *CYCD7;1* in seeds would be similar to reducing the activity of RBR prior to and post fertilization. This would result in failure to cell cycle arrest in the central cell leading to overproliferation of central cell nuclei as has been observed in a loss-of function *rbr* mutant. This phenotype will be discussed further in the final discussion (chapter 6).

Whilst the multi-nucleus phenotype is observed in all of the $_{seed}$*CYCD7;1* lines, 80% of the ovules of the lowest $_{seed}$*CYCD7;1* expression (12489 and 14054) display this phenotype whereas the stronger expresser 6499 and 6484 had 55% and 30% of ovules with multiple nuclei, respectively. Interestingly, it does not correlate with the lethality proportion in the different lines. The lines 6499 and 6484 have the highest levels of lethality (80% and 65% respectively) whereas the lower expressers have 50%. It does not appear that the multi nucleate phenotype is the cause or the main factor causing lethality since, for example, in line 12489 out of the 80% of ovules with multiple nuclei, 60 % could develop into a seed, as the lethality is 50%.

Here I showed that *CYCD7;1* expression in the mature central cell and the endosperm acts non-autonomously on embryo and seed coat growth (Fig. 4.10). $_{seed}$*CYCD7;1* influences seed development by promoting cell division in the embryo and the seed coat throughout seed development. Due to the observed accelerated embryo development and the similar size of heart stage embryos in *WT* and $_{seed}$*CYCD7;1*, I propose that the rate of cell division is increased and the window of cell division is prolonged.

Figure 4.10. Overview of the effects of *CYCD7;1* expression in the ovule central cell and the developing endosperm on seed development.

Seed development starts from the fertilization of the ovule. It is characterized by the development of two zygotic tissues, the embryo and the endosperm, and the maternal integuments giving rise to the seed coat. Pictures show a mature ovule (on the left) and the different stages of seed development. The stages of embryo development are written in blue and the stages of endosperm development are written in black. The stages of seed development are recorded days after pollination (DAP) and are based on the Fig. 4.6B.
Under the control of the *FWA* promoter, *CYCD7;1* is expressed in the mature central cell and the developing syncytial endosperm when the embryo reaches the heart stage (beige) . The ovule and seed compartments affected by the expression of *CYCD7;1* are visualized with a diamond shape.
Phenotypes observed in seed-targeted *CYCD7;1* expression are

- nucleus proliferation in the central cell in absence of fertilization.
- seed lethality (grey) during early stages of fertilization/seed development (dark gray) and embryo arrest at globular stage (light gray).
- accelerated embryo development until heart stage (dark blue) correlated with an accelerated rate of cell divisions (cyan).
- seed enlargement visible 4 DAP correlated with a transition stage of embryo development (red), an endosperm enlargement and mature embryo and seed coat size increase (orange).

Scale bar: 50 µm.

Abbreviations: cc, central cell; e, embryo; en, endosperm; I, integuments

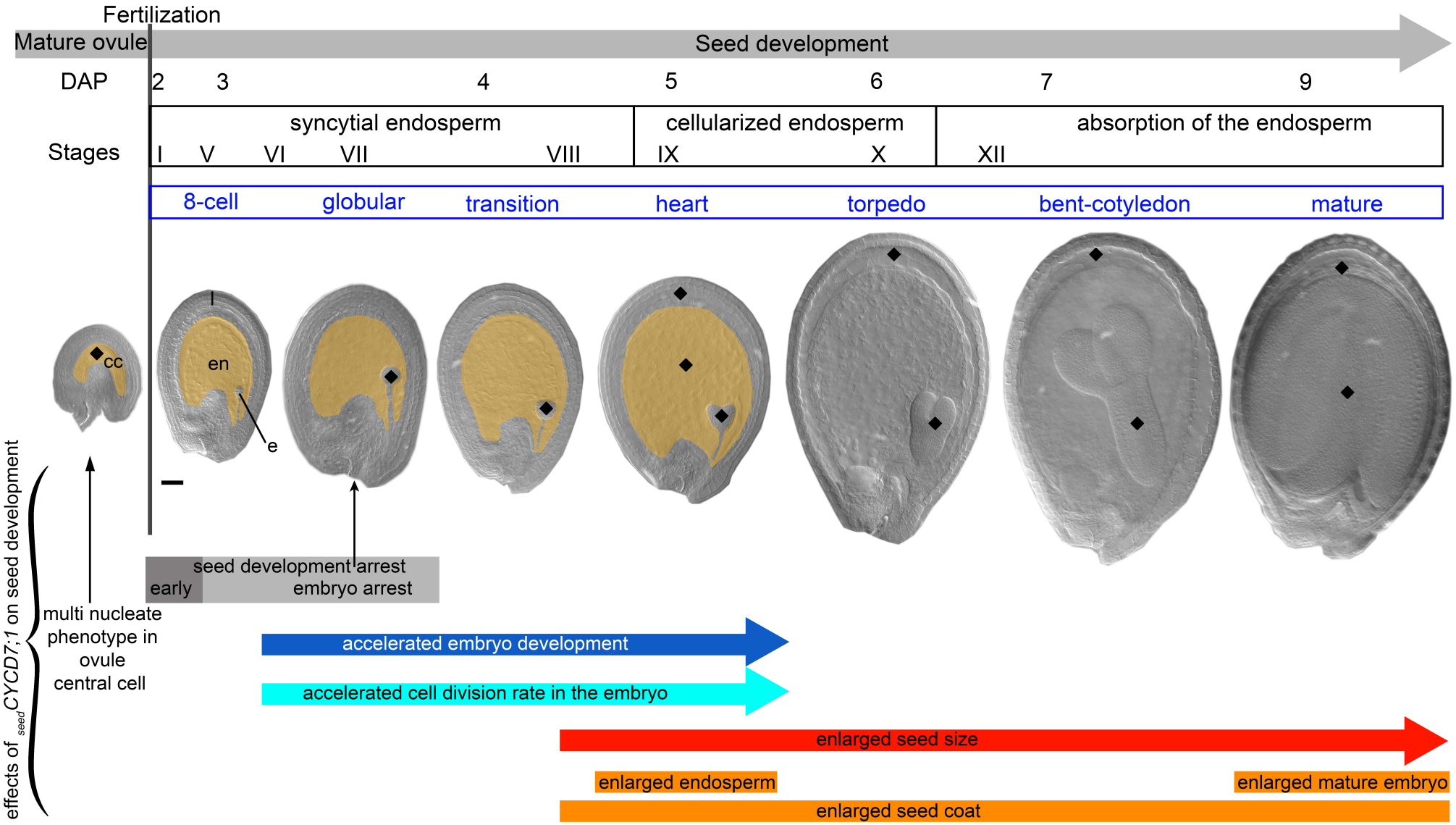
Fertilization
Mature ovule
Seed development
DAP
2
3
4
5
6
7
9
Stages
syncytial endosperm
cellularized endosperm
absorption of the endosperm
I
V
VI
VII
VIII
IX
X
XII
8-cell
globular
transition
heart
torpedo
bent-cotyledon
mature
cc
en
e
seed development arrest
early
embryo arrest
effects of pseed CYCD7;1 on seed development
multi nucleate phenotype in ovule central cell
accelerated embryo development
accelerated cell division rate in the embryo
enlarged seed size
enlarged endosperm
enlarged mature embryo
enlarged seed coat
CYCD7;1 expression under the activity of the FWA promoter
Ovule and seed compartments affected by CYCD7;1 expression in the endosperm

Chapter 5

Interaction of CYCD7;1 with CDK and KRP proteins

Chapter 5
Interaction of CYCD7;1 with CDK and KRP proteins

Introduction

In all Eukaryotes, the cell cycle is governed by CDKs in association with cyclins (Meijer and Murray, 2000). In Arabidopsis, fives CDKs are known to be involved in regulating the cell cycle (Vandepoele *et al.*, 2002). CDKA;1 is association with D-type cyclin control the commitment of cells to the mitotic cell cycle by regulating the transition G1-to-S through the *RBR/E2F* pathway. This is supported by studies of loss-of-function *cycd* mutants that are impaired in the cell cycle and thus have reduced cell numbers in leaves (Dewitte *et al.*, 2007), fewer mitotic figures in germinating roots (Masubelele *et al.*, 2005) and a decreased lateral root density (Sanz *et al.*, 2011) to cite a few examples. Gain-of-function *CYCD* mutants, on the contrary, display cell overproliferation leading to impaired differentiation (Dewitte *et al.*, 2003).

In Chapters 3 and 4, I demonstrated a possible role for *CYCD7;1* in stimulating seed enlargement by promoting cell division. These results corroborate with the study showing that overexpression of *CYCD7;1* in proliferation tissue during seed development under the RPS5A promoter leads to outgrowth of embryos and endosperm by promoting cell division and cell enlargement (Collins *et al.*, 2012). Little is known otherwise about the role of *CYCD7;1*. Recent studies show that native *CYCD7;1* is expressed in late meristemoids and guard mother cells during stomatal development and in sperm cells of the pollen grain (Patell *et al.*, manuscript under revision). It appears that *CYCD7;1* promotes the last symmetric division of the guard mother cell , but paradoxically it appears to inhibit cell cycle progression in stomatal guard cells and in pollen. The molecular mechanism by which *CYCD7;1* may be involved in regulating the cell cycle needs to be elucidated. In this chapter, the aim is to identify potential CYCD7;1 interactors such as CDKs and KRPs to help understand its mode of action.

During the past decade, the interaction between core cycle proteins has been broadly investigated. Protein-protein interactions have been analyzed using high-throughput methods (Van Leene *et al.*, 2007; Braun *et al.*, 2013) . Protein-fragment complementation assays (PCA) such as yeast-two-hybrid (Y2H), bimolecular fluorescence complementation

(BiFC), is based on reconstituting a functional transcription factor and a reporter respectively from two inactive fragments. PCA is used to study direct and targeted interaction between two proteins of interest. In contrast, affinity purification-mass spectrometry (AP-MS) (eg. tandem affinity purification, TAP) highlights direct and indirect interactions between proteins found in complexes. TAP is based on a 2-step protein complex immunoprecipitation with immobilized antibodies and mass spectrometry to identify the purified proteins. BiFC and TAP are *in planta* methods, whereas Y2H is an *in vivo* heterologous system that could be affected by problems of protein expression or toxic effects in yeast. All three methods can give false positives with BiFC and TAP due to an overexpression that could potentially lead to unspecific interactions and, in Y2H, potential auto-activation. Steric hindrance caused by the protein fusions could cause false negative results. Using these technologies over 100 proteins have been studied, 416 interactions were tested and 35 interactions are confirmed using the 3 methods (Van Leene *et al.*, 2011).

In this chapter, using a yeast-three-hybrid (Y3H) assay, I investigated the potential interactions between CYCD7;1, CDKA;1 and all KRPs. The interaction with CDKBs was also tested. I then analyzed the expression pattern of the confirmed interactors by the yeast-hybrid assay. Finally, to test whether the interaction is relevant in respect to the enhanced seed size phenotype, I analyzed the seed size phenotype of the $_{seed}$*CYCD7;1* in the *knock-out* mutant backgrounds of the interactors identified.

Results

5.1. Identification of CYCD7;1 cell cycle partners

5.1.1. Yeast three-hybrid assay: to test interaction between three proteins

To investigate the potential interaction between CDKs, CYCD7;1 and KRPs, a yeast-three-hybrid assay was performed (Drees, 1999) (Fig. 5.1). In Yeast, such as *Saccharomyces cerevisiae*, the GAL4 transcription factor binds to a specific DNA sequence to induce gene expression. The GAL4 contains a DNA binding domain (BD), allowing interaction with DNA sequences, and an activation domain (AD), inducing gene expression (Fig. 5.1A). In the Y2H assay, these domains are spilt and binding and activation domains are each fused to proteins of interest (Fig. 5.1B,C). The fusions are made in frame with the N-terminus of the protein of interest. If the two proteins interact, the BD and AD of GAL4 form an active transcription factor that can activate the expression of reporter genes (Fig. 5.1E). In the Y3H assay (Fig. 5.1F-G), a third protein is co-expressed in the yeast. To achieve this, the appropriate native cDNA sequence was cloned under the phosphosglycerate kinase promoter (PGK) in pFL61. The third construct is not fused to any GAL4 component (see chapter 2). *CYCD7;1* and the 5 Arabidopsis CDKs were fused to both the GAL4-AD and GAL4-BD and the 7 KRPs were fused to the AD. The KRPs were also expressed unfused in pFL61. KRP proteins were not fused to the BD as it has been demonstrated that they can self-activate (C Forzani, unpublished data). The Y3H was performed using the yeast strain PJ694A which carries under GAL4/UAS control a *lacZ* reporter gene as well as *HIS3* and *ADE2* providing auxotrophy on histidine and adenine. Interaction between 2 and/or 3 proteins is revealed by the yeast growth on media lacking of histidine or adenine. In the L*acZ* assay, interaction is visualized by the appearance of a blue reaction product after several hour incubation with the substrate X-gal.

Figure 5.1. Schematic representation of the yeast-two-hybrid and yeast-three-hybrid assays.

Yeast-hybrid assay test for protein-protein interaction *in vivo*. The yeast transcription factor (TF) GAL4 has two distinct domains, the DNA-binding domain (BD) and the transcriptional activation domain (AD). These two domains form a functional transcription factor that binds to a *UAS* promoter leading to the transcription of the adjacent gene. In the yeast-two-hybrid assay two putative interacting proteins X and Y are fused to the BD and AD. The two hybrid proteins BD-X and AD-Y are co-expressed in a yeast strain (here, PJ69-4A) exhibiting histidine and adenine auxotrophy or *lacZ*, a reporter gene under the control of *UAS*. When X and Y interact, the TF is reconstituted, leading to expression of the reporter. With PJ69-4A, the yeast will grow on media lacking of histidine and adenine. During the *LacZ* assay, the X-Gal is added and cleaved by the enzyme product of *LacZ* gene expression, the yeast colonies will turn blue.

In the yeast-three-hybrid assay, a yeast strain is co-transformed with BD-X and AD-Y and a third protein Z. Z is expressed under the control of a strong constitutive promoter (*PGK*). The reporter genes are transcribed only when Z interacts with X and Y at the same time (modified from Dees, 1999).

(A) Native TF with BD and AD, leads to reporter gene expression

(B,C) Negative control. (B) BD-X expression on its own or with AD (without Y fused), the reporter gene is not active. (C) AD-Y expression on its own or with BD (without X fused), the TF is not reconstituted and the reporter gene not expressed. In the latter case, if the reporter gene is active, Y-AD self activates, and positive results cannot be concluded.

(D) When X and Y do not interact, the reporter gene is not expressed.

(E) Interaction between X and Y allow formation of an active TF leading to reporter gene expression.

(F,G) In a yeast-three hybrid assay, a third protein Z is tested for the interaction with Y and X. If Z does not interact with both of them or interacts with only one of them, the TF is not active and the reporter gene is not expressed (F). The interaction between X and Z and Y allows the expression of the reporter gene (G).

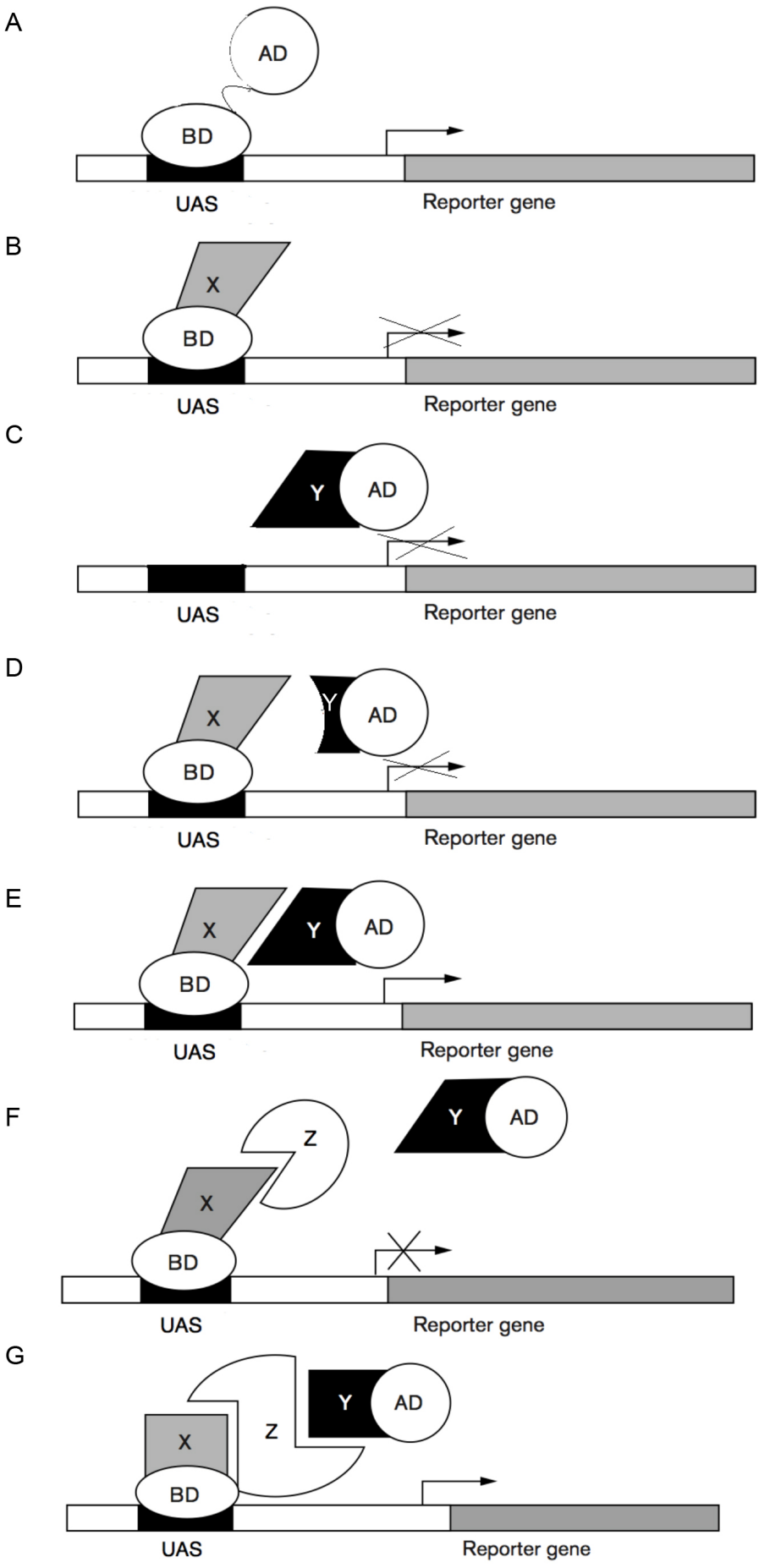
A
AD
BD
UAS
Reporter gene
B
X
BD
UAS
Reporter gene
C
Y
AD
UAS
Reporter gene
D
X
Y
AD
BD
UAS
Reporter gene
E
X
Y
AD
BD
UAS
Reporter gene
F
Z
Y
AD
X
BD
UAS
Reporter gene
G
Y
AD
Z
X
BD
UAS
Reporter gene

5.1.2. CYCD7;1 interacts with CDKA;1 in the presence of KRP2

Unlike other D-type cyclins, a recent study showed that CYCD2;1 does not interact with CDKA;1 directly but requires KRP2 to allow the formation of the CYCD-CDKA;1 complex (Sanz *et al.*, 2011). Based on this observation, the interaction between CYCD7;1, CDKA;1 and KRP2 was tested. In addition, the interactions with CDKBs were also probed in the assay (Fig. 5.2).

Before investigating the interaction of the proteins of interest, several controls were performed. First, it was necessary to check that the simultaneous expression of the three proteins in yeast is not lethal for the strain. After transformation, yeast was grown on media lacking tryptophan, leucine and uracil, selecting for the transformants containing the 3 plasmids of interest (see chapter 2; Fig 5.2, first column). All combinations were found to be viable, except CYCD7;1-BD and CDKB2;2-AD (Fig.5.2, first column, row 45). However, since the reciprocal combination CYCD7;1-AD and CDKB2;2-BD was viable, conclusions about the interaction could be drawn (Fig.5.2, first column, row 50).

Next, to eliminate potential false positives several controls were carried out. To check for self-activation, yeast containing CYCD7;1-BD or CDK-BD were transformed with the empty AD vector together with either the pFL61 empty vector (Fig.5.2, rows 2,5,22,31,40,49) that or expressing KRP2 (Fig.5.2, rows 9,14,24,33,42,51). In all cases, no yeast growth could be observed on - his or - ade media and no blue colour appeared. In parallel, to ensure that the AD did not forms an active TF with an unfused BD and activate the expression of the reporter gene, CYCD7;1-AD, CDKA-AD and KRP2-AD were transformed with empty BD and pFL61 empty vector (Fig.5.2, rows 4,7,17,26,35,44) or pFL61_KRP2 (Fig.5.2, rows 8,10,19,28,37,46). On media selective for the interaction none of the above combinations could grow whereas they could grow on media selecting for transformants with the 3 plasmids, suggesting that no interaction between protein-AD and unfused BD occurred. Therefore, all controls were negative.

The interactions between CDKA;1, CYCD7;1 and KRP2 were investigated. Direct interactions were detected between CDKA;1 and KRP2 as revealed by growth and blue colour in the CDKA;1-BD/KRP2-AD combination (Fig. 5.2, row 13). No direct interaction of CYCD7;1 with either CDKA;1 or KRP2 was observed in this system as no yeast growth or blue color could be observed in the CYCD7;1-BD/CDKA;1-AD, CDKA;1-BD/CYCD7;1-AD and CYCD7;1-BD/KRP2-AD combinations (Fig. 5.2, rows 3,6/16,12). Since KRP2 has been shown to promote the interaction between a different CYCD (CYCD2;1) and CDKA;1 (Sanz *et al.*, 2011), its ability to promote possible CYCD7;1 and CDKA;1 interaction was tested. Results show that KRP2 expressed as a native protein promoted CDKA;1/CYCD7;1

interaction in both the CYCD7;1-BD/CDKA;1-AD and CDKA;1-AD/CYCD7;1-BD combinations (Fig. 5.2, row 11,15).

5.1.3. CYCD7;1 does not interact with CDKBs in yeast

The analysis was further extended to test whether CYCD7;1 can bind CDKBs in the presence or absence of KRP2. No direct interaction of KRP2 with any of the four CDKBs (CDKB1;1, CDKB1;2, CDKB2;1, CDKB2;2) was observed (Fig. 5.2, rows 21,30,39,48), as previously reported (Zhou *et al.*, 2002a; Nakai *et al.*, 2006). Furthermore no direct interaction of CDKBs with CYCD7;1 was observed (Fig. 5.2, rows 18,23,27,32,36,41,45,50). Finally the co-expression of KRP2 was unable to promote CDKBs-CYCD7;1 interaction (Fig. 5.2, rows 20,25,29,34,38,43,47,52).

The KRP family has seven members in Arabidopsis. The question asked is whether CYCD7;1 binds specifically to CDKA;1 in the presence of KRP2 or whether CYCD7;1 could interact with any CDKs in presence of other KRPs.

5.1.4. CYCD7;1 can also interact with CDKA;1 in the presence of KRP1

The most closely related of the other KRPs to KRP2 is KRP1 (Zhou *et al.*, 2002a; Torres Acosta *et al.*, 2011). The previous investigation was therefore repeated using KRP1 instead of KRP2. The same controls as mentioned above were run to ensure the validity of the results of this experiment (Fig. 5.3): no yeast growth was observed on - his or - ade media and no blue colour appeared with transformants containing (1) CYCD7;1-BD or CDK-BD, empty AD vector together with pFL61 expressing KRP1 (Fig. 5.3 row 2,7,13,18,23,28), (2) empty BD with CYCD7;1-AD or CDK-AD and pFL61_KRP1 (Fig. 5.3, row 8,3,10,15,20,25), and (3) empty BD with KRP1-AD and pFL61 empty vector (Fig. 5.3 row 5)

Similar results to KRP2 were found with KRP1. Interaction between KRP1 and CDKA;1 (Fig. 5., row 6) and not any other CDKBs (Fig. 5.3 row 12,17,22,27), was observed as yeast could grow on media lacking his and ade, as well as a positive result with the *lacZ* reporter. Like KRP2, CYCD7;1 did not interact with KRP1 (Fig. 5.3, row 1), but interaction with CDKA;1 was observed when KRP1 was co-expressed (Fig. 5.3, row 4,9). Furthermore the interaction between CYCD7;1 was specific for CDKA;1. When CDKBs, KRP1 and CYCD7;1 were co-expressed the yeast did not grow on media lacking of his and ade, indicating that KRP1 also did not promote the interaction between CDKBs and CYCD7;1 (Fig. 5.3, row 11,14,16,19,21,24,26,29).

Figure 5.2. CYCD7;1 interacts with CDKA;1 in the presence of KRP2.

Interaction between CYCD7;1, CDKs (CDKA;1/ CDKB1;1/CDKB1;2/CDKB2;1 and CDKB2;2) and KRP2 was tested using Y3H assays. The first column shows growth on a medium non-selective for the interaction but selective for co-transformation with the three plasmids (medium depleted of TLU).
– his column is a medium depleted of TLUH and supplemented with 30 mM 3-AT. – ade is a medium depleted of TLUA. Yeast growth on –TLUH or –TLUA reflects an interaction between the proteins expressed.
X-Gal column shows colonies grown on –TLU (selection for co-transformant) for 3 days on which the overlay X-Gal assay was performed (see chapter 2). Interaction between the expressed proteins is detected by the development of a blue color.

Abbreviations: T, tryptophan; L, leucine; U, uracil; H/his, histidine; A/ade, adenine; 3-AT, 3-Amino-1,2,4-triazole.

	BD	AD	pFL61
1	empty	empty	empty
2	CYCD7;1	empty	empty
3	CYCD7;1	CDKA;1	empty
4	empty	CDKA;1	empty
5	CDKA;1	empty	empty
6	CDKA;1	CYCD7;1	empty
7	empty	CYCD7;1	empty
8	empty	CYCD7;1	KRP2
9	CYCD7;1	empty	KRP2
10	empty	CDKA;1	KRP2
11	**CYCD7;1**	**CDKA;1**	**KRP2**
12	**CYCD7;1**	**KRP2**	**empty**
13	**CDKA;1**	**KRP2**	**empty**
14	CDKA;1	empty	KRP2
15	**CDKA;1**	**CYCD7;1**	**KRP2**
16	CDKA;1	CYCD7;1	empty

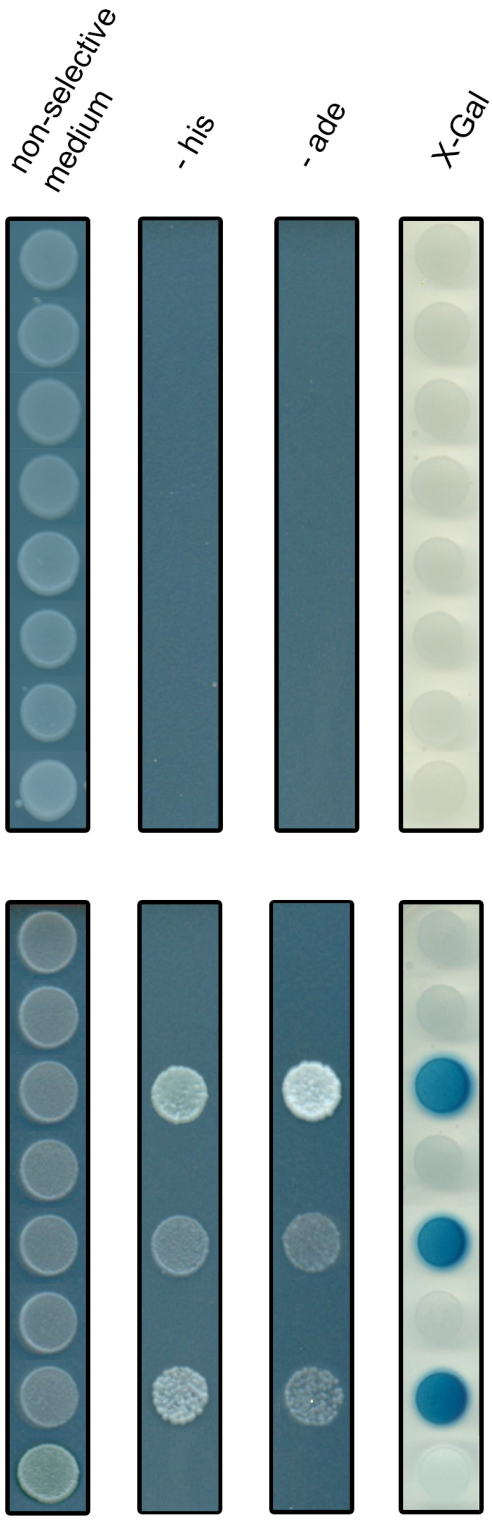

	BD	AD	pFL61
17	empty	CDKB1;1	empty
18	CYCD7;1	CDKB1;1	empty
19	empty	CDKB1;1	KRP2
20	CYCD7;1	CDKB1;1	KRP2
21	CDKB1;1	KRP2	empty
22	CDKB1;1	empty	empty
23	CDKB1;1	CYCD7;1	empty
24	CDKB1;1	empty	KRP2
25	CDKB1;1	CYCD7;1	KRP2
26	empty	CDKB1;2	empty
27	CYCD7;1	CDKB1;2	empty
28	empty	CDKB1;2	KRP2
29	CYCD7;1	CDKB1;2	KRP2
30	CDKB1;2	KRP2	empty
31	CDKB1;2	empty	empty
32	CDKB1;2	CYCD7;1	empty
33	CDKB1;2	empty	KRP2
34	CDKB1;2	CYCD7;1	KRP2

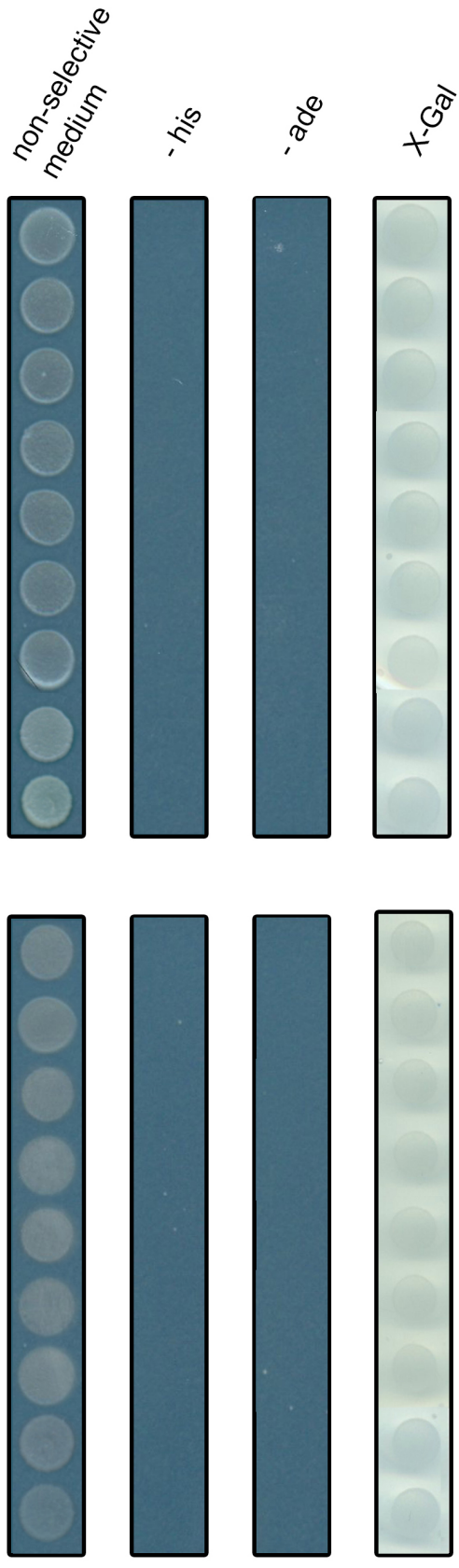

Figure 5.2. CYCD7;1 interacts with CDKA;1 in presence of KRP2 (continued).

	BD	AD	pFL61
35	empty	CDKB2;1	empty
36	CYCD7;1	CDKB2;1	empty
37	empty	CDKB2;1	KRP2
38	CYCD7;1	CDKB2;1	KRP2
39	CDKB2;1	KRP2	empty
40	CDKB2;1	empty	empty
41	CDKB2;1	CYCD7;1	empty
42	CDKB2;1	empty	KRP2
43	CDKB2;1	CYCD7;1	KRP2
44	empty	CDKB2;2	empty
45	CYCD7;1	CDKB2;2	empty
46	empty	CDKB2;2	KRP2
47	CYCD7;1	CDKB2;2	KRP2
48	CDKB2;2	KRP2	empty
49	CDKB2;2	empty	empty
50	CDKB2;2	CYCD7;1	empty
51	CDKB2;2	empty	KRP2
52	CDKB2;2	CYCD7;1	KRP2

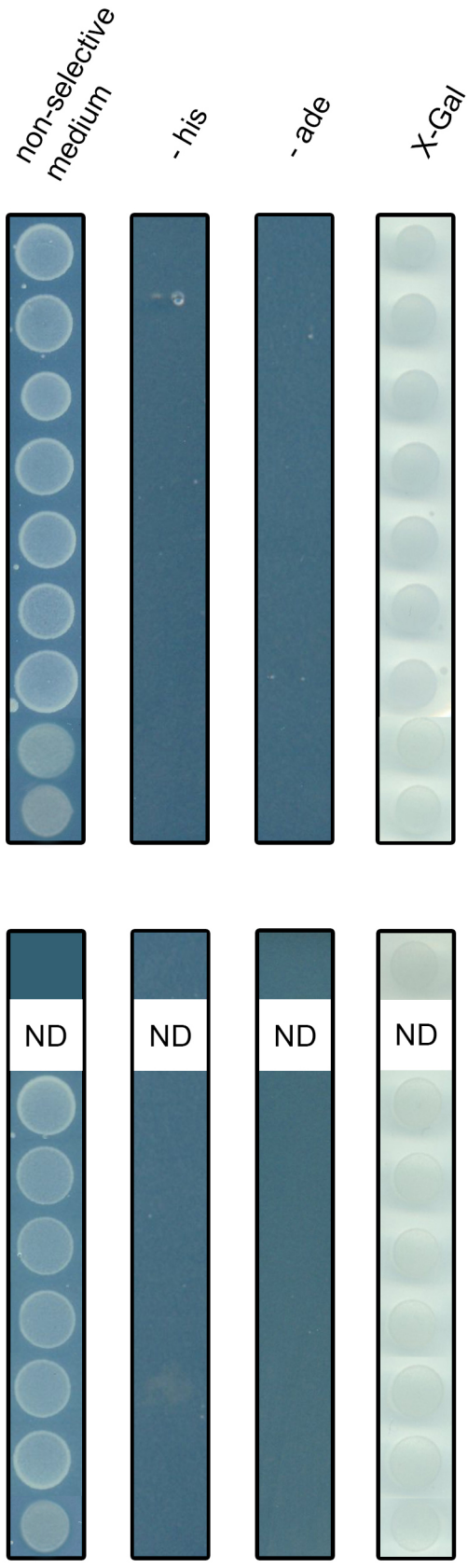

Figure 5.2. CYCD7;1 interacts with CDKA;1 in presence of KRP2 (continued).

Figure 5.3. CYCD7;1 interacts with CDKA;1 in the presence of KRP1.

Interaction between CYCD7;1, CDKs (CDKA;1/ CDKB1;1/CDKB1;2/CDKB2;1 and CDKB2;2) and KRP1 was tested using Y3H assays. The first column shows growth on a medium non-selective for the interaction but selective for co-transformation with the three plasmids (medium depleted of TLU).
– his column is a medium depleted of TLUH and supplemented with 30 mM 3-AT. – ade is a medium depleted of TLUA. Yeast growth on –TLUH or –TLUA reflects an interaction between the proteins expressed.
X-Gal column shows colonies grown on –TLU (selection for co-transformant) for 3 days on which the overlay X-Gal assay was performed (see chapter 2). Interaction between the expressed proteins is detected by the development of a blue color.

Abbreviations: T, tryptophan; L, leucine; U, uracil; H/his, histidine; A/ade, adenine; 3-AT, 3-Amino-1,2,4-triazole.

	BD	AD	pFL61
1	**CYCD7;1**	**KRP1**	**empty**
2	CYCD7;1	empty	KRP1
3	empty	CDKA;1	KRP1
4	**CYCD7;1**	**CDKA;1**	**KRP1**
5	empty	KRP1	empty
6	**CDKA;1**	**KRP1**	**empty**
7	CDKA;1	empty	KRP1
8	empty	CYCD7;1	KRP1
9	**CDKA;1**	**CYCD7;1**	**KRP1**
10	empty	CDKB1;1	KRP1
11	CYCD7;1	CDKB1;1	KRP1
12	CDKB1;1	KRP1	empty
13	CDKB1;1	empty	KRP1
14	CDKB1;1	CYCD7;1	KRP1

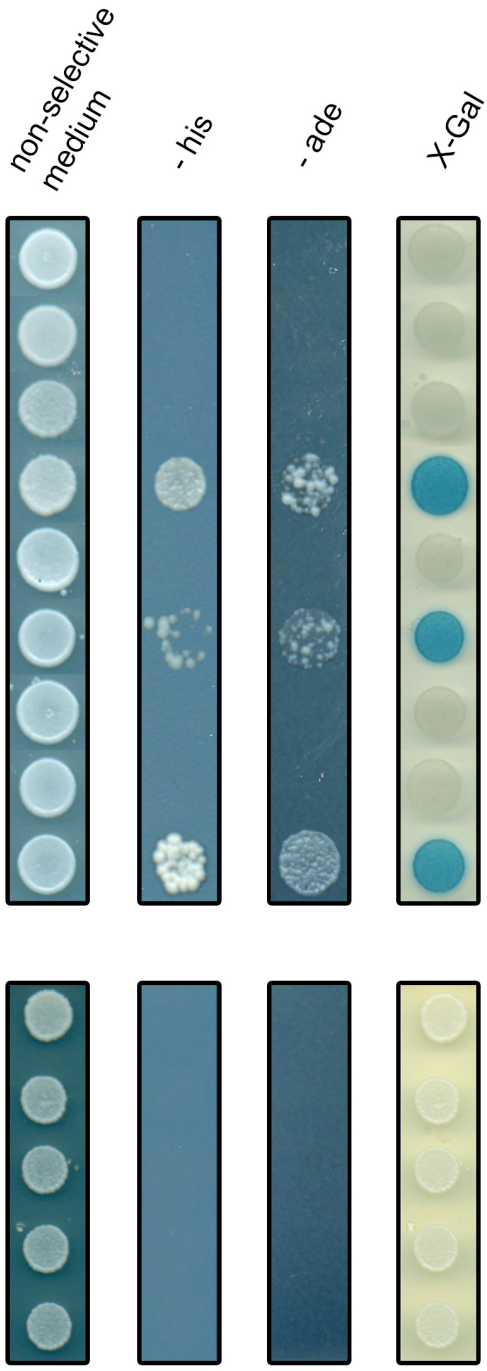

	BD	AD	pFL61
15	empty	CDKB1;2	KRP1
16	CYCD7;1	CDKB1;2	KRP1
17	CDKB1;2	KRP1	empty
18	CDKB1;2	empty	KRP1
19	CDKB1;2	CYCD7;1	KRP1
20	empty	CDKB2;1	KRP1
21	CYCD7;1	CDKB2;1	KRP1
22	CDKB2;1	KRP1	empty
23	CDKB2;1	empty	KRP1
24	CDKB2;1	CYCD7;1	KRP1
25	empty	CDKB2;2	KRP1
26	CYCD7;1	CDKB2;2	KRP1
27	CDKB2;2	KRP1	empty
28	CDKB2;2	empty	KRP1
29	CDKB2;2	CYCD7;1	KRP1

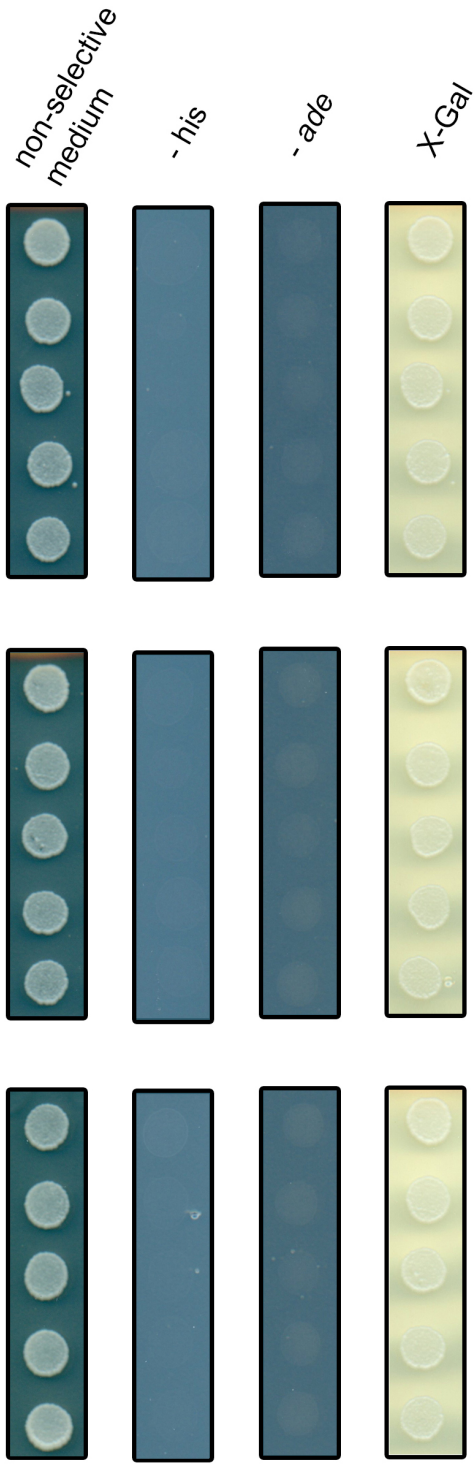

Figure 5.3. CYCD7;1 interacts with CDKA;1 in presence of KRP1 (continued).

5.1.5. Other members of the KRP family do not interact with CYCD7;1

KRP1 and KRP2 appear to be involved in allowing or promoting the interaction between the catalytic sub-unit CDKA;1 and the regulatory sub unit CYCD7;1. To ensure that no other members of the KRP family are disregarded, a yeast-three-hybrid was performed with KRP3, KRP4, KRP5, KRP6, KRP7 and the 5 CDKs.

When CDKA;1-BD and KRP-AD are co-expressed, only yeast with KRP3-AD can grow suggesting that CDKA;1 interacts with KRP3 but not with KRP4, KRP5, KRP6 or KRP7 (Fig. 5.4). However, CYCD7;1 does not bind CDKA;1 in the presence of KRP3 as yeast growth does not occur and the colonies stay white in the X-Gal assay. This demonstrates that KRP binding to CDKA;A is not sufficient to promote CDKA;1 interaction with CYCD7;1, and this promotion is specific to KRP1 and KRP2.

CYCD7;1-BD or - AD, CDKA;1-BD or –AD, KRP1/2/3 with or without AD appear to be functional as they could interact with one or more partner proteins. On the other hand, as no interaction was detected with KRP4/5/6/7 with or without the AD, I needed to ensure that the proteins were both expressed in yeast and were functional. Positive controls showing an interaction between CYCD2;1 and KRP4, KRP5 and KRP7 were included (Sanz *et al.*, 2011). As no positive control was available for KRP6, the absence of yeast growth should be interpreted carefully and might not reflect an absence of interaction.

Finally the interaction between CYCD7;1 and the other 5 KRPs and the 4 CDKBs was tested (Fig. 5.5). Using this system it appeared that CYCD7;1 did not interact with CDKBs nor did KRP3-7. However, the absence of interaction between CYCD7;1 and CDKBs has to interpreted carefully as the absence of positive control binding for the CDKBs was not available and results could be caused by a production of non functional CDKBs or CDKBs with an abnormal conformation in yeast.

Using Y3H assay, the interaction between CYCD7;1 and CDKA;1 in the presence of KRP1 or KRP2 was revealed. To investigate if the interaction is required *in planta* to give rise to the enhanced seed size phenotype, KRP1 and KRP2 expression patterns were analyzed to assess the likelihood of the proteins coming into contact.

Figure 5.4. CDKA;1 can also interact with KRP3 but this does not allow the interaction with CYCD7;1.

Interaction between CYCD7;1, CDKA;1 and KRP3-7 is tested using Y3H assay. The first column shows growth on a medium non-selective for the interaction but selective for co-transformation with the three plasmids (medium depleted of TLU).
– his column is a medium depleted of TLUH and supplemented with 30 mM 3-AT. – ade is a medium depleted of TLUA. Yeast growth on –TLUH or –TLUA reflects an interaction between the proteins expressed.
X-Gal column shows colonies grown on –TLU (selection for co-transformant) for 3 days on which the overlay X-Gal assay was performed (see chapter 2). Interaction between the expressed proteins is detected by the development of a blue color.

Abbreviations: T, tryptophan; L, leucine; U, uracil; H/his, histidine; A/ade, adenine; 3-AT, 3-Amino-1,2,4-triazole.

BD	AD	pFL61
CYCD7;1	**KRP3**	**empty**
CYCD7;1	empty	KRP3
empty	CDKA;1	KRP3
CYCD7;1	CDKA;1	KRP3
empty	KRP3	empty
CDKA;1	**KRP3**	**empty**
CDKA;1	empty	KRP3
empty	CYCD7;1	KRP3
CDKA;1	**CYCD7;1**	**KRP3**
CYCD7;1	**KRP4**	**empty**
CYCD2;1	**KRP4**	**empty**
CYCD7;1	empty	KRP4
empty	CDKA;1	KRP4
CYCD7;1	**CDKA;1**	**KRP4**
empty	KRP4	empty
CDKA;1	KRP4	empty
CDKA;1	empty	KRP4
empty	CYCD7;1	KRP4
CDKA;1	**CYCD7;1**	**KRP4**

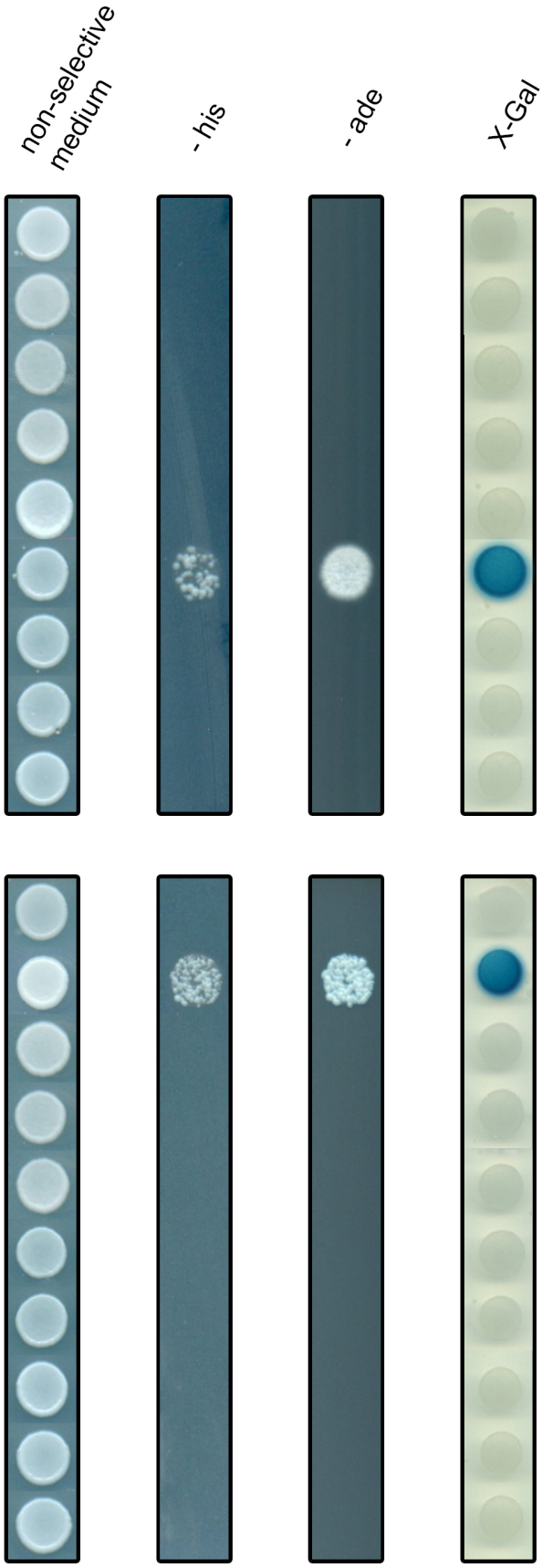

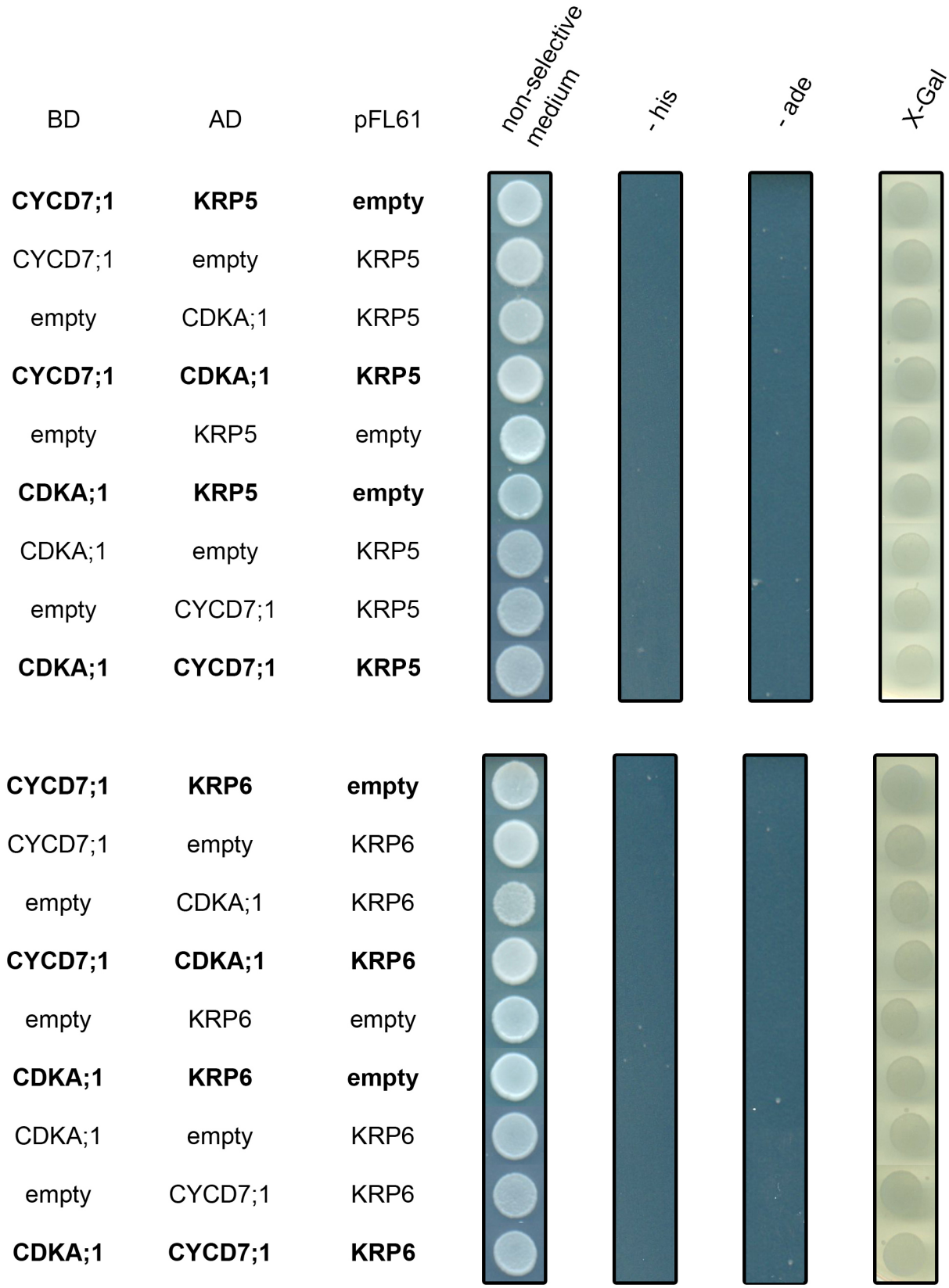

Figure 5.4. CDKA;1 can also interact KRP3 but this does not allow the interaction CYCD7;1 (continued).

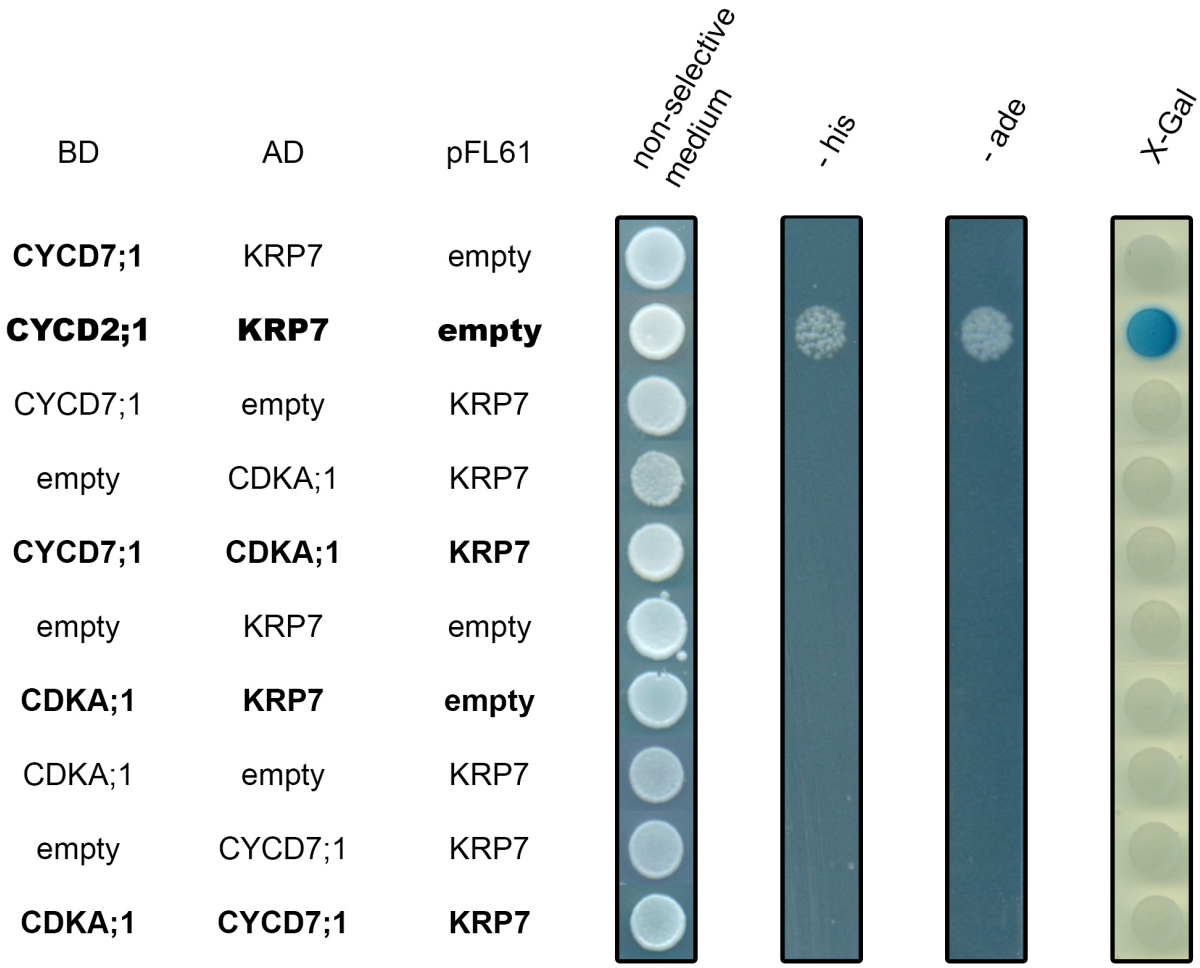

Figure 5.4. CDKA;1 can also interact KRP3 but this does not allow the interaction CYCD7;1 (continued).

Figure 5.5. CYCD7;1 does not appear to bind any CDKBs.

Interaction between CYCD7;1, CDKBs (CDKB1;1/CDKB1;2/CDKB2;1 and CDKB2;2) and KRP3, KRP4, KRP5, KRP6 and KRP7 was tested using Y3H assays. The first column shows growth on a medium non-selective for the interaction but selective for co-transformation with the three plasmids (medium depleted of TLU).
– his column is a medium depleted of TLUH and supplemented with 30 mM 3-AT. – ade is a medium depleted of TLUA. Yeast growth on –TLUH or –TLUA reflects an interaction between the proteins expressed.
X-Gal column shows colonies grown on –TLU (selection for co-transformant) for 3 days on which the overlay X-Gal assay was performed (see chapter 2). Interaction between the expressed proteins is detected by the development of a blue color.

Abbreviations: T, tryptophan; L, leucine; U, uracil; H/his, histidine; A/ade, adenine; 3-AT, 3-Amino-1,2,4-triazole.

BD	AD	pFL61
empty	CDKB1;1	KRP3
CYCD7;1	CDKB1;1	KRP3
CDKB1;1	KRP3	empty
CDKB1;1	empty	KRP3
CDKB1;1	CYCD7;1	KRP3
empty	CDKB1;2	KRP3
CYCD7;1	CDKB1;2	KRP3
CDKB1;2	KRP3	empty
CDKB1;2	empty	KRP3
CDKB1;2	CYCD7;1	KRP3
empty	CDKB2;1	KRP3
CYCD7;1	CDKB2;1	KRP3
CDKB2;1	KRP3	empty
CDKB2;1	empty	KRP3
CDKB2;1	CYCD7;1	KRP3
empty	CDKB2;2	KRP3
CYCD7;1	CDKB2;2	KRP3
CDKB2;2	KRP3	empty
CDKB2;2	empty	KRP3
CDKB2;2	CYCD7;1	KRP3

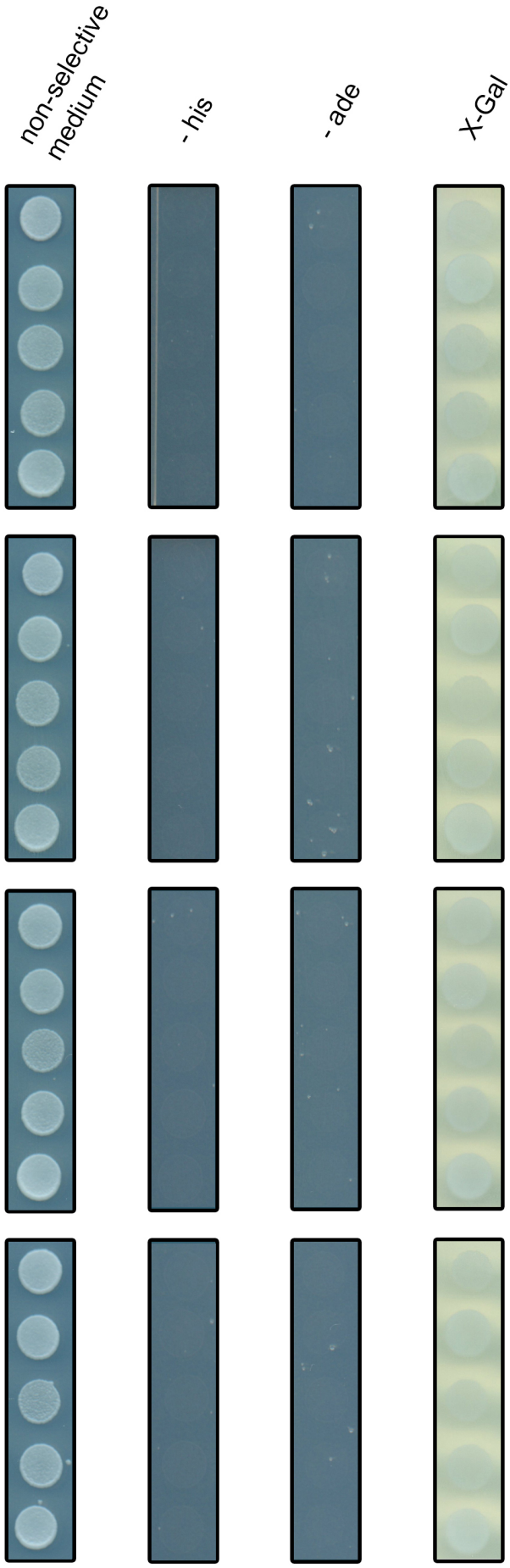

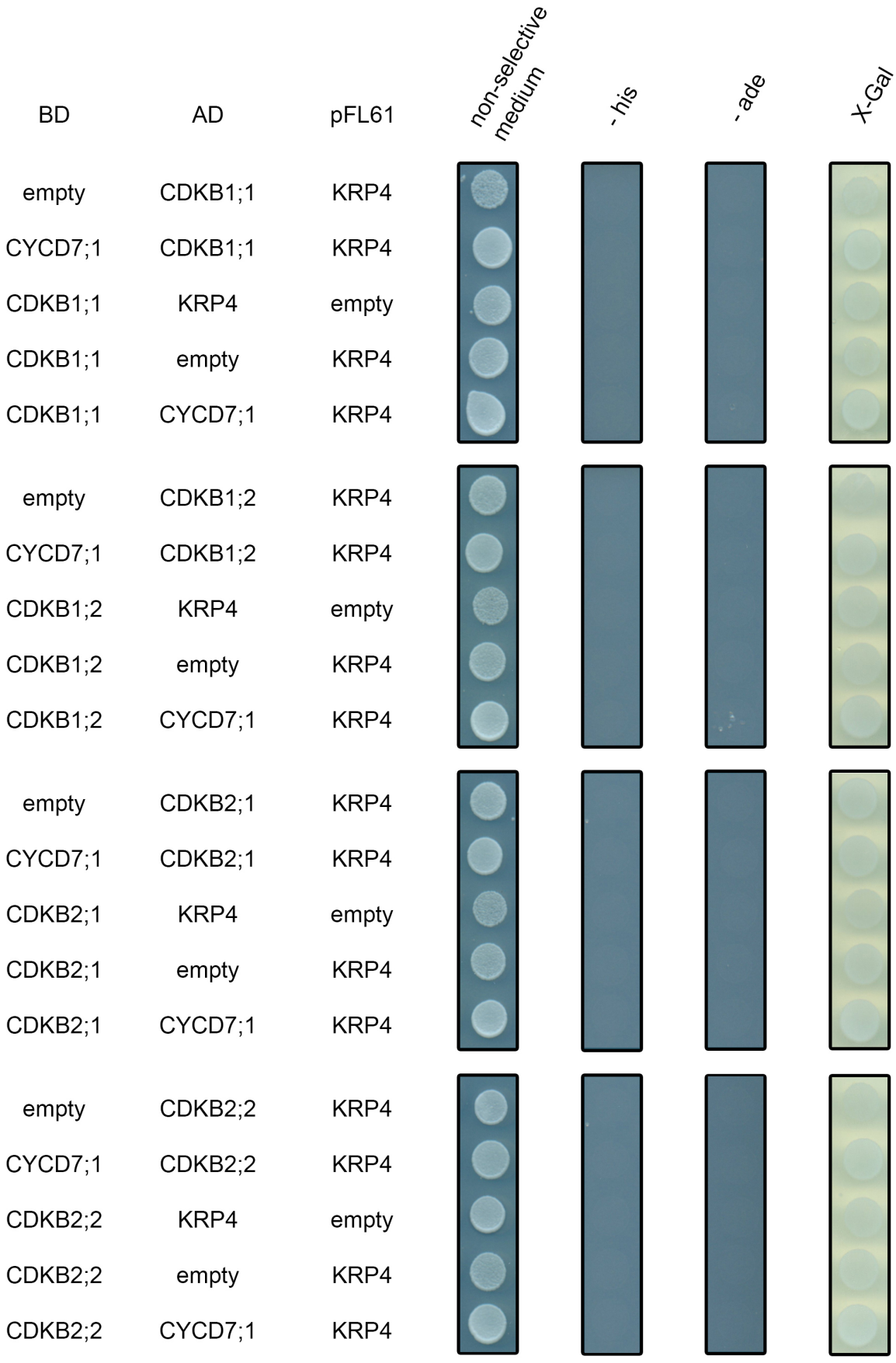

Figure 5.5. CYCD7;1 does not appear to bind any CDKBs (continued).

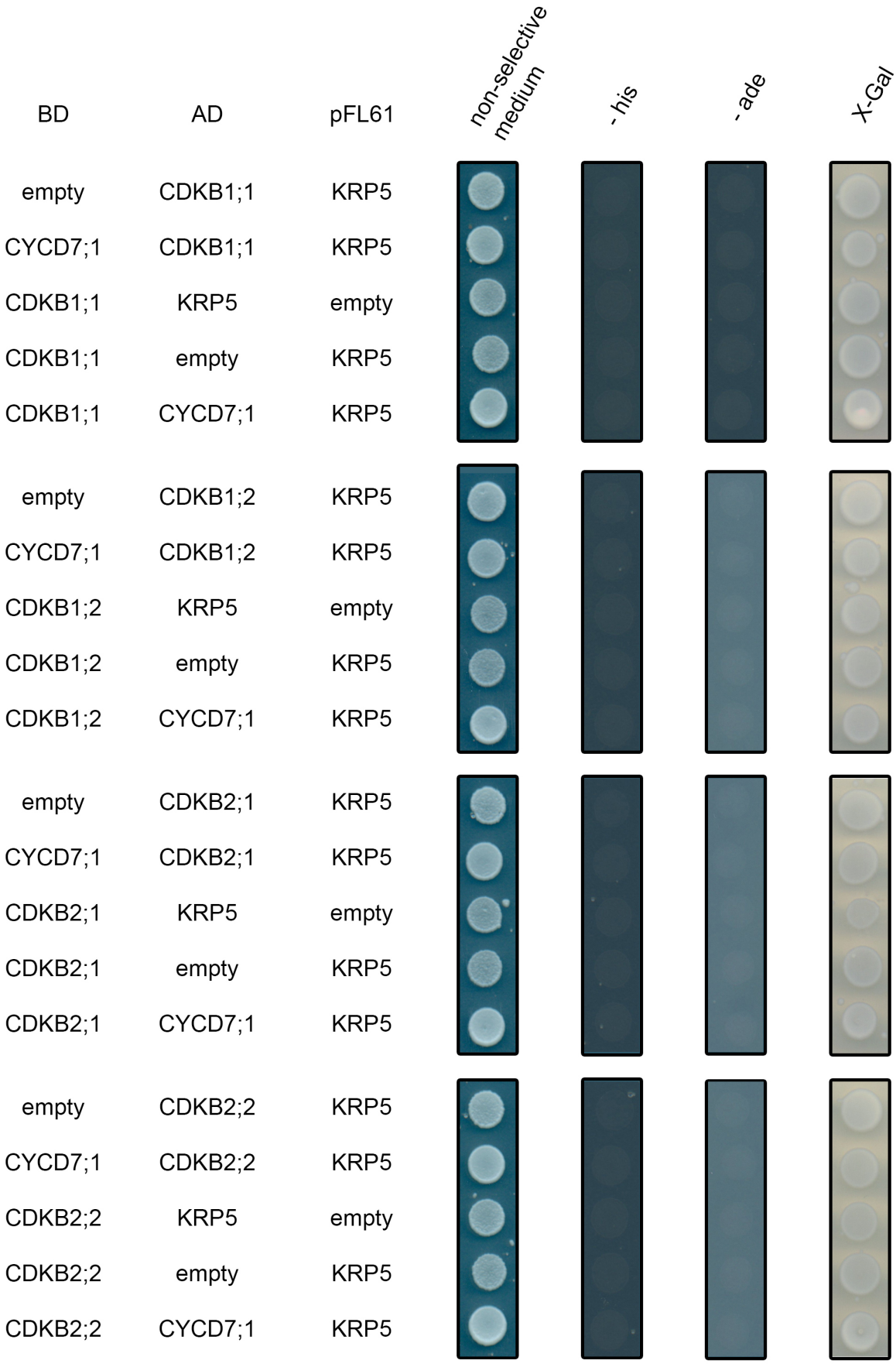

Figure 5.5. CYCD7;1 does not appear to bind any CDKBs (continued).

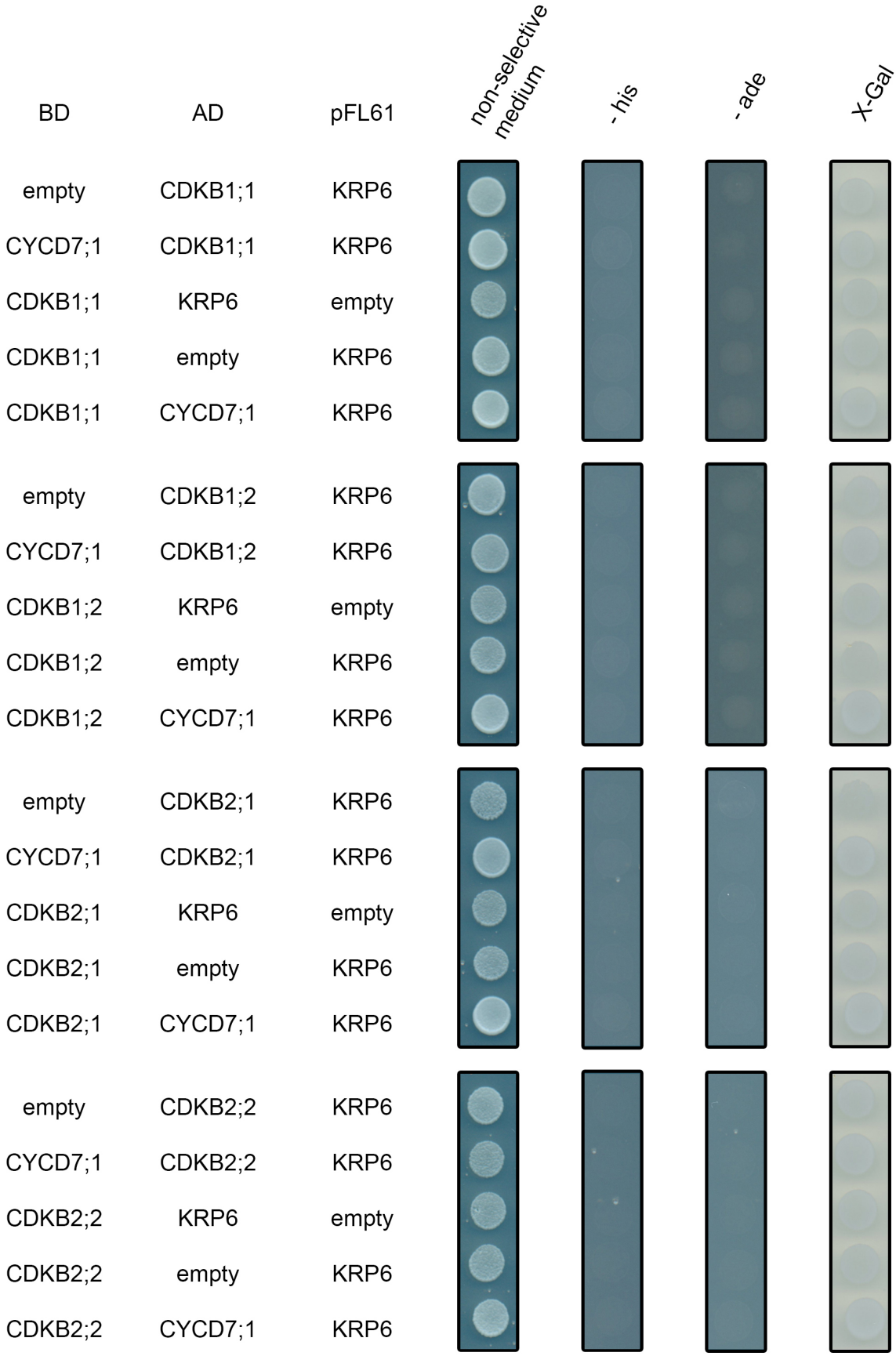

Figure 5.5. CYCD7;1 does not appear to bind any CDKBs (continued).

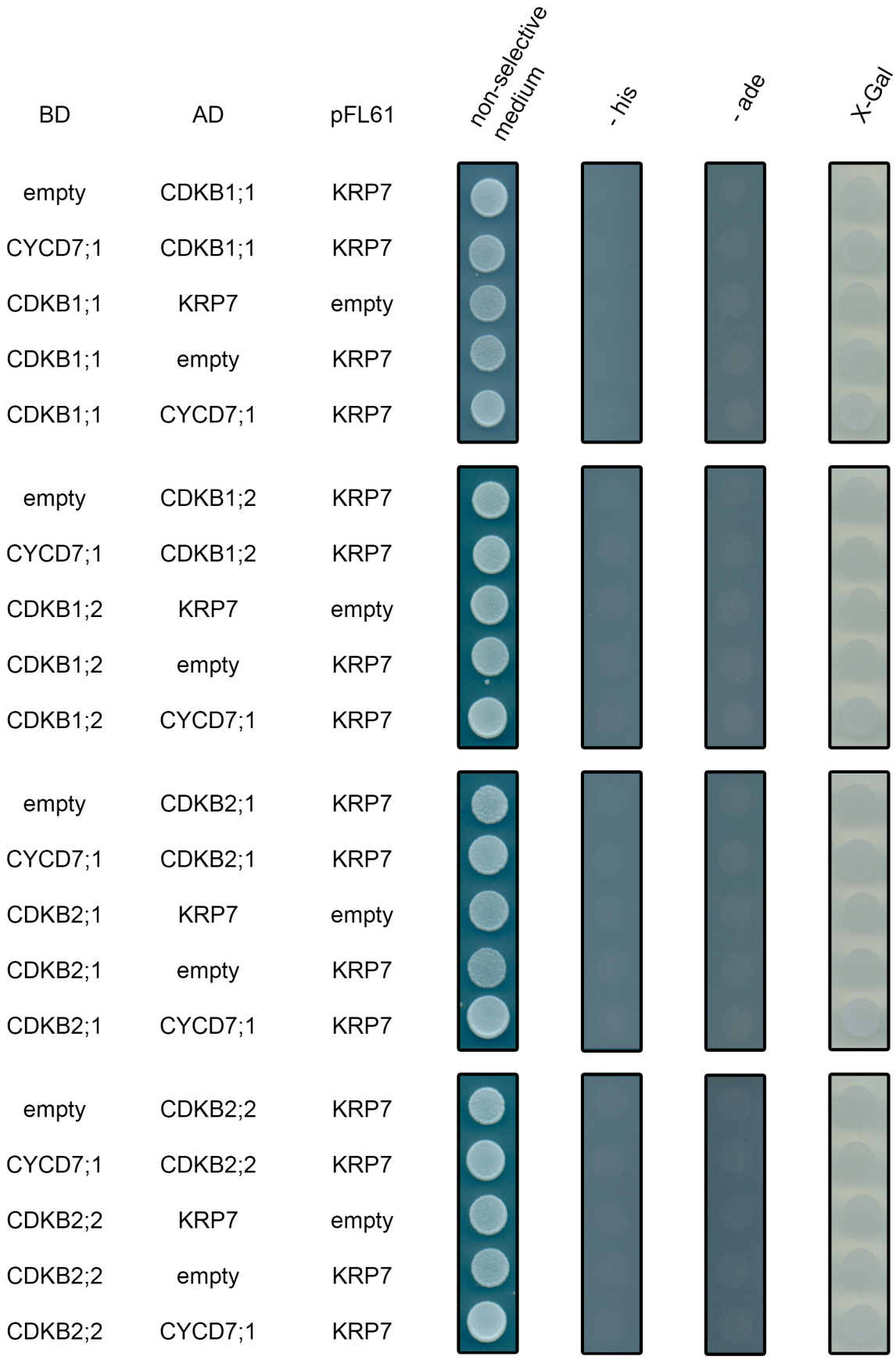

Figure 5.5. CYCD7;1 does not appear to bind any CDKBs (continued).

5.2. Activity of *KRP1* and *KRP2* genes during plant development

5.2.1. Expression pattern of *KRP1* during plant development

KRP1 expression was examined using RT-PCR of total RNA, and the reporter line *KRP1:GUS* (Ren *et al.*, 2008). Analyses were carried out on seedlings and on reproductive structures as a positive control and on different stages of developing seeds pooled together to perform the RT-PCR. For RT-PCR, *WT* (*Col-0*) was used to assess basal expression, and the *krp1-1* loss-of-function mutant as a negative control. The *KRP1:KRP1-GUS* transgenic line (overexpressor in the native domain of expression) was used as a positive control (Ren *et al.*, 2008; Sanz *et al.*, 2011). *WT* and *KRP1:KRP1-GUS* seedlings showed detectable mRNA, whereas *krp1-1* seedlings did not show any mRNA, confirming previous data (Fig. 5.6A). *KRP1* transcript could be detected in developing seeds of *WT* and in the overexpressor *KRP1:KRP1-GUS* but not in *krp1-1* seeds. To gain a better insight of *KRP1* spatio-temporal expression, the reporter *KRP1:GUS* was studied. The *KRP1:KRP1-GUS* transgenic line was also available but no GUS signal was detected in these seeds.

As previously described, a 7day-old seedling showed *KRP1:GUS* activity in cotyledons and 2 emerging leaves but could not be seen in the petiole or in roots (Fig. 5.6B). In the inflorescence, GUS staining was visible in sepals throughout flower development from stage 10 to stage 16 as described by Smyth *et al.* (1990)(Fig. 5.6C-F). At stage 16, in addition to the expression in sepals, *KRP1:GUS* expression is detectable in mature anthers (Fig. 5.6F,G) and specifically in mature pollen grains (Fig. 5.6G). In pistils that appeared to be pollinated, ovules/seeds showed staining (Fig. 5.6H). Detailed analysis of *KRP1* expression in developing seeds revealed that the promoter was not active before the dermatogene stage (Fig. 5.6I). *KRP1:GUS* was strongly expressed in the micropylar endosperm at the globular embryo stage (Fig. 5.6J) and more weakly at heart stage (Fig. 5.6K). From later heart/early torpedo stage (Fig. 5.6L) to bent cotyledon stage (Fig. 5.6M), the expression appeared in the cellularized endosperm. In mature-green-stage seeds, *KRP1* activity seemed to be restricted to the mature embryo (Fig. 5.6N).

The data suggest that *KRP1* was expressed during seed development. *KRP1* activity in the endosperm at globular stage would be concomitant with *CYCD7;1* expression under the *FWA* promoter and *CDKA;1* expression that has been shown to be expressed in mature central cell and seed development (Le *et al.*, 2010; Zhao *et al.*, 2012). The spatio-temporal overlap of *CYCD7;1, KRP1* and *CDKA;1* expression supports that fact that *CYCD7;1*, *KRP1*, and CDKA;1 might be involved in enhancing seed size.

Figure 5.6. *KRP1* is expressed during vegetative, flower and seed development.

(A) cDNA was prepared from seedlings and seeds at different developmental stages pooled together. RT-PCR was performed using *ACTIN 2* (*ACT2*, primer pair 9 and 10 in chapter 2) for normalization and gene-specific primers (*KRP1*, primer pair 14 and 15 in chapter 2). *Col-0 WT* was used to assess the basal level of expression, the *krp1-1* mutant as a negative control and the *KRP1:KRP1-GUS* transgenic line (Ren *et al.*, 2008) as an overexpressor in the native domain of expression.

KRP1:GUS line (Ren *et al.*, 2008) was used to examine *KRP1* promoter activity by GUS assay (0.5 mM $K_3Fe(CN)_6/K_4Fe(CN)_6$ and 3h incubation at 37°C). After incubation, blue staining appeared in expressing tissues. Floral developmental stages used are those described by Smyth et al. (1990). Seed developmental stages used are described in Bowman and Mansfield (1994) and reviewed by West and Harada (1993) and, Le *et al.* (2010).

(B) Expression is detectable in cotyledons and young leaves of 7-day old seedlings.

C-G, Expression during flower development and reproductive structures:

In the inflorescence (C), GUS staining is visible in the sepals of flowers at different developmental stages from stage 10 (D) to stage 12 (E). At stage 16 (F), expression is still noticeable in sepals and appears in mature anthers. Detailed view of pollen sac (G) reveals promoter activity in the mature pollen grain (in box, pollen grain extracted from pollen sac). (H) Flower to which sepals, petals and stamen were removed to reveal a pistil where the seeds in the ovary chamber show a blue staining.

I-N, Expression during seed development:

(I) At dermatogen stage, expression is not detectable in any of the seed compartments.
(J) *KRP1* is expressed in the micropylar endosperm at globular stage
(K) Weak expression detected in micropylar endosperm at heart phase
(L) Blue stain is visible in cellularized endosperm at the transition heart-torpedo
(M) Blue stain is visible in cellularized endosperm at bent cotyledon
(N) GUS activity seems to be restricted to mature embryo at mature-green-stage

Scale bars: B,C, 1 mm; D,E,F,H, 500 µm; G, 50 µm; I,J,K,L,M,N, 75 µm.

Abbreviations: se, sepal; gy, gynoecium; a, anther; I, integuments; en, endosperm; e, embryo; su, suspensor; ch, chalzal pole; mp, micropylar pole.

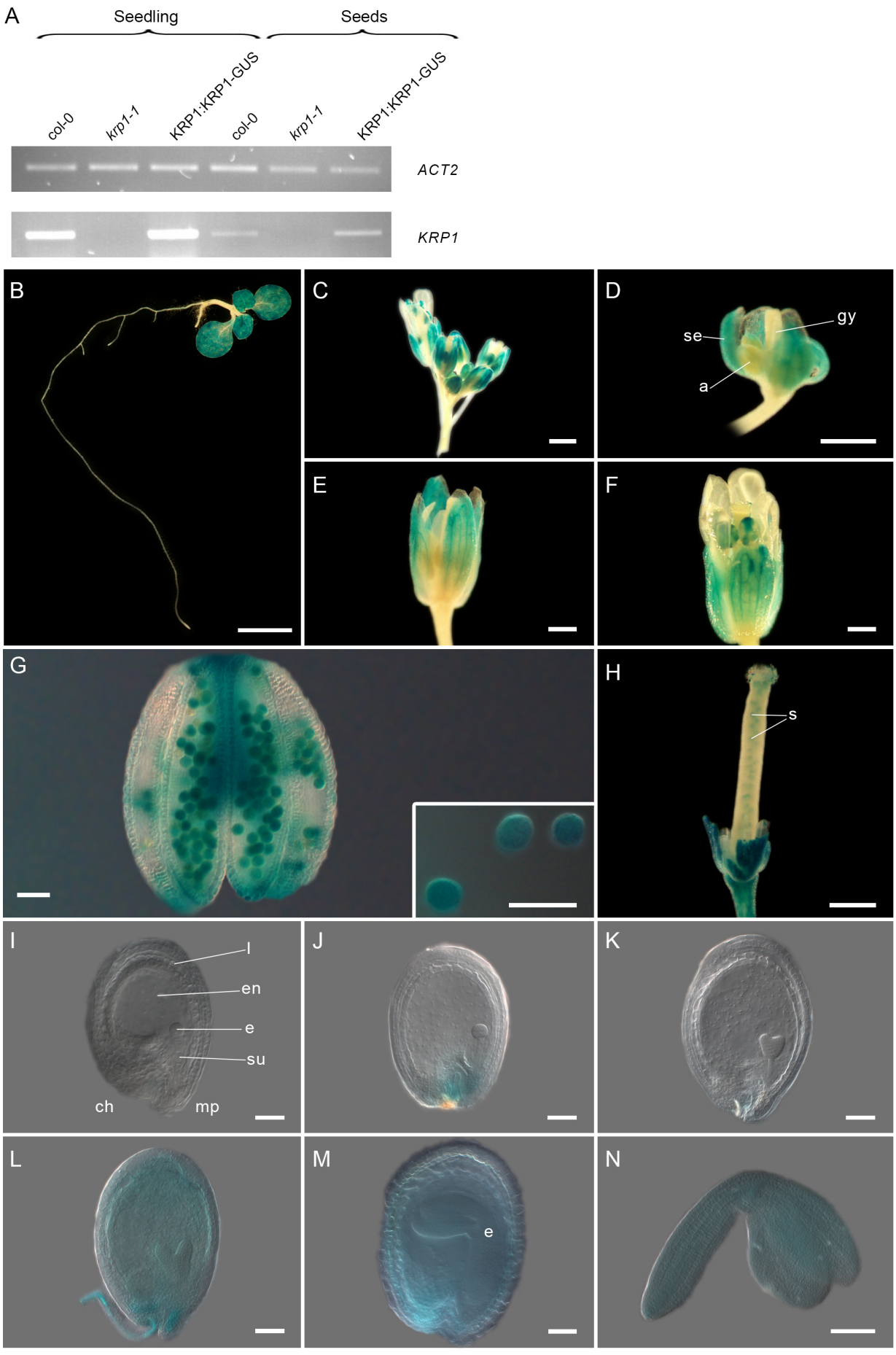
A
Seedling
Seeds
col-0
krp1-1
KRP1:KRP1-GUS
col-0
krp1-1
KRP1:KRP1-GUS
ACT2
KRP1
B
C
D
gy
se
a
E
F
G
H
s
I
l
en
e
su
ch
mp
J
K
L
M
e
N

5.2.2. Expression pattern of *KRP2* during plant development

KRP2 promoter activity was examined using RT-PCRs on total RNA, the reporter line *KRP2:GUS* and the protein fusion transgenic line *KRP2:KRP2-GFP* (Sanz *et al.*, 2011). As for *KRP1,* analyses were carried out on seedlings and reproductive structures as positive controls and different stages of developing seeds pooled together to perform the RT-PCR. *WT* (*Col-0*) was used to assess basal expression by RT-PCR, the *krp2-3* loss-of-function mutant as a negative control (Sanz *et al.*, 2011) and the *KRP2:KRP2-GFP* transgenic line as a control. *WT* and *KRP2:KRP2-GFP* seedlings showed detectable mRNA, whereas in *krp2-3* seedlings, no KRP2 transcripts were detected, confirming previous results (Fig. 5.7A). *WT* and overexpressor *KRP2:KRP2-GFP* showed a detectable level of mRNA but the *krp2-3* mutant did not. In both seedling and seed, as the *ACTIN2* levels were similar, it appears that addition of one copy of *KRP2* under its own promoter was sufficient to produce a detectable difference in mRNA level.

KRP2:GUS and *KRP2:KRP2-GFP* lines were used to confirm *KRP2:GUS* expression in vegetative and reproductive tissues. *KRP2* activity was visible in the vascular tissues of emerging leaves and the primary root of 7day-old seedling (Fig. 5.7B). A close-up of root tissues showed that *KRP2* expression was detectable by GUS staining in the vasculature from the vascular initials (Fig. 5.7C) up to the shoot. The KRP2 protein fusion with GFP reveals that KRP2 protein was present in the root where the protein activity was previously observed (Fig. 5.7D)(Sanz *et al.*, 2011). At 24 hours after exposure to light, a germinating embryo showed blue staining in the vasculature of the root and the cotyledons (Fig. 5.7E). This suggests that the *KRP2* promoter is active early during germination events in the root and cotyledon vasculature.

KRP2 expression was further followed during flower development. No blue staining could be observed in any of the sterile (sepals and petals) or reproductive (androecium and gynoecium) floral organs at stage 10 (Fig. 5.7F), stage 12 (Fig. 5.7G) or stage 15-16 (Fig. 5.7H-I). At stage 17, *KRP2* promoter activity was not detectable in the mature green silique (Fig. 5.7J). From the 2-4-cell embryo to the mature green embryo, *KRP2:GUS* activity was not detectable (Fig. 5.7K-R). These data appear to be contradictory with RT-PCR results showing the presence of *KRP2* mRNA during seed development. This could be explained by the combined fact that RT-PCR was performed on bulked up seeds at different stages of development, increasing the total amount of RNA extracted, or the presence of intron sequences in the precursor mRNA needed for *KRP2:GUS* expression in the endogenous domain. However, the second hypothesis seems unlikely as analysis of the *KRP2:KRP2-GFP* line, containing the genomic sequence fused to the GFP, revealed that no GFP signal

could be seen in any of the seed compartments at any of the different stages of seed development (data not shown).

Taken together, the data suggest that *KRP2* is expressed in vegetative organs and specifically in the vasculature. Non-correlating data for *KRP2* expression during seed development prevent us from drawing a clear conclusion. However, *KRP2* mRNA is detectable during seed development but the timing of expression and the tissue are not yet determined. The presence of *KRP2* mRNA during seed development supports the proposal that KRP2 is a potential interactor of CYCD7;1 and CDKA;1 and may be involved in the enhanced seed size phenotype in seed-targeted *CYCD7;1* transgenic lines. To confirm or deny this hypothesis, lines with seed-targeted *CYCD7;1* expression in *krp1-1* and *krp2-3* knockout backgrounds were generated and the seed size phenotype investigated.

Figure 5.7. *KRP2* is expressed during vegetative and seed development.

(A) cDNA was prepared from seedlings and seeds at different developmental stages pooled together. RT-PCR was performed using *ACTIN 2* (*ACT2*, primer pair 9 and 10 in chapter 2) for normalization and gene-specific primers (*KRP2*, primer pair 16 and 17 in chapter 2). *Col-0 WT* was used to assess the basal level of expression, the *krp2-3* mutant as a negative control and the *KRP2:KRP2-GFP* transgenic line (Sanz *et al.*, 2011) as an overexpressor in the native domain of expression.

KRP2:GUS line (De Veylder *et al.*, 2001) was used to examine *KRP2* promoter activity by GUS assay (0.5 mM $K_3Fe(CN)_6/K_4Fe(CN)_6$ and 24h incubation at 37°C). After incubation, blue staining appears in expressing tissues. The *KRP2:KRP2-GFP* reporter line was imaged using a confocal microscope to detect the protein localization.
Floral developmental stages used are those described by Smyth *et al.* (1990). Seed developmental stages used are described in Bowman and Mansfield (1994) and reviewed by West and Harada (1993) and, Le *et al.* (2010).

(B-E) Expression is detectable in vasculature of shoots and roots (B-C) of 7-day-old seedlings. KRP2 protein is localized in the vasculature of the root (D). Blue stain is visible in the vasculature of 24h-light seedling (E).

F-J, Expression during flower development and in reproductive structures:

KRP2 activity was not detectable in flowers at stage 10 (F), stage 12 (G) or at stage 15-16 (H). No staining was visible in mature reproductive structures (stage 15-16, I). Siliques at stage 17-18 did not exhibit blue staining (J)

K-R, Expression is not detectable in any of the seed compartments at the 2/4-cell stage (K), 8-cell (L), globular (M), triangular (N), heart (O), torpedo (P), walking-stick (Q) and mature-green-stage (R).

Scale bars: B,J, 2mm; C,D,F, 200 µm; E, K-R, 50 µm; G,H,I, 500 µm.

Abbreviations: se, sepal; gy, gynoecium; a, anther; I, integuments; en, endosperm; e, embryo; su, suspensor; ch, chalzal pole; mp, micropylar pole.

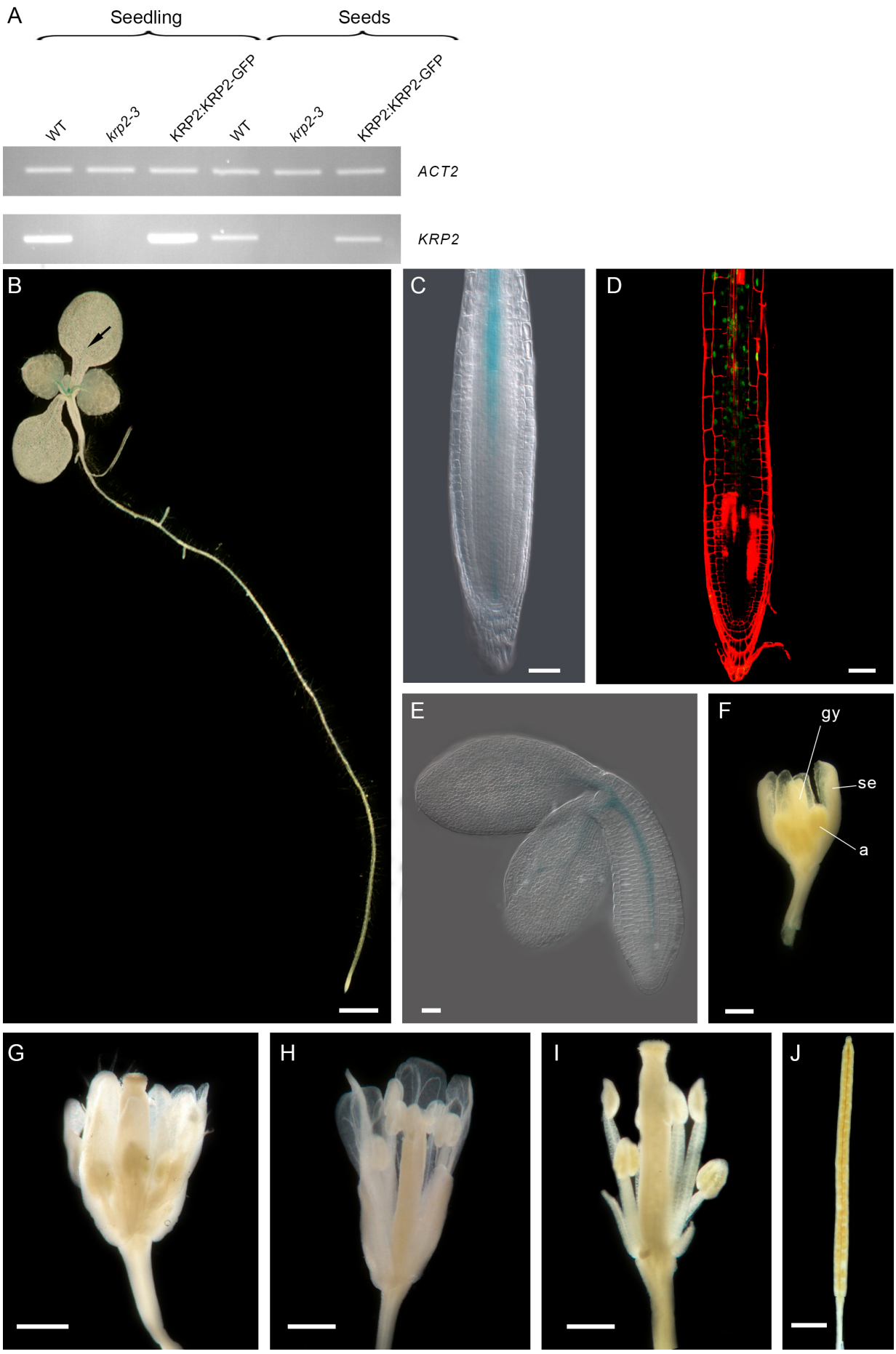
A
Seedling
Seeds
WT
krp2-3
KRP2:KRP2-GFP
WT
krp2-3
KRP2:KRP2-GFP
ACT2
KRP2
B
C
D
E
F
gy
se
a
G
H
I
J

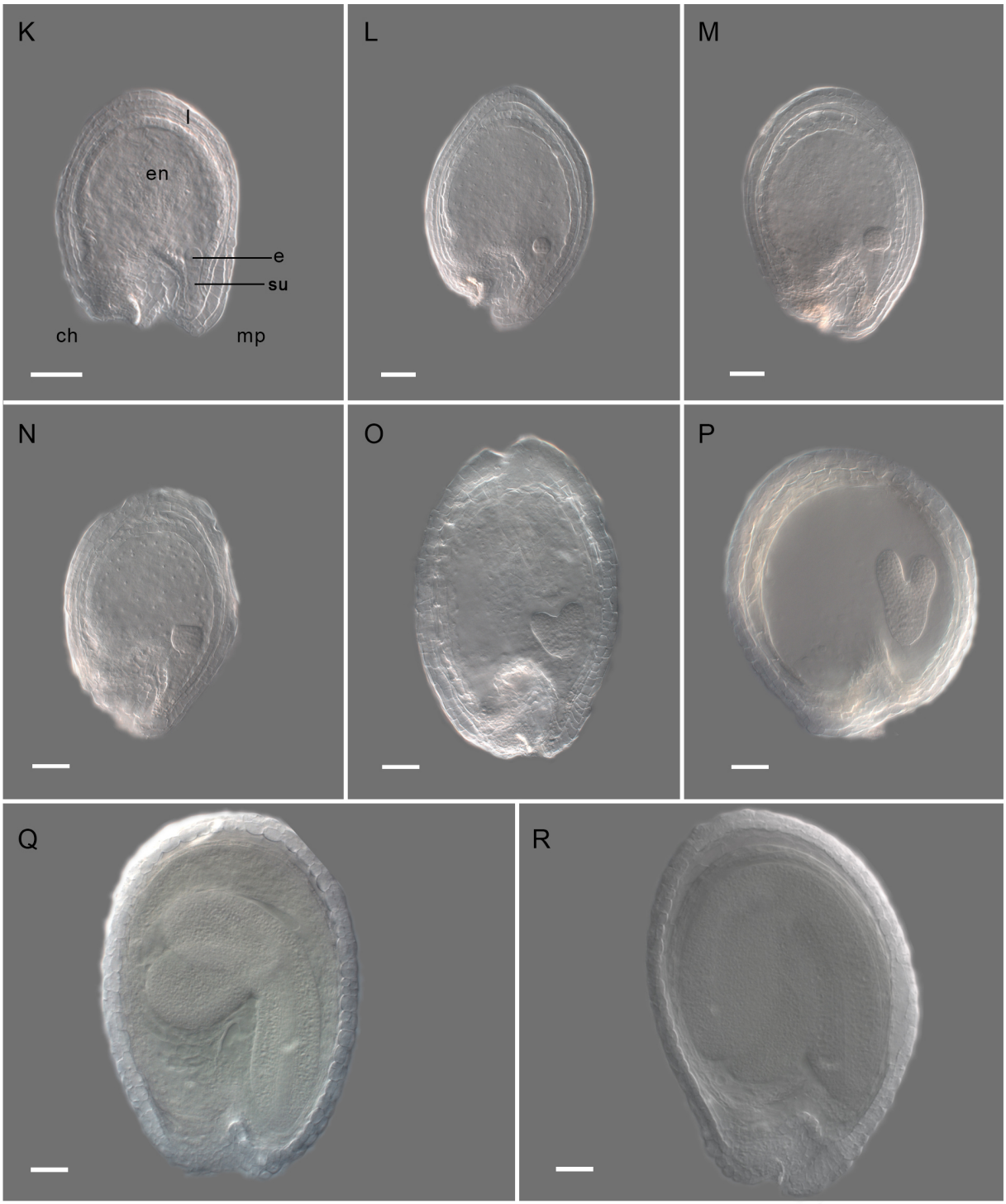

Figure 5.7. *KRP2* is expressed during vegetative and seed development (continued).

5.3. Biological roles of the CDKA;1-CYCD7;1-KRP1/2 interaction in the seed size phenotype

In this study, the *FWA* promoter is used to drive the expression of *CYCD7;1* in the mature central cell and in the endosperm of the developing seed (chapter 3). Moreover endosperm-targeted *CYCD7;1* lines produce enlarged seeds. Several studies show that D-type cyclins act with CDKA;1 to regulate the cell cycle progression (Dewitte *et al.*, 2003; Dewitte *et al.*, 2007; Nieuwland *et al.*, 2009; Sozzani *et al.*, 2010; Sanz *et al.*, 2011; Zhao *et al.*, 2012). Here I showed, using a Y3H assay, that CYCD7;1 can indeed interact with the catalytic subunit CDKA;1, but also that this interaction requires KRP2 or KRP1 as a partner. To investigate whether the interaction is necessary *in planta* to obtain seeds with an enhanced size, lines with endosperm-targeted *CYCD7;1* expression were crossed into *krp1-1* and *krp2-3* backgrounds. If KRP1 and KRP2 are indeed required for the size enhancement mediated by CYCD7;1 ectopic expression, it might be expected that the size enhancement be reduced or abolished in these lines.

krp1-1 (SALK 100189) and *krp2-3* (SALK 110338) are T-DNA insertion mutants and are publicly available from the SALK institute. *krp1-1* and *krp2-3* lines were genotyped by PCR. Primer pairs (20+15) and (20+16) respectively were used to determine where the T-DNA insert is localized in the gene and (13+14) and (16+17) respectively were used to amplify the native *KRP1* and *KRP2* genes (Fig. 5.8A). *krp1-1* had a T-DNA inserted at the beginning of the last exon (exon 4). The study of interaction between KRP1 and CDKA;1, and KRP1 and CYCD3;1 shows that the CDKA;1/CYCD binding domain is localized on the C-terminal of KRP1, between the amino acid positions 152 and 191, corresponding to the end of exon 3 and the beginning of exon 4 (Wang *et al.*, 1998). In *krp2-3*, T-DNA was situated in exon 3 (Fig. 5.8A). To confirm that *krp1-1* and *krp2-3* are knock out mutants, RT-PCR was performed on seedling mRNA, using primer pairs (15+14) and (16+17) respectively. Similarly to KRP1, it has been shown that the CDKA;1/CYCD binding domain is localized at the C-terminal of KRP2 spanning exons 3 and 4 (De Veylder *et al.*, 2001; Torres Acosta *et al.*, 2011). Both *krp1-1* and *krp2-3* showed no presence of full length mRNA, as previously demonstrated (Sanz *et al.*, 2011), and the two seed-targeted *CYCD7;1* lines have *KRP1* and *KRP2* mRNAs (Fig. 5.8B).

$_{seed}$*CYCD7;1* lines 6499 and 12489 were used to perform crosses with *krp1-1* and *krp2-3*. As shown in chapter 3, line 6499 is the strongest expressor available and line 12489 has a weaker expression. F3 homozygous *krp1-1* x $_{seed}$*CYCD7;1* and *krp2-3* x $_{seed}$*CYCD7;1* lines were generated. *krp1-1*, *krp2-3*, $_{seed}$*CYCD7;1* and *WT* were isolated from the cross. The

genotypes of these lines were confirmed by PCR using the primer pairs above. For *krp1-1* and *krp2-3* and for $_{seed}$*CYCD7;1* (11+12, see chapter 3) were used (Fig. 5.8C,F).

The seed sizes of the different genotypes were compared using a two-way ANOVA (with normality assumptions met and homoscedasticity verified) and the number of seeds measured ranged from 188 to 227 (Fig. 5.8D,E,G,H). *WT* seeds had a mean projected area of 96,594 μm^2 ranging from 95,726 μm^2 to 97123 μm^2, *krp1-1* seeds of 97,434 μm^2 and *krp2-3* of 97,350 μm^2. *krp1-1* and *krp2-2* seeds were not significantly larger than the *WT* ($p=0.002$ and $p=1.48x10^{-18}$ respectively). $_{seed}$*CYCD7;1*$_{6499}$ seeds have a size of 135,117 μm^2 on average, which was significantly greater than the *WT* ($p=1.26x10^{-78}$), representing a size increase of 39%. *krp1-1* x $_{seed}$*CYCD7;1* and *krp2-3* x $_{seed}$*CYCD7;1* had seed areas of 136,125 μm^2 and 130,581 μm^2 respectively. *krp1-1* or *krp2-3* x $_{seed}$*CYCD7;1* seeds were not significantly smaller than $_{seed}$*CYCD7;1*$_{6499}$ ($p=1$ and $p=0.45$ respectively) and both were significantly larger than the *WT* ($p=1.6x10^{-8}$ and $p=1.47x10^{-15}$ respectively).

The $_{seed}$*CYCD7;1* line 12489 had a seed size 104,509 μm^2 on average. These seeds were significantly greater than the *WT* ($p=6.04x10^{-7}$) representing a size increase of 8% respectively. *krp1-1* x $_{seed}$*CYCD7;1* and *krp2-3* x $_{seed}$*CYCD7;1* showed seed sizes of 103,043 μm^2 and 103,691 μm^2 respectively, which were not significantly different from $_{seed}$*CYCD7;1*$_{12489}$ ($p=1$ and $p=0.7$ respectively) but were significantly larger than the *WT* (p-value $2.58x10^{-8}$ for cross with *krp1-1* and $1.05x10^{-5}$ for the cross with *krp2-3*) and single *krp* insertion mutants ($p=3.8x10^{-4}$ for cross with *krp1-1* and $p=2.63x10^{-6}$ for the cross with *krp2-3*).

These data shows that $_{seed}$*CYCD7;1* seeds are larger than *WT* and there is a correlation between the magnitude of the seed size increase and the ectopic level of *CYCD7;1* expression in the seed. This piece of information corroborates results shown in chapter 3. The loss of *KRP1* or *KRP2* function does not affect final seed size. Therefore the loss of a single putative interactor, KRP1 or KRP2, in $_{seed}$*CYCD7;1* lines does not appear to influence the seed size phenotype.

Figure 5.8. Biological roles of CDKA;1, CYCD7;1 and KRP1/2 interaction in the seed size phenotype.

(A) Schematic representation of *krp1-1* (SALK 100189) and *krp2-3* (SALK 110338) insertion mutants showing the relative positions of 5' and 3' UTR (grey box), exons (black box), introns, (black line), CDK/CYCD binding domain (stripe box), T-DNA inserts indicated by RB and LB and primers.

(B) RT-PCR showing the absence of full length transcript of *KRP1* in *krp1-1* and *KRP2* in *krp2-3* using primer pairs (15+14) and (16+17) respectively. *ACT2* was used a loading control.

(C-H) Crosses generated between $_{seed}$*CYCD7;1* x *krp1-1* (C-E) and between $_{seed}$*CYCD7;1* x *krp2-3* (F-H).

(C) Genotyping by PCR to identify *WT*, $_{seed}$*CYCD7;1*, *krp1-1* from the cross (indicated with a * *and* $_{seed}$*CYCD7;1* x *krp1-1*. Primers pairs used are (11+12 amplifying a ~ 940 bp fragment) for $_{seed}$*CYCD7;1,* for the native KRP1 (13+14 amplifying a ~ 580 bp fragment) and (20+15 giving a DNA band of ~ 350 bp) for the insert (see chapter 2).

(D,G) Projected seed area was measured on at least 188 seeds. Mean seed size is plotted. Errors bars represent ± SE. * indicates a p-value < 0.05

(E) Seed from *WT*, *krp2-3*, $_{seed}$*CYCD7;1* and $_{seed}$*CYCD7;1* x *krp2-3.*

(C) Genotyping by PCR to isolate *WT*, $_{seed}$*CYCD7;1*, *krp2-3* from the cross (indicated with a * *and* $_{seed}$*CYCD7;1* x *krp2-3*. Primers pairs used are (11+12 amplifying a ~ 940 bp fragment) for $_{seed}$*CYCD7;1,* for the native KRP2 (16+17 giving a DNA band of ~ 800 bp) and (20+16 giving a DNA band of ~ 750 bp) for the insert (see chapter 2).

(H) Seed from *WT, krp2-3*, $_{seed}$*CYCD7;1* and $_{seed}$*CYCD7;1* x *krp2-3.*

Scale bars: 200 µm

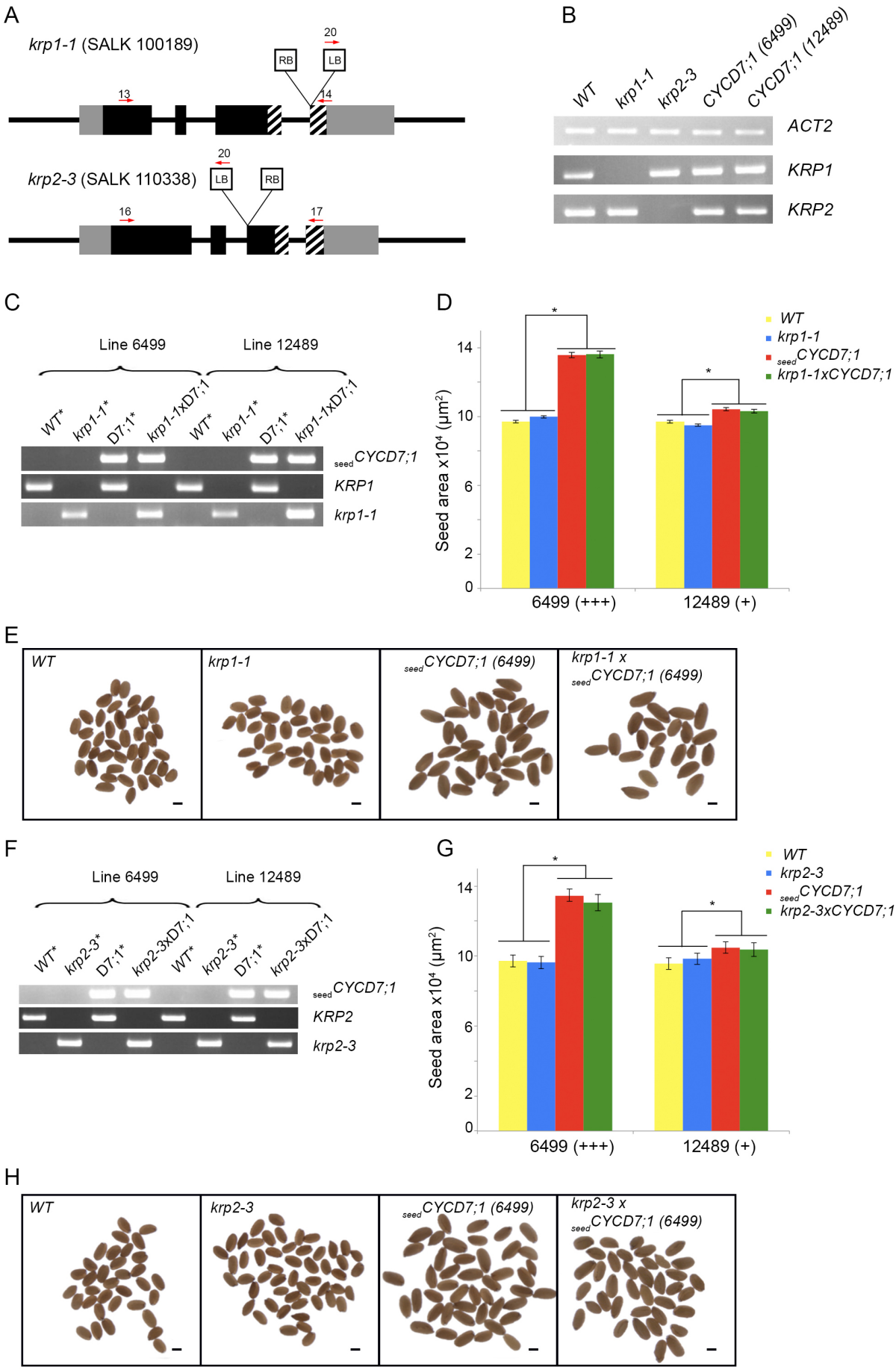
A
krp1-1 (SALK 100189)
20
RB
LB
13
14
krp2-3 (SALK 110338)
20
LB
RB
16
17
B
WT
krp1-1
krp2-3
CYCD7;1 (6499)
CYCD7;1 (12489)
ACT2
KRP1
KRP2
C
Line 6499
Line 12489
WT*
krp1-1*
D7;1*
krp1-1xD7;1
WT*
krp1-1*
D7;1*
krp1-1xD7;1
seedCYCD7;1
KRP1
krp1-1
D
Seed area x10⁴ (µm²)
14
10
6
2
0
6499 (+++)
12489 (+)
WT
krp1-1
seedCYCD7;1
krp1-1xCYCD7;1
E
WT
krp1-1
seedCYCD7;1 (6499)
krp1-1 x seedCYCD7;1 (6499)
F
Line 6499
Line 12489
WT*
krp2-3*
D7;1*
krp2-3xD7;1
WT*
krp2-3*
D7;1*
krp2-3xD7;1
seedCYCD7;1
KRP2
krp2-3
G
Seed area x10⁴ (µm²)
14
10
6
2
0
6499 (+++)
12489 (+)
WT
krp2-3
seedCYCD7;1
krp2-3xCYCD7;1
H
WT
krp2-3
seedCYCD7;1 (6499)
krp2-3 x seedCYCD7;1 (6499)

Discussion

Y3H assays were performed to determine potential direct interaction between proteins. CDKA;1 was shown to interact with KRP1, KRP2 and KRP3. This corroborates previous findings using Y2H assays and co-immunoprecipitation (Wang *et al.*, 1998; Lui *et al.*, 2000; De Veylder *et al.*, 2001; Zhou *et al.*, 2002a; Nakai *et al.*, 2006; Ren *et al.*, 2008; Sanz *et al.*, 2011; Pusch *et al.*, 2012; Zhao *et al.*, 2012). Interestingly, whereas I could not show the interaction between CDKA;1 and KRP4, Zhou *et al.* previously showed that KRP4/ICK7 could interact with CDKA;1/Cdc2a, using the same KRP plasmid DNA for expression in yeast (Zhou *et al.*, 2002a). The absence of interaction between CDKA;1 and KRP6/ICK4 and KRP7/ICK5 was also demonstrated by Zhou *et al*. The controversial results found regarding the CDKA;1/KRP4 interaction may be due to the yeast strain used to perform the yeast assays, since they were different. Thus, it is likely that the yeast strain PJ69-4A used is more stringent than MaV203 used by Zhou *et al*, and requires a stronger interaction between tested proteins to be able to grow on media selecting for the interaction. Furthermore, the CDKA;1/KRP4 as well as CDKA;1/KRP6 interactions have been shown using TAP-MS (Van Leene *et al.*, 2010). As previously mentioned the TAP-MS method reveals interaction between proteins forming a complex. The detection of KRP4 and KRP6 interaction with CDKA;1 using TAP- MS could suggest that CDKA;1/KRP4 or KRP6 interactions require additional proteins to allow the binding. The interaction between KRP and CDK appears to be specific to CDKA;1. In the yeast assays performed, I could not detect interaction between KRPs and CDKBs. These results corroborate interaction studies on one hand performed in the yeast that could not detect direct interactions between CDKB1;1 and all KRPs except KRP5 and on the other hand co-immunoprecipation also showing that KRPs bind CDKA;1 but not CDKB1;1 (Lui *et al.*, 2000; De Veylder *et al.*, 2001; Zhou *et al.*, 2002a; Verkest *et al.*, 2005a; Pusch *et al.*, 2012). However, an 87-amino-acid fragment of KRP5 has been shown to interact with CDKB1;1 in a yeast-hybrid assay (Lui *et al.*, 2000). Similarly, a co-immonuprecipitation assay shows that CDKB2;1 cannot bind directly KRPs. However, this study also shows that the complex CYCD2;1/CDKB;2;1 can bind all the KRPs (Nakai *et al.*, 2006). These data also highlight the role of KRP as a bridging factor (discussed below).

Furthermore the Y3H assay suggests that CDKA;1 does not interact with CYCD7;1 on its own whereas the interaction seems to be allowed when KRP1 or KRP2 act as a mediator. The absence of direct interaction between CDKA;1 and CYCD7;1 could be explained (1) by a change in conformation of CYCD7;1 or CDKA;1 fused to AD or BD and the interaction may dependent on post-translational modifications such as disulphide bridge,

phosphorylation which does not occur properly in yeast or (2) KRP1 or KRP1 are required to bind first CKDA;1 inducing a conformational change promoting the interaction between CDKA;1 and CYCD7;1. To support the biological relevance of KRP1/2 as a mediator, as opposed to these conclusions being derived from a technical issue, Van Leene *et al.* (2010) showed an interaction between CYCD7;1 and CDKA;1 using a TAP method. This methods also showed that CKS1, CKS2, SMR4 and SMR6 are part of the protein complex in which CDKA;1 and CYCD7;1 were found to interact. The requirement of KRP1/2 presence to promote CDKA;1 and CYCD7;1 interaction highlights a new role for KRP. Similarly, it has been shown that the interaction between CYCD2;1 and CDKA;1 requires the presence of KRP2 (Sanz *et al.*, 2011). In this study, the authors propose that KRP2 is required for CYCD2;1 to translocate into the nucleus, and for the interaction between CYCD2;1 and CDKA;1 to form an active kinase complex. In mammals, it also been reported that Cip/Kip, KRP orthologs help to activate the G1 kinase Cdk4 and Cdk6 since Cdk4/6 and its functional interactor Cyclin D do not bind with high affinity (Sherr and Roberts, 1999; Bockstaele *et al.*, 2006). The formation of the complex is enhanced in presence of Cip proteins, analogous to the role of KRP.

The relevance of the interaction between CDKA;1, CYCD7;1 and KRP1 and KRP2, *in planta,* for the enhanced seed size phenotype requires that the proteins (1) are expressed in the same time-window or are present at the time and (2) come into contact either by being expressed in the same cell or moving into a common cell. *CYCD7;1* expressed under the *FWA* promoter is present in the mature central cell prior to fertilization and in endosperm from just before fertilization until endosperm cellularization when its expression is no longer detectable (see chapter 3). Recently, *CDKA;1* has been shown to be expressed throughout ovule development and especially in the nuclei of the egg cell and central cell in mature ovules (Zhao *et al.*, 2012; Belmonte *et al.*, 2013). Microarray data of CDKA;1 expression available on the eFP brower revealed that CDKA;1 is expressed is all the three seed tissues and throughout the seed development (Fig. 5.9D) (Winter *et al.*, 2007). The expression of *KRP1* and *KRP2* has been studied during vegetative and reproductive development. Several methods investigating the expression at different levels were used. Promoter activity was analyzed using a reporter gene (Gonzalez-Garcia *et al.*, 2011). RNA transcript levels were highlighted using northern blot (Lui *et al.*, 2000), RT-PCR (De Veylder *et al.*, 2001), micro-array (De Almeida Engler *et al.*, 2009) and *in situ* hybridization (Ormenese *et al.*, 2004). The protein abundance was determined using fusion tags (De Veylder *et al.*, 2001). These studies show that KRP1 and KRP2 are both expressed in leaves, stems, root, anthers, sepals and at the base of siliques. However, the

level of expression of KRP1 and KRP2 differs depending on the tissue. For example KRP2 is strongly expressed in the stem whereas KRP1 has a lower level of expression in the stem. More specifically, KRP1 and KRP2 expression has also been shown in endoreduplicating tissues using *in-situ* hybridization (Ormenese *et al.*, 2004). In contrast, *KRP1* and *KRP2* expression in seeds has been little explored. Microarray analysis performed by De Almeida and co-workers showed inconclusive results in the range of settings used (De Almeida Engler *et al.*, 2009). In 2010, the global analysis of gene expression during seed development using microarrays did not disclose *KRP* expression (Le *et al.*, 2010). In this study, the investigation of *KRP1* and *KRP2* expression showed that *KRP1* and *KRP2* full-length transcripts are present in seedlings, confirming published results, and in seeds during their development. Since mRNA was detectable in developing seeds, reporter lines *KRP1:GUS* (Ren *et al.*, 2008), *KRP2:GUS* (De Veylder *et al.*, 2001) and *KRP2:KRP2-GFP* (Sanz *et al.*, 2011) were used to document the expression pattern in developing seeds. *KRP1* activity was detectable in the micropylar endosperm when the embryo reaches the globular stage, corresponding to the beginning of endosperm cellularization at the micropylar pole, confirming the RT-PCR results (Berger, 2003). This result also corroborates microarray data of KRP1 expression available on the eFP brower (Fig. 5.9B) (Winter *et al.*, 2007).

However, despite the presence of KRP2 mRNA in developing seeds, no KRP2 promoter activity or KRP2-GFP protein could be detected in developing seeds. The RT-PCR and expression pattern contradictory data may be explained, as suggested previously, by low KRP2 activity, but as the RT-PCR was performed on many seeds, the total amount of RNA extracted was increased allowing for KRP2 mRNA detection. Moreover, microarray data of KRP2 expression suggest that KRP2 is expressed in the seed integument from heart-stage to mature seed (Fig. 5.9C) (Winter *et al.*, 2007).

CYCD7;1 is a putative regulatory subunit of the CDKA-CYCD complex, hence *CYCD7;1* function in the seed size phenotype is linked to the interaction between the 2 subunits leading to the kinase activity. As shown in the Y3H assay, the interaction between CDKA;1 and CYCD7;1 is conditioned by the presence of KRP1 or KRP2 proteins. Since KRP1 and KRP2 are expressed during seed development, the three partners could potentially physically interact.

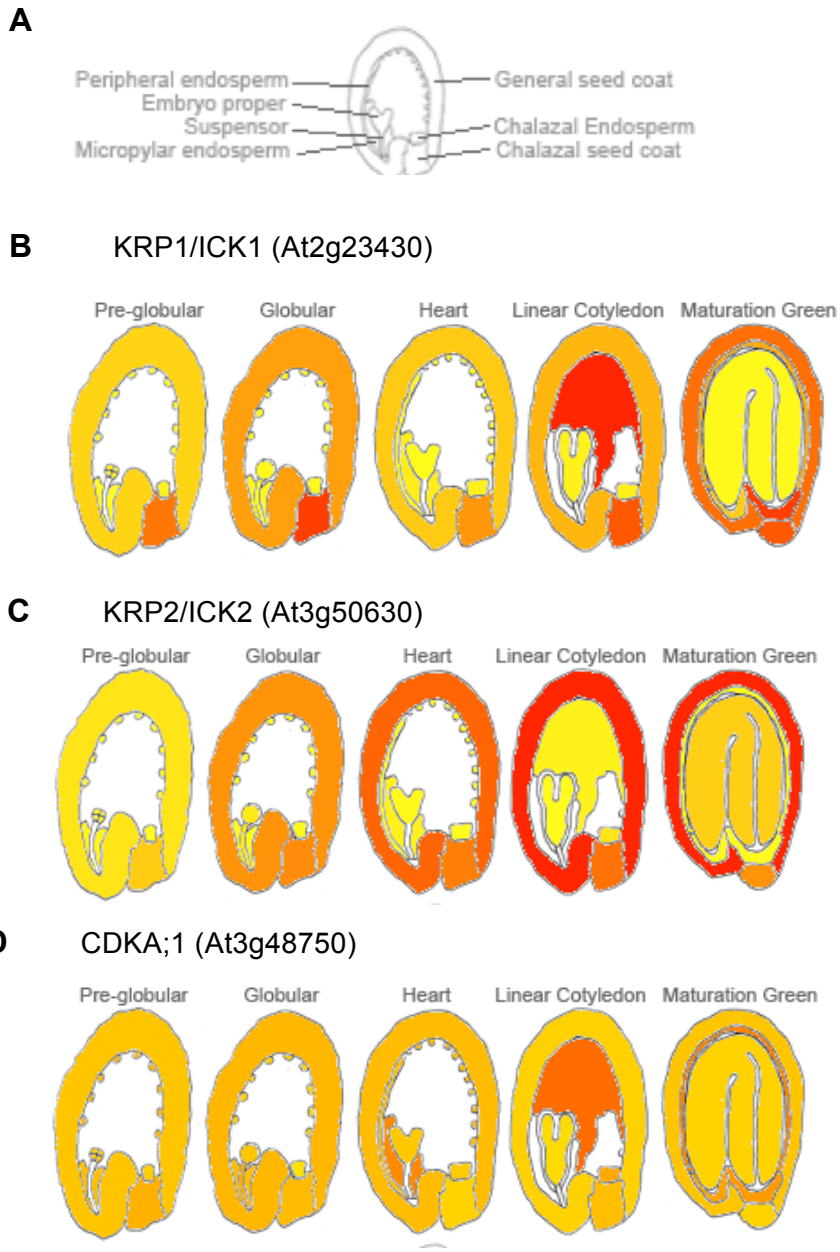

Figure 5.9. KRP1 and KRP2 expression as revealed by microarray data. (A) Schematic representation of a developing seed. KRP1 (B), KRP2 (C) and CDKA;1 (D) expression in developing Arabidopsis *Ws* seeds based on microarray data. Modified from Arabidopsis eFP browser (Winter *et al.*, 2007).

The strategy taken to investigate if $_{seed}$*CYCD7;1* acts with CDKA;1, KRP1 or KRP2 *in planta* to give rise to the enhanced seed size phenotype, was to express $_{seed}$*CYCD7;1* in

loss-of function *krp* mutants. *CDKA;1* loss-of-function is lethal and as KRP1 and KRP2 are required for the interaction CDKA;1-CYCD7;1, using loss-of-function *krp1-1* and *krp2-3* mutants was the approach adopted. *krp1-1* and *krp2-3* did not show full length transcripts and no 3' transcript encoding the CYC/CDK binding motifs were detected, so they are loss-of-function mutants. These mutants were crossed with $_{seed}$*CYCD7;1*. Loss of *KRP1* or *KRP2* did not have an effect on seed size. The loss of function of *KRP1* or *KRP2* in $_{seed}$*CYCD7;1* does not affect the enlarged seed size compared to the $_{seed}$*CYCD7;1* in *WT* background. This result could have several explanations. (1) KRP1 and KRP2 are redundant and losing the function of a single KRP is not sufficient to reduce the size of enlarged seeds. To rule out the redundancy of *KRP1* and *KRP*2, the generation of $_{seed}$*CYCD7;1* in a double mutant *krp1-1/krp2-3* background would be required. (2) KRP1 and KRP2 are not involved in the phenotype since CYCD7;1 and CDKA;1 interact without the KRP1 and KRP2 as a mediator *in planta* and the direct interaction revealed using a heterologous yeast system does not reflect the mechanism *in planta*. (3) As the T-DNA insertion in KRP1 and KRP2 genes is at the 3' of the gene, it is possible that a shorter mRNA from the 5' is still produced. However, it is unlikely to mediate binding since the CDKA;1/CYCD binding domain is located in the 3' region disrupted by the T-DNA insertion (Torres Acosta *et al.*, 2011). Thus even though the 5' mRNA could be synthesized, the protein produced would not have the functional domain to bind CDKA;1/CYCD7;1. Using a knock-down mutant of *CDKA;1* (Dissmeyer *et al.*, 2007; Zhao *et al.*, 2012) in the $_{seed}$*CYCD7;1* background would be a way to rule out the requirement of KRP1 and KRP2 to obtain a complex. An *in vitro* kinase assay could also be used to determine if the complex CYCD7;1-CDKA;1 is functional. However, it is also possible that CYCD7;1 exerts its effect without interacting with CDKA;1. This could be tested from the phenotype of CYCD7;1 with a mutation in the CDK-binding domain which prevents the interaction. The molecular mechanism by which CYCD7;1 acts to give rise to the enhanced seed size phenotype still needs to be clarified.

Chapter 6

Final Discussion

Chapter 6
Final Discussion

Crop productivity must be increased in order to cover the food needs of the world population. For human consumption, seeds are the main edible component of grain crops. Therefore, seed size is one of the key features for seed yield improvement. Over the past 25 years, extensive studies have been done to identify genes involved in the determination of seed size, and to characterize their interactions and functions (Kesavan *et al.*, 2013) although no strong unifying picture has emerged. These genes encode various proteins such as transcription factors, kinases and enzymes for pigment synthesis, and are involved in a range of cellular processes including hormone signaling and epigenetic modifications. In the meantime, increasing knowledge of seed development following ovule fertilization highlights that (1) cell cycle activity is essential and, (2) the coordination of seed tissue development and therefore seed size determination involves on signals between seed components (Nowack *et al.*, 2010; Collins *et al.*, 2012).

Initiation of the cell cycle depends on the decision of quiescent cells to re-enter the cell cycle. It occurs upon the integration of exogenous and endogenous signals controlling the G1 phase acting on the CDKA;1/CYCD complex (Oakenfull *et al.*, 2002; Dewitte and Murray, 2003; Kono *et al.*, 2006; Menges *et al.*, 2006; Dewitte *et al.*, 2007). Until last year, little was known about the expression or function of D-type cyclins during seed development (Collins *et al.*, 2012). This study shows that *CYCD* genes have discrete but partially overlapping expression patterns, with the exception of *CYCD7;1* that is not expressed during seed development. In addition, both overexpression of *CYCD3;1* and loss-of-function of the three *CYCD3* genes impair seed development. Interestingly, in both gain- and loss-of-function mutants, embryo patterning is disrupted and embryo development is delayed. The endosperm is shriveled, pointing to abnormal development (Collins *et al.*, 2012). These data suggest that proper expression of *CYCD3* genes is required for normal seed development. This study also shows that strong ectopic expression of *CYCD7;1* in the seed increases final seed size. In addition, *CYCD7;1* is the only member of the conserved family of D-type cyclins that has been little characterized during embryonic and postembryonic plant development. A further recent study shows that *CYCD7;1* is expressed in stomatal lineage cells, especially late meristemoids and guard mother cells, as well as in the two sperm cells of the pollen grain (Patell *et al.*, manuscript under revision). In this study, data suggest antagonistic functions depending of the time of expression in these cells. *CYCD7;1* stimulates the final cell divisions of the guard mother

cell to produce guard cells, and of the generative cell to produce two sperm cells. Upon the final divisions of the stomata guard cells and sperm cells, *CYCD7;1* promotes an arrest in S-phase in each case preventing further mitotic divisions. The reasons for the S-phase arrest and the mechanism of *CYCD7;1* action in these cell types are unknown.

In this present study, ectopic expression of *CYCD7;1* in seeds is used on one hand to illustrate a novel method to target seed size increase using a cell cycle regulator, and on the other hand to attempt to understand more about its molecular mechanisms of action.

6.1. Endosperm-targeted *CYCD7;1* expression promotes seed size enlargement

Endosperm-targeted expression of the *CYCD7;1* gene to the endosperm under the *FWA* promoter led to the formation of seeds with an increased final size compared to *WT* seeds (Chapter 1). Seeds are composed of three different tissues (the zygotic embryo, the zygotic endosperm and the maternal-tissue-derived seed coat) that require developmental coordination (Bowman, 1994; Nowack *et al.*, 2010). Therefore the increase of final seed size could be due to a coordinated increase of the three compartments or only the increase of the specific tissue where the *CYCD7;1* gene is expressed.

I observed that mature embryos from *FWA:CYCD7;1* lines showed an enlargement. Several other studies have also revealed that larger seeds contain larger embryos, as it is the case in the *EOD3* overexpresser, *mnt* and *ap2*, mutants as well as in interploidy crosses with paternal excess (Scott *et al.*, 1998; Ohto *et al.*, 2005; Schruff *et al.*, 2006; Ohto *et al.*, 2009; Fang *et al.*, 2012). Similarly, mutants with a reduced level of cytokinin sensing such as the *Arabidopsis thaliana sensor histidine kinase* (*ahk2/ahk3/ahk4*) triple mutant (known to be cytokinin receptors) or cytokinin-deficient mutants such as an overexpresser of *CYTOKININ OXIDASE/DEHYDROGENASE1* (*AtCKX1*) mutants show enlarged seeds containing larger embryos (Werner *et al.*, 2003; Riefler *et al.*, 2006). Conversely, interploidy crosses with maternal excess, *ttg2*, *mini3* and *short hypocotyl underblue1* (*SHB*) mutants show that smaller seeds develop smaller embryos (Johnson *et al.*, 2002; Luo *et al.*, 2005; Zhou *et al.*, 2009).

The development of enlarged embryos was expected to be coordinated with enlargement of the seed coat of mature seeds, a hypothesis confirmed by measurements of the projected seed area. This increase of embryo size and seed coat surface in *FWA:CYCD7;1* lines, in which *CYCD7;1* expression was restricted to the mature central cell and the developing endosperm until full cellularization using the *FWA* promoter, is presumably one more example of the communication between seed compartment during its development

(see below, Nowack *et al.*, 2010). As the size of the embryo and the seed coat of mature seeds is enhanced in *CYCD7;1* endosperm-targeted expression lines, it is not unreasonable to hypothesize that the aleurone layer, a single cell layer remaining from the endosperm at seed maturity, is also thickened either by an increase of cell size or an increase in the number of layers. During the analysis of seed developmental progression, preliminary observation revealed that in mature seeds, the aleurone was a single cell layer in both the *WT* and the *CYCD7;1* endosperm-targeted expression lines (Chapter 4). However, no detailed quantification was performed regarding thickness of the layer. I chose not to performed further investigations because, after the completion of endosperm development, this latter is metabolized in order to sustain the final stages of embryo development (Berger, 1999). Therefore I assumed that if the *CYCD7;1* has an effect on endosperm development itself, it would occur during the earlier stages of seed development when the endosperm undergoes, first nucleus proliferation and then cellularization. The endosperm is fully developed after cellularization when the embryo reaches the heart-torpedo stages (Boisnard-Lorig *et al.*, 2001). Analysis of the size of seeds during their development showed that the enlargement arose 4 DAP, correlating with the embryo reaching the heart stage and the presence of cell walls in the endosperm, indicating that the cellularization process was happening (Chapter 4). Moreover, the comparison of area of heart stage embryos between the *WT* and the $_{seed}$*CYCD7;1* revealed no difference even though embryos reach this stage faster and the overall size of the developing seed is larger. Therefore, since the $_{seed}$*CYCD7;1* final seed size is larger than the *WT* but the embryos had a similar size 4 DAP, this suggests that the seed cavity in which the endosperm developed is increased. Therefore it is reasonable to infer that the endosperm is larger. On the contrary, smaller mature seeds have a reduced endosperm cavity at heart stage as suggested by loss-of-function of the *IKU2* and *MINI3* genes that are natively expressed in the endosperm (Garcia *et al.*, 2003; Luo *et al.*, 2005).

6.2. Endosperm-targeted *CYCD7;1* expression promotes cell proliferation in enlarged seed

As mentioned above, *FWA:CYCD7;1* lines produced larger mature seeds compared to *WT* lines. Many studies show that altered organ size is due to a modification of cell proliferation and/or of cell growth (Tsukaya, 2003; Breuninger and Lenhard, 2010). Moreover, enlarged cells that undergo extensive growth, such as trichomes or epidermal cells, frequently display a higher ploidy level correlated with endoreduplication (Traas *et al.*, 1998; Joubes and Chevalier, 2000; De Veylder *et al.*, 2001). Therefore the determination of organ size depends on the regulation of the mitotic cell cycle and the endocycle. D-type cyclins have

been demonstrated, using loss and gain of function mutants, to promote cell cycle progression in plants (Menges *et al.*, 2006). Constitutive overexpression of *CYCD2;1* in Arabidopsis led to an increased number of stomata as well as an increased number of cells in roots and in the primordia of aerial organs (Qi and John, 2007). Similarly, constitutive overexpression of *CYCD3;1* caused hyperproliferation of leaf cells and *RPS5A>>CYCD3;1* promotes cell proliferation in the embryo and the suspensor of developing seeds (Dewitte *et al.*, 2003; Collins *et al.*, 2012). Reciprocally, loss-of-function of the three *CYCD3* genes leads to a reduction of cell numbers in petals correlated with a cell size increase, whereas the loss-of-function of single or double *CYCD3* genes does not display an effect on cell proliferation (Dewitte *et al.*, 2007). *CYCD4* genes have been shown to control cell division in the initial step of stomata formation in the hypocotyls and to therefore control the proliferation of stomatal lineage progenitors (Kono *et al.*, 2007). *CYCD4;1* loss-of-function leads to a reduced lateral root density. Because *CYCD4;1* is involved in the regulation of cell divisions which are required for the formation and emergence of lateral roots (De Veylder *et al.*, 1999; Nieuwland *et al.*, 2009). Similarly, it has been shown that *CYCD2;1* is an auxin-regulated mediator of lateral formation (Sanz *et al.*, 2011). *CYCD6;1* has been shown to be involved in regulating formative division in cortex/endodermis layers in Arabidopsis root (Sozzani *et al.*, 2010; Cruz-Ramírez *et al.*, 2012). All these lines of evidence are consistent with the view the *CYCD* genes promote cell division in plants.

Given the regulatory function of D-type cyclins in the mitotic cell cycle and the recent evidence showing that *CYCD7;1* stimulates cell divisions in stomatal lineage cells and in generative cells of the pollen grain, it is not unreasonable to postulate that when ectopically expressed, *CYCD7;1* will stimulate cell divisions during seed development and therefore lead to an enlargement of the mature embryo, seed coat and developing endosperm. However, in non-disrupted organ development, cell division and cell expansion act synergistically in order to achieve correct the organ morphogenesis program. And so, cell division and cell expansion are only tools to achieve final organ size and shape partially determined by other genes than cell cycle regulating genes. Therefore, since the final organ size is the determined endpoint, modifying either the cell cycle or cell expansion could be compensated by the other that is not affected (Bogre *et al.*, 2008). Hence, identification and disruption of genes involved in determining seed size show that both cell division and cell expansion are affected. In the literature, mutants affecting seed size have variable effects on cell number and cell expansion. For example, increases in cell number and cell size contribute to larger seeds in the *EOD3* and *AtCKX1* overexpressers and *mnt* mutants (Schruff *et al.*, 2006; Fang *et al.*, 2012). Reciprocally, smaller seeds in *ttg2* and

iku2 mutants show a reduction of cell size number (Garcia *et al.*, 2005). Another example from *klu* mutant analysis shows that smaller seeds have a smaller number of larger cells (Adamski *et al.*, 2009). All these examples suggest that the change of seed size is normally due to a combined effect of cell division and cell expansion. Therefore, considering the role of CYCDs in cell proliferation, it is obvious to postulate that *CYCD7;1* should stimulate cell division, but given the general linkage between cell division and expansion, I cannot discard the hypothesis that cell expansion also plays a role in the enlarged seed of *$_{seed}$CYCD7;1* lines. However, the results presented here show that the epidermal pavement cells of the embryo, the embryonic root cortical cells and the outer seed coat cells have a similar area in the *$_{seed}$CYCD7;1* lines and the *WT*, suggesting that cell expansion is not affected. The embryo, cotelydons and final seed size are larger, leading to the conclusion that cell proliferation is increased. Therefore this study is, to my knowledge, a unique example during seed development where seed enlargement is due a modification of cell cycle program exclusively and where the cell expansion is not affected.

$_{seed}$CYCD7;1 lines produce larger seeds composed of more cells in the embryo and the seed coat. The generation of a higher number of cells appeared to be due to an accelerated rate of cell proliferation. In *$_{seed}$CYCD7;1* lines, the embryos reached the heart-stage quicker than the *WT* embryos (Chapter 4). However, the morphological comparison of heart stage embryos showed that *$_{seed}$CYCD7;1* embryos are identical to *WT* embryos. The accelerated embryo development and the absence of embryo patterning defects are consistent with a faster cell cycle rate during early development. In addition, the accelerated rate of embryo development occurred up to 4-5 DAP and from 5-6 DAP onwards the progression of embryo development is similar in *$_{seed}$CYCD7;1* and *WT* lines (Chapter 4). 4-5 DAP embryos reached heart-stage and the point at which the endosperm was cellularizing. At this stage the activity of the *FWA* promoter starts decreasing and the expression of *FWA:CYCD7;1* was no longer visible in the seed and especially in the endosperm (Chapter 3). These data suggest that the cell overproliferation in the embryo is due to an accelerated rate of cell divisions and the timing of accelerated rate of cell divisions in the embryo correlates with the timing of *CYCD7;1* expression in the endosperm.

This study suggests that endosperm-targeted *CYCD7;1* expression promotes seed enlargement by increasing the rate of cell division in the embryo and seed coat. Under the *FWA* promoter, *CYCD7;1* is expressed in the mature central cell and in the endosperm until cellularization (Chapter 3). However, the effects on endosperm still need to be investigated

in detail. The time-course study of seed development showed that the endosperm is enlarged 4 DAP, correlating with the first manifestation of seed enlargement. Preliminary microscopic analysis showed that nuclei proliferation in the endosperm is increased, leading to an endosperm with an enlarged size. However, detailed quantification should be performed to confirm this. The endosperm nucleus proliferation hypothesis is supported by the analysis of seed development mutants such as *mea, ttg2* and *iku2*. Similarly, *mea* mutants display larger seeds with lengthened endosperm mitotic activity and an enlarged chalazal endosperm (Grossniklaus *et al.*, 1998; Kiyosue *et al.*, 1999). Reciprocally, in *ttg2* and *iku2* mutants, seeds are smaller due to reduced embryo and integument size and less endosperm growth during the cellularization process (Garcia *et al.*, 2003; Garcia *et al.*, 2005). The *mnt* mutant is a counter example. In *mtn* larger seeds, the mature embryo is larger whereas the endosperm is not hypertrophic. This suggests that in larger seeds not all of the three tissues are always affected by the size increase (Schruff *et al.*, 2006).

All these studies show that effects of the final seed size can originate from modification of cell proliferation and expansion in the three components of the size. Hence, although it is still possible that endosperm-specific *CYCD7;1* expression has no effect on the endosperm, from my preliminary analysis and *mea, ttg2* and *iku2* studies, I can predict that *CYCD7;1* might have an effect on endosperm proliferation during the syncytial phase and maybe during the cellularization phase.

6.3. *CYCD7;1* acts in an autonomous and non-autonomous manner

Seed development lies in the coordination of growth of three tissues, with three different genetic backgrounds, that develop concomitantly (the diploid embryo m/p, the triploid endosperm 2m/p and the diploid integument 2m) (Nowack *et al.*, 2010). Therefore it is not surprising that gene expression is different in the three seed tissues, nor that the coordination of their developments requires communication. Most of the seed development mutant examples mentioned above show that the genes controlling seed growth act in both an autonomous and non-autonomous manner. *MINI3* and *IKU2* genes are specifically expressed in developing endosperm shortly after fertilization, and loss-of-function of these genes affects seed integument and embryo development in a non-autonomous manner (Garcia *et al.*, 2003). *MEA*, which is expressed in the endosperm upon fertilization, triggers seed integument and embryo proliferation (Grossniklaus *et al.*, 1998). Reciprocally *TTG2,* which is expressed in the integument, triggers cell proliferation in the seed integuments and the endosperm, as suggested by the loss-of-function mutant showing a defect of integument and endosperm growth upon fertilization (Garcia *et al.*, 2005). Similarly, *AP2* is expressed in the ovule and seed integuments, and prevents cell overproliferation in the

endosperm and embryo since the *ap2* seeds display hypertrophic embryo and endosperm due to an increase in mitotic activity (Ohto *et al.*, 2005; Ohto *et al.*, 2009). Therefore its effects on the embryo are presumably indirect consequences of its expression in the ovule and integuments.

In this study, I showed that *CYCD7;1* expression was targeted to the endosperm. However, the stimulating effect on cell proliferation was noticeable in the embryo, the seed coat and in the endosperm, suggesting that *CYCD7;1* acts autonomously in the endosperm and non-autonomously in the seed coat and embryo. Hence stimulating proliferation within the endosperm up to 4 DAP appears to be sufficient to promote larger seed.

6.4. CYCD7;1 forms a complex with CDKA;1 in the presence of KRP1 and/or KRP2 and may act through the *RBR* pathway to regulate the cell cycle

6.4.1. CYCD7;1 interacts with CDKA;1 in the presence of KRP1 or KRP2

As reviewed above and in chapter 1, D-type cyclins are cell cycle regulators known to bind CDKA;1, in order to regulate the G1-to-S transition of the cell cycle. The interaction between CYCDs and CDKA;1 has been demonstrated using various methods such as yeast-hybrid assays, BiFC, co-immunoprecipitation and TAP experiments (Boruc *et al.*, 2010; Van Leene *et al.*, 2010; Van Leene *et al.*, 2011; Pusch *et al.*, 2012; Zhao *et al.*, 2012). Control of the G1-S transition by the CYCD/CDKA;1 complex has been supported by the detailed analysis of *CYCD* expression, as well as the overexpression of *CYCD3* genes in synchronized Arabidopsis cell cultures. Broadly speaking, all 10 D-type cyclins are expressed during the G1 phase, with some variations (Menges and Murray, 2002; Menges *et al.*, 2003; Menges *et al.*, 2005). Moreover, in *CYCD3;1*-overexpressing cells, the increased proportion of cells in the G2 phase, the prolonged G2 phase, and enhanced level of S-phase gene expression suggests that cells go through the G1-S transition quicker and highlights the role of *CYCD3;1* in controlling this transition (Menges *et al.*, 2006). Control of the G1-S transition by CYCD2;1 and CYCD3;1, both of which can form a complex with CDKA;1, has also been demonstrated *in planta* and not surprisingly in dividing cells (Healy *et al.*, 2001). Here, I showed that CYCD7;1 interacts with CDKA;1, but this interaction is possible in yeast only when KRP1 or KRP2 have first bound CDKA;1. Moreover I showed that in this assay, none of the four CDKBs can bind CYCD7;1 or KRP1/2, and the complex formation is specific to the presence of CDKA;1. As previously discussed in chapter 5, several studies using yeast-hybrid-assays, BiFC and co-immunoprecipitation show similar results regarding the binding of CDKA;1 to KRP1 or KRP2 and the absence of interaction between CDKB1 and KRPs (Wang *et al.*, 1998; Lui *et al.*, 2000; De Veylder *et al.*, 2001; Zhou *et al.*, 2002a; Nakai *et al.*, 2006; Van Leene *et al.*, 2007; Ren *et al.*, 2008; Sanz *et al.*,

2011; Pusch *et al.*, 2012; Zhao *et al.*, 2012). Unlike the results I showed, that CYCD7;1 cannot bind KRP1 or KRP2, these studies showed that the D-type cyclins investigated can also bind KRPs on their own (CYCD2;1 and KRP2, (Sanz *et al.*, 2011); CYCD3;1 and KRP1, (Nakai *et al.*, 2006)). Sanz *et al.* proposed that KRP2 acts as a linker promoting between CYCD2;1 and CDKA;1 that could not bind in absence of KRP2 (2011). In addition, the results from the study of the interaction between CDKA;1, KRPs and CYCD3;1 suggest that KRP preferentially targets the CDK-cyclin dimer since CDKA;1 with a modified CYCD binding motif that prevents the CDKA;1/CYCD complex formation, cannot interact with any of the KRPs (Zhao *et al.*, 2012). Similar to the results I showed, a core cell cycle component interactomic study reveals that CDKA;1 and CYCD7;1 sit in the same complex *in vivo* (Van Leene *et al.*, 2010). However, whereas I detected the binding of KRP1/2 with CDKA;1 and CYCD7;1, the interactomic study identifies SMR4 and SMR6, two additional CYCD/CDK, inhibitors, as part of the complex as well as the CYCD/CDK co-factors, CKS1 and CKS2.

Here I demonstrated the prerequisite for binding of KRP1 or KRP2 with CDKA;1 for the formation of the CYCD7;1/CDKA;1 regulatory complex. This suggests that CYCD7;1 alone has a low affinity for CDKA;1, but this affinity is increased when CDKA;1 is bound to KRP1/2, possibly due to a conformational change of CDKA;1 promoting therefore, the interaction with CYCD7;1. However in this study some questions remain unanswered. I could not demonstrate *in planta* that KRP1 or KRP2 was required for the formation of a functional CDKA;1/CYCD7;1 complex based on its ability to generate the enhanced seed size phenotype. The *knock-out* of *krp1* or *krp2* did not have any effect on the seed size in endosperm-targeted *CYCD7;1* expression lines. However, as both KRP1 and KRP2 are expressed in the seed, they may act redundantly and the effect on seed size might be present when the loss-of-function *krp1* and *krp2* genes will be in the *CYCD7;1* seed-targeted expression lines. The kinase activity of the CYCD7;1/CDKA;1 complex could also be assessed *in vitro* in the presence and absence of KRP1/2. This method would not however discern whether or not the CYCD7;1/CDKA;1 kinase activity is the key element promoting cell proliferation during seed development and therefore the seed enlargement. Another explanation of the lack of an effect on final seed size in *krp1-krp2-*$_{seed}$*CYCD7;1* lines is that other inhibitors such as SIM or SMR are involved in the CYCD7;1/CDKA;1 complex. Indeed, this has been demonstrated by Van Leene (2010). Finally, it is also possible that CYCD7;1 acts independently of complex formation with CDKA;1 to give rise to the enlarged seed size phenotype in endosperm-specific *CYCD7;1* expression lines.

6.4.2. CYCD7;1/CDKA;1 may act through the *RBR* pathway and may have an effect on the imprinting of the maternal genome

Endosperm-targeted *CYCD7;1* expression leads to a final seed size increase promoted by cell proliferation. CYCD/CDKA regulates the progression through the G1-S transition and therefore the commitment of the cell to enter the cell cycle (Boniotti and Gutierrez, 2001). In addition, it has been demonstrated that the entry of the cell into S-phase of the cell cycle is initiated by relieving the inhibition of the E2F/DP transcription factors by RBR, allowing the transcription of S-phase genes (Dyson, 1998). The release of RBR inhibition occurs upon phosphorylation of the latter by the CYCD/CDKA;1 complex during the progression to the G1-S transition (Boniotti and Gutierrez, 2001).

A plausible explanation of the cell proliferation stimulation in $_{seed}$*CYCD7;1* lines is that the CYCD7;1/CDKA;1 complex acts by phosphorylating RBR and therefore permitting cell cycle progression, leading to cell proliferation. CYCD7;1 contains a canonical LxCxE amino acid motif known to be required for the interaction of cyclins with RBR (Menges *et al.*, 2007). Moreover, in cell suspension *CYCD7;1* is expressed late in G1 (Menges *et al.*, 2005). These results are consistent with the hypothesis that *CYCD7;1* may act through the RBR pathway to promote cell division. Another piece of evidence is that $_{seed}$*CYCD7;1* expression in the mature central cell phenocopies the *rbr1-1* mutants that show nucleus overproliferation prior to fertilization (Ingouff *et al.*, 2006; Johnston *et al.*, 2008). In addition, several studies show that RBR is involved in genome imprinting and therefore in endosperm development. Mutants in the Polycomb group genes of the *FIS* class such as *mea/fis1* (Grossniklaus *et al.*, 1998; Kiyosue *et al.*, 1999), *fis2* (Luo *et al.*, 1999), *fie/fis3* (Ohad *et al.*, 1996), *msi1* (Kohler *et al.*, 2003; Guitton *et al.*, 2004; Ingouff *et al.*, 2006), also display nuclear proliferation in the absence of fertilization. Despite the apparently similar phenotype, the use of endosperm-specific reporters reveals that the central cell of the *rbr* mutants does not acquire endosperm identity, whereas that in *fis* mutants does (Ingouff *et al.*, 2006). These results suggest that the *rbr* mutant fails to arrest cell cycle in the mature female gametophyte prior to fertilization, whereas in *fis* mutants re-entry into the cell cycle occurs despite the absence of a fertilization signal, leading to autonomous endosperm development. A direct consequence of this different arrest in the cell cycle between the *rbr* and *fis* mutant is that some of the additional nuclei in *rbr* are haploid, as the fusion of the two haploid nuclei into a diploid polar nucleus in the central cell does not always occur, and some nuclei are diploid, whereas in the *fis* mutants, a mature central cell displays a single diploid nucleus undergoing extra cell cycles, and therefore the multiple nuclei in *fis* mutant are always diploid (Johnston *et al.*, 2008). As the $_{seed}$*CYCD7;1* phenotype observed in the central cell is similar to that in *rbr* and *fis* mutants, a question arises as to whether the central cell acquires endosperm identity and whether the nucleus DNA content is diploid or

haploid. Preliminary observation of the unfertilized ovules of $_{seed}$*CYCD7;1* would suggest that the phenotype is similar to that in the *rbr* mutant, as the central cell did not acquire the typical shape of a developing endosperm that undergoes growth, and therefore nuclei fail to arrest cell division in the mature central cell prior to fertilization. However further analyses need to be done to confirm this hypothesis.

RBR has been demonstrated to interact with MSI1 and DNA methytransferase1 (MET1), leading to the transcriptional repression of *MET1* (Jullien *et al.*, 2008). MET1 has been shown to be involved in methylating DNA of the *MEA*, *FIS2* and *FWA* genes, which is required for their genome imprinting (Kinoshita *et al.*, 1999; Kinoshita *et al.*, 2004; Jullien *et al.*, 2006; Xiao *et al.*, 2006). Paternal alleles of *MEA, FIS2* and *FWA* are hypermethylated, leading to their silencing in the endosperm, whereas the maternal alleles are hypomethylated in the endosperm allowing their expression (Huh *et al.*, 2007; Hsieh *et al.*, 2011). In *mea* and *fis2* mutants, the autonomous endosperm development is due to an increase of methylation leading to the repression of maternal allele expression in the endosperm (Kinoshita *et al.*, 1999; Kinoshita *et al.*, 2004; Schmidt *et al.*, 2013). In *mea* mutants, as well as in interploidy crosses with paternal genome excess, developing seeds display an increased number of peripheral endosperm nuclei and an enlarged chalazal endosperm (Grossniklaus *et al.*, 1998; Scott *et al.*, 1998; Kiyosue *et al.*, 1999). In the *rbr* loss-function-mutant, *MET1* is less repressed leading to hypermethylation of genes such as *MEA* or *FIS2*. Hypermethylated *MEA* and *FIS2* are then silenced, leading to autonomous development of the endosperm. Conceptually, hypermethylation of *MEA* or *FIS2* could be interpreted as effectively changing the maternal and paternal genome expression balance, potentially leading to larger seeds on a similar way to an excess of paternal genome. Relating this to the experiments here, CYCD7;1/CDKA;1 can phosphorylate RBR and inhibit its function, leading to the induction of higher expression of MET1 that can then hypermethylate maternal genome. This would lead to a change in maternal/paternal genome expression balance. Therefore, the hypothesis is consistent with an enlarged seed size phenotype in $_{seed}$*CYCD7;1* lines, similar to the enlarged seed phenotype observed in plants with an excess of paternal genome.

6.5. *CYCD7;1* expression in the central cell might reduce fertility

Proper formation of the female gametophyte is crucial for fertilization, as well as seed development. In $_{seed}$*CYCD7;1* lines, 50% to 75 % of seeds did not reach maturity. As described in chapter 4, 20 to 50 % of these non-developing seeds, fail to reach maturity due to an embryo arrest at globular stage. No apparent defect of embryo patterning was

observed (Chapter 4). In contrast, in lines overexpressing *CYCD3;1* or *CYCD7;1* in the embryo, 40-50% of embryos fail to establish a proper pattern: the protoderm fails to differentiate into a distinguishable outer single cell layer, the division of the hypophysis is transversal instead of longitudinal prior to the incorporation of the upper into the embryo and/or the globular embryo undergoes uncoordinated outgrowth. The embryo defects are correlated with seed abortion in these lines overexpressing *CYCD3;1* or *CYCD7;1* in the embryo (Collins *et al.*, 2012). The embryo arrest in $_{seed}$*CYCD7;1* lines could be due a defect arising in the endosperm, since my work show that the *CYCD7;1* expression in the endosperm has a non-autonomous effect on embryo development. Even though no visible defects in the endosperm are observed, this is a likely explanation as many examples of embryo arrest due endosperm developmental impairment have been reported. In mutants failing to cellularize the endosperm, embryo arrest can be due to a failure in proper patterning of the embryo, such as in *endosperm defective1* (*ede1*) mutants, or show no visible defects in embryo patterning, as reported for the *capulet2* mutant (Grini *et al.*, 2002; Pignocchi *et al.*, 2009). However, in both mutants, the seed stops its development. In the *glauce* mutant, *WT* pollen can fertilize the egg cell but not the central cell. Therefore the endosperm does not develop. Eventually seeds abort (Ngo *et al.*, 2007). Similarly, the single fertilization event of the egg cell in the *cdka;1* mutant leads to the development of the embryo and in some cases non-autonomous endosperm development. At the 32-nuclei stage the endosperm stops both its own development and the seeds (Ungru *et al.*, 2008). The targeted degeneration of the endosperm using tissue-specific expression of the diphtheria toxin A also leads to embryo arrest and subsequent seed abortion (Weijers *et al.*, 2003). Further investigations need to be performed to unravel the roles of *CYCD7;1* expressed in the endosperm on embryo arrest at globular stages.

Embryo arrest at the globular stage explains 40-50% of seed abortion. However, I also showed that the seed abortion is also due to an earlier event of seed development. The question that remains unclear is whether the ovules degenerated before fertilization or shortly after fertilization. According to the non-fertilization hypothesis, three scenarios can be considered: (1) the pollen tube does not the reach the ovules, (2) the pollen tube reaches the ovule but the sperm cells are either not released or sperm cell nuclei do not fuse with the female nuclei and therefore do not trigger seed development, and (3) the ovule degenerates before reaching maturity. Defects of pollen tube guidance are observed in *central cell guidance* (*ccg*) mutants. *CCG* encodes a transcription factor that when expressed under an endosperm specific promoter in the *ccg* mutant rescues the defect in pollen tube guidance, suggesting that the central cell may also have a role in pollen tube

guidance in addition to the synergids (Chen and Tian, 2007). As discussed before, the expression of *CYCD7;1* in the mature central cell has some effect on central cell polar nucleus formation and it is therefore not unlikely to have more subtle effects that were not found in this study. To rule out a defect in fertilization, use of a sperm cell nucleus marker such as *HTR12* (discussed in chapter 5) would be a great help (Ingouff *et al.*, 2007). Moreover, use of an endosperm-specific marker such as MEA could also determine whether the seed development program has been initiated (Luo *et al.*, 2000). As the endosperm starts its development even before the zygote development is activated, it would seem beneficial to use an endosperm-specific marker rather than a zygote-specific marker. The effect of *CYCD7;1* on the central cell and the *CYCD7;1* involvement in causing early seed lethality are still unclear. For example the proportion of ovules displaying nucleus proliferation in the central cell does not match the proportion of early aborting seeds: 10 to 25% of the total seeds abort early in development whereas 50-85% of ovules display extra nucleus proliferation in the central cell. However, as leaky expression of CYCD7;1 was observed in the pollen grain, it is possible that pollen grains from $_{seed}$*CYCD7;1* can fertilize only the egg cell, and as the nuclei in the endosperm are already proliferating, the endosperm development program is triggered allowing the continuation of its growth and therefore seed development. Similar results have been reported when a *cdka;1* single sperm cell pollen fertilizated a *FIS*-class mutant. In this case, the *cdka;1* single sperm cell fertilized the egg cell initiating the zygotic developmental program, and endosperm proliferation was initiated by the loss-of-function of the *FIS*-class genes. The endosperm cellularization process that marks the arrest of endosperm development in *FIS*-class mutants is restored and the seed develops (Nowack *et al.*, 2007).

6.6. Trade-off between seed size and number

Seeds develop within enclosed fruit pods. Therefore, their final size is affected by the spatial constraint of the silique. It has been commonly acknowledged that an increase in seed size is accompanied by a decrease in seed number per silique. However, quantification of lethality in enlarged seed mutants or, reciprocally, quantification of seed size increase in seed lethal mutants, has been poorly investigated in detail or reported. For example, in *ap2* and *ahk2-3-4 triple* mutants, seed size underwent an increase of 20-70% and 150% respectively. Although the authors mentioned a possible reduction of seed yield, no data quantify this reduction (Jofuku *et al.*, 2005; Riefler *et al.*, 2006). In *AtCKX1,2,3,4* overexpressors, seed size was quantified and seed lethality was visualized with pictures of opened siliques, but determination of the level of seed lethality was not mentioned (Werner *et al.*, 2003). Reciprocally, in *cdka1-1*$^{+/-}$, 50% of seeds abort but variation in seed size has

not been reported (Nowack *et al.*, 2006). More recently, Fang and co-workers showed that in *EOD3* overexpressers, seed size is increased by 100% and is accompanied by 21% lethality (2012). House *et al.* showed that the relationship between seed number and seed size in inter-ploidy crosses is not significant (2010). Here I showed that $_{seed}$*CYCD7;1* lines with the higher level of *CYCD7;1* have higher lethality and higher seed size increase and, reciprocally, $_{seed}$*CYCD7;1* lines with a lower level of *CYCD7;1* expression have a lower lethality proportion and a lower seed size increase. It sill remains unclear whether *CYCD7;1* endosperm-specific expression induces lethality and, as a consequence of reduced steric bulk, seed size increases, or whether *CYCD7;1* induces both seed size increase and lethality independently. I demonstrated that *CYCD7;1* endosperm-specific expression has a direct effect on cell proliferation, therefore it is unlikely that the only effect of *CYCD7;1* is inducing lethality and that seed size increase is solely a consequence of this high lethality proportion. Another way of addressing this issue would be to quantify the seed size of a seed lethal mutant such as *cdka;1-1*$^{+/-}$. If the seeds of the lethal mutant do not show a size increase, it would suggest that lethality does not always lead to larger seeds, but reduces the steric bulk in the silique. However, in this study it appeared that expression of *CYCD7;1* under the *FWA* promoter has the drawback of inducing lethality. Thus the choice of promoter to drive CYCD7;1 expression seems critical.

6.7. Concluding remarks and future work

CYCD7;1 is a good candidate to target its expression in seed in order to manipulate seed size and therefore seed yield in agronomically important crop plants, if lethality issues can be addressed.

As mentioned above, the choice of promoter to drive the expression of *CYCD7;1* is essential for usefully engineering seed size. Endosperm development is a key element to control seed size by affecting embryo and seed coat development, thus an endosperm-specific promoter appears to be an obvious choice. In addition, the parental-origin dosage in the endosperm is also a key element for endosperm development. Therefore an imprinted endosperm-specific promoter such as the *FWA* promoter was a good candidate for targeting the expression in the central cell and developing endosperm. However, two improvements could be considered: first, from this study, it appears that the early expression of *CYCD7;1* in the mature central cell might cause seed lethality. Secondly, as the seed integument also creates a constraint to seed development, using an integument-specific promoter as well as a maternal genome endosperm-specific promoter might increase the yield. Hence, *MEDEA* or *FIS2* promoters could be used to target the

expression of *CYCD7;1*. In addition, a recent study reveals a new gene, specific to the seed integument, *DIRIGENT PROTEIN1* (*DP1*) (Esfandiari *et al.*, 2013).

Endosperm-targeted expression of *CYCD7;1* also phenocopies cytokinin-deficient and cytokinin receptor-deficient mutants. Since it has been shown that one mechanism of cytokinin action is the control of the cell cycle components (*CYCDs*) and more specifically *CYCD3s* (Dewitte *et al.*, 2007), it would be interesting to investigate the effects of cytokinin on endosperm-targeted *CYCD7;1* expression.

An interesting feature of endosperm-targeted *CYCD7;1* expression was larger seedling than the *WT* after seven days indicating a potential faster seedling establishment. In annual crops, seedling establishment is a critical point at which biotic and abiotic stresses can influence the yield of the crop for the whole year. Therefore, reducing the time window of seedling establishment is one way of reducing the influence of external factors impairing the harvest yield. Investigations to determine whether seedlings with larger cotyledons display faster vegetative growth and whether the flowering transition is earlier could be done.

References

Abe, M., Katsumata, H., Komeda, Y. & Takahashi, T. 2003. Regulation of shoot epidermal cell differentiation by a pair of homeodomain proteins in *Arabidopsis*. *Development.* **130**: 635-43.

Ach, R. A., Durfee, T., Miller, A. B., Taranto, P., Hanley-Bowdoin, L., Zambryski, P. C. & Gruissem, W. 1997. *RRB1* and *RRB2* encode maize retinoblastoma-related proteins that interact with a plant D-type cyclin and geminivirus replication protein. *Molecular and Cellular Biology.* **17**: 5077-86.

Adamski, N. M., Anastasiou, E., Eriksson, S., O'neill, C. M. & Lenhard, M. 2009. Local maternal control of seed size by *KLUH/CYP78A5*-dependent growth signaling. *Proceedings of the National Academy of Sciences.* **106**: 20115-20.

Aida, M., Beis, D., Heidstra, R., Willemsen, V., Blilou, I., Galinha, C., Nussaume, L., Noh, Y. S., Amasino, R. & Scheres, B. 2004. The *PLETHORA* genes mediate patterning of the Arabidopsis root stem cell niche. *Cell.* **119**: 109-20.

Aida, M., Ishida, T. & Tasaka, M. 1999. Shoot apical meristem and cotyledon formation during *Arabidopsis* embryogenesis: interaction among the *CUP-SHAPED COTYLEDON* and *SHOOT MERISTEMLESS* genes. *Development.* **126**: 1563-70.

Aida, M., Vernoux, T., Furutani, M., Traas, J. & Tasaka, M. 2002. Roles of *PIN-FORMED1* and *MONOPTEROS* in pattern formation of the apical region of the Arabidopsis embryo. *Development.* **129**: 3965-74.

Albani, D., Mariconti, L., Ricagno, S., Pitto, L., Moroni, C., Helin, K. & Cella, R. 2000. DcE2F, a functional plant E2F-like transcriptional activator from *Daucus carota*. *The Journal of Biological Chemistry.* **275**: 19258-67.

Alberts, B., Johnson, A., Lewis, J., Raff, M., Roberts, K. & Walter, P. 2002. Molecular Biology of the Cell. *In:* SCIENCE, N. Y. G. (ed.) 4th ed.: New York: Garland Science.

Alvarez-Buylla, E. R., Benitez, M., Corvera-Poire, A., Chaos Cador, A., De Folter, S., Gamboa De Buen, A., Garay-Arroyo, A., Garcia-Ponce, B., Jaimes-Miranda, F., Perez-Ruiz, R. V., Pineyro-Nelson, A. & Sanchez-Corrales, Y. E. 2010. Flower development. *Arabidopsis Book.* **8**: e0127.

Amberg, D. C., Burke, D. J. & Strathern, J. N. 2006. High-Efficiency Transformation of Yeast. *Cold Spring Harbor Protocols.* **2006**: pdb.prot4145.

Andrietta, M. H., Eloy, N. B., Hemerly, A. S. & Ferreira, P. C. G. 2001. Identification of sugarcane cDNAs encoding components of the cell cycle machinery. *Genetics and Molecular Biology.* **24**: 61-88.

Barroco, R. M., De Veylder, L., Magyar, Z., Engler, G., Inzé, D. & Mironov, V. 2003. Novel complexes of cyclin-dependent kinases and a cyclin-like protein from *Arabidopsis thaliana* with a function unrelated to cell division. *Cellular and Molecular Life Sciences* **60**: 401-12.

Barroco, R. M., Van Poucke, K., Bergervoet, J. H., De Veylder, L., Groot, S. P., Inze, D. & Engler, G. 2005. The role of the cell cycle machinery in resumption of postembryonic development. *Plant Physiology.* **137**: 127-40.

Becker, D., Kemper, E., Schell, J. & Masterson, R. 1992. New plant binary vectors with selectable markers located proximal to the left T-DNA border. *Plant Molecular Biology.* **20**: 1195-7.

Belmonte, M. F., Kirkbride, R. C., Stone, S. L., Pelletier, J. M., Bui, A. Q., Yeung, E. C., Hashimoto, M., Fei, J., Harada, C. M., Munoz, M. D., Le, B. H., Drews, G. N., Brady, S. M., Goldberg, R. B. & Harada, J. J. 2013. Comprehensive developmental profiles of gene activity in regions and subregions of the *Arabidopsis* seed. *Proceedings of the National Academy of Sciences.* **110**: 435-44.

Benfey, P. N., Ren, L. & Chua, N. H. 1989. The CaMV 35S enhancer contains at least two domains which can confer different developmental and tissue-specific expression patterns. *The EMBO journal.* **8**: 2195-202.

Benkova, E., Michniewicz, M., Sauer, M., Teichmann, T., Seifertova, D., Jurgens, G. & Friml, J. 2003. Local, efflux-dependent auxin gradients as a common module for plant organ formation. *Cell.* **115**: 591-602.

Berger, F. 1999. Endosperm development. *Current Opinion in Plant Biology.* **2**: 28-32.

Berger, F. 2003. Endosperm: the crossroad of seed development. *Current Opinion in Plant Biology.* **6**: 42-50.

Berger, F., Grini, P. E. & Schnittger, A. 2006. Endosperm: an integrator of seed growth and development. *Current Opinion in Plant Biology.* **9**: 664-70.

Bockstaele, L., Kooken, H., Libert, F., Paternot, S., Dumont, J. E., De Launoit, Y., Roger, P. P. & Coulonval, K. 2006. Regulated activating Thr172 phosphorylation of cyclin-dependent kinase 4(CDK4): its relationship with cyclins and CDK "inhibitors". *Molecular and Cellular Biology.* **26**: 5070-85.

Bogre, L., Magyar, Z. & Lopez-Juez, E. 2008. New clues to organ size control in plants. *Genome Biology.* **9**: 226.

Boisnard-Lorig, C., Colon-Carmona, A., Bauch, M., Hodge, S., Doerner, P., Bancharel, E., Dumas, C., Haseloff, J. & Berger, F. 2001. Dynamic Analyses of the Expression of the HISTONE::YFP Fusion Protein in Arabidopsis Show That Syncytial Endosperm Is Divided in Mitotic Domains. *The Plant Cell.* **13**: 495-509.

Boniotti, M. B. & Gutierrez, C. 2001. A cell-cycle-regulated kinase activity phosphorylates plant retinoblastoma protein and contains, in *Arabidopsis*, a CDKA/cyclin D complex. *The Plant Journal.* **28**: 341-50.

Boruc, J., Van Den Daele, H., Hollunder, J., Rombauts, S., Mylle, E., Hilson, P., Inzé, D., De Veylder, L. & Russinova, E. 2010. Functional Modules in the *Arabidopsis* Core Cell Cycle Binary Protein-Protein Interaction Network. *The Plant Cell.* **22**: 1264-80.

Boudolf, V., Lammens, T., Boruc, J., Van Leene, J., Van Den Daele, H., Maes, S., Van Isterdael, G., Russinova, E., Kondorosi, E., Witters, E., De Jaeger, G., Inzé, D. & De Veylder, L. 2009. CDKB1;1 Forms a Functional Complex with CYCA2;3 to Suppress Endocycle Onset. *Plant Physiology.* **150**: 1482-93.

Boudolf, V., Rombauts, S., Naudts, M., Inze, D. & De Veylder, L. 2001. Identification of novel cyclin-dependent kinases interacting with the CKS1 protein of *Arabidopsis*. *Journal of Experimental Botany.* **52**: 1381-2.

Bowman, J. L. 1994. *Arabidopsis : an atlas of morphology and development.* New York, Springer-Verlag.

Brand, A. H. & Perrimon, N. 1993. Targeted gene expression as a means of altering cell fates and generating dominant phenotypes. *Development.* **118**: 401-15.

Braun, P., Aubourg, S., Van Leene, J., De Jaeger, G. & Lurin, C. 2013. Plant protein interactomes. *Annual Review of Plant Biology.* **64**: 161-87.

Brenchley, R., Spannagl, M., Pfeifer, M., Barker, G. L., D'amore, R., Allen, A. M., Mckenzie, N., Kramer, M., Kerhornou, A., Bolser, D., Kay, S., Waite, D., Trick, M., Bancroft, I., Gu, Y., Huo, N., Luo, M. C., Sehgal, S., Gill, B., Kianian, S., Anderson, O., Kersey, P., Dvorak, J., Mccombie, W. R., Hall, A., Mayer, K. F., Edwards, K. J., Bevan, M. W. & Hall, N. 2012. Analysis of the bread wheat genome using whole-genome shotgun sequencing. *Nature.* **491**: 705-10.

Breuninger, H. & Lenhard, M. 2010. Chapter Seven - Control of Tissue and Organ Growth in Plants. *In:* MARJA, C. P. T. (ed.) *Current Topics in Developmental Biology.* Academic Press.

Breuninger, H., Rikirsch, E., Hermann, M., Ueda, M. & Laux, T. 2008. Differential expression of *WOX* genes mediates apical-basal axis formation in the *Arabidopsis* embryo. *Developmental Cell.* **14**: 867-76.

Buendía-Monreal, M., Rentería-Canett, I., Guerrero-Andrade, O., Bravo-Alberto, C. E., Martínez-Castilla, L. P., García, E. & Vázquez-Ramos, J. M. 2011. The family of maize D-type cyclins: genomic organization, phylogeny and expression patterns. *Physiologia Plantarum.* **143**: 297-308.

Burssens, S., De Almeida Engler, J., Beeckman, T., Richard, C., Shaul, O., Ferreira, P., Van Montagu, M. & Inzé, D. 2000. Developmental expression of the *Arabidopsis thaliana CycA2;1* gene. *Planta.* **211**: 623-31.

Byrne, M. E., Barley, R., Curtis, M., Arroyo, J. M., Dunham, M., Hudson, A. & Martienssen, R. A. 2000. *Asymmetric leaves1* mediates leaf patterning and stem cell function in *Arabidopsis*. *Nature.* **408**: 967-71.

Capron, A., Chatfield, S., Provart, N. & Berleth, T. 2009. Embryogenesis: pattern formation from a single cell. *Arabidopsis Book.* **7**: e0126.

Chanvivattana, Y., Bishopp, A., Schubert, D., Stock, C., Moon, Y.-H., Sung, Z. R. & Goodrich, J. 2004. Interaction of Polycomb-group proteins controlling flowering in *Arabidopsis*. *Development.* **131**: 5263-76.

Chaudhury, A. M. & Berger, F. 2001. Maternal control of seed development. *Seminars in Cell & Developmental Biology.* **12**: 381-86.

Chen, Z., Hafidh, S., Poh, S. H., Twell, D. & Berger, F. 2009. Proliferation and cell fate establishment during *Arabidopsis* male gametogenesis depends on the Retinoblastoma protein. *Proceedings of the National Academy of Sciences.* **106**: 7257-62.

Chen, Z., Higgins, J. D., Hui, J. T., Li, J., Franklin, F. C. & Berger, F. 2011. Retinoblastoma protein is essential for early meiotic events in *Arabidopsis*. *The EMBO Journal.* **30**: 744-55.

Chen, Z. J. & Tian, L. 2007. Roles of dynamic and reversible histone acetylation in plant development and polyploidy. *Biochimica et Biophysica Acta (BBA) - Gene Structure and Expression.* **1769**: 295-307.

Chevray, P. M. & Nathans, D. 1992. Protein interaction cloning in yeast: identification of mammalian proteins that react with the leucine zipper of Jun. *Proceedings of the National Academy of Sciences.* **89**: 5789-93.

Choi, Y., Harada, J. J., Goldberg, R. B. & Fischer, R. L. 2004. An invariant aspartic acid in the DNA glycosylase domain of *DEMETER* is necessary for transcriptional activation of the imprinted *MEDEA* gene. *Proceedings of the National Academy of Sciences.* **101**: 7481-86.

Chuang, C. F. & Meyerowitz, E. M. 2000. Specific and heritable genetic interference by double-stranded RNA in *Arabidopsis thaliana*. *Proceedings of the National Academy of Sciences.* **97**: 4985-90.

Churchman, M. L., Brown, M. L., Kato, N., Kirik, V., Hülskamp, M., Inzé, D., De Veylder, L., Walker, J. D., Zheng, Z., Oppenheimer, D. G., Gwin, T., Churchman, J. & Larkin, J. C. 2006. SIAMESE, a Plant-Specific Cell Cycle Regulator, Controls Endoreplication Onset in *Arabidopsis thaliana*. *The Plant Cell.* **18**: 3145-57.

Cockcroft, C. E., Den Boer, B. G., Healy, J. M. & Murray, J. A. 2000. Cyclin D control of growth rate in plants. *Nature.* **405**: 575-9.

Collins, C. 2008. *CYCD Gene Function in Arabidopsis Seed Development.* University of Cambridge.

Collins, C., Dewitte, W. & Murray, J. A. 2012. D-type cyclins control cell division and developmental rate during *Arabidopsis* seed development. *Journal of Experimental Botany.* **63**: 3571-86.

Criqui, M. C. & Genschik, P. 2002. Mitosis in plants: how far we have come at the molecular level? *Current Opinion in Plant Biology.* **5**: 487-93.

Cruz-Ramírez, A., Díaz-Triviño, S., Blilou, I., Grieneisen, V. A., Sozzani, R., Zamioudis, C., Miskolczi, P., Nieuwland, J., Benjamins, R., Dhonukshe, P., Caballero-Pérez, J., Horvath, B., Long, Y., Mähönen, A. P., Zhang, H. L., Xu, J., Murray, J. A., Benfey, P. N., Bako, L., Marée, A. F. M. & Scheres, B. 2012. A Bistable Circuit Involving SCARECROW-RETINOBLASTOMA Integrates Cues to Inform Asymmetric Stem Cell Division. *Cell.* **150**: 1002-15.

De Almeida Engler, J., De Veylder, L., De Groodt, R., Rombauts, S., Boudolf, V., De Meyer, B., Hemerly, A., Ferreira, P., Beeckman, T., Karimi, M., Hilson, P., Inzé, D. & Engler, G. 2009. Systematic analysis of cell-cycle gene expression during Arabidopsis development. *The Plant Journal.* **59**: 645-60.

De Jager, S. M. & Murray, J. A. 1999. Retinoblastoma proteins in plants. *Plant Molecular Biology.* **41**: 295-9.

De Veylder, L., Beeckman, T., Beemster, G. T., De Almeida Engler, J., Ormenese, S., Maes, S., Naudts, M., Van Der Schueren, E., Jacqmard, A., Engler, G. & Inze, D. 2002. Control of proliferation, endoreduplication and differentiation by the *Arabidopsis* E2Fa-DPa transcription factor. *The EMBO journal.* **21**: 1360-8.

De Veylder, L., Beeckman, T., Beemster, G. T. S., Krols, L., Terras, F., Landrieu, I., Van Der Schueren, E., Maes, S., Naudts, M. & Inzé, D. 2001. Functional Analysis of Cyclin-Dependent Kinase Inhibitors of Arabidopsis. *The Plant Cell.* **13**: 1653-68.

De Veylder, L., Beeckman, T. & Inze, D. 2007. The ins and outs of the plant cell cycle. *Nature reviews.* **8**: 655-65.

De Veylder, L., De Almeida Engler, J., Burssens, S., Manevski, A., Lescure, B., Van Montagu, M., Engler, G. & Inzé, D. 1999. A new D-type cyclin of *Arabidopsis thaliana* expressed during lateral root primordia formation. *Planta.* **208**: 453-62.

De Veylder, L., Segers, G., Glab, N., Casteels, P., Van Montagu, M. & Inzé, D. 1997. The *Arabidopsis* Cks1At protein binds the cyclin-dependent kinases Cdc2aAt and Cdc2bAt. *FEBS letters.* **412**: 446-52.

De Veylder, L. D., Joubès, J. & Inzé, D. 2003. Plant cell cycle transitions. *Current Opinion in Plant Biology.* **6**: 536-43.

Debeaujon, I., Nesi, N., Perez, P., Devic, M., Grandjean, O., Caboche, M. & Lepiniec, L. 2003. Proanthocyanidin-Accumulating Cells in Arabidopsis Testa: Regulation of Differentiation and Role in Seed Development. *The Plant Cell.* **15**: 2514-31.

Del Pozo, J. C., Boniotti, M. B. & Gutierrez, C. 2002. Arabidopsis E2Fc Functions in Cell Division and Is Degraded by the Ubiquitin-SCFAtSKP2 Pathway in Response to Light. *The Plant Cell.* **14**: 3057-71.

Dewitte, W. & Murray, J. A. 2003. The plant cell cycle. *Annual Review of Plant Biology.* **54**: 235-64.

Dewitte, W., Riou-Khamlichi, C., Scofield, S., Healy, J. M. S., Jacqmard, A., Kilby, N. J. & Murray, J. A. 2003. Altered Cell Cycle Distribution, Hyperplasia, and Inhibited Differentiation in Arabidopsis Caused by the D-Type Cyclin CYCD3. *The Plant Cell.* **15**: 79-92.

Dewitte, W., Scofield, S., Alcasabas, A. A., Maughan, S. C., Menges, M., Braun, N., Collins, C., Nieuwland, J., Prinsen, E., Sundaresan, V. & Murray, J. A. 2007. *Arabidopsis* CYCD3 D-type cyclins link cell proliferation and endocycles and are rate-limiting for cytokinin responses. *Proceedings of the National Academy of Sciences.* **104**: 14537-42.

Dissmeyer, N., Nowack, M. K., Pusch, S., Stals, H., Inzé, D., Grini, P. E. & Schnittger, A. 2007. T-Loop Phosphorylation of *Arabidopsis* CDKA;1 Is Required for Its Function and Can Be Partially Substituted by an Aspartate Residue. *The Plant Cell.* **19**: 972-85.

Dissmeyer, N., Weimer, A. K., Pusch, S., De Schutter, K., Alvim Kamei, C. L., Nowack, M. K., Novak, B., Duan, G. L., Zhu, Y. G., De Veylder, L. & Schnittger, A. 2009. Control of cell proliferation, organ growth, and DNA damage response operate independently of dephosphorylation of the *Arabidopsis* Cdk1 homolog CDKA;1. *The Plant Cell.* **21**: 3641-54.

Doan, D. N., Linnestad, C. & Olsen, O. A. 1996. Isolation of molecular markers from the barley endosperm coenocyte and the surrounding nucellus cell layers. *Plant Molecular Biology.* **31**: 877-86.

Drees, B. L. 1999. Progress and variations in two-hybrid and three-hybrid technologies. *Current Opinion in Chemical Biology.* **3**: 64-70.

Drews, G. N. & Koltunow, A. M. 2011. The female gametophyte. *Arabidopsis Book.* **9**: e0155.

Dumas, C. 2001. Reproduction et développement des plantes à fleurs. *Comptes Rendus de l'Académie des Sciences - Series III - Sciences de la Vie.* **324**: 517-21.

Duttweiler, H. M. 1996. A highly sensitive and non-lethal β-galactosidase plate assay for yeast. *Trends in Genetics.* **12**: 340-41.

Dyson, N. 1998. The regulation of E2F by pRB-family proteins. *Genes & development.* **12**: 2245-62.

Ebel, C., Mariconti, L. & Gruissem, W. 2004. Plant retinoblastoma homologues control nuclear proliferation in the female gametophyte. *Nature.* **429**: 776-80.

Edgar, B. A. & Orr-Weaver, T. L. 2001. Endoreplication cell cycles: more for less. *Cell.* **105**: 297-306.

Emery, J. F., Floyd, S. K., Alvarez, J., Eshed, Y., Hawker, N. P., Izhaki, A., Baum, S. F. & Bowman, J. L. 2003. Radial patterning of *Arabidopsis* shoots by class III HD-ZIP and KANADI genes. *Current Biology.* **13**: 1768-74.

Enugutti, B., Oelschner, M. & Schneitz, K. 2013. Microscopic Analysis of Ovule Development in *Arabidopsis thaliana*. *In:* DE SMET, I. (ed.) *Plant Organogenesis.* Humana Press.

Esfandiari, E., Jin, Z., Abdeen, A., Griffiths, J. S., Western, T. L. & Haughn, G. W. 2013. Identification and analysis of an outer-seed-coat-specific promoter from *Arabidopsis thaliana*. *Plant Molecular Biology.* **81**: 93-104.

Evans, T., Rosenthal, E. T., Youngblom, J., Distel, D. & Hunt, T. 1983. Cyclin: a protein specified by maternal mRNA in sea urchin eggs that is destroyed at each cleavage division. *Cell.* **33**: 389-96.

Fang, W., Wang, Z., Cui, R., Li, J. & Li, Y. 2012. Maternal control of seed size by *EOD3/CYP78A6* in *Arabidopsis thaliana*. *The Plant Journal.* **70**: 929-39.

Fao. 2009. *How to feed the world in 2050?* [Online]. Available: http://www.fao.org/wsfs/forum2050/en/.

Faure, J. E., Rotman, N., Fortune, P. & Dumas, C. 2002. Fertilization in *Arabidopsis thaliana* wild type: developmental stages and time course. *The Plant Journal.* **30**: 481-8.

Field, C., Li, R. & Oegema, K. 1999. Cytokinesis in eukaryotes: a mechanistic comparison. *Current Opinion in Cell Biology.* **11**: 68-80.

Fischer, J. A., Giniger, E., Maniatis, T. & Ptashne, M. 1988. GAL4 activates transcription in *Drosophila*. *Nature.* **332**: 853-56.

Friedman, W. E. 1999. Expression of the cell cycle in sperm of *Arabidopsis*: implications for understanding patterns of gametogenesis and fertilization in plants and other eukaryotes. *Development.* **126**: 1065-75.

Friml, J., Vieten, A., Sauer, M., Weijers, D., Schwarz, H., Hamann, T., Offringa, R. & Jurgens, G. 2003. Efflux-dependent auxin gradients establish the apical-basal axis of *Arabidopsis*. *Nature.* **426**: 147-53.

Friml, J., Yang, X., Michniewicz, M., Weijers, D., Quint, A., Tietz, O., Benjamins, R., Ouwerkerk, P. B., Ljung, K., Sandberg, G., Hooykaas, P. J., Palme, K. & Offringa, R. 2004. A PINOID-dependent binary switch in apical-basal PIN polar targeting directs auxin efflux. *Science.* **306**: 862-5.

Fujimoto, R., Kinoshita, Y., Kawabe, A., Kinoshita, T., Takashima, K., Nordborg, M., Nasrallah, M. E., Shimizu, K. K., Kudoh, H. & Kakutani, T. 2008. Evolution and control of imprinted *FWA* genes in the genus *Arabidopsis*. *PLoS Genetics.* **4**: e1000048.

Galbraith, D. W., Harkins, K. R. & Knapp, S. 1991. Systemic Endopolyploidy in *Arabidopsis thaliana*. *Plant Physiology.* **96**: 985-9.

Garcia, D., Fitz Gerald, J. N. & Berger, F. 2005. Maternal control of integument cell elongation and zygotic control of endosperm growth are coordinated to determine seed size in Arabidopsis. *The Plant Cell.* **17**: 52-60.

Garcia, D., Saingery, V., Chambrier, P., Mayer, U., Jurgens, G. & Berger, F. 2003. Arabidopsis *haiku* mutants reveal new controls of seed size by endosperm. *Plant Physiology.* **131**: 1661-70.

Gehring, M., Huh, J. H., Hsieh, T. F., Penterman, J., Choi, Y., Harada, J. J., Goldberg, R. B. & Fischer, R. L. 2006. DEMETER DNA glycosylase establishes *MEDEA* polycomb gene self-imprinting by allele-specific demethylation. *Cell.* **124**: 495-506.

Goldberg, R. B., De Paiva, G. & Yadegari, R. 1994. Plant embryogenesis: zygote to seed. *Science.* **266**: 605-14.

Gonzalez-Garcia, M.-P., Vilarrasa-Blasi, J., Zhiponova, M., Divol, F., Mora-Garcia, S., Russinova, E. & Cano-Delgado, A. I. 2011. Brassinosteroids control meristem size by promoting cell cycle progression in *Arabidopsis* roots. *Development.* **138**: 849-59.

Goodrich, D. W. & Lee, W.-H. 1993. Molecular characterization of the retinoblastoma susceptibility gene. *Biochimica et Biophysica Acta (BBA) - Reviews on Cancer.* **1155**: 43-61.

Grafi, G., Burnett, R. J., Helentjaris, T., Larkins, B. A., Decaprio, J. A., Sellers, W. R. & Kaelin, W. G., Jr. 1996. A maize cDNA encoding a member of the retinoblastoma protein family: involvement in endoreduplication. *Proceedings of the National Academy of Sciences.* **93**: 8962-7.

Grini, P. E., Jurgens, G. & Hulskamp, M. 2002. Embryo and endosperm development is disrupted in the female gametophytic *capulet* mutants of Arabidopsis. *Genetics.* **162**: 1911-25.

Grossniklaus, U., Vielle-Calzada, J. P., Hoeppner, M. A. & Gagliano, W. B. 1998. Maternal control of embryogenesis by *MEDEA*, a polycomb group gene in *Arabidopsis*. *Science.* **280**: 446-50.

Guitton, A. E. & Berger, F. 2005. Loss of function of MULTICOPY SUPPRESSOR OF IRA1 produces nonviable parthenogenetic embryos in *Arabidopsis*. *Current Biology.* **15**: 750-4.

Guitton, A. E., Page, D. R., Chambrier, P., Lionnet, C., Faure, J. E., Grossniklaus, U. & Berger, F. 2004. Identification of new members of Fertilisation Independent Seed Polycomb Group pathway involved in the control of seed development in *Arabidopsis thaliana*. *Development.* **131**: 2971-81.

Gusti, A., Baumberger, N., Nowack, M., Pusch, S., Eisler, H., Potuschak, T., De Veylder, L., Schnittger, A. & Genschik, P. 2009. The *Arabidopsis thaliana* F-box protein FBL17 is essential for progression through the second mitosis during pollen development. *PLoS One.* **4**: e4780.

Gutierrez, C., Ramirez-Parra, E., Castellano, M. M. & Del Pozo, J. C. 2002. G(1) to S transition: more than a cell cycle engine switch. *Current Opinion in Plant Biology.* **5**: 480-6.

Haecker, A., Gross-Hardt, R., Geiges, B., Sarkar, A., Breuninger, H., Herrmann, M. & Laux, T. 2004. Expression dynamics of *WOX* genes mark cell fate decisions during early embryonic patterning in Arabidopsis thaliana. *Development.* **131**: 657-68.

Hajheidari, M., Farrona, S., Huettel, B., Koncz, Z. & Koncz, C. 2012. CDKF;1 and CDKD Protein Kinases Regulate Phosphorylation of Serine Residues in the C-Terminal Domain of *Arabidopsis* RNA Polymerase II. *The Plant Cell.* **24**: 1626-42.

Hamamura, Y., Nagahara, S. & Higashiyama, T. 2012. Double fertilization on the move. *Current Opinion in Plant Biology.* **15**: 70-77.

Haseloff, J. 1999. GFP variants for multispectral imaging of living cells. *Methods in Cell Biology.* **58**: 139-51.

Haseloff, J. P. & Hodge, S. 2001. Gene expression. United States patent application.

Healy, J. M., Menges, M., Doonan, J. H. & Murray, J. A. 2001. The Arabidopsis D-type cyclins CycD2 and CycD3 both interact in vivo with the PSTAIRE cyclin-dependent kinase Cdc2a but are differentially controlled. *The Journal of Biological Chemistry.* **276**: 7041-7.

Hehenberger, E., Kradolfer, D. & Kohler, C. 2012. Endosperm cellularization defines an important developmental transition for embryo development. *Development.* **139**: 2031-9.

Heisler, M. G., Ohno, C., Das, P., Sieber, P., Reddy, G. V., Long, J. A. & Meyerowitz, E. M. 2005. Patterns of auxin transport and gene expression during primordium development revealed by live imaging of the Arabidopsis inflorescence meristem. *Current biology : CB.* **15**: 1899-911.

Helariutta, Y., Fukaki, H., Wysocka-Diller, J., Nakajima, K., Jung, J., Sena, G., Hauser, M. T. & Benfey, P. N. 2000. The *SHORT-ROOT* gene controls radial patterning of the *Arabidopsis* root through radial signaling. *Cell.* **101**: 555-67.

Hemerly, A. S., Ferreira, P. C. G., Van Montagu, M., Engler, G. & Inzé, D. 2000. Cell division events are essential for embryo patterning and morphogenesis: studies on dominant-negative *cdc2aAt* mutants of *Arabidopsis*. *The Plant Journal.* **23**: 123-30.

Herridge, R. P., Day, R. C., Baldwin, S. & Macknight, R. C. 2011. Rapid analysis of seed size in *Arabidopsis* for mutant and QTL discovery. *Plant Methods.* **7**: 3.

Higashiyama, T., Kuroiwa, H., Kawano, S. & Kuroiwa, T. 1998. Guidance in Vitro of the Pollen Tube to the Naked Embryo Sac of *Torenia fournieri*. *The Plant Cell.* **10**: 2019-31.

House, C., Roth, C., Hunt, J. & Kover, P. X. 2010. Paternal effects in *Arabidopsis* indicate that offspring can influence their own size. *Proceedings of the Royal Society.* **277**: 2885-93.

Hsieh, T. F., Shin, J., Uzawa, R., Silva, P., Cohen, S., Bauer, M. J., Hashimoto, M., Kirkbride, R. C., Harada, J. J., Zilberman, D. & Fischer, R. L. 2011. Regulation of imprinted gene expression in *Arabidopsis* endosperm. *Proceedings of the National Academy of Sciences.* **108**: 1755-62.

Huang, X., Lu, T. & Han, B. 2013. Resequencing rice genomes: an emerging new era of rice genomics. *Trends in Genetics.* **29**: 225-32.

Huh, J. H., Bauer, M. J., Hsieh, T. F. & Fischer, R. 2007. Endosperm gene imprinting and seed development. *Current Opinion in Genetics & Development.* **17**: 480-5.

Imai, K. K., Ohashi, Y., Tsuge, T., Yoshizumi, T., Matsui, M., Oka, A. & Aoyama, T. 2006. The A-type cyclin CYCA2;3 is a key regulator of ploidy levels in *Arabidopsis* endoreduplication. *The Plant Cell.* **18**: 382-96.

Ingouff, M., Hamamura, Y., Gourgues, M., Higashiyama, T. & Berger, F. 2007. Distinct Dynamics of HISTONE3 Variants between the Two Fertilization Products in Plants. *Current Biology.* **17**: 1032-37.

Ingouff, M., Jullien, P. E. & Berger, F. 2006. The female gametophyte and the endosperm control cell proliferation and differentiation of the seed coat in *Arabidopsis*. *The Plant Cell.* **18**: 3491-501.

International Rice Genome Sequencing, P. 2005. The map-based sequence of the rice genome. *Nature.* **436**: 793-800.

Inze, D. & De Veylder, L. 2006. Cell cycle regulation in plant development. *Annual Review of Genetics.* **40**: 77-105.

Ito, M., Araki, S., Matsunaga, S., Itoh, T., Nishihama, R., Machida, Y., Doonan, J. H. & Watanabe, A. 2001. G2/M-phase-specific transcription during the plant cell cycle is mediated by c-Myb-like transcription factors. *The Plant Cell.* **13**: 1891-905.

Ito, M., Iwase, M., Kodama, H., Lavisse, P., Komamine, A., Nishihama, R., Machida, Y. & Watanabe, A. 1998. A novel *cis*-acting element in promoters of plant B-type cyclin genes activates M phase-specific transcription. *The Plant Cell.* **10**: 331-41.

Jacqmard, A., De Veylder, L., Segers, G., De Almeida Engler, J., Bernier, G., Van Montagu, M. & Inze, D. 1999. Expression of *CKS1At* in *Arabidopsis thaliana* indicates a role for the protein in both the mitotic and the endoreduplication cycle. *Planta.* **207**: 496-504.

Jakoby, M. & Schnittger, A. 2004. Cell cycle and differentiation. *Current Opinion in Plant Biology.* **7**: 661-69.

James, P., Halladay, J. & Craig, E. A. 1996. Genomic Libraries and a Host Strain Designed for Highly Efficient Two-Hybrid Selection in Yeast. *Genetics.* **144**: 1425-36.

Jefferson, R. A., Kavanagh, T. A. & Bevan, M. W. 1987. GUS fusions: beta-glucuronidase as a sensitive and versatile gene fusion marker in higher plants. *The EMBO journal.* **6**: 3901-7.

Jofuku, K. D., Den Boer, B. G., Van Montagu, M. & Okamuro, J. K. 1994. Control of Arabidopsis flower and seed development by the homeotic gene *APETALA2*. *The Plant Cell.* **6**: 1211-25.

Jofuku, K. D., Omidyar, P. K., Gee, Z. & Okamuro, J. K. 2005. Control of seed mass and seed yield by the floral homeotic gene *APETALA2*. *Proceedings of the National Academy of Sciences.* **102**: 3117-22.

Johnson, C. S., Kolevski, B. & Smyth, D. R. 2002. *TRANSPARENT TESTA GLABRA2*, a trichome and seed coat development gene of Arabidopsis, encodes a WRKY transcription factor. *The Plant Cell.* **14**: 1359-75.

Johnston, A. J., Matveeva, E., Kirioukhova, O., Grossniklaus, U. & Gruissem, W. 2008. A Dynamic Reciprocal *RBR*-PRC2 Regulatory Circuit Controls *Arabidopsis* Gametophyte Development. *Current Biology.* **18**: 1680-86.

Joubes, J. & Chevalier, C. 2000. Endoreduplication in higher plants. *Plant Molecular Biology.* **43**: 735-45.

Joubes, J., Chevalier, C., Dudits, D., Heberle-Bors, E., Inze, D., Umeda, M. & Renaudin, J. P. 2000. CDK-related protein kinases in plants. *Plant Molecular Biology.* **43**: 607-20.

Jullien, N. 2004. AmplifX. 1.6.2. CNRS, Aix-Marseille Université. http://crn2m.univ-mrs.fr/pub/amplifx-dist.

Jullien, P. E., Katz, A., Oliva, M., Ohad, N. & Berger, F. 2006. Polycomb group complexes self-regulate imprinting of the Polycomb group gene *MEDEA* in *Arabidopsis*. *Current Biology.* **16**: 486-92.

Jullien, P. E., Mosquna, A., Ingouff, M., Sakata, T., Ohad, N. & Berger, F. 2008. Retinoblastoma and its binding partner MSI1 control imprinting in *Arabidopsis*. *PLoS Biology.* **6**: e194.

Jura, N., Zhang, X., Endres, Nicholas f., Seeliger, Markus a., Schindler, T. & Kuriyan, J. 2011. Catalytic Control in the EGF Receptor and Its Connection to General Kinase Regulatory Mechanisms. *Molecular Cell.* **42**: 9-22.

Kakidani, H. & Ptashne, M. 1988. GAL4 activates gene expression in mammalian cells. *Cell.* **52**: 161-67.

Kang, I. H., Steffen, J. G., Portereiko, M. F., Lloyd, A. & Drews, G. N. 2008. The AGL62 MADS domain protein regulates cellularization during endosperm development in *Arabidopsis*. *The Plant Cell.* **20**: 635-47.

Kaplan, D. R. & Cooke, T. J. 1997. Fundamental Concepts in the Embryogenesis of Dicotyledons: A Morphological Interpretation of Embryo Mutants. *The Plant Cell.* **9**: 1903-19.

Kawamura, K., Murray, J. A., Shinmyo, A. & Sekine, M. 2006. Cell Cycle Regulated D3-type Cyclins form Active Complexes with Plant-specific B-type Cyclin-dependent Kinase *in vitro*. *Plant Molecular Biology.* **61**: 311-27.

Kesavan, M., Song, J. T. & Seo, H. S. 2013. Seed size: a priority trait in cereal crops. *Physiologia Plantarum.* **147**: 113-20.

Kinoshita, T., Miura, A., Choi, Y., Kinoshita, Y., Cao, X., Jacobsen, S. E., Fischer, R. L. & Kakutani, T. 2004. One-way control of *FWA i*mprinting in *Arabidopsis* endosperm by DNA methylation. *Science.* **303**: 521-3.

Kinoshita, T., Yadegari, R., Harada, J. J., Goldberg, R. B. & Fischer, R. L. 1999. Imprinting of the *MEDEA* polycomb gene in the Arabidopsis endosperm. *The Plant Cell.* **11**: 1945-52.

Kitsios, G., Alexiou, K. G., Bush, M., Shaw, P. & Doonan, J. H. 2008. A cyclin-dependent protein kinase, CDKC2, colocalizes with and modulates the distribution of spliceosomal components in Arabidopsis. *The Plant Journal.* **54**: 220-35.

Kiyosue, T., Ohad, N., Yadegari, R., Hannon, M., Dinneny, J., Wells, D., Katz, A., Margossian, L., Harada, J. J., Goldberg, R. B. & Fischer, R. L. 1999. Control of fertilization-independent endosperm development by the *MEDEA* polycomb gene in *Arabidopsis*. *Proceedings of the National Academy of Sciences.* **96**: 4186-91.

Kohler, C., Hennig, L., Bouveret, R., Gheyselinck, J., Grossniklaus, U. & Gruissem, W. 2003. *Arabidopsis* MSI1 is a component of the MEA/FIE *Polycomb* group complex and required for seed development. *The EMBO journal.* **22**: 4804-14.

Kondorosi, E. & Kondorosi, A. 2004. Endoreduplication and activation of the anaphase-promoting complex during symbiotic cell development. *FEBS letters.* **567**: 152-7.

Kono, A., Ohno, R., Umeda-Hara, C., Uchimiya, H. & Umeda, M. 2006. A distinct type of cyclin D, *CYCD4;2*, involved in the activation of cell division in *Arabidopsis*. *Plant Cell Reports.* **25**: 540-5.

Kono, A., Umeda-Hara, C., Adachi, S., Nagata, N., Konomi, M., Nakagawa, T., Uchimiya, H. & Umeda, M. 2007. The *Arabidopsis* D-Type Cyclin CYCD4 Controls Cell Division in the Stomatal Lineage of the Hypocotyl Epidermis. *The Plant Cell.* **19**: 1265-77.

Kono, A., Umeda-Hara, C., Lee, J., Ito, M., Uchimiya, H. & Umeda, M. 2003. Arabidopsis D-type cyclin CYCD4;1 is a novel cyclin partner of B2-type cyclin-dependent kinase. *Plant Physiology.* **132**: 1315-21.

Kosugi, S. & Ohashi, Y. 2002. E2Ls, E2F-like Repressors of Arabidopsis That Bind to E2F Sites in a Monomeric Form. *Journal of Biological Chemistry.* **277**: 16553-58.

Krupnova, T., Sasabe, M., Ghebreghiorghis, L., Gruber, C. W., Hamada, T., Dehmel, V., Strompen, G., Stierhof, Y.-D., Lukowitz, W., Kemmerling, B., Machida, Y., Hashimoto, T., Mayer, U. & Jurgens, G. 2009. Microtubule-Associated Kinase-like Protein RUNKEL Needed for Cell Plate Expansion in *Arabidopsis* Cytokinesis. *Current Biology.* **19**: 518-23.

Landrieu, I., Da Costa, M., De Veylder, L., Dewitte, F., Vandepoele, K., Hassan, S., Wieruszeski, J.-M., Faure, J.-D., Van Montagu, M., Inzé, D. & Lippens, G. 2004. A small CDC25 dual-specificity tyrosine-phosphatase isoform in *Arabidopsis thaliana*. *Proceedings of the National Academy of Sciences.* **101**: 13380-85.

Le, B. H., Cheng, C., Bui, A. Q., Wagmaister, J. A., Henry, K. F., Pelletier, J., Kwong, L., Belmonte, M., Kirkbride, R., Horvath, S., Drews, G. N., Fischer, R. L., Okamuro, J. K.,

Harada, J. J. & Goldberg, R. B. 2010. Global analysis of gene activity during *Arabidopsis* seed development and identification of seed-specific transcription factors. *Proceedings of the National Academy of Sciences.* **107**: 8063-70.

Leroy, O., Hennig, L., Breuninger, H., Laux, T. & Kohler, C. 2007. Polycomb group proteins function in the female gametophyte to determine seed development in plants. *Development.* **134**: 3639-48.

Li, Y., Zheng, L., Corke, F., Smith, C. & Bevan, M. W. 2008. Control of final seed and organ size by the *DA1* gene family in *Arabidopsis thaliana*. *Genes & Development.* **22**: 1331-6.

Liu, C.-M., Mcelver, J., Tzafrir, I., Joosen, R., Wittich, P., Patton, D., Van Lammeren, A. a. M. & Meinke, D. 2002. Condensin and cohesin knockouts in *Arabidopsis* exhibit a *titan* seed phenotype. *The Plant Journal.* **29**: 405-15.

Lopes, M. A. & Larkins, B. A. 1993. Endosperm origin, development, and function. *Plant Cell.* **5**: 1383-99.

Lu, P., Porat, R., Nadeau, J. A. & O'neill, S. D. 1996. Identification of a meristem L1 layer-specific gene in Arabidopsis that is expressed during embryonic pattern formation and defines a new class of homeobox genes. *The Plant Cell.* **8**: 2155-68.

Lui, H., Wang, H., Delong, C., Fowke, L. C., Crosby, W. L. & Fobert, P. R. 2000. The *Arabidopsis* Cdc2a-interacting protein ICK2 is structurally related to ICK1 and is a potent inhibitor of cyclin-dependent kinase activity i*n vitro*. *The Plant Journal.* **21**: 379-85.

Lukowitz, W., Mayer, U. & Jurgens, G. 1996. Cytokinesis in the Arabidopsis embryo involves the syntaxin-related KNOLLE gene product. *Cell.* **84**: 61-71.

Luo, M., Bilodeau, P., Dennis, E. S., Peacock, W. J. & Chaudhury, A. 2000. Expression and parent-of-origin effects for *FIS2*, *MEA*, and *FIE* in the endosperm and embryo of developing *Arabidopsis* seeds. *Proceedings of the National Academy of Sciences.* **97**: 10637-42.

Luo, M., Bilodeau, P., Koltunow, A., Dennis, E. S., Peacock, W. J. & Chaudhury, A. M. 1999. Genes controlling fertilization-independent seed development in A*rabidopsis thaliana*. *Proceedings of the National Academy of Sciences.* **96**: 296-301.

Luo, M., Dennis, E. S., Berger, F., Peacock, W. J. & Chaudhury, A. 2005. *MINISEED3* (*MINI3*), a WRKY family gene, and *HAIKU2* (*IKU2*), a leucine-rich repeat (*LRR*) *KINASE* gene, are regulators of seed size in *Arabidopsis*. *Proceedings of the National Academy of Sciences.* **102**: 17531-6.

Lynn, K., Fernandez, A., Aida, M., Sedbrook, J., Tasaka, M., Masson, P. & Barton, M. K. 1999. The *PINHEAD/ZWILLE* gene acts pleiotropically in Arabidopsis development and has overlapping functions with the *ARGONAUTE1* gene. *Development.* **126**: 469-81.

Ma, J., Przibilla, E., Hu, J., Bogorad, L. & Ptashne, M. 1988. Yeast activators stimulate plant gene expression. *Nature.* **334**: 631-33.

Mansfield, S. G. & Briarty, L. G. 1991. Early embryogenesis in *Arabidopsis thaliana*. II. The developing embryo. *Canadian Journal of Botany.* **69**: 461-76.

Mansfield, S. G., Briarty, L. G. & Erni, S. 1991. Early embryogenesis in *Arabidopsis thaliana*. I. The mature embryo sac. *Canadian Journal of Botany.* **69**: 447-60.

Marchant, A., Kargul, J., May, S. T., Muller, P., Delbarre, A., Perrot-Rechenmann, C. & Bennett, M. J. 1999. AUX1 regulates root gravitropism in *Arabidopsis* by facilitating auxin uptake within root apical tissues. *The EMBO journal.* **18**: 2066-73.

Masubelele, N. H., Dewitte, W., Menges, M., Maughan, S., Collins, C., Huntley, R., Nieuwland, J., Scofield, S. & Murray, J. A. 2005. D-type cyclins activate division in the root apex to promote seed germination in *Arabidopsis*. *Proceedings of the National Academy of Sciences.* **102**: 15694-99.

Mayer, K. F., Schoof, H., Haecker, A., Lenhard, M., Jurgens, G. & Laux, T. 1998. Role of *WUSCHEL* in regulating stem cell fate in the Arabidopsis shoot meristem. *Cell.* **95**: 805-15.

Mayer, U., Buttner, G. & Jurgens, G. 1993. Apical-basal pattern formation in the *Arabidopsis* embryo: studies on the role of the *gnom* gene. *Development.* **117**: 149-62.

Mayer, U., Herzog, U., Berger, F., Inzé, D. & Jürgens, G. 1999. Mutations in the *PILZ* group genes disrupt the microtubule cytoskeleton and uncouple cell cycle progression from cell division in *Arabidopsis* embryo and endosperm. *European Journal of Cell Biology.* **78**: 100-08.

Meijer, M. & Murray, J. A. 2000. The role and regulation of D-type cyclins in the plant cell cycle. *Plant Molecular Biology.* **43**: 621-33.

Melaragno, J. E., Mehrotra, B. & Coleman, A. W. 1993. Relationship between Endopolyploidy and Cell Size in Epidermal Tissue of Arabidopsis. *The Plant Cell.* **5**: 1661-68.

Menges, M., De Jager, S. M., Gruissem, W. & Murray, J. A. 2005. Global analysis of the core cell cycle regulators of Arabidopsis identifies novel genes, reveals multiple and highly specific profiles of expression and provides a coherent model for plant cell cycle control. *The Plant Journal.* **41**: 546-66.

Menges, M., Hennig, L., Gruissem, W. & Murray, J. A. 2002. Cell cycle-regulated gene expression in *Arabidopsis*. *The Journal of Biological Chemistry.* **277**: 41987-2002.

Menges, M., Hennig, L., Gruissem, W. & Murray, J. A. 2003. Genome-wide gene expression in an *Arabidopsis* cell suspension. *Plant Molecular Biology.* **53**: 423-42.

Menges, M. & Murray, J. A. 2002. Synchronous *Arabidopsis* suspension cultures for analysis of cell-cycle gene activity. *The Plant Journal.* **30**: 203-12.

Menges, M., Pavesi, G., Morandini, P., Bogre, L. & Murray, J. A. 2007. Genomic organization and evolutionary conservation of plant D-type cyclins. *Plant Physiology.* **145**: 1558-76.

Menges, M., Samland, A. K., Planchais, S. & Murray, J. A. 2006. The D-type cyclin CYCD3;1 is limiting for the G1-to-S-phase transition in Arabidopsis. *Plant Cell.* **18**: 893-906.

Minet, M., Dufour, M.-E. & Lacroute, F. 1992. Complementation of *Saccharomyces cerevisiae* auxotrophic mutants by Arabidopsis thaliana cDNAs. *The Plant Journal.* **2**: 417-22.

Mironov, V., De Veylder, L., Van Montagu, M. & Inzé, D. 1999. Cyclin-Dependent Kinases and Cell Division in Plants—The Nexus. *The Plant Cell.* **11**: 509-21.

Moller, B. & Weijers, D. 2009. Auxin control of embryo patterning. *Cold Spring Harbor Perspectives in Biology.* **1**: a001545.

Moore, I., Samalova, M. & Kurup, S. 2006. Transactivated and chemically inducible gene expression in plants. *The Plant Journal.* **45**: 651-83.

Müller, S., Fuchs, E., Ovecka, M., Wysocka-Diller, J., Benfey, P. N. & Hauser, M.-T. 2002. Two New Loci, *PLEIADE* and *HYADE*, Implicate Organ-Specific Regulation of Cytokinesis in Arabidopsis. *Plant Physiology.* **130**: 312-24.

Muranaka, T. 2011. Plant gateway vectors for RNAi as a tool for functional genomic studies. *Methods in Molecular Biology.* **744**: 27-35.

Nagai, T., Ibata, K., Park, E. S., Kubota, M., Mikoshiba, K. & Miyawaki, A. 2002. A variant of yellow fluorescent protein with fast and efficient maturation for cell-biological applications. *Nature Biotechnology.* **20**: 87-90.

Nakai, T., Kato, K., Shinmyo, A. & Sekine, M. 2006. *Arabidopsis* KRPs have distinct inhibitory activity toward cyclin D2-associated kinases, including plant-specific B-type cyclin-dependent kinase. *FEBS letters.* **580**: 336-40.

Nakajima, K., Sena, G., Nawy, T. & Benfey, P. N. 2001. Intercellular movement of the putative transcription factor SHR in root patterning. *Nature.* **413**: 307-11.

Ngo, Q. A., Moore, J. M., Baskar, R., Grossniklaus, U. & Sundaresan, V. 2007. Arabidopsis *GLAUCE* promotes fertilization-independent endosperm development and expression of paternally inherited alleles. *Development.* **134**: 4107-17.

Nieuwland, J., Maughan, S., Dewitte, W., Scofield, S., Sanz, L. & Murray, J. A. 2009. The D-type cyclin CYCD4;1 modulates lateral root density in *Arabidopsis* by affecting the basal meristem region. *Proceedings of the National Academy of Sciences.* **106**: 22528-33.

Noble, M. E., Endicott, J. A., Brown, N. R. & Johnson, L. N. 1997. The cyclin box fold: protein recognition in cell-cycle and transcription control. *Trends in Biochemical Sciences.* **22**: 482-7.

Novak, B., Csikasz-Nagy, A., Gyorffy, B., Nasmyth, K. & Tyson, J. J. 1998. Model scenarios for evolution of the eukaryotic cell cycle. *Philosophical Transactions of the Royal Society B: Biological Sciences.* **353**: 2063-76.

Nowack, M. K., Grini, P. E., Jakoby, M. J., Lafos, M., Koncz, C. & Schnittger, A. 2006. A positive signal from the fertilization of the egg cell sets off endosperm proliferation in angiosperm embryogenesis. *Nature Genetics.* **38**: 63-7.

Nowack, M. K., Shirzadi, R., Dissmeyer, N., Dolf, A., Endl, E., Grini, P. E. & Schnittger, A. 2007. Bypassing genomic imprinting allows seed development. *Nature.* **447**: 312-5.

Nowack, M. K., Ungru, A., Bjerkan, K. N., Grini, P. E. & Schnittger, A. 2010. Reproductive cross-talk: seed development in flowering plants. *Biochemical Society Transactions.* **38**: 604-12.

Nugent, J. H., Alfa, C. E., Young, T. & Hyams, J. S. 1991. Conserved structural motifs in cyclins identified by sequence analysis. *Journal of Cell Science.* **99**: 669-74.

Nurse, P. 2000. A long twentieth century of the cell cycle and beyond. *Cell.* **100**: 71-8.

Oakenfull, E. A., Riou-Khamlichi, C. & Murray, J. A. 2002. Plant D-type cyclins and the control of G1 progression. *Philosophical transactions of the Royal Society of London. Series B, Biological sciences.* **357**: 749-60.

Ohad, N., Margossian, L., Hsu, Y. C., Williams, C., Repetti, P. & Fischer, R. L. 1996. A mutation that allows endosperm development without fertilization. *Proceedings of the National Academy of Sciences.* **93**: 5319-24.

Ohto, M. A., Fischer, R. L., Goldberg, R. B., Nakamura, K. & Harada, J. J. 2005. Control of seed mass by *APETALA2*. *Proceedings of the National Academy of Sciences.* **102**: 3123-8.

Ohto, M. A., Floyd, S. K., Fischer, R. L., Goldberg, R. B. & Harada, J. J. 2009. Effects of *APETALA2* on embryo, endosperm, and seed coat development determine seed size in Arabidopsis. *Sexual Plant Reproduction.* **22**: 277-89.

Ormenese, S., De Almeida Engler, J., De Groodt, R., De Veylder, L., Inzé, D. & Jacqmard, A. 2004. Analysis of the Spatial Expression Pattern of Seven Kip Related Proteins (KRPs) in the Shoot Apex of *Arabidopsis thaliana*. *Annals of Botany.* **93**: 575-80.

Paul-Victor, C. & Turnbull, L. A. 2009. The effect of growth conditions on the seed size/number trade-off. *PloS One.* **4**: e6917.

Peres, A., Churchman, M. L., Hariharan, S., Himanen, K., Verkest, A., Vandepoele, K., Magyar, Z., Hatzfeld, Y., Van Der Schueren, E., Beemster, G. T. S., Frankard, V., Larkin, J. C., Inzé, D. & De Veylder, L. 2007. Novel Plant-specific Cyclin-dependent Kinase Inhibitors Induced by Biotic and Abiotic Stresses. *Journal of Biological Chemistry.* **282**: 25588-96.

Peris, C. I., Rademacher, E. H. & Weijers, D. 2010. Green beginnings - pattern formation in the early plant embryo. *Current Topics in Developmental Biology.* **91**: 1-27.

Pickett-Heaps, J. D., Gunning, B. E. S., Brown, R. C., Lemmon, B. E. & Cleary, A. L. 1999. The cytoplast concept in dividing plant cells: cytoplasmic domains and the evolution of spatially organized cell division. *American Journal of Botany.* **86**: 153-72.

Pignocchi, C., Minns, G. E., Nesi, N., Koumproglou, R., Kitsios, G., Benning, C., Lloyd, C. W., Doonan, J. H. & Hills, M. J. 2009. *ENDOSPERM DEFECTIVE1* Is a Novel Microtubule-Associated Protein Essential for Seed Development in *Arabidopsis*. *The Plant Cell.* **21**: 90-105.

Pines, J. 1995. Cyclins and cyclin-dependent kinases: theme and variations. *Advances in Cancer Research.* **66**: 181-212.

Prasher, D. C., Eckenrode, V. K., Ward, W. W., Prendergast, F. G. & Cormier, M. J. 1992. Primary structure of the *Aequorea victoria* green-fluorescent protein. *Gene.* **111**: 229-33.

Price, D. H. 2000. P-TEFb, a cyclin-dependent kinase controlling elongation by RNA polymerase II. *Methods in Molecular Biology*
Molecular and Cellular Biology. **20**: 2629-34.

Pusch, S., Harashima, H. & Schnittger, A. 2012. Identification of kinase substrates by bimolecular complementation assays. *The Plant Journal.* **70**: 348-56.

Qi, R. & John, P. C. L. 2007. Expression of Genomic *AtCYCD2;1* in Arabidopsis Induces Cell Division at Smaller Cell Sizes: Implications for the Control of Plant Growth. *Plant Physiology.* **144**: 1587-97.

Ramirez-Parra, E. & Gutierrez, C. 2007. The many faces of chromatin assembly factor 1. *Trends in Plant Science.* **12**: 570-76.

Ramirez-Parra, E., López-Matas, M. A., Fründt, C. & Gutierrez, C. 2004. Role of an Atypical E2F Transcription Factor in the Control of Arabidopsis Cell Growth and Differentiation. *The Plant Cell.* **16**: 2350-63.

Ramirez-Parra, E., Xie, Q., Boniotti, M. B. & Gutierrez, C. 1999. The cloning of plant E2F, a retinoblastoma-binding protein, reveals unique and conserved features with animal G(1)/S regulators. *Nucleic Acids Research.* **27**: 3527-33.

Ray, A., Lang, J. D., Golden, T. & Ray, S. 1996a. *SHORT INTEGUMENT* (*SIN1*), a gene required for ovule development in *Arabidopsis*, also controls flowering time. *Development.* **122**: 2631-8.

Ray, S., Golden, T. & Ray, A. 1996b. Maternal effects of the *short integument* mutation on embryo development in *Arabidopsis*. *Developmental Biology.* **180**: 365-9.

Ren, H., Santner, A., Pozo, J. C. D., Murray, J. A. & Estelle, M. 2008. Degradation of the cyclin-dependent kinase inhibitor KRP1 is regulated by two different ubiquitin E3 ligases. *The Plant Journal.* **53**: 705-16.

Renaudin, J.-P., Doonan, J., Freeman, D., Hashimoto, J., Hirt, H., Inzé, D., Jacobs, T., Kouchi, H., Rouzé, P., Sauter, M., Savouré, A., Sorrell, D., Sundaresan, V. & Murray, J. A. 1996. Plant cyclins: a unified nomenclature for plant A-, B- and D-type cyclins based on sequence organization. *Plant Molecular Biology.* **32**: 1003-18.

Riefler, M., Novak, O., Strnad, M. & Schmulling, T. 2006. *Arabidopsis* cytokinin receptor mutants reveal functions in shoot growth, leaf senescence, seed size, germination, root development, and cytokinin metabolism. *The Plant Cell.* **18**: 40-54.

Riou-Khamlichi, C., Huntley, R., Jacqmard, A. & Murray, J. A. 1999. Cytokinin activation of *Arabidopsis* cell division through a D-type cyclin. *Science.* **283**: 1541-4.

Robinson-Beers, K., Pruitt, R. E. & Gasser, C. S. 1992. Ovule Development in Wild-Type Arabidopsis and Two Female-Sterile Mutants. *The Plant Cell.* **4**: 1237-49.

Rossignol, P., Stevens, R., Perennes, C., Jasinski, S., Cella, R., Tremousaygue, D. & Bergounioux, C. 2002. AtE2F-a and AtDP-a, members of the E2F family of transcription factors, induce Arabidopsis leaf cells to re-enter S phase. *Molecular Genetics and Genomics.* **266**: 995-1003.

Russell, P. & Nurse, P. 1986. *cdc25+* functions as an inducer in the mitotic control of fission yeast. *Cell.* **45**: 145-53.

Russo, A. A., Jeffrey, P. D. & Pavletich, N. P. 1996. Structural basis of cyclin-dependent kinase activation by phosphorylation. *Nature Structural & Molecular Biology.* **3**: 696-700.

Sabelli, P. A., Dante, R. A., Leiva-Neto, J. T., Jung, R., Gordon-Kamm, W. J. & Larkins, B. A. 2005. RBR3, a member of the retinoblastoma-related family from maize, is regulated by the RBR1/E2F pathway. *Proceedings of the National Academy of Sciences.* **102**: 13005-12.

Sambrook, J. & Russell, D. W. 2001. *Molecular cloning : a laboratory manual.* Cold Spring Harbor, N.Y., Cold Spring Harbor Laboratory Press.

Sanz, L., Dewitte, W., Forzani, C., Patell, F., Nieuwland, J., Wen, B., Quelhas, P., De Jager, S., Titmus, C., Campilho, A., Ren, H., Estelle, M., Wang, H. & Murray, J. A. 2011. The *Arabidopsis* D-Type Cyclin CYCD2;1 and the Inhibitor ICK2/KRP2 Modulate Auxin-Induced Lateral Root Formation. *The Plant Cell.* **23**: 641-60.

Schlereth, A., Moller, B., Liu, W., Kientz, M., Flipse, J., Rademacher, E. H., Schmid, M., Jurgens, G. & Weijers, D. 2010. *MONOPTEROS* controls embryonic root initiation by regulating a mobile transcription factor. *Nature.* **464**: 913-6.

Schmidt, A., Wohrmann, H. J., Raissig, M. T., Arand, J., Gheyselinck, J., Gagliardini, V., Heichinger, C., Walter, J. & Grossniklaus, U. 2013. The *Polycomb* group protein MEDEA and the DNA methyltransferase MET1 interact to repress autonomous endosperm development in Arabidopsis. *The Plant Journal.* **73**: 776-87.

Schmutz, J., Cannon, S. B., Schlueter, J., Ma, J., Mitros, T., Nelson, W., Hyten, D. L., Song, Q., Thelen, J. J., Cheng, J., Xu, D., Hellsten, U., May, G. D., Yu, Y., Sakurai, T., Umezawa, T., Bhattacharyya, M. K., Sandhu, D., Valliyodan, B., Lindquist, E., Peto, M., Grant, D., Shu, S., Goodstein, D., Barry, K., Futrell-Griggs, M., Abernathy, B., Du, J., Tian, Z., Zhu, L., Gill, N., Joshi, T., Libault, M., Sethuraman, A., Zhang, X. C., Shinozaki, K., Nguyen, H. T., Wing, R. A., Cregan, P., Specht, J., Grimwood, J., Rokhsar, D., Stacey, G., Shoemaker, R. C. & Jackson, S. A. 2010. Genome sequence of the palaeopolyploid soybean. *Nature.* **463**: 178-83.

Schneitz, K., Hülskamp, M. & Pruitt, R. E. 1995. Wild-type ovule development in *Arabidopsis thaliana*: a light microscope study of cleared whole-mount tissue. *The Plant Journal.* **7**: 731-49.

Schoof, H., Lenhard, M., Haecker, A., Mayer, K. F., Jurgens, G. & Laux, T. 2000. The stem cell population of Arabidopsis shoot meristems in maintained by a regulatory loop between the CLAVATA and WUSCHEL genes. *Cell.* **100**: 635-44.

Schruff, M. C., Spielman, M., Tiwari, S., Adams, S., Fenby, N. & Scott, R. J. 2006. The *AUXIN RESPONSE FACTOR 2* gene of *Arabidopsis* links auxin signalling, cell division, and the size of seeds and other organs. *Development.* **133**: 251-61.

Scott, R. J., Spielman, M., Bailey, J. & Dickinson, H. G. 1998. Parent-of-origin effects on seed development in *Arabidopsis thaliana*. *Development.* **125**: 3329-41.

Sherr, C. J. & Roberts, J. M. 1999. CDK inhibitors: positive and negative regulators of G1-phase progression. *Genes & Development.* **13**: 1501-12.

Shi, D. Q. & Yang, W. C. 2011. Ovule development in Arabidopsis: progress and challenge. *Current Opinion in Plant Biology.* **14**: 74-80.

Shimotohno, A., Umeda-Hara, C., Bisova, K., Uchimiya, H. & Umeda, M. 2004. The Plant-Specific Kinase CDKF;1 Is Involved in Activating Phosphorylation of Cyclin-Dependent Kinase-Activating Kinases in Arabidopsis. *The Plant Cell.* **16**: 2954-66.

Smyth, D. R., Bowman, J. L. & Meyerowitz, E. M. 1990. Early flower development in *Arabidopsis*. *The Plant Cell.* **2**: 755-67.

Soppe, W. J. J., Jacobsen, S. E., Alonso-Blanco, C., Jackson, J. P., Kakutani, T., Koornneef, M. & Peeters, A. J. M. 2000. The Late Flowering Phenotype of *fwa* Mutants Is Caused by Gain-of-Function Epigenetic Alleles of a Homeodomain Gene. *Molecular Cell.* **6**: 791-802.

Sorensen, M. B., Mayer, U., Lukowitz, W., Robert, H., Chambrier, P., Jurgens, G., Somerville, C., Lepiniec, L. & Berger, F. 2002. Cellularisation in the endosperm of *Arabidopsis thaliana* is coupled to mitosis and shares multiple components with cytokinesis. *Development.* **129**: 5567-76.

Sorrell, D., Marchbank, A., Mcmahon, K., Dickinson, R., Rogers, H. & Francis, D. 2002. A *WEE1* homologue from *Arabidopsis thaliana*. *Planta.* **215**: 518-22.

Sozzani, R., Cui, H., Moreno-Risueno, M. A., Busch, W., Van Norman, J. M., Vernoux, T., Brady, S. M., Dewitte, W., Murray, J. A. & Benfey, P. N. 2010. Spatiotemporal regulation of cell-cycle genes by SHORTROOT links patterning and growth. *Nature.* **466**: 128-32.

Spadafora, N. D., Doonan, J. H., Herbert, R. J., Bitonti, M. B., Wallace, E., Rogers, H. J. & Francis, D. 2011. Arabidopsis T-DNA insertional lines for *CDC25* are hypersensitive to hydroxyurea but not to zeocin or salt stress. *Annals of Botany.* **107**: 1183-92.

Stangeland, B. & Salehian, Z. 2002. An improved clearing method for GUS assay in *Arabidopsis* endosperm and seeds. *Plant Molecular Biology Reporter.* **20**: 107-14.

Steinborn, K., Maulbetsch, C., Priester, B., Trautmann, S., Pacher, T., Geiges, B., Küttner, F., Lepiniec, L., Stierhof, Y.-D., Schwarz, H., Jürgens, G. & Mayer, U. 2002. The *Arabidopsis PILZ* group genes encode tubulin-folding cofactor orthologs required for cell division but not cell growth. *Genes & Development.* **16**: 959-71.

Steinmann, T., Geldner, N., Grebe, M., Mangold, S., Jackson, C. L., Paris, S., Galweiler, L., Palme, K. & Jurgens, G. 1999. Coordinated polar localization of auxin efflux carrier PIN1 by GNOM ARF GEF. *Science.* **286**: 316-8.

Strompen, G., El Kasmi, F., Richter, S., Lukowitz, W., Assaad, F. F., Jurgens, G. & Mayer, U. 2002. The *Arabidopsis HINKEL* gene encodes a kinesin-related protein involved in cytokinesis and is expressed in a cell cycle-dependent manner. *Current Biology.* **12**: 153-8.

Swaminathan, K., Yang, Y., Grotz, N., Campisi, L. & Jack, T. 2000. An Enhancer Trap Line Associated with a D-Class Cyclin Gene in Arabidopsis. *Plant Physiology.* **124**: 1658-67.

Tassan, J. P., Jaquenoud, M., Léopold, P., Schultz, S. J. & Nigg, E. A. 1995. Identification of human cyclin-dependent kinase 8, a putative protein kinase partner for cyclin C. *Proceedings of the National Academy of Sciences.* **92**: 8871-75.

Thorstensen, T., Grini, P. E. & Aalen, R. B. 2011. SET domain proteins in plant development. *Biochimica et Biophysica Acta (BBA) - Gene Regulatory Mechanisms.* **1809**: 407-20.

Torres Acosta, J. A., Fowke, L. C. & Wang, H. 2011. Analyses of phylogeny, evolution, conserved sequences and genome-wide expression of the ICK/KRP family of plant CDK inhibitors. *Annals of Botany.* **107**: 1141-57.

Traas, J., Hülskamp, M., Gendreau, E. & Höfte, H. 1998. Endoreduplication and development: rule without dividing? *Current Opinion in Plant Biology.* **1**: 498-503.

Tromas, A., Paponov, I. & Perrot-Rechenmann, C. 2010. AUXIN BINDING PROTEIN 1: functional and evolutionary aspects. *Trends in Plant Science.* **15**: 436-46.

Truernit, E., Bauby, H., Dubreucq, B., Grandjean, O., Runions, J., Barthélémy, J. & Palauqui, J.-C. 2008. High-Resolution Whole-Mount Imaging of Three-Dimensional Tissue Organization and Gene Expression Enables the Study of Phloem Development and Structure in *Arabidopsis*. *The Plant Cell.* **20**: 1494-503.

Tsukaya, H. 2003. Organ shape and size: a lesson from studies of leaf morphogenesis. *Current Opinion in Plant Biology.* **6**: 57-62.

Twell, D. 2011. Male gametogenesis and germline specification in flowering plants. *Sexual Plant Reproduction.* **24**: 149-60.

Ueda, M., Zhang, Z. & Laux, T. 2011. Transcriptional activation of *Arabidopsis* axis patterning genes *WOX8/9* links zygote polarity to embryo development. *Developmental Cell.* **20**: 264-70.

Umeda, M., Bhalerao, R. P., Schell, J., Uchimiya, H. & Koncz, C. 1998. A distinct cyclin-dependent kinase-activating kinase of *Arabidopsis thaliana*. *Proceedings of the National Academy of Sciences.* **95**: 5021-6.

Un News, C. 2013. *World population projected to reach 9.6 billion by 2050* [Online]. Available: http://www.un.org/apps/news/story.asp?NewsID=45165 - .UcRRN79mPAI.

Ungru, A., Nowack, M. K., Reymond, M., Shirzadi, R., Kumar, M., Biewers, S., Grini, P. E. & Schnittger, A. 2008. Natural variation in the degree of autonomous endosperm formation reveals independence and constraints of embryo growth during seed development in *Arabidopsis thaliana*. *Genetics.* **179**: 829-41.

Van Leene, J., Boruc, J., De Jaeger, G., Russinova, E. & De Veylder, L. 2011. A kaleidoscopic view of the *Arabidopsis* core cell cycle interactome. *Trends in Plant Science.* **16**: 141-50.

Van Leene, J., Hollunder, J., Eeckhout, D., Persiau, G., Van De Slijke, E., Stals, H., Van Isterdael, G., Verkest, A., Neirynck, S., Buffel, Y., De Bodt, S., Maere, S., Laukens, K., Pharazyn, A., Ferreira, P. C. G., Eloy, N., Renne, C., Meyer, C., Faure, J.-D., Steinbrenner, J., Beynon, J., Larkin, J. C., Van De Peer, Y., Hilson, P., Kuiper, M., De Veylder, L., Van Onckelen, H., Inze, D., Witters, E. & De Jaeger, G. 2010. Targeted interactomics reveals a complex core cell cycle machinery in *Arabidopsis thaliana*. *Molecular Systems Biology.* **6**.

Van Leene, J., Stals, H., Eeckhout, D., Persiau, G., Van De Slijke, E., Van Isterdael, G., De Clercq, A., Bonnet, E., Laukens, K., Remmerie, N., Henderickx, K., De Vijlder, T., Abdelkrim, A., Pharazyn, A., Van Onckelen, H., Inzé, D., Witters, E. & De Jaeger, G. 2007. A Tandem Affinity Purification-based Technology Platform to Study the Cell Cycle Interactome in *Arabidopsis thaliana*. *Molecular & Cellular Proteomics.* **6**: 1226-38.

Van't Hof, J. 1985. Control points within the cell cycle. *In:* BRYANT, J. A. & FRANCIS, D. (eds.) *The Cell division cycle in plants.* Cambridge Cambridgeshire ; New York: Cambridge University Press.

Vandepoele, K., Raes, J., De Veylder, L., Rouze, P., Rombauts, S. & Inze, D. 2002. Genome-wide analysis of core cell cycle genes in Arabidopsis. *The Plant Cell.* **14**: 903-16.

Verkest, A., Manes, C. L., Vercruysse, S., Maes, S., Van Der Schueren, E., Beeckman, T., Genschik, P., Kuiper, M., Inze, D. & De Veylder, L. 2005a. The cyclin-dependent kinase inhibitor KRP2 controls the onset of the endoreduplication cycle during Arabidopsis leaf development through inhibition of mitotic CDKA;1 kinase complexes. *The Plant Cell.* **17**: 1723-36.

Verkest, A., Weinl, C., Inze, D., De Veylder, L. & Schnittger, A. 2005b. Switching the cell cycle. Kip-related proteins in plant cell cycle control. *Plant Physiology.* **139**: 1099-106.

Vlieghe, K., Boudolf, V., Beemster, G. T. S., Maes, S., Magyar, Z., Atanassova, A., De Almeida Engler, J., De Groodt, R., Inzè, D. & De Veylder, L. 2005. The DP-E2F-like Gene *DEL1* Controls the Endocycle in *Arabidopsis thaliana*. *Current Biology* **15**: 59-63.

Walker, J. D., Oppenheimer, D. G., Concienne, J. & Larkin, J. C. 2000. *SIAMESE*, a gene controlling the endoreduplication cell cycle in *Arabidopsis thaliana* trichomes. *Development.* **127**: 3931-40.

Wang, G., Kong, H., Sun, Y., Zhang, X., Zhang, W., Altman, N., Depamphilis, C. W. & Ma, H. 2004. Genome-wide analysis of the cyclin family in Arabidopsis and comparative phylogenetic analysis of plant cyclin-like proteins. *Plant Physiology.* **135**: 1084-99.

Wang, H., Fowke, L. C. & Crosby, W. L. 1997. A plant cyclin-dependent kinase inhibitor gene. *Nature.* **386**: 451-2.

Wang, H., Qi, Q., Schorr, P., Cutler, Adrian j., Crosby, W. L. & Fowke, L. C. 1998. ICK1, a cyclin-dependent protein kinase inhibitor from *Arabidopsis thaliana* interacts with both Cdc2a and CycD3, and its expression is induced by abscisic acid. *The Plant Journal.* **15**: 501-10.

Waterhouse, P. M., Graham, M. W. & Wang, M. B. 1998. Virus resistance and gene silencing in plants can be induced by simultaneous expression of sense and antisense RNA. *Proceedings of the National Academy of Sciences.* **95**: 13959-64.

Weigel, D. & Glazebrook, J. 2006. *In Planta* Transformation of *Arabidopsis*. *Cold Spring Harbor Protocols.* **2006**: pdb.prot4668.

Weijers, D., Franke-Van Dijk, M., Vencken, R.-J., Quint, A., Hooykaas, P. & Offringa, R. 2001. An *Arabidopsis* Minute-like phenotype caused by a semi-dominant mutation in a *RIBOSOMAL PROTEIN S5* gene. *Development.* **128**: 4289-99.

Weijers, D., Schlereth, A., Ehrismann, J. S., Schwank, G., Kientz, M. & Jurgens, G. 2006. Auxin triggers transient local signaling for cell specification in *Arabidopsis* embryogenesis. *Developmental Cell.* **10**: 265-70.

Weijers, D., Van Hamburg, J.-P., Van Rijn, E., Hooykaas, P. J. J. & Offringa, R. 2003. Diphtheria Toxin-Mediated Cell Ablation Reveals Interregional Communication during Arabidopsis Seed Development. *Plant Physiology.* **133**: 1882-92.

Weinl, C., Marquardt, S., Kuijt, S. J. H., Nowack, M. K., Jakoby, M. J., Hülskamp, M. & Schnittger, A. 2005. Novel Functions of Plant Cyclin-Dependent Kinase Inhibitors, ICK1/KRP1, Can Act Non-Cell-Autonomously and Inhibit Entry into Mitosis. *The Plant Cell.* **17**: 1704-22.

Werner, T., Motyka, V., Laucou, V., Smets, R., Van Onckelen, H. & Schmulling, T. 2003. Cytokinin-deficient transgenic Arabidopsis plants show multiple developmental alterations indicating opposite functions of cytokinins in the regulation of shoot and root meristem activity. *The Plant Cell.* **15**: 2532-50.

Werner, T., Motyka, V., Strnad, M. & Schmulling, T. 2001. Regulation of plant growth by cytokinin. *Proceedings of the National Academy of Sciences.* **98**: 10487-92.

West, M. & Harada, J. J. 1993. Embryogenesis in Higher Plants: An Overview. *The Plant Cell.* **5**: 1361-69.

Wildwater, M., Campilho, A., Perez-Perez, J. M., Heidstra, R., Blilou, I., Korthout, H., Chatterjee, J., Mariconti, L., Gruissem, W. & Scheres, B. 2005. The *RETINOBLASTOMA-RELATED* gene regulates stem cell maintenance in *Arabidopsis* roots. *Cell.* **123**: 1337-49.

Windsor, J. B., Symonds, V. V., Mendenhall, J. & Lloyd, A. M. 2000. *Arabidopsis* seed coat development: morphological differentiation of the outer integument. *The Plant Journal.* **22**: 483-93.

Winter, D., Vinegar, B., Nahal, H., Ammar, R., Wilson, G. V. & Provart, N. J. 2007. An "Electronic Fluorescent Pictograph" browser for exploring and analyzing large-scale biological data sets. *PLoS One.* **2**: e718.

Wolters, H., Anders, N., Geldner, N., Gavidia, R. & Jurgens, G. 2011. Coordination of apical and basal embryo development revealed by tissue-specific GNOM functions. *Development.* **138**: 117-26.

Xiao, W., Brown, R. C., Lemmon, B. E., Harada, J. J., Goldberg, R. B. & Fischer, R. L. 2006. Regulation of seed size by hypomethylation of maternal and paternal genomes. *Plant Physiology.* **142**: 1160-8.

Xie, Q., Sanz-Burgos, A. P., Hannon, G. J. & Gutierrez, C. 1996. Plant cells contain a novel member of the retinoblastoma family of growth regulatory proteins. *The EMBO journal.* **15**: 4900-8.

Xu, C. & Min, J. 2011. Structure and function of WD40 domain proteins. *Protein & Cell.* **2**: 202-14.

Yoo, S., Bomblies, K., Yoo, S., Yang, J., Choi, M., Lee, J., Weigel, D. & Ahn, J. 2005. The 35S promoter used in a selectable marker gene of a plant transformation vector affects the expression of the transgene. *Planta.* **221**: 523-30.

Young, T. E., Gallie, D. R. & Demason, D. A. 1997. Ethylene-Mediated Programmed Cell Death during Maize Endosperm Development of *Wild-Type* and *shrunken2* Genotypes. *Plant Physiology.* **115**: 737-51.

Yu, Y., Steinmetz, A., Meyer, D., Brown, S. & Shen, W.-H. 2003. The Tobacco A-Type Cyclin, *Nicta;CYCA3;2*, at the Nexus of Cell Division and Differentiation. *The Plant Cell.* **15**: 2763-77.

Zhao, X. A., Harashima, H., Dissmeyer, N., Pusch, S., Weimer, A. K., Bramsiepe, J., Bouyer, D., Rademacher, S., Nowack, M. K., Novak, B., Sprunck, S. & Schnittger, A. 2012. A General G1/S-Phase Cell-Cycle Control Module in the Flowering Plant *Arabidopsis thaliana*. *PLoS Genetics.* **8**: e1002847.

Zheng, X., Deng, W., Luo, K., Duan, H., Chen, Y., Mcavoy, R., Song, S., Pei, Y. & Li, Y. 2007. The cauliflower mosaic virus (CaMV) 35S promoter sequence alters the level and patterns of activity of adjacent tissue- and organ-specific gene promoters. *Plant Cell Reports.* **26**: 1195-203.

Zhou, Y., Fowke, L. & Wang, H. 2002a. Plant CDK inhibitors: studies of interactions with cell cycle regulators in the yeast two-hybrid system and functional comparisons in transgenic *Arabidopsis* plants. *Plant Cell Reports.* **20**: 967-75.

Zhou, Y., Wang, H., Gilmer, S., Whitwill, S. & Fowke, L. 2003. Effects of co-expressing the plant CDK inhibitor ICK1 and D-type cyclin genes on plant growth, cell size and ploidy in *Arabidopsis thaliana*. *Planta.* **216**: 604-13.

Zhou, Y., Wang, H., Gilmer, S., Whitwill, S., Keller, W. & Fowke, L. C. 2002b. Control of petal and pollen development by the plant cyclin-dependent kinase inhibitor ICK1 in transgenic Brassica plants. *Planta.* **215**: 248-57.

Zhou, Y., Zhang, X., Kang, X., Zhao, X., Zhang, X. & Ni, M. 2009. *SHORT HYPOCOTYL UNDER BLUE1* associates with *MINISEED3* and *HAIKU2* promoters *in vivo* to regulate *Arabidopsis* seed development. *The Plant Cell.* **21**: 106-17.